IEC 62359

Edition 2.1 2017-09

CONSOLIDATED VERSION

colour inside

Ultrasonics – Field characterization – Test methods for the determination of thermal and mechanical indices related to medical diagnostic ultrasonic fields

IEC 62359:2010-10+AMD1:2017-09 CSV(en)

IEC Central Office
3, rue de Varembé
CH-1211 Geneva 20
Switzerland

Tel.: +41 22 919 02 11
Fax: +41 22 919 03 00
info@iec.ch
www.iec.ch

About the IEC

The International Electrotechnical Commission (IEC) is the leading global organization that prepares and publishes International Standards for all electrical, electronic and related technologies.

About IEC publications

The technical content of IEC publications is kept under constant review by the IEC. Please make sure that you have the latest edition, a corrigenda or an amendment might have been published.

IEC Catalogue - webstore.iec.ch/catalogue

The stand-alone application for consulting the entire bibliographical information on IEC International Standards, Technical Specifications, Technical Reports and other documents. Available for PC, Mac OS, Android Tablets and iPad.

IEC publications search - www.iec.ch/searchpub

The advanced search enables to find IEC publications by a variety of criteria (reference number, text, technical committee,…). It also gives information on projects, replaced and withdrawn publications.

IEC Just Published - webstore.iec.ch/justpublished

Stay up to date on all new IEC publications. Just Published details all new publications released. Available online and also once a month by email.

Electropedia - www.electropedia.org

The world's leading online dictionary of electronic and electrical terms containing 20 000 terms and definitions in English and French, with equivalent terms in 16 additional languages. Also known as the International Electrotechnical Vocabulary (IEV) online.

IEC Glossary - std.iec.ch/glossary

65 000 electrotechnical terminology entries in English and French extracted from the Terms and Definitions clause of IEC publications issued since 2002. Some entries have been collected from earlier publications of IEC TC 37, 77, 86 and CISPR.

IEC Customer Service Centre - webstore.iec.ch/csc

If you wish to give us your feedback on this publication or need further assistance, please contact the Customer Service Centre: csc@iec.ch.

IEC 62359

Edition 2.1 2017-09

CONSOLIDATED VERSION

colour inside

Ultrasonics – Field characterization – Test methods for the determination of thermal and mechanical indices related to medical diagnostic ultrasonic fields

INTERNATIONAL ELECTROTECHNICAL COMMISSION

ICS 17.140.50

ISBN 978-2-8322-4885-0

IEC 62359

Edition 2.1 2017-09

REDLINE VERSION

colour inside

Ultrasonics – Field characterization – Test methods for the determination of thermal and mechanical indices related to medical diagnostic ultrasonic fields

IEC 62359:2010-10+AMD1:2017-09 CSV(en)

CONTENTS

INTERNATIONAL ELECTROTECHNICAL COMMISSION

ULTRASONICS – FIELD CHARACTERIZATION – TEST METHODS FOR THE DETERMINATION OF THERMAL AND MECHANICAL INDICES RELATED TO MEDICAL DIAGNOSTIC ULTRASONIC FIELDS

FOREWORD

1) The International Electrotechnical Commission (IEC) is a worldwide organization for standardization comprising all national electrotechnical committees (IEC National Committees). The object of IEC is to promote international co-operation on all questions concerning standardization in the electrical and electronic fields. To this end and in addition to other activities, IEC publishes International Standards, Technical Specifications, Technical Reports, Publicly Available Specifications (PAS) and Guides (hereafter referred to as "IEC Publication(s)"). Their preparation is entrusted to technical committees; any IEC National Committee interested in the subject dealt with may participate in this preparatory work. International, governmental and non-governmental organizations liaising with the IEC also participate in this preparation. IEC collaborates closely with the International Organization for Standardization (ISO) in accordance with conditions determined by agreement between the two organizations.
2) The formal decisions or agreements of IEC on technical matters express, as nearly as possible, an international consensus of opinion on the relevant subjects since each technical committee has representation from all interested IEC National Committees.
3) IEC Publications have the form of recommendations for international use and are accepted by IEC National Committees in that sense. While all reasonable efforts are made to ensure that the technical content of IEC Publications is accurate, IEC cannot be held responsible for the way in which they are used or for any misinterpretation by any end user.
4) In order to promote international uniformity, IEC National Committees undertake to apply IEC Publications transparently to the maximum extent possible in their national and regional publications. Any divergence between any IEC Publication and the corresponding national or regional publication shall be clearly indicated in the latter.
5) IEC itself does not provide any attestation of conformity. Independent certification bodies provide conformity assessment services and, in some areas, access to IEC marks of conformity. IEC is not responsible for any services carried out by independent certification bodies.
6) All users should ensure that they have the latest edition of this publication.
7) No liability shall attach to IEC or its directors, employees, servants or agents including individual experts and members of its technical committees and IEC National Committees for any personal injury, property damage or other damage of any nature whatsoever, whether direct or indirect, or for costs (including legal fees) and expenses arising out of the publication, use of, or reliance upon, this IEC Publication or any other IEC Publications.
8) Attention is drawn to the Normative references cited in this publication. Use of the referenced publications is indispensable for the correct application of this publication.
9) Attention is drawn to the possibility that some of the elements of this IEC Publication may be the subject of patent rights. IEC shall not be held responsible for identifying any or all such patent rights.

This Consolidated version of IEC 62359 bears the edition number 2.1. It consists of the second edition (2010-10) [documents 87/445/FDIS and 87/453/RVD] and its corrigendum 1 (2011-03), and its amendment 1 (2017-09) [documents 87/661/FDIS and 87/665/RVD]. The technical content is identical to the base edition and its amendment.

In this Redline version, a vertical line in the margin shows where the technical content is modified by amendment 1. Additions are in green text, deletions are in strikethrough red text. A separate Final version with all changes accepted is available in this publication.

International standard IEC 62359 has been prepared by IEC technical committee 87: Ultrasonics.

This second edition It constitutes a technical revision.

Major changes with respect to the previous edition include the following:

- The methods of determination set out in the first edition of this standard were based on those contained in the American standard for Real–Time Display of Thermal and Mechanical Acoustic Output Indices on Diagnostic Ultrasound Equipment (ODS) and were intended to yield identical results. While this second edition also follows the ODS in principal and uses the same basic formulae and assumptions (see Annex A), it contains a few significant modifications which deviate from the ODS.

- One of the primary issues dealt with in preparing this second edition of IEC 62359 was “missing” TI equations. In Edition 1 there were not enough equations to make complete “at-surface” and “below-surface” summations for TIS and TIB in combined-operating modes. Thus major changes with respect to the previous edition are related to the introduction of new calculations of thermal indices to take into account both "at-surface" and "below-surface" thermal effects.

For the specific technical changes involved please see Annex E.

This publication has been drafted in accordance with the ISO/IEC Directives, Part 2.

This standard may be used to support the requirements of IEC 60601-2-37.

In this particular standard, the following print types are used:

– requirements, compliance with which can be tested, and definitions: in roman type
– notes, explanations, advice, introductions, general statements, exceptions, and references: in smaller type
– *test specifications: in italic type*
– words in **bold** are defined terms in Clause 3

The committee has decided that the contents of the base publication and its amendment will remain unchanged until the stability date indicated on the IEC web site under "http://webstore.iec.ch" in the data related to the specific publication. At this date, the publication will be

- reconfirmed,
- withdrawn,
- replaced by a revised edition, or
- amended.

A bilingual version of this publication may be issued at a later date.

IMPORTANT – The 'colour inside' logo on the cover page of this publication indicates that it contains colours which are considered to be useful for the correct understanding of its contents. Users should therefore print this document using a colour printer.

INTRODUCTION

Medical diagnostic ultrasonic equipment is widely used in clinical practice for imaging and monitoring purposes. Equipment normally operates at frequencies in the low megahertz frequency range and comprises an ultrasonic transducer acoustically coupled to the patient and associated electronics. There is an extremely wide range of different types of systems in current clinical practice.

The ultrasound entering the patient interacts with the patient's tissue, and this interaction can be considered in terms of both thermal and non-thermal effects. The purpose of this International standard is to specify methods of determining thermal and non-thermal exposure indices that can be used to help in assessing the hazard caused by exposure to a particular ultrasonic field used for medical diagnosis or monitoring. It is recognised that these indices have limitations, and knowledge of the indices at the time of an examination is not sufficient in itself to make an informed clinical risk assessment. It is intended that these limitations will be addressed in future revisions of this standard and as scientific understanding increases. While such increases remain pending, several organizations have published **prudent-use statements.**

Under certain conditions specified in IEC 60601-2-37, these indices are displayed on medical ultrasonic equipment intended for these purposes.

INTRODUCTION to Amendment

The second edition of IEC 62359 was published in 2010. Since then, IEC 60601-2-37:2007/AMD1:2015 has been published and calls for provision of **attenuated spatial peak temporal average intensity**, $I_{\mathrm{spta},\alpha}$, and **attenuated spatial peak pulse average intensity**, $I_{\mathrm{sppa},\alpha}$, at specific spatial maximum points in the ultrasonic field on the **beam axis**. No IEC standard describes the determination of these quantities at these specific positions. IEC 62359 for determining the thermal indices currently uses similar values at other positions, therefore, the determination of **attenuated spatial peak temporal average intensity**, $I_{\mathrm{spta},\alpha}$, and **attenuated spatial peak pulse average intensity**, $I_{\mathrm{sppa},\alpha}$, has been added as an annex in this amendment.

Additionally, references to newly published collateral standards have been updated.

ULTRASONICS – FIELD CHARACTERIZATION – TEST METHODS FOR THE DETERMINATION OF THERMAL AND MECHANICAL INDICES RELATED TO MEDICAL DIAGNOSTIC ULTRASONIC FIELDS

1 Scope

This International standard is applicable to medical diagnostic ultrasound fields.

This standard establishes

– parameters related to thermal and non-thermal exposure aspects of diagnostic ultrasonic fields;
– methods for the determination of an exposure parameter relating to temperature rise in theoretical tissue-equivalent models, resulting from absorption of ultrasound;
– methods for the determination of an exposure parameter appropriate to certain non-thermal effects.

NOTE 1 In Clause 3 of this standard, SI units are used (per ISO/IEC Directives, Part 2, ed. 5, Annex I b) in the Notes below definitions of certain parameters, such as beam areas and intensities; it may be convenient to use decimal multiples or submultiples in practice. Users must take care of decimal prefixes used in combination with the units when using and calculating numerical data. For example, beam area may be specified in cm^2 and intensities in W/cm^2 or mW/cm^2.

NOTE 2 Underlying calculations have been done from 0,25 MHz to 15 MHz for MI and 0,5 MHz to 15 MHz for *TI*.

NOTE 3 The thermal indices are steady state estimates based on the acoustic **output power** required to produce a 1°C temperature rise in tissue conforming to the "homogeneous tissue 0,3 $dBcm^{-1}MHz^{-1}$ attenuation model" [1] [1)] and may not be appropriate for radiation force imaging, or similar techniques that employ pulses or pulse bursts of sufficient duration to create a significant transient temperature rise. [2]

2 Normative references

The following referenced documents are indispensable for the application of this document. For dated references, only the edition cited applies. For undated references, the latest edition of the referenced document (including any amendments) applies.

IEC 60601-2-37:2007, *Medical electrical equipment – Part 2-37: Particular requirements for the basic safety and essential performance of ultrasonic medical diagnostic and monitoring equipment*
IEC 60601-2-37:2007/AMD1:2015

IEC 61157:2007, *Standard means for the reporting of the acoustic output of medical diagnostic ultrasonic equipment*
IEC 61157:2007/AMD1:2013

IEC 61161:~~2006~~ 2013, *Ultrasonics – Power measurement – Radiation force balances and performance requirements*

IEC 61828:2001, *Ultrasonics – Focusing transducers – Definitions and measurement methods for the transmitted fields*

---

1) Figures in square brackets refer to Bibliography.

IEC 62127-1:2007, *Ultrasonics – Hydrophones – Part 1: Measurement and characterization of medical ultrasonic fields up to 40 MHz*
IEC 62127-1:2007/AMD1:2013

IEC 62127-2:2007, *Ultrasonics – Hydrophones – Part 2: Calibration for ultrasonic fields up to 40 MHz*

IEC 62127-3:2007, *Ultrasonics – Hydrophones – Part 3: Properties of hydrophones for ultrasonic fields up to 40 MHz*

3 Terms and definitions

For the purposes of this document, the terms and definitions given in IEC 60601-2-37, IEC 62127-1~~:2007~~, IEC 62127-2~~:2007~~, IEC 62127-3~~:2007~~, IEC 61157~~:2007~~ and IEC 61161~~:2006 (several of which are repeated below for convenience)~~ apply. Several of these are repeated below for convenience and others are listed because they have been modified for application to this standard.

NOTE Units below definitions are given is SI units as per ISO/IEC Directives, Part 2, ed. 5, Annex I b). Users must be alert to possible need to convert units when using this standard in situations where data are received in units that are different from those used in the SI system.

3.1
acoustic attenuation coefficient
α
coefficient intended to account for ultrasonic attenuation of tissue between the **external transducer aperture** and a specified point

NOTE 1 A linear dependence on frequency is assumed.

NOTE 2 **Acoustic attenuation coefficient** is expressed in decibels per metre per hertz (dB m^{-1} Hz^{-1}).

3.2
acoustic absorption coefficient
μ_0
coefficient intended to account for ultrasonic absorption of tissue in the region of interest

NOTE 1 A linear dependence on frequency is assumed.

NOTE 2 **Acoustic absorption coefficient** is expressed in neper per metre per hertz (Np m^{-1} Hz^{-1}).

3.3
acoustic repetition period
arp
time interval between corresponding points of consecutive cycles~~ for continuous wave systems~~, pulses or scans, depending on the current operating mode

NOTE 1 The **acoustic repetition period** is equal to the **pulse repetition period** for non-automatic scanning systems and to the **scan repetition period** for automatic scanning systems**.**

NOTE 2 For continuous wave modes, the **acoustic repetition period** is the time interval between corresponding points of consecutive cycles

NOTE 3 For **combined operating modes** where transmit pulsing of the constituent modes may be interrupted, the ***arp*** determination should take into account non-pulsing time to calculate an average period.

NOTE ~~2~~4 The **acoustic repetition period** is expressed in seconds (s).

[IEC 62127-1:2007, definition 3.2, modified]

3.4
acoustic working frequency
frequency of an acoustic signal based on the observation of the output of a **hydrophone** placed in an acoustic field ~~at the position corresponding to the **spatial-peak temporal-peak acoustic pressure**~~ on the **beam axis**, beyond the **break-point depth**, corresponding to **depth of maximum pulse-intensity integral** z_{pii}.

NOTE 1 The signal is analysed using either the **zero-crossing acoustic-working frequency** technique or a spectrum analysis method. Specific acoustic-working frequencies are defined in 3.4.1 and 3.4.2.

NOTE 2 For pulsed waveforms the **acoustic-working frequency** shall be measured at the ~~position of maximum **pulse-pressure-squared integral**~~ **depth for peak pulse-intensity integral**.

NOTE 3 **Acoustic frequency** is expressed in hertz (Hz).

[IEC 62127-1:2007, definition 3.3, modified]

3.4.1
zero-crossing acoustic-working frequency
f_{awf}
number of consecutive half-cycles (irrespective of polarity) divided by twice the time between the commencement of the first half-cycle and the end of the n-th half-cycle

NOTE 1 Any half-cycle in which the waveform shows evidence of phase change shall not be counted.

NOTE 2 The measurement should be performed at terminals in the receiver, that are as close as possible to the receiving transducer (hydrophone) and, in all cases, before rectification.

NOTE 3 This frequency is determined according to the procedure specified in IEC/TR 60854 [3].

NOTE 4 This frequency is intended for continuous-wave systems only.

3.4.2
arithmetic-mean acoustic-working frequency
f_{awf}
arithmetic mean of the most widely separated frequencies f_1 and f_2, within the range of three times f_1, at which the magnitude of the acoustic pressure spectrum is 3 dB below the peak magnitude

NOTE 1 This frequency is intended for pulse-wave systems only.

NOTE 2 It is assumed that $f_1 < f_2$.

NOTE 3 If f_2 is not found within the range < 3 f_1, f_2 is to be understood as the lowest frequency above this range at which the spectrum magnitude is -3 dB from the peak magnitude.

3.5
attenuated bounded-square output power
$P_{1x1,\alpha}(z)$
The maximum value of the **attenuated output power** passing through any one square centimeter of the plane perpendicular to the **beam axis** at depth z

NOTE 1 At $z = 0$ (the transducer surface) $P_{1x1,\alpha}(z)$ becomes the **bounded-square output power**, that is, at $z = 0$, $P_{1x1,\alpha} = P_{1x1}$.

NOTE 2 **Attenuated bounded-square output power** is expressed in watts (W).

3.6
attenuated output power
$P_\alpha(z)$
value of the acoustic **output power** after attenuation, at a specified distance from the **external transducer aperture**, and given by

$$P_\alpha(z) = P\,10^{(-\alpha z\, f_{awf}/10\,dB)} \quad (1)$$

where

α is the **acoustic attenuation coefficient**;

z is the distance from the **external transducer aperture** to the point of interest;

f_{awf} is the **acoustic working frequency**;

P is the **output power** measured in water.

NOTE 1 **Attenuated output power** is expressed in watts (W).

NOTE 2 In the case of stand-offs the P should represent the **output power** emanating from the stand-off.

3.7
attenuated peak-rarefactional acoustic pressure
$p_{r,\alpha}(z)$
value of the **peak-rarefactional acoustic pressure** after attenuation, on a plane perpendicular to the **beam axis** at a specified distance z from the **external transducer aperture**, and given by

$$p_{r,\alpha}(z) = p_r(z) 10^{(-\alpha z f_{awf}/20\,dB)} \quad (2)$$

where

α is the **acoustic attenuation coefficient**;

z is the distance from the **external transducer aperture** along the **beam axis** to the plane containing the point of interest;

f_{awf} is the **acoustic working frequency**;

$p_r(z)$ is the **peak-rarefactional acoustic pressure** measured in water.

NOTE Attenuated peak-rarefactional acoustic pressure is expressed in pascals (Pa).

3.8
attenuated pulse-intensity integral
***pii*$_\alpha$ (*z*)**
value of the **pulse-intensity integral** after attenuation, on a plane perpendicular to the **beam axis** at a specified distance z from the **external transducer aperture**, and given by

$$pii_\alpha(z) = pii\, 10^{(-\alpha z f_{awf}/10\,dB)} \quad (3)$$

where

α is the **acoustic attenuation coefficient**;

z is the distance from the **external transducer aperture** along the **beam axis** to the plane containing the point of interest;

f_{awf} is the **acoustic working frequency**;

pii is the **pulse-intensity integral** measured in water.

NOTE 1 **Attenuated pulse-intensity integral** is expressed in joules per metre squared, (J m^{-2}).

NOTE 2 For measurement purposes of this standard, pii_α is equivalent to $1/(\rho c)$ times the **attenuated pulse-pressure-squared integral** at depth z, with ρc denoting the characteristic acoustic impedance of pure water.

3.9
attenuated spatial-average temporal-average intensity
$I_{sata,\alpha}(z)$
value of the **spatial-average temporal-average intensity** after attenuation, on a plane perpendicular to the **beam axis** at a specified distance z from the **external transducer aperture**, and given by

$$I_{sata,\alpha}(z) = I_{sata}\, 10^{(-\alpha z f_{awf}/10\,dB)} \quad (4)$$

where

α is the **acoustic attenuation coefficient**;

z is the distance from the **external transducer aperture** along the **beam axis** to the plane containing the point of interest;

f_{awf} is the **acoustic working frequency**;

I_{sata} is the **spatial-average temporal-average intensity**, at a specified distance z measured in water.

NOTE **Attenuated spatial-average temporal-average intensity** is expressed in watts per metre squared, (W m^{-2}).

3.10
attenuated spatial-peak temporal-average intensity
$I_{spta,\alpha}(z)$
value of the **spatial-peak temporal-average intensity** after attenuation, on a plane perpendicular to the **beam axis** at a specified distance z from the **external transducer aperture**, and given by

$$I_{spta,\alpha}(z) = I_{spta}\, 10^{(-\alpha z\, f_{awf}/10dB)} \quad (5)$$

where

α is the **acoustic attenuation coefficient**;

z is the distance from the **external transducer aperture** along the **beam axis** to the plane containing the point of interest;

f_{awf} is the **acoustic working frequency**;

I_{spta} is the **spatial-peak temporal-average intensity**, at a specified distance z measured in water.

NOTE **Attenuated spatial-peak temporal-average intensity** is expressed in watts per metre squared, (W m^{-2}).

3.11
attenuated temporal-average intensity
$I_{ta,\alpha}(z)$
value of the **temporal-average intensity** after attenuation, on a plane perpendicular to the **beam axis** at a specified distance z from the **external transducer aperture**, and given by

$$I_{ta,\alpha}(z) = I_{ta}(z)\, 10^{(-\alpha z\, f_{awf}/10dB)} \quad (6)$$

where

α is the **acoustic attenuation coefficient**;

z is the distance from the **external transducer aperture** along the **beam axis** to the plane containing the point of interest;

f_{awf} is the **acoustic working frequency**;

$I_{ta}(z)$ is the **temporal-average intensity** measured in water.

NOTE **Attenuated temporal-average intensity** is expressed in watts per metre squared, (W m^{-2}).

3.12
beam area
$A_b(z)$
area in a specified plane perpendicular to the **beam axis** consisting of all points at which the **pulse-pressure-squared integral** is greater than a specified fraction of the maximum value of the **pulse-pressure-squared integral** in that plane

NOTE 1 If the position of the plane is not specified, it is the plane passing through the point corresponding to the **spatial-peak temporal-peak acoustic pressure** in the whole acoustic field.

NOTE 2 In a number of cases, the term **pulse-pressure-squared integral** is replaced everywhere in the above definition by any linearly related quantity, e.g.:

a) in the case of a continuous wave signal the term **pulse-pressure-squared integral** is replaced by mean square acoustic pressure as defined in IEC 61689 [4];

b) in cases where signal synchronisation with the scanframe is not available, the term **pulse-pressure-squared integral** may be replaced by **temporal average intensity.**

NOTE 3 Some specified levels are 0,25 and 0,01 for the -6 dB and -20 dB beam areas, respectively.

NOTE 4 Beam area is expressed in metres squared (m^2).

[IEC 62127-1:2007, definition 3.7, modified]

3.13
beam- axis
straight line that passes through the beam centrepoints of two planes perpendicular to the line which connects the point of maximal pulse-pressure-squared integral with the centre of the external transducer aperture

NOTE 1 See Figure 1.

NOTE 2 The location of the first plane is the location of the plane containing the maximum **pulse-pressure-squared integral** or, alternatively, is one containing a single main lobe which is in the focal Fraunhofer zone. The location of the second plane is as far as is practicable from the first plane and parallel to the first with the same two orthogonal scan lines (*x* and *y* axes) used for the first plane.

NOTE 3 In a number of cases, the term **pulse-pressure-squared integral** is replaced in the above definition by any linearly related quantity, e.g.:

a) in the case of a continuous wave signal the term **pulse-pressure-squared integral** is replaced by mean square acoustic pressure as defined in IEC 61689,

b) in cases where signal synchronisation with the scan frame is not available the term **pulse-pressure-squared integral** may be replaced by **temporal average intensity**.

[IEC 62127-1:2007, definition 3.8]

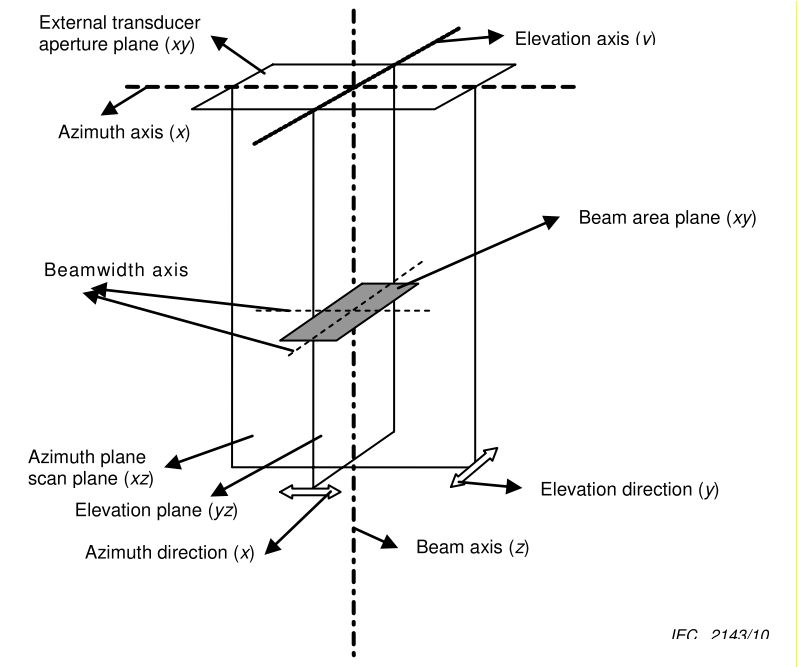

Figure 1 – Schematic diagram of the different planes and lines in an ultrasonic field
(modified from IEC 61828 and IEC 62127-1)

3.14
beam centrepoint

position determined by the 2D centroid of a set of **pulse-pressure-squared integrals** measured over the -6dB beam-area in a specified plane

NOTE Methods for determining 2D centroids are described in Annex B and C of IEC 61828.

3.15
beamwidth midpoint
linear average of the coordinates of the locations midway between each pair of points determining a **beamwidth** in a specified plane

NOTE The average is taken over as many **beamwidth** levels given in B.2 of IEC 61828 as signal level permits.

[IEC 62127-1:2007, definition 3.10, modified]

3.16
beamwidth
w_6, w_{12}, w_{20}
greatest distance between two points on a specified axis perpendicular to the **beam axis** where the **pulse-pressure-squared integral** falls below its maximum on the specified axis by a specified amount

NOTE 1 In a number of cases, the term **pulse-pressure-squared integral** is replaced in the above definition by any linearly related quantity, e.g.:

a) in the case of a continuous wave signal the term **pulse-pressure-squared integral** is replaced by mean square acoustic pressure as defined in IEC 61689 [4],

b) in cases where signal synchronisation with the scan frame is not available the term **pulse-pressure-squared integral** may be replaced by **temporal average intensity**.

NOTE 2 Commonly used **beamwidth**s are specified at –6 dB, –12 dB and –20 dB levels below the maximum. The decibel calculation implies taking 10 times the logarithm to the base of 10 of the ratios of the integrals.

NOTE 3 **Beamwidth** is expressed in metres (m).

[IEC 62127-1:2007, definition 3.11]

3.17
bone thermal index
TIB
thermal index for applications, such as foetal (second and third trimester) ~~or neonatal cephalic (through the fontanelle)~~, in which the ultrasound beam passes through soft tissue and a focal region is in the immediate vicinity of bone

NOTE 1 See 5.4.2 and 5.5.2 for methods of determining the bone thermal index.

NOTE 2 See Annex A for rationale and derivation notes.

3.18
bounded-square output power
P_{1x1}
maximum value of the time average **acoustic output power** emitted from any one-centimetre square region of the active area of the transducer, the one-centimetre square region having 1 cm dimensions in the x- and y-directions

NOTE 1 The side of the 1 cm × 1 cm square should be aligned with the azimuth axis in accordance with Figure 1. See A.4.1.4 and Annex B for more detail.

NOTE 2 **Bounded-square output power** is expressed in watts (W).

3.19
break-point depth
z_{bp}
closest distance, to the solid surface of the transducer or the enclosure of any stand-off path, used during a search to determine below-surface *TIS* and *TIB* **acoustic working frequency** and intensity parameters (such as **attenuated spatial-peak temporal-average intensity**)

$$z_{bp} = 1{,}5 \text{ x } D_{eq} \quad (7)$$

where D_{eq} is the **equivalent aperture diameter** for **non-scanning modes**.

NOTE 1 Specifically, for the **mechanical index**: the search should continue till the depth z_{MI}. Reasonable care should be taken not to go so close to the transducer face as to risk the integrity of the hydrophone or the validity of the measurement.

NOTE 2 For **scanning modes,** ~~D_{eq} is calculated using the **output beam area** of one **ultrasonic scan line**~~ use the **non-scanning mode** D_{eq} value calculation [Equation (8)]. Do this using the **output beam area** of one **ultrasonic scan line**; the central scan line, corresponding to the **beam axis** (i.e. the line where pii, MI, *and* f_{awf} are measured).

NOTE 3 See Annex A for rationale and derivation notes.

NOTE 4 **Breakpoint depth** is expressed in metres (m).

3.20
combined-operating mode
mode of operation of an **equipment** that combines more than one **discrete-operating mode**

[IEC 61157:2007, definition 3.17.1]

3.21
cranial-bone thermal index
TIC
thermal index for applications~~, such as paediatric and adult cranial applications,~~ in which the ultrasound beam passes through bone near the beam entrance into the body, such as paediatric and adult cranial or neonatal cephalic applications

NOTE 1 See 5.4.2.1 and 5.5.2.1 for methods of determining the **cranial bone thermal index**.

NOTE 2 See Annex A for rationale and derivation notes.

3.22
default setting
specific state of control that the ~~**ultrasonic**~~ **medical diagnostic ultrasonic equipment** will enter upon power-up, new **patient** selection or change from non-foetal to foetal applications

3.23
depth for mechanical index
z_{MI}
depth on the **beam axis** from the **external transducer aperture** to the plane of maximum **attenuated** ~~**pulse-intensity integral** (pii_{α})~~ **pulse-pressure-squared-integral** ($ppsi_{\alpha}$)

NOTE 1 Because z_{MI} may occur closer to the transducer than the **break-point depth** z_{bp}, use of $ppsi_{\alpha}$ rather than pii_{α} is technically more appropriate. If $z_{ppsi,\alpha}$ is larger than z_{bp}, then $z_{ppsi,\alpha}$ and $z_{pii,\alpha}$ are equal.

NOTE 2 **Depth for mechanical index** is expressed in metres (m).

3.24
depth for ~~**peak**~~ **maximum pulse**~~-~~ **intensity integral**
~~z_{pii}~~
~~depth on the **beam axis** from the **external transducer aperture** to the plane of maximum **pulse-intensity integral** (pii) as approximated by the **pulse-pressure-squared integral** ($ppsi$)~~

depth z on the **beam axis** and beyond the **break-point depth** z_{bp} from the **external transducer aperture** to the plane of maximum **pulse-intensity integral** (*pii*) as approximated by the **pulse-pressure-squared integral** (*ppsi*)

NOTE 1 **Depth for** ~~**peak pulse-intensity integral**~~ **maximum** ***pii*** is expressed in metres (m).

NOTE 2 **Depth for maximum** ***pii*** is termed "depth for peak pulse-intensity integral" in IEC 60601-2-37:2007/AMD1:2015.

NOTE 3 At this depth the **acoustic working frequency** is determined.

3.25
depth for *TIB*
$z_{b,ns}$ for **non-scanning modes**
for **non-scanning modes**, the distance along the **beam axis** from the **external transducer aperture** to the plane where the product of **attenuated output power** and **attenuated spatial-peak temporal-average intensity** is a maximum over the distance range equal to, or greater than, the **break-point depth**, z_{bp}

NOTE 1 **Depth for *TIB*** is expressed in metres (m).

NOTE 2 See Annex A for rationale and derivation notes.

3.26
depth for *TIS*
$z_{s,ns}$ for **non-scanning modes**
for **non-scanning modes**, the distance along the **beam axis** from the **external transducer aperture** to the plane at which the lower value of the **attenuated output power** and the product of the **attenuated spatial-peak temporal-average intensity** and 1 cm^2 is maximized over the distance range equal to, or greater than, the **break-point depth**, z_{bp}

NOTE 1 In this standard, the restricted definition of **spatial-peak temporal-average intensity** from IEC 62127-1, relating to a specified plane, is used where **spatial-peak temporal-average intensity** is replaced by **attenuated spatial-peak temporal-average intensity**.

NOTE 2 Depth for *TIS* is expressed in metres (m).

NOTE 3 See Annex A for rationale and derivation notes.

3.27
~~**Discrete-perating**~~ **discrete-operating mode**
mode of operation of ~~**ultrasonic**~~ **medical diagnostic ultrasonic equipment** in which the purpose of the excitation of the **ultrasonic transducer** or **ultrasonic transducer** element group is to utilize only one diagnostic methodology

[IEC 61157:2007, definition 3.17.2, modified]

3.28
equivalent aperture diameter
D_{eq}
diameter of a circle ~~whose area is the **output beam area** and~~ the area A of which is the –12 dB **output beam area** A_{ob} for **non-scanning modes** and the –12 dB **scanned aperture area** A_{sa} for **scanning modes**, given by

$$\sout{D_{eq} = \sqrt{\frac{4}{\pi} A_{ob}}} \qquad D_{eq} = \sqrt{\frac{4}{\pi} A} \tag{8}$$

where A_{ob} is the **output beam area**.

NOTE 1 ~~This formula gives the diameter of a circle whose area is the –12 dB **output beam area**. It is used in the calculation of the **cranial-bone thermal index** and the **soft tissue thermal index.**~~ Equation (8) is used in the calculation of the **cranial-bone thermal index**; for **non-scanning modes** with $A = A_{ob}$ and for **scanning modes** with $A = A_{sa}$.

NOTE 2 Equation (8) with $A = A_{ob}$ is also used in calculating the **break-point depth**.

NOTE ~~2~~ 3 **Equivalent aperture diameter** is expressed in metres (m).

3.29
equivalent beam area
$A_{eq}(z)$
area of the acoustic beam at the distance z in terms of power and intensity and given by

$$A_{eq}(z) = \frac{P_{\alpha}(z)}{I_{spta,\alpha}(z)} = \frac{P}{I_{spta}} \quad (9)$$

where

$P_{\alpha}(z)$ is the **attenuated output power**, at the distance z;

$I_{spta,\alpha}(z)$ is the **attenuated spatial-peak temporal-average intensity**, at the distance z;

P is the **output power**;

I_{spta} is the **spatial-peak temporal-average intensity**, at the distance z; and

z is the distance from the **external transducer aperture** to the specified point.

NOTE **Equivalent beam area** is expressed in metres squared (m^2).

3.30
equivalent beam diameter
$d_{eq}(z)$
diameter of the acoustic beam at the distance z in terms of the **equivalent beam area** and given by

$$d_{eq}(z) = \sqrt{\frac{4}{\pi} A_{eq}(z)} \quad (10)$$

where

$A_{eq}(z)$ is the **equivalent beam area**;

z is the distance from the **external transducer aperture** to the specified point.

NOTE **Equivalent beam diameter** is expressed in metres (m).

3.31
external transducer aperture
part of the surface of the **ultrasonic transducer** or **ultrasonic transducer** element group assembly that emits ultrasonic radiation into the propagation medium

NOTE 1 This surface is assumed to be either directly in contact with the patient or in contact with a water or liquid path to the patient. See Figure 1.

NOTE 2 The **ultrasonic transducer** element group is usually offset from this surface by a lens, matching layers and possibly fluid.

[IEC 62127-1:2007, definition 3.27, modified]

3.32
mechanical index
MI
mechanical index is given by

$$MI = \frac{p_{r,\alpha}(z_{MI})\, f_{awf}^{-1/2}}{C_{MI}} \quad (11)$$

where

C_{MI} = 1 MPa·MHz$^{-1/2}$

$p_{r,a}(z_{MI})$ is the **attenuated peak-rarefactional acoustic pressure** at the depth z_{MI}

f_{awf} is the **acoustic-working frequency**.

NOTE 1 See Annex A for rationale and derivation notes.

3.33
medical diagnostic ultrasonic equipment (or **system**)
combination of the **ultrasound instrument console** and the **transducer assembly** making up a complete diagnostic system

[IEC 61157:2007, definition 3.15]

NOTE 1 For the purpose of this standard, **medical diagnostic ultrasonic equipment (or system)** means **electrical equipment** that is intended for *in vivo* ultrasonic examination and monitoring for obtaining a medical diagnosis.

NOTE 2 IEC 60601-2-37:2007 uses the term "ultrasonic diagnostic equipment" instead of **medical diagnostic ultrasonic equipment**.

3.34
non-scanning mode
mode of operation of ~~**ultrasonic**~~ **medical diagnostic ultrasonic equipment** that involves a sequence of ultrasonic pulses which give rise to **ultrasonic scan lines** that follow the same acoustic path

[IEC 62127-1:2007, definition 3.39.4, modified]

3.35
output beam area
A_{ob}
area of the ultrasonic beam derived from the -12 dB **beam area** at the **external transducer aperture**

NOTE 1 For reasons of measurement accuracy, the –12 dB **output beam area** may be derived from measurements at a distance chosen to be as close as possible to the face of the transducer, and, if possible, no more than 1 mm from the face.

NOTE 2 For contact transducers, this area can be taken as the geometrical area of the **ultrasonic transducer** or **ultrasonic transducer** element group.

NOTE 3 The **output beam area** is expressed in metres squared (m^2).

NOTE 4 Methodology for finding the beam area using the **pulse-pressure-squared integral** for focused fields is described in clauses 6.2 and 6.3 of IEC 61828.

[IEC 62127-1:2007, definition 3.40]

3.36
output beam dimensions
X_{ob} , Y_{ob}
dimensions of the ultrasonic beam (–12 dB **beamwidth**) in specified directions perpendicular to each other and in a direction normal to the **beam axis** and at the **external transducer aperture**

NOTE 1 For reasons of measurement accuracy, the –12 dB **output beam dimensions** may be derived from measurements at a distance chosen to be as close as possible to the face of the transducer and, if possible, no more than 1 mm from the face.

NOTE 2 For contact transducers, these dimensions can be taken as the geometrical dimensions of the **ultrasonic transducer** or **ultrasonic transducer** element group.

NOTE 3 **Output beam dimensions** are expressed in metres (m).

NOTE 4 Methodology for finding the beam area using the **pulse-pressure-squared integral** for focused fields is described in 6.2 and 6.3 of IEC 61828.

[IEC 62127-1:2007, definition 3.41, modified]

3.37
output power
P
time-average ultrasonic power emitted by an **ultrasonic transducer** into an approximately free field under specified conditions in a specified medium, preferably water

[IEC 61161:~~2006~~ 2013, definition 3.3]

NOTE 1 "time-average" means averaged over an integral multiple of the temporal periodicity.

NOTE 2 **Output power** is expressed in watts (W).

3.38
peak-rarefactional acoustic pressure
p_r
maximum of the modulus of the negative **instantaneous acoustic pressure** in an acoustic field or in a specified plane during an **acoustic repetition period**

NOTE 1 **Peak-rarefactional acoustic pressure** is expressed as a positive number.

NOTE 2 **Peak-rarefactional acoustic pressure** is expressed in pascals (Pa).

NOTE 3 The definition of **peak-rarefactional acoustic pressure** also applies to peak-negative acoustic pressure which is also in use in literature.

[IEC 62127-1:2007, definition 3.44]

3.39
power parameter
P_p
beam-related power quantity used in the numerator of the general **thermal index** relationship

NOTE 1 See Equation A.4

NOTE 2 The meaning of this quantity depends on the TI to be evaluated, see A.5.1 and A.5.2. In general terms, it will be the measured quantity responsible for the estimation of the specific temperature rise.

NOTE 3 **Power parameter** is expressed in watts (W).

3.40
prudent-use statements
affirmations of the principle~~ advising avoidance of primarily high exposure levels and secondarily long exposure times while acquiring necessary clinical information~~ that only necessary clinical information should be acquired and that high exposure levels and long exposure times should be avoided

NOTE See Bibliography [5,6,7,8].

3.41
pulse duration
t_d
1,25 times the interval between the time when the time integral of the square of the **instantaneous acoustic pressure** reaches 10 % and 90 % of its final value

NOTE 1 The final value of the time integral of the square of the **instantaneous acoustic pressure** is the **pulse-pressure-squared integral**.

NOTE 2 **Pulse duration** is expressed in seconds (s).

NOTE 3 See Figure 2 of IEC 62127-1.

[IEC 62127-1:2007, definition 3.48]

3.42
pulse-intensity integral
pii
time integral of the **instantaneous intensity** at a particular point in an acoustic field integrated over the **acoustic pulse waveform**

NOTE 1 For measurement purposes referred to in this International Standard, **pulse-intensity integral** is proportional to **pulse-pressure-squared integral**.

NOTE 2 The **pulse-intensity integral** is expressed in joules per metre squared (Jm^{-2}).

[IEC 62127-1:2007, definition 3.49]

3.43
pulse-pressure-squared integral
ppsi
time integral of the square of the **instantaneous acoustic pressure** at a particular point in an acoustic field integrated over the **acoustic pulse waveform**

NOTE The **pulse-pressure-squared integral** is expressed in pascal squared seconds (Pa^2s).

[IEC 62127-1:2007, definition 3.50]

3.44
pulse repetition period
prp
time interval between equivalent points on successive pulses or tone-bursts

NOTE 1 In general, for **non-scanning modes** the **pulse repetition period** needs to be adjusted to represent a 'per-second' average taking into account interruptions-in, or non-constant, pulsing; e.g. such as may occur in **combined operating modes**.

NOTE 2 The **pulse repetition period** is expressed in seconds (s).

[IEC 62127-1:2007, definition 3.51]

3.45
pulse repetition rate
prr
reciprocal of the **pulse repetition period**

NOTE The **pulse repetition rate** is expressed in hertz (Hz).

[IEC 62127-1:2007, definition 3.52]

3.46
scanned aperture area
A_{sa}
area at the **external transducer aperture** consisting of all points at which the **pulse-pressure-squared integral** is greater than -12 dB of the maximum value of the **pulse-pressure-squared integral** in that plane

NOTE 1 For reasons of measurement accuracy, the –12 dB **scanned aperture area** may be derived from measurements at a distance chosen to be as close as possible to the face of the transducer, and, if possible, no more than 1 mm from the face.

NOTE 2 For contact transducers, this area can be taken as the geometrical area of the active elements during one frame scan of the **ultrasonic transducer** or **ultrasonic transducer** element group.

NOTE 3 In a number of cases, the term **pulse-pressure-squared integral** is replaced everywhere in the above definition by any linearly related quantity, e.g.:

a) in the case of a continuous wave signal the term **pulse-pressure-squared integral** is replaced by mean square acoustic pressure as defined in IEC 61689,

b) in cases where signal synchronisation with the scanframe is not available the term **pulse-pressure-squared integral** may be replaced by **temporal average intensity**.

NOTE 4 **Scanned aperture area** is expressed in metres squared (m^2).

3.47
scan direction
for **systems** with scanning modes, the direction in the **scan plane** and perpendicular to a specified **ultrasonic scan line**

NOTE During one acquisition frame the scan direction may be azimuthal (x) and/or elevational (y) and may include combinations, e.g., polar.

[IEC 61157: 2007, definition 3.27]

3.48
scan plane
for automatic scanning systems, a plane containing all the **ultrasonic scan lines**

NOTE 1 See Figure 1.

NOTE 2 Some scanning systems have the ability to steer the ultrasound beam in two directions. In this case, there is no **scan plane** that meets this definition. However, it might be useful to consider a plane through the major-axis of symmetry of the **ultrasound transducer** and perpendicular to the transducer face (or another suitable plane) as being equivalent to the scan plane.

[IEC 62127-1:2007, definition 3.56]

3.49
scanning mode
mode of operation of ~~an **ultrasonic**~~ **a medical diagnostic ultrasonic equipment** that involves a sequence of ultrasonic pulses which give rise to scan lines that do not follow the same acoustic path

[IEC 61157:2007, definition 3.17.5]

3.50
scan repetition period
srp
time interval between identical points on two successive frames, sectors or scans, applying to automatic scanning systems with a periodic scan sequence only

NOTE 1 In general, this International Standard assumes that an individual **ultrasonic scan line** repeats exactly after a number of acoustic pulses.

NOTE 2 The scan repetition period is expressed in seconds (s).

3.51
scanwidth
w_s
greatest distance between two points on the axis in the **scan plane** perpendicular to the central **ultrasonic scan line** where the **temporal average intensity** falls below its maximum in the **scan plane** by 12 dB at the distance of interest from the transducer surface

NOTE 1 This dimension may be determined by hydrophone measurements or by calculation using knowledge of the dimensions of the transducer aperture and scanning geometry.

NOTE 2 **Scanwidth** is expressed in metres (m).

3.52
soft tissue thermal index
TIS
thermal index related to soft tissues

NOTE 1 See 5.4.1 and the following sub-clauses and 5.5.1 for methods of determining the **soft tissue thermal index.**

NOTE 2 For the purposes of this document, soft tissue includes all body tissues and fluids except skeletal tissues.

NOTE 3 See Annex A for rationale and derivation notes.

3.53
spatial-average temporal-average intensity
I_{sata}
equal to the **temporal-average intensity** averaged over the **scan-area, beam area** or other defined area as appropriate

NOTE **Spatial-average temporal-average intensity** is expressed in watts per metre squared (Wm^{-2}).

[IEC 62127-1:2007, definition 3.59 slightly modified]

3.54
spatial-peak temporal-average intensity
I_{spta}
maximum value of the **temporal-average intensity** in an acoustic field or in a specified plane

NOTE 1 For systems in **combined-operating mode**, ~~the time interval over which the temporal average is taken is sufficient to include any period during which scanning may not be taking place~~ the averaging time period needs to be sufficient to include periods in which scanning or pulsing is interrupted.

NOTE 2 **Spatial-peak temporal-average intensity** is expressed in watts per metre squared (Wm^{-2}).

[IEC 62127-1:2007, definition 3.62]

3.55
temporal-average intensity
I_{ta}
time-average of the **instantaneous intensity** at a particular point in an acoustic field

NOTE 1 The time-average is taken normally over an integral number of **acoustic repetition periods**; if not, the period for averaging should be specified.

NOTE 2 **Temporal-average intensity** is expressed in watts per metre squared (Wm^{-2}).

[IEC 62127-1:2007, definition 3.65]

3.56
thermal index
TI
ratio of **attenuated** ~~**acoustic**~~ **output power** at a specified point to the **attenuated** ~~**acoustic**~~ **output power** required to raise the temperature at that point in a specific tissue model by 1 °C

NOTE See Annex A for rationale and derivation notes.

3.57
transducer assembly
those parts of **medical diagnostic ultrasonic equipment** comprising the **ultrasonic transducer** and/or **ultrasonic transducer** element group, together with any integral components, such as an acoustic lens or integral stand-off

NOTE The **transducer assembly** is usually separable from the ultrasound instrument console.

[IEC 62127-1:2007, definition 3.69]

3.58
transmit pattern
combination of a specific set of transducer beam-forming characteristics (determined by the transmit aperture size, apodization shape and relative timing/phase delay pattern across the

aperture, resulting in a specific focal length and direction) and an electrical drive waveform of a specific fixed shape but variable amplitude

3.59
ultrasonic scan line
for scanning systems, the **beam axis** for a particular **ultrasonic transducer** element group, or for a particular excitation of an **ultrasonic transducer** or **ultrasonic transducer** element group

NOTE 1 Here an **ultrasonic scan line** refers to the path of acoustic pulses and not to a line on an image on the display screen of a system.

NOTE 2 The case where a single excitation produces ultrasonic beams propagating along more than one **beam axis** is not considered.

[IEC 62127-1:2007, definition 3.71, modified]

3.60
ultrasonic transducer
device capable of converting electrical energy to mechanical energy within the ultrasonic frequency range and/or reciprocally of converting mechanical energy to electrical energy

[IEC 62127-1:2007, definition 3.73]

3.61
instantaneous acoustic pressure
$p(t)$
pressure minus the ambient pressure at a particular instant in time and at a particular point in an acoustic field

NOTE **Instantaneous acoustic pressure** is expressed in pascals (Pa).

[SOURCE: IEC 62127-1:2007, 3.33, modified – The reference to IEV 801-01-19 has been removed in the definition]

3.62
attenuated instantaneous acoustic pressure
$p_\alpha(z,t)$
value of the **instantaneous acoustic pressure** at time t after attenuation on a plane perpendicular to the **beam axis** at a specified distance z from the source, and given by

$$p_\alpha(z,t) = p(z,t)10^{(-\alpha\, z\, f_{\text{awf}}/20\ \text{dB})} \tag{26}$$

where

α is the **acoustic attenuation coefficient**;

z is the distance from the source to the point (plane) of interest;

f_{awf} is the **acoustic working frequency**;

$p(z,t)$ is the **instantaneous acoustic pressure**

NOTE **Attenuated instantaneous acoustic pressure** is expressed in pascals (Pa).

3.63
attenuated pulse-pressure-squared integral
$ppsi_\alpha(z)$
time integral of the square of the **attenuated instantaneous acoustic pressure**, integrated over the acoustic pulse waveform, on a plane perpendicular to the **beam axis** at a specified distance z in an acoustic field

$$ppsi_{\alpha}(z) = \int p_{\alpha}^{2}(z,t)dt = \int \left[p(z,t)10^{(-\alpha\, z\, f_{\text{awf}}/20\ \text{dB})}\right]^{2} dt = ppsi(z) \times 10^{(-\alpha\, z\, f_{\text{awf}}/10\ \text{dB})} \quad (27)$$

where

$p(z,t)$ is the **instantaneous acoustic pressure** at depth z.

α is the **acoustic attenuation coefficient**;

z is the distance from the source to the point (plane) of interest;

f_{awf} is the **acoustic working frequency**;

$ppsi$ is the **pulse-pressure-squared integral**

NOTE 1 **Attenuated pulse-pressure-squared integral** is expressed in pascal squared seconds (Pa^2s).

NOTE 2 See definition 3.43 for the non-attenuated version; with the addition here of the perpendicular plane at depth z.

3.64
attenuated scan intensity integral
$sii_{\alpha}(z)$

sum of the **attenuated pulse intensity integrals** in one scan (one frame of **ultrasonic scan lines**) at depth z

NOTE 1 **Attenuated scan intensity integral** is expressed in joules per square metre (Jm^{-2}).

NOTE 2 For measurement purposes of this standard, $sii_{\alpha}(z)$ is equivalent to $1/(\rho c)$ times the **sum of attenuated pulse-pressure-squared integrals** at depth z, for $z \geq z_{\text{bp}}$, with ρc denoting the characteristic acoustic impedance of pure water.

NOTE 3 See definition 3.79 for the non-attenuated version.

3.65
attenuated spatial-peak pulse-average intensity
$I_{\text{sppa},\alpha}(z)$

maximum value of the **spatial-peak pulse-average intensity** after attenuation, on a plane perpendicular to the **beam axis** at a specified distance z from the source, and given by

$$I_{\text{sppa},\alpha}(z) = \frac{1}{t_{\text{d}}(z)}\, pii_{\alpha}(z) \quad (28)$$

where

$t_{\text{d}}(z)$ is the **pulse duration** at the same depth z;

$pii_{\alpha}(z)$ is the **attenuated pulse-intensity integral** at depth z

NOTE 1 **Attenuated spatial-peak pulse-average intensity** is expressed in watts per square metre (Wm^{-2}).

NOTE 2 For measurement purposes of this standard, $pii_{\alpha}(z)$ is equivalent to $1/(\rho c)$ times the **attenuated pulse-pressure-squared integrals** at depth z, $ppsi_{\alpha}(z)$, for $z \geq z_{\text{bp}}$, with ρc denoting the characteristic acoustic impedance of pure water.

NOTE 3 See definition 3.81 for the non-attenuated version.

3.66
attenuated sum of pulse-pressure-squared integrals
$s_{\alpha}ppsi\,(z)$

attenuated value of the sum of **pulse-pressure-squared integrals** in one scan (one frame of **ultrasonic scan lines)** at depth z

NOTE 1 **Attenuated sum of pulse-pressure-squared integrals** is expressed in pascal squared seconds (Pa^2s).

NOTE 2 The **attenuated sum of pulse-pressure-squared integrals** at depth z will be equal to the **sum of attenuated pulse-pressure-squared integrals** if each **ultrasonic scan line** in the frame which is included in the sum has the same **acoustic working frequency**.

NOTE 3 See F.3.1.4.2 for additional explanation.

NOTE 4 See definition 3.83 for the non-attenuated version.

3.67
depth for maximum I_{sppa}

$z_{sppa,max}$
depth z on the **beam axis** and beyond the **break-point depth** z_{bp} of maximum **spatial-peak pulse-average intensity**

NOTE 1 **Depth for maximum I_{sppa}** is expressed in metres (m).

NOTE 2 This depth is equivalent to the **depth for maximum pii**.

3.68
depth for maximum $I_{sppa,\alpha}$

$z_{sppa,\alpha,max}$
depth z on the **beam axis** and beyond the **break-point depth** z_{bp} of maximum **attenuated spatial-peak pulse-average intensity**

NOTE 1 **Depth for maximum $I_{sppa,\alpha}$** is expressed in metres (m).

NOTE 2 This depth is equivalent to the **depth for maximum pii_{α}**.

3.69
depth for maximum I_{spta}

$z_{spta,max}$
depth z on the **beam axis** and beyond the **break-point depth** z_{bp} of maximum **spatial-peak temporal-average intensity**

NOTE 1 **Depth for maximum I_{spta}** is expressed in metres (m).

NOTE 2 For **non-scanning modes**, this depth is equivalent to the **depth for maximum pii**. For **scanning modes**, it is equivalent to the **depth for maximum sii**.

3.70
depth for maximum $I_{spta,\alpha}$

$z_{spta,\alpha,max}$
depth z on the **beam axis** and beyond the **break-point depth** z_{bp} of maximum **attenuated spatial-peak temporal-average intensity**

NOTE 1 **Depth for maximum $I_{spta,\alpha}$** is expressed in metres (m).

NOTE 2 For **non-scanning modes**, this depth is equivalent to the **depth for maximum pii_{α}**. For **scanning modes**, it is equivalent to the **depth for maximum sii_{α}**.

3.71
depth for maximum pii_{α}

$z_{pii,\alpha}$
depth z on the **beam axis** and beyond the **break-point depth** z_{bp} of maximum **attenuated pulse-intensity integral**

NOTE 1 **Depth for maximum pii_{α}** is expressed in metres (m).

NOTE 2 This depth is equivalent to the **depth for maximum $ppsi_{\alpha}$**, $z_{ppsi,\alpha}$, when $z_{ppsi,\alpha}$ occurs beyond the **break-point depth** (see 3.73).

NOTE 3 **Depth for maximum pii_{α}** is termed "depth for peak attenuated pulse-intensity integral" in IEC 60601-2-37:2007+IEC 60601-2-37:2007/AMD1:2015.

3.72
depth for maximum $ppsi$

z_{ppsi}
depth z on the **beam axis** of maximum **pulse-pressure-squared integral**

NOTE 1 **Depth for maximum** ***ppsi*** is expressed in metres (m).

NOTE 2 When it occurs beyond the **break-point depth**, this depth is equivalent to the **depth for maximum** ***pii***, z_{pii} (see 3.24).

3.73
depth for maximum $ppsi_\alpha$

$z_{ppsi,\alpha}$
depth z on the **beam axis** of maximum **attenuated pulse-pressure-squared integral**

NOTE 1 **Depth for maximum** $ppsi_\alpha$ is expressed in metres (m).

NOTE 2 When it occurs beyond the **break-point depth**, this depth is equivalent to the **depth for maximum** pii_α, $z_{pii,\alpha}$ (i.e. depth for maximum **attenuated pulse-intensity integral**).

NOTE 3 This depth is the **depth for mechanical index**, z_{MI} (see 3.23).

3.74
depth for maximum *sii*

z_{sii}
depth z on the **beam axis** and beyond the **break-point depth** z_{bp} of maximum **scan-intensity integral**

NOTE 1 **Depth for maximum** ***sii*** is expressed in metres (m).

NOTE 2 This depth is equivalent to the **depth for maximum** ***sppsi,*** z_{sppsi}, when z_{sppsi} occurs beyond the **break-point depth** (see 3.76).

NOTE 3 **Depth for maximum** ***sii*** is termed "depth for peak sum of pulse-intensity integrals" in IEC 60601-2-37:2007+IEC 60601-2-37:2007/AMD1:2015.

3.75
depth for maximum sii_α

$z_{sii,\alpha}$
depth z on the **beam axis** and beyond the **break-point depth** z_{bp} of maximum **attenuated scan-intensity integral**

NOTE 1 **Depth for maximum** sii_α is expressed in metres (m).

NOTE 2 This depth is equivalent to the **depth for maximum** ***sppsi*****$_\alpha$**, $z_{sppsi,\alpha}$, when $z_{sppsi,\alpha}$ occurs beyond the **break-point depth** (see 3.77).

NOTE 3 **Depth for maximum** sii_α is termed "depth for peak sum of attenuated pulse-intensity integrals" in IEC 60601-2-37:2007+IEC 60601-2-37:2007/AMD1:2015.

3.76
depth for maximum *sppsi*

z_{sppsi}
depth z on the **beam axis** of maximum **sum of pulse-pressure-squared integrals**

NOTE 1 **Depth for maximum** ***sppsi*** is expressed in metres (m).

NOTE 2 When it occurs beyond the **break-point depth**, this depth is equivalent to the **depth for maximum** ***sii***, z_{sii} (see 3.74).

NOTE 3 **Depth for maximum** ***sppsi*** is termed "depth for peak sum of pulse-intensity integrals" in IEC 60601-2-37:2007+IEC 60601-2-37:2007/AMD1:2015.

3.77
depth for maximum $sppsi_\alpha$

$z_{sppsi,\alpha}$
depth z on the **beam axis** of maximum **sum of attenuated pulse-pressure-squared integrals**

NOTE 1 **Depth for maximum** $sppsi_\alpha$ is expressed in metres (m).

NOTE 2 When it occurs beyond the **break-point depth**, this depth is equivalent to the **depth for maximum** sii_α, $z_{sii,\alpha}$ (see 3.75).

NOTE 3 **Depth for maximum** $sppsi_\alpha$ is termed "depth for peak sum of attenuated pulse-intensity integrals" in IEC 60601-2-37:2007+IEC 60601-2-37:2007/AMD1:2015.

3.78
pulse-average intensity
I_{pa}

quotient of the **pulse-intensity integral** to the **pulse duration** at a particular point in an acoustic field

NOTE 1 This definition applies to pulses and bursts.

NOTE 2 **Pulse-average intensity** is expressed in watts per square metre (Wm^{-2}).

[IEC 62127-1:2007+IEC 62127-1:2007/AMD1:2013, 3.47]

3.79
scan intensity integral
sii

sum of the **pulse intensity integrals** in one scan (one frame of **ultrasonic scan lines**) at depth z in the acoustic field

NOTE 1 **Scan intensity integral** is expressed in joules per square metre (Jm^{-2}).

NOTE 2 For measurement purposes of this standard, sii is equivalent to $1/(\rho c)$ times the **sum of pulse-pressure-squared integral** at depth z where ρc is the characteristic acoustic impedance of pure water.

3.80
scan repetition rate
srr

inverse of the **scan repetition period** (see 3.50)

NOTE **Scan repetition rate** is expressed in hertz (Hz).

3.81
spatial-peak pulse-average intensity
$I_{sppa}(z)$

maximum value of the **pulse-average intensity** on a plane perpendicular to the **beam axis** at a specified distance z from the source, and given by

$$I_{sppa}(z) = \frac{1}{t_d(z)}\, pii(z) \tag{29}$$

where

$t_d(z)$ is the **pulse duration** at the same depth z;

$pii(z)$ is the **pulse-intensity integral** at depth z

NOTE 1 **Spatial-peak pulse-average intensity** is expressed in watts per square metre (Wm^{-2}).

NOTE 2 For measurement purposes of this standard, $pii(z)$ is equivalent to $1/(\rho c)$ times the **pulse-pressure-squared integral** at depth z, $ppsi(z)$, for $z \geq z_{bp}$, with ρc denoting the characteristic acoustic impedance of pure water.

NOTE 3 See IEC 62127-1:2007, 3.60, which has been modified to specify the perpendicular plane at depth z. Equation (29) and Note 2 have been added, in accordance with IEC 62127-1:2007, Equation (15).

3.82
sum of attenuated pulse-pressure-squared integrals
$sppsi_{\alpha}(z)$
sum of the **attenuated pulse-pressure-squared integrals** in one scan (one frame of **ultrasonic scan lines**) at depth z

NOTE 1 **Sum of attenuated pulse-pressure-squared integrals** is expressed in pascal squared seconds (Pa^2s).

NOTE 2 Closely related to the **attenuated scan intensity integral**, see 3.64.

NOTE 3 The **sum of attenuated pulse-pressure-squared integrals** at depth z will be equal to the **attenuated sum of pulse-pressure-squared integrals** at depth z if each **ultrasonic scan line** in the frame which is included in the sum has the same **acoustic working frequency**.

3.83
sum of pulse-pressure-squared integrals
$sppsi(z)$
sum of **pulse-pressure-squared integrals** in one scan (one frame of **ultrasonic scan lines**) at depth z

NOTE 1 **Sum of pulse-pressure-squared integrals** is expressed in pascal squared seconds (Pa^2s).

NOTE 2 The $sppsi$ at depth z may also be referred to as the scan pulse pressure squared integral and is proportional to the **scan intensity integral** for $z \geq z_{bp}$.

4 List of symbols

α	**acoustic attenuation coefficient**
$A_b(z)$	**beam area**
$A_{eq}(z)$	**equivalent beam area**
A_{ob}	**output beam area**
A_{sa}	scanned aperture area
arp	**acoustic repetition period**
C_{MI}	normalizing coefficient
$C_{TIS,1}$	normalizing coefficient
$C_{TIS,2}$	normalizing coefficient
$C_{TIB,1}$	normalizing coefficient
$C_{TIB,2}$	normalizing coefficient
C_{TIC}	normalizing coefficient
C_K	normalizing coefficient
C_{sb}	normalizing coefficient
d_6	–6 dB beam diameter
D_{eq}	**equivalent aperture diameter**
$d_{eq}(z)$	**equivalent beam diameter**
f_{awf}	**acoustic working frequency**
I_{ta}	**temporal-average intensity**
$I_{ta,\alpha}(z)$	**attenuated temporal-average intensity**
I_{sata}	**spatial-average temporal-average intensity**
$I_{sata,\alpha}(z)$	attenuated spatial-average temporal-average intensity
I_{sppa}	**spatial-peak pulse-average intensity**
$I_{sppa,\alpha}$	**attenuated spatial-peak pulse-average intensity**
I_{spta}	**spatial-peak temporal-average intensity**

$I_{spta,\alpha^{(z)}}$	**attenuated spatial-peak temporal-average intensity**
I_{ta}	**temporal-average intensity**
K	thermal conductivity
MI	**mechanical index**
μ_0	**acoustic absorption coefficient**
P	**output power**
$P_{\alpha^{(z)}}$	**attenuated output power**
P_{1x1}	**bounded-square output power**
$P_{1x1,\alpha^{(z)}}$	**attenuated bounded-square output power**
pii	**pulse-intensity integral**
$pii_{\alpha^{(z)}}$	**attenuated pulse-intensity integral**
P_p	**power parameter**
$ppsi_\alpha$	**attenuated pulse-pressure-squared integral**
$ppsi(z)$	**pulse-pressure-squared integral**
p_r	**peak-rarefactional acoustic pressure**
$p_{r,\alpha^{(z)}}$	**attenuated peak-rarefactional acoustic pressure**
prp	**pulse repetition period**
prr	**pulse repetition rate**
sii	**scan intensity integral**
sii_α	**attenuated scan intensity integral**
$sppsi$	**sum of pulse-pressure-squared integrals**
$s_\alpha ppsi$	**attenuated sum of pulse-pressure-squared integrals**
$sppsi_\alpha$	**sum of attenuated pulse-pressure-squared integrals**
srp	**scan repetition period**
srr	**scan repetition rate**
TI	**thermal index**
TIB	**bone thermal index**
~~$TIB_{as,sc}$~~ TIC_{sc}	**bone thermal index** at-surface, scanning
~~$TIB_{as,ns}$~~ TIC_{ns}	**bone thermal index** at surface, non-scanning
$TIB_{bs,sc}$	**bone thermal index** below surface, scanning
$TIB_{bs,ns}$	**bone thermal index** below surface, non-scanning
TIC	**cranial-bone thermal index**
TIS	**soft tissue thermal index**
$TIS_{as,sc}$	**soft tissue thermal index** at-surface, scanning
$TIS_{as,ns}$	**soft tissue thermal index** at surface, non-scanning
$TIS_{bs,sc}$	**soft tissue thermal index** below surface, scanning
$TIS_{bs,ns}$	**soft tissue thermal index** below surface, non-scanning
t_d	**pulse duration**
w_6, w_{12}, w_{20}	**beamwidth**
X_{ob} , Y_{ob}	**output beam dimensions**
z	distance from the **external transducer aperture** to a specified point
$z_{b,ns}$	**depth for *TIB*** below surface for non- scanned modes
z_{bp}	**break-point depth**

z_{pii}	**depth for ~~peak pulse-intensity integral~~ maximum** pii
$z_{pii,\alpha}$	**depth for maximum** pii_{α}
z_{ppsi}	**depth for maximum** $ppsi$
$z_{ppsi,\alpha}$	**depth for maximum** $ppsi_{\alpha}$
z_{MI}	**depth for** MI
z_{sii}	**depth for maximum** sii
$z_{sii,\alpha}$	**depth for maximum** sii_{α}
$z_{s,ns}$	**depth for** TIS below surface for non- scanned modes
$z_{sppa,max}$	**depth for maximum** I_{sppa}
$z_{sppa,\alpha,max}$	**depth for maximum** $I_{sppa,\alpha}$
$z_{spta,max}$	**depth for maximum** I_{spta}
$z_{spta,\alpha,max}$	**depth for maximum** $I_{spta,\alpha}$
z_{sppsi}	**depth for maximum** $sppsi$
$z_{sppsi,\alpha}$	**depth for maximum** $sppsi_{\alpha}$

5 Test methods for determining the mechanical index and the thermal index

5.1 General

This clause defines methods for determining an exposure parameter relating to temperature rise in theoretical tissue-equivalent models, and also an exposure parameter for non-thermal effects. These exposure parameters, referred to as indices, are related to the safe use of ~~ultrasonic~~ **medical diagnostic ultrasonic equipment**. The indices are intended to be used in IEC 60601-2-37.

These indices shall be determined in accordance with 5.2 to 5.5 for a particular ultrasonic field configuration generated by a **discrete-operating mode** of specific ~~ultrasonic~~ **medical diagnostic ultrasonic equipment**. For **combined-operating modes**, the procedures specified in 5.6 shall be used. Background material is given in Annex A. “Rationale and derivation”.

Acoustic output measurements shall be undertaken using test methods based on the use of hydrophones in accordance with IEC 62127-1 or the use of radiation force balances for power measurements in accordance with IEC 61161. All such measurements shall be made in water (see also Annex B). The measurement uncertainty is to be determined by following [9].

In all cases where **bounded-square output power** is determined, the location of the bounding mask or equivalent means (see Annex B) shall be such as to determine the largest value.

The value of the **acoustic attenuation coefficient** shall be 0,3 dB cm^{-1} MHz^{-1}. This value is selected as an appropriate attenuating coefficient for a homogeneous model intended to be equivalent to the attenuation in reasonable worst-case conditions of clinical use.

The **output beam area** may be determined by using a line scanning or a raster-scanning hydrophone. If the output beam area is expected to be circular it may be sufficient to measure the w_{20} **beamwidth** along the x and y axes. If the **beamwidth**s are equal within 5 %, then also measure the diagonal widths of the aperture at ± 45° to the x axis. If the diagonal widths are also within 5 %, then the symmetry is circular for present purposes. If the diagonal widths differ by more than 5 % compared to the x or y widths, the symmetry is not circular and measurements may be performed by raster scanning, but not line scanning. See IEC 61828 for more.

NOTE 1 Temperature rise in tissue due to transducer surface self-heating has not been taken into account in the determination of the **thermal index** [10]. See Annex C.

NOTE 2 The attenuation model used is not always applicable. Recent literature suggests that sometimes other models should be used [11]. See Annex D for more discussion.

NOTE 3 See Annex D for more discussion of 'reasonable worst case'.

NOTE 4 Basic SI units have been specified in Clause 3. The expressions in the following clauses and annexes were formulated using, e.g. centimetres (cm), milliwatts (mW), and megahertz (MHz)

5.2 Determination of mechanical index

5.2.1 Determination of attenuated peak-rarefactional acoustic pressure

The calculation of **mechanical index** requires determination of the value of the **attenuated peak-rarefactional acoustic pressure** at the location of the maximum **attenuated pulse-intensity integral** ($z_{pii,\alpha}$). This location should be determined according to the procedures set out in IEC 62127-1 for the location of peak **pulse-pressure-squared integral**, with the addition that for all measurement locations an **acoustic attenuation coefficient** shall be applied to the **pulse-pressure-squared integral.**

5.2.2 Calculation of mechanical index

The **mechanical index** shall be calculated, at depth z_{MI}, from the expression as defined under 3.32:

$$MI = \frac{p_{\mathrm{r},\alpha} \cdot f_{\mathrm{awf}}^{-1/2}}{C_{MI}} \qquad (11)$$

where

C_{MI} = 1 MPa MHz$^{-1/2}$

$p_{\mathrm{r},\alpha}(z_{MI})$ is the **attenuated peak-rarefactional acoustic pressure** at the depth z_{MI}

f_{awf} is the **acoustic-working frequency**.

5.3 Determination of thermal index – general

The method of determination of the **thermal index** depends on the tissue model being assumed (*TIS*, *TIB* or *TIC* tissue model) and, for the *TIS* and *TIB* models, it requires the calculation of 'at surface' and 'below surface' values and taking the larger. For **combined-operating modes**, 'at surface' and 'below surface' contributions from **scanning modes** and **non-scanning modes** are calculated and summed, the displayed *TI* being the larger sum.

The determination methods for these 'at surface', 'below surface', 'scanning' and 'non-scanning' components are described in the following sections.

NOTE 1 The thermal indices are steady state estimates based on the acoustic **output power** required to produce a 1 °C temperature rise in tissue conforming to the "homogeneous tissue 0,3 dBcm^{-1}MHz^{-1} attenuation model" [1] and may not be appropriate for radiation force imaging, or similar techniques that employ pulses or pulse bursts of sufficient duration to create a significant transient temperature rise. [2].

NOTE 2 At present the heat conduction from transducer surface is not evaluated nor included in the methods for determining the exposure parameters. See Annex C.

5.4 Determination of thermal index in non-scanning mode

5.4.1 Determination of soft tissue thermal index for non-scanning modes

5.4.1.1 Determination of soft tissue thermal index at-surface for non-scanning modes, $TIS_{\mathrm{as,ns}}$

For each **transmit pattern** in a **non-scanning mode** the **soft tissue thermal index** at-surface for a **non-scanning mode**, $TIS_{\mathrm{as,ns}}$, shall be calculated from:

$$TIS_{\text{as,ns}} = \frac{P_{1x1}\ f_{\text{awf}}}{C_{TIS,1}} \tag{12}$$

where

$C_{TIS,1}$ = 210 mW MHz;

P_{1x1} is the **bounded-square output power**;

f_{awf} is the **acoustic working frequency**.

5.4.1.2 Determination of soft tissue thermal index *TIS* below-surface for non-scanning modes, $TIS_{\text{bs,ns}}$

For each **transmit pattern** in a **non-scanning mode,** the **depth for** ***TIS***, $z_{\text{s,ns}}$, shall be determined by the range along the **beam axis** to the plane at which the lower value of the **attenuated output power** and the product of the **attenuated spatial-peak temporal-average intensity** multiplied by 1 cm^2 is maximized. The position of the maximum value of this parameter, for $z \geq z_{\text{bp}}$, shall be $z_{\text{s,ns}}$.

$$z_{\text{s,ns}} = \text{depth of max}\left[\ \min\left(I_{\text{spta},\alpha}(z)\times 1\,\text{cm}^2, P_\alpha(z)\right)\ \right] \tag{13}$$

NOTE See Annex A for discussion of the $z_{\text{s,ns}} \geq z_{\text{bp}}$ convention.

For each **transmit pattern** in a **non-scanning mode** the **soft tissue thermal index** below surface for a **non-scanning mode**, $TIS_{\text{bs,ns}}$, shall be calculated from:

$$TIS_{\text{bs,ns}} = \frac{P_\alpha\left(z_{\text{s,ns}}\right) f_{\text{awf}}}{C_{TIS,1}} \tag{14}$$

or

$$TIS_{\text{bs,ns}} = \frac{I_{\text{spta},\,\alpha}\left(z_{\text{s,ns}}\right) f_{\text{awf}}}{C_{TIS,2}} \tag{15}$$

whichever yields the smaller value,

where

$C_{TIS,1}$ = 210 mW MHz;

$C_{TIS,2}$ = 210 mW cm^{-2} MHz;

$P_\alpha(z_{\text{s,ns}})$ is the **attenuated output power** at $z_{\text{s,ns}}$, the **depth for *TIS***

f_{awf} is the **acoustic working frequency**;

$I_{\text{spta},\alpha}(z_{\text{s,ns}})$ is the attenuated spatial-peak temporal-average intensity at $z_{\text{s,ns}}$, the **depth for *TIS*.**

NOTE As $TIS_{\text{bs,ns}}$ is to be determined on the beam axis, $I_{\text{spta}}(z)$, may be approximated by taking the $I_{\text{ta}}(z)$ value on the beam axis.

Thus, $TIS_{\text{bs,ns}}$ is determined at depth $z_{\text{s,ns}}$ from:

$$TIS_{\text{bs,ns}} = \min\left[\frac{P_\alpha\left(z_{\text{s,ns}}\right) f_{\text{awf}}}{C_{TIS,1}}, \frac{I_{\text{spta},\alpha}\left(z_{\text{s,ns}}\right) f_{\text{awf}}}{C_{TIS,2}}\right] \tag{16}$$

[see Table A.2 “B”]

5.4.2 Determination of bone thermal index, TIB, for non-scanning modes

5.4.2.1 Determination of bone thermal index at surface for non-scanning modes, TIC_{ns} ~~(= $TIB_{as,ns}$)~~

For each **transmit pattern** in a **non-scanning mode**, the (**cranial) bone thermal index** at-surface shall be calculated from:

$$\sout{TIC_{ns} = TIB_{as,ns} = \frac{P / D_{eq}}{C_{TIC}}} \quad TIC_{ns} = \frac{P / D_{eq}}{C_{TIC}} \tag{17}$$

where

C_{TIC} = 40 mW cm^{-1};

P is the **output power**;

D_{eq} is the **equivalent aperture diameter**; calculation for **non-scanning modes** as described in 3.28 using the **output beam area** A_{ob}.

NOTE ~~$TIB_{as,ns}$ is also known as the cranial bone thermal index, TIC_{ns}.~~ TIC_{ns} applies to the bone-at-surface case for **non-scanning modes**.

5.4.2.2 Determination of bone thermal index below-surface for non-scanning modes, $TIB_{bs,ns}$

For each **transmit pattern** in a **non-scanning mode,** the **depth for *TIB*** shall be determined from the dependence, on distance, of the product of the **attenuated output power and** the **attenuated spatial-peak temporal-average intensity**, or equivalently the square root of this product. The position of the maximum value of this product, for depths >= z_{bp}, shall determine $z_{b,ns}$.

$$z_{b,ns} = \text{depth of max } \left(P_\alpha(z) \times I_{spta,\alpha}(z)\right) \tag{18}$$

NOTE 1 See Annex A for discussion of the $z_{b,ns} \geq z_{bp}$ convention.

The **bone thermal index** below-surface for **non-scanning mode**, $TIB_{bs,ns}$, shall be calculated from:

$$TIB_{bs,ns} = \frac{\sqrt{P_\alpha(z_{b,ns}) I_{spta,\alpha}(z_{b,ns})}}{C_{TIB,1}} \tag{19}$$

or

$$TIB_{bs,ns} = \frac{P_\alpha(z_{b,ns})}{C_{TIB,2}} \tag{20}$$

whichever yields the smallest value;

where

$C_{TIB,1}$ = 50 mW cm^{-1};

$C_{TIB,2}$ = 4,4 mW;

$P_\alpha(z_{b,ns})$ is the **attenuated output power** at the **depth for *TIB***;

$I_{spta,\alpha}(z_{b,ns})$ is the **attenuated spatial-peak temporal-average intensity** at the **depth for *TIB***.

NOTE As $TIB_{bs,ns}$ is to be determined on the beam axis, $I_{spta}(z)$, may be approximated by taking the $I_{ta}(z)$ value on the beam axis.

Thus, $TIB_{\mathrm{bs,ns}}$ is determined at depth $z_{\mathrm{b,ns}}$ from:

$$TIB_{\mathrm{bs,ns}} = \min\left[\frac{\sqrt{P_{\alpha}\left(z_{\mathrm{b,ns}}\right) I_{\mathrm{spta},\alpha}\left(z_{\mathrm{b,ns}}\right)}}{C_{TIB,1}}, \frac{P_{\alpha}\left(z_{\mathrm{b,ns}}\right)}{C_{TIB,2}}\right] \tag{21}$$

[see Table A.2 “D1”]

5.5 Determination of thermal index in scanning modes

5.5.1 Determination of soft tissue thermal index for scanning modes

5.5.1.1 Determination of soft tissue thermal index at-surface for scanning modes, $TIS_{\mathrm{as,sc}}$

For each **transmit pattern** in a **scanning mode**, the **soft tissue thermal index** at-surface shall be calculated from:

$$TIS_{\mathrm{as,sc}} = \frac{P_{1\mathrm{x}1}\, f_{\mathrm{awf}}}{C_{TIS,1}} \tag{22}$$

where

$C_{TIS,1}$ = 210 mW MHz;

$P_{1\mathrm{x}1}$ is the **bounded-square-output-power** (z = 0);

f_{awf} is the **acoustic working frequency**.

5.5.1.2 Determination of soft tissue thermal index below-surface for scanning modes, $TIS_{\mathrm{bs,sc}}$

For each **transmit pattern** in a **scanning mode** the **soft tissue thermal index** below-surface for a **scanning mode**, $TIS_{\mathrm{bs,sc}}$, shall be calculated from:

$$TIS_{\mathrm{bs,sc}} = TIS_{\mathrm{as,sc}} = \frac{P_{1\mathrm{x}1}\, f_{\mathrm{awf}}}{C_{TIS,1}} \tag{23}$$

[see Table A.2 “B2”]

5.5.2 Determination of bone thermal index for scanning modes

5.5.2.1 Determination of bone thermal index at surface for scanning modes, TIC_{sc} ~~(= $TIB_{\mathrm{as,sc}}$)~~

The determination of the **bone thermal index** at-surface for **scanning modes** shall be identical to that for **bone thermal index** at-surface for **non-scanning modes**, as specified in 5.4.2.1, except that D_{eq} is calculated by using the **scanned aperture area** A_{sa} as described in 3.28.

~~$TIC_{\mathrm{sc}} = TIB_{\mathrm{as,sc}} = \frac{P / D_{\mathrm{eq}}}{C_{TIC}}$~~ $\qquad TIC_{\mathrm{sc}} = \frac{P / D_{\mathrm{eq}}}{C_{TIC}}$ (24)

where

C_{TIC} = 40 mW cm^{-1};

P is the **output power**;

D_{eq} is the **equivalent aperture diameter**; calculation for **scanning modes** as described in 3.28 using the **scanned aperture area** A_{sa}.

NOTE ~~$TIB_{as,sc}$ is also known as the cranial bone thermal index, TIC_{sc}~~ TIC_{sc} applies to the bone-at-surface case for **scanning modes.**

5.5.2.2 Determination of bone thermal index below-surface for scanning mode, $TIB_{bs,sc}$

The **bone thermal index** below-surface, $TIB_{bs,sc}$, shall be calculated from:

$$TIB_{bs,sc} = TIS_{as,sc} = \frac{P_{1x1}\, f_{awf}}{C_{TIS1}} \qquad (25)$$

where

$C_{TIS,1}$ = 210 mW MHz;

P_{1x1} is the **bounded-square-output-power** (z = 0);

f_{awf} is the **acoustic working frequency**.

[see Table A.2 “D.2”]

5.6 Calculations for combined-operating mode

5.6.1 Acoustic working frequency

In a **combined-operating mode** with more than one type of **transmit pattern** employed during the scan period, the **acoustic working frequency** shall be considered separately for each different **transmit pattern** as appropriate in calculating the **thermal index** or the **mechanical index**.

5.6.2 Thermal index

For **combined-operating modes**, the at-surface and the below-surface **thermal index** contributions for each **discrete-operating mode** shall be calculated separately and the individual values summed appropriately, as shown in Table 1. For *TIC* the location of the maximum temperature increase is near the surface of the **transducer assembly**. For *TIB* the location of the maximum temperature increase depends on whether (as shown in Table 1) the at-surface *TIS*-summation or the below-surface *TIB*-summation is larger. In the latter case, choose z_b as the depth corresponding to the non-scanning mode, $TIB_{bs,ns}$, since the scanning mode contribution to TIB_{bs} is estimated from the at-surface value. For *TIS* the location of the maximum temperature increase depends on the combination process. *TIS* shall be the summation of at-surface TIS_{as} contributions for all modes, or the summation of below-surface TIS_{bs} contributions for all modes, whichever is the larger. If the at-surface *TIS*-summation is larger, z_s is equal to 0. If the below-surface *TIS*-summation is larger choose z_s as the depth corresponding to the non-scanning mode, $TIS_{bs,ns}$, since the scanning mode contribution to TIS_{bs} is estimated from the at-surface value. Table 1 summarizes the combination formulae for each of the **thermal index** categories.

Table 1 – Summary of combination formulae for each of the THERMAL INDEX categories

Thermal index categories	Combinations of discrete mode values of thermal index [equations for each discrete mode are shown in Tables A.2]
TIC	$\sum_{\substack{Discrete\\Modes}} TIC_{as} = \sum_{non-scanned\_TPs} TIC_{as,ns} + \sum_{scanned\_TPs} TIC_{as,sc}$ $\sum_{\substack{Discrete\\Modes}} TIC_{as} = \sum_{non-scanned\_TPs} TIC_{ns} + \sum_{scanned\_TPs} TIC_{sc}$
TIB	$\mathrm{Max}\left[\sum_{\substack{Discrete\\Modes}} TIS_{as}, \sum_{\substack{Discrete\\Modes}} TIB_{bs}\right]$ $= \sum_{scanned\_TPs} TIS_{as,sc} + \mathrm{Max}\left[\sum_{non-scanned\_TPs} TIS_{as,ns}, \sum_{non-scanned\_TPs} TIB_{bs,ns}\right]$
TIS	$\mathrm{Max}\left[\sum_{\substack{Discrete\\Modes}} TIS_{as}, \sum_{\substack{Discrete\\Modes}} TIS_{bs}\right]$ $= \sum_{scanned\_TPs} TIS_{as,sc} + \mathrm{Max}\left[\sum_{non-scanned\_TPs} TIS_{as,ns}, \sum_{non-scanned\_TPs} TIS_{bs,ns}\right]$ NOTE *'scanned_TPs'* means Scanned **Transmit Patterns** e.g. B mode, Color Mode *'non-scanned_TPs'* means Non-Scanned **Transmit Patterns** e.g. Pulsed Doppler, CW, M

5.6.3 Mechanical index

For **combined-operating modes**, the **mechanical index** shall be that for the **discrete-operating mode** with the largest **mechanical index**.

5.7 Summary of measured quantities for index determination

Table 2 gives a summary of the acoustic quantities required for the determination of each of the defined safety-related indices. Since attenuated quantities are derived by calculation from associated measured free-field quantities, both attenuated and free-field quantities are included.

Table 2 – Summary of the acoustic quantities required for the determination of the indices

Index	*MI*	TIS_{as} (at surface)	TIS_{bs} *(below surface)*		TIB_{bs} *(below surface)*		TIC ~~*(TIB_{as})*~~ *(at surface)*
Mode		**Scanning and non-scanning**	**Scanning** (=$TIS_{as,sc}$)	**non-scanning**	**Scanning** (= $TIS_{as,sc}$)	**non-scanning**	**Scanning and non-scanning**
f_{awf} at z_{pii}	x	x	x	x	x	x	
P							x
P_{1x1}		x	x		x		
P_{α}				x		x	
$I_{spta,\alpha}$				x		x	
pii	x			x		x	
pii_{α}	x			x		x	
$p_{r,\alpha}$	x						
d_{eq}						x	
D_{eq}							x
z_{bp}	x			x		x	
$z_{s,ns}$				x			
$z_{b,ns}$						x	
z_{MI}	x						
z_{pii}	x			x		x	

Annex A
(informative)

Rationale and derivation of index models

A.1 Overview

This annex provides in summary a rationale and derivation guidance for the formulas presented in the body of this standard for **mechanical index** and **thermal index**. Numerous references are made to the root publications from which the formulas were derived. As will be discussed in the derivation notes that follow, key parts of the MI and TI models rely on experimental data. This annex does not attempt to do more than describe relevant results of the experiments. A thorough reading of the referenced papers is strongly recommended in order to obtain a full understanding of the model derivation notes presented herein.

The relationship of various acoustic output parameters (for example, acoustic intensity, pressure, power, etc.) to biological endpoints is not well understood at the present time. Evidence to date has identified two fundamental mechanisms, thermal and mechanical, by which ultrasound may induce bio-effects [12,13]. This standard provides a uniform means for the calculation of acoustic output parameters relevant to these potential biological effects. The rationale behind these calculation methods is twofold:

a) that information be provided that is representative of what is occurring *in vivo* with regard to mechanical and thermal bio-effects. It is for this reason that indices were chosen as opposed to absolute quantities not shown to have a direct correlation to bio-effects;
b) that ultrasonically induced heating and acoustic pressure levels should be maintained at a level as low as practical while still providing acceptable diagnostic information (the "ALARA Principle").

A.2 General rationale

A.2.1 Rationale for attenuation coefficient of the tissue path used

The **absorption coefficient** of typical soft tissue is 0,87 dB cm^{-1} MHz^{-1}. Since the **attenuation coefficient** includes scattering and diffusion as well as absorption, the **attenuation coefficient** is always greater than the **absorption coefficient** for the same tissue and conditions. However, the **attenuation coefficient** of 0,3 dB cm^{-1} MHz^{-1} is frequently used to provide a conservative safety margin when modelling the attenuation of the sound path reaching a target tissue.

The choice of a homogeneous tissue path to the region of interest and an **acoustic attenuation coefficient** of 0,3 dB cm^{-1} MHz^{-1} is a compromise. Other attenuation models were evaluated and rejected, such as fixed distance models [14] and the use of a homogeneous tissue model with an attenuation coefficient of 0,5 dB cm^{-1} MHz^{-1}, a value more representative of many radiological and cardiac imaging applications. However, use of more than one attenuation model would entail an increase in **equipment** complexity and could create a further need for user input to select appropriate attenuation schemes. With the selected compromise in the attenuation model, the **mechanical index** and **thermal index** are simple to implement and use and, most importantly, are sufficient to allow users to minimize acoustic output and any corresponding potential mechanical or thermal bio-effects.

A.2.2 Thermal properties of tissue used in calculation of the thermal index

The rationale related to tissue properties used in the determination of the **thermal index** (TI) is given in [14,22,25,27].

A.2.3 Mechanical properties of tissue used in calculation of the mechanical index

The rationale related to tissue properties used in the determination of the **mechanical index** (MI) is given in [21,22,24,27].

A.3 Mechanical index (MI)

A.3.1 Rationale

A **mechanical index** is selected as a value to be calculated as an indicator related to mechanical effects. The index is intended to estimate the potential for mechanical bio-effects. Examples of mechanical effects include motion (or streaming) around compressible gas bubbles as ultrasound pressure waves pass through tissues, and energy released in the inertial collapse, i.e., cavitation, of micrometer-sized gas bubbles.

While no adverse mechanical bio-effects in humans have been reported to date from exposure to ultrasound output levels typical of ~~ultrasonic~~ **medical diagnostic ultrasonic equipment**, several observations have contributed to the development of the **mechanical index**.

– In lithotripsy, mechanical bio-effects are induced by ultrasound with peak pressures in the same range as those that are sometimes used in diagnostic imaging, albeit at significantly lower frequencies.

– *In vitro* experiments and observations with lower organisms have demonstrated the possibility of cavitation at ultrasound peak pressures and frequencies in ranges utilized by some ~~ultrasonic~~ **medical diagnostic ultrasonic equipment** [15].

– Lung haemorrhage has been demonstrated in several laboratory animal models exposed to levels of pulsed ultrasound similar to those used in ~~ultrasonic~~ **medical diagnostic ultrasonic equipment.** Although this effect has been demonstrated in juvenile and adult animals, similar effects have not been found in foetuses [16,17].

A.3.2 Derivation notes

The conditions that affect the likelihood of mechanical effects are not yet well understood; however, it is generally agreed that the likelihood increases as **peak-rarefactional acoustic pressure** increases, and decreases as the ultrasound frequency increases. Further, it is generally believed to be a threshold effect, such that no effect occurs unless a certain output level is exceeded [18,19,20].

While the existing limited experimental data [21] suggest a linear frequency relationship, a more conservative root-frequency relationship was selected. The **mechanical index** is defined as in 3.32 as

$$MI = \frac{p_{\mathrm{r},\alpha}\left(z_{MI}\right) \times f_{\mathrm{awf}}{}^{-1/2}}{C_{MI}} \tag{A.1}$$

where

C_{MI} = 1 MPa MHz$^{-1/2}$

$p_{\mathrm{r},\alpha}(z_{MI})$ is the **attenuated peak-rarefactional acoustic pressure** at the depth z_{MI}

z_{MI} is the **depth for** MI

f_{awf} is the **acoustic-working frequency**.

The convention adopted in [22] and continued here is to use the $p_{\mathrm{r},\alpha}$ value determined at the position on the beam axis of maximum **attenuated pulse-intensity integral**, z_{MI}. The intent is to reduce measurement burden, as the position and value of $p_{\mathrm{r},\alpha}(z_{MI})$ is assumed to be close to the position and value of the maximum $p_{\mathrm{r},\alpha}(z)$. This assumption is more accurate when pressure wave propagation is more nearly linear. While, the position and value of the maximum $p_{\mathrm{r},\alpha}(z)$ diverges (typically becoming shallower and larger) from that of $p_{\mathrm{r},\alpha}(z_{MI})$ as the effects of nonlinear propagation become more pronounced.

A.4 Thermal index (TI)

A.4.1 Rationales

A.4.1.1 General

The relationship between temperature rise and thermal bio-effects in tissues is well established (numerous studies,[1,5,7,8,14,23,24]). While present acoustic output measurement parameters, such as

P **output power**,

I_{ta} **temporal-average intensity**, and

I_{spta} **spatial-peak temporal-average intensity**

are not suitable individually as indicators or estimators of ultrasound-induced temperature rise, combinations of these parameters (together with specific geometric information) can be used to calculate indices that provide an estimate of risk of hazard from temperature rise in soft tissue or bone.

Because of the difficulties of anticipating and thermally modelling the many possible ultrasound scan planes of the human body, simplified models based on average conditions are used. Three user-selectable **thermal index** categories corresponding to different anatomical combinations of soft tissue and bone that are encountered in imaging applications are defined (see Table A.1). Each category uses one or more TI-models. Values for each model listed in Table A.1 are calculated and the larger or largest value is displayed.

A.4.1.2 Rationale for the location of the maximum temperature increase

The location of the maximum temperature increase depends on the ultrasound propagation conditions in the human body. The maximum temperature increase is assumed to be near the surface if the ultrasound beam passes through bone near the surface (TIC). For TIB, the assumption is that the maximum temperature rise is either below the surface at the tissue/bone interface, or at the soft tissue surface, thus the at-surface soft tissue equation (Equation A in Table A.2) and the below-surface bone equation (Equation D in Table A.2)) are both calculated and the maximum displayed. Likewise, for the homogeneous soft tissue model, the maximum temperature rise may be at the surface or below the surface, so TIS is the maximum value of the results of evaluating Equations A and B in Table A.2.

A.4.1.3 Rationale for choosing a break-point depth (z_{bp})

Searching the beam axis methodically up to but no closer than the **break-point depth**, z_{bp}, is imposed on the measurement of all below-surface TI parameters.

The intent of the z_{bp} as originally stated [22] was to prevent measurements from being made in the acoustic field too close to the transducer. One reason for this is to reduce violation of the assumption that acoustic particle velocity and pressure are in phase when estimating the **pulse-intensity integral**, (pii), from the **pulse-pressure-squared integral**, ($ppsi$).

NOTE 1 As discussed in section A.4.1.6 and A.4.1.7, below-surface **thermal index** values are basically functions of **acoustic output power**, and the **mechanical index** is a function of acoustic pressure. Therefore the phase between particle velocity and acoustic pressure may not seem so important. However due to the approximations and conventions used in this standard, the measurement of intensity, by way of the **pulse-pressure-squared integral** is required.

NOTE 2 In AIUM / NEMA measurement standards prior to UD-3 ([22] and all previous editions thereof), a break-point value of z_min = min(X_Dim, Y_Dim), i.e. the minimum dimension of the active transmit aperture, was used. This value proved to be inside the acoustic field close to the transducer of some transducer/system combinations.

A.4.1.4 Rationale for the bounded-square output power and attenuated bounded-square output power

As discussed in A.4.1.2, A.4.3.1 and A.4.3.2, for the soft tissue case, the interaction between acoustic beam dimensions and the cooling effect of perfusion determines the position of maximum temperature increase. A perfusion rate characterized by a perfusion length of 1 cm is assumed. This translates to a situation where, for **beam areas** less than 1 cm^2, **output power** is the relevant **power parameter,** and for **beam areas** greater than 1 cm^2, spatial average acoustic intensity multiplied by 1 cm^2 is the relevant **power parameter**. This leads to the concept of the **bounded-square output power,** P_{1x1}, as the **power parameter** "at-surface", and the **"attenuated bounded-square output power,** $P_{1x1,\alpha}(z)$, as the **power parameter** "below-surface".

Interpretation of [25] and the information in [22] have led previously, in [22], to using $\frac{P}{X}$ = '**output power** per unit scan length' as the power parameter of interest for 'at-surface' *TIS* estimates for **scanning modes**. In Edition 1 of this standard $\frac{P}{X}$ was symbolized as P_1 and titled the 'bounded output power'. Edition 1 of this standard also used an approximation of the, presently used, **bounded-square output power**, P_{1x1}, for the at-surface *TIS* for **non-scanning modes**, calculated only when the output beam area, A_{ob}, is <= 1,0 cm^2, and an approximation of **attenuated bounded-square output power**, $P_{1x1,\alpha}(z)$, for below-surface **non-scanning modes**.

In the present 2nd edition of the IEC 62359 standard the at-surface *TIS*-equations for all modes (**scanning** and **non-scanning**) use P_{1x1}. And the at-surface *TIS* is calculated for all aperture sizes. This is rationalized as follows:

A) Clearly P_{1x1} should be used for **non-scanning modes** for the at-surface *TIS* and $P_{1x1,\alpha}(z)$ for the below surface *TIS*.

B) There is an expectation that **scanned mode** and **non-scanned mode** *TIS value*s should converge smoothly as the number of scan lines narrows to 1 (from the **scanned mode** case to the **non-scanned mode** case). This occurs when P_{1x1} is used for both cases.

C) A majority of the 70 probes/cases simulated in [25] had *Y* aperture dimensions ('transducer width') ≤ 1,0 cm, in which case $\frac{P}{X}$ (P_1) and P_{1x1} yield the same numerical magnitude.

D) Many modern diagnostic ultrasound scanners and probes are capable of scanning in multiple scan planes (e.g. 3D / 4D scanning). The previously used $\frac{P}{X}$ (P_1) parameter ('power per unit length in the scan direction') is ill-defined and/or inadequate for these cases.

An approximation of the **attenuated bounded-square output power** is used in equation B in Table A.2, for the below-surface *TIS*.

A.4.1.5 Rationale for at surface *TI* in non-scanning mode and scanning mode

Implementation of the **soft tissue thermal index** (*TIS*) assumes a homogenous tissue-path model. One basic equation covers all cases for the at-surface case, **scanning modes** (such as colour-flow mapping and B-mode) and **non-scanning modes** (such as Doppler and M-mode).

~~Interpretation of [25] and the information in A.4.3 have led previously to using $\frac{P}{X}$ = '**output power** per unit scan length' as the power parameter of interest for 'at-surface' *TIS* estimates for **scanning modes**. In Edition 1 of this standard $\frac{P}{X}$ was symbolized as P_1 and titled the 'bounded output power'. Edition 1 of this standard also used an approximation~~

~~of the, presently used, **bounded-square output power**, P_{1x1}, for the at-surface *TIS* for **non-scanning modes**, calculated only when the output beam area, A_{ob}, is ≤ 1,0 cm^2, and an approximation of **attenuated bounded-square output power**, $P_{1x1,\alpha}(z)$, for below-surface **non-scanning modes**.~~

~~In the present second edition of the IEC 62359 standard the at-surface *TIS*-equations for all modes (**scanning** and **non-scanning**) use P_{1x1}. And the at-surface *TIS* is calculated for all aperture sizes. This is rationalized as follows:~~

~~a) There is an expectation that **scanning mode** and **non-scanning mode** *TIS values* should converge smoothly as the number of scan lines narrows to 1 (non-scanned), and as the depth of interest moves from 'below the surface' ($z > 0$) to the surface ($z = 0$).~~

~~b) A majority of the 70 probes/cases simulated in [25] and mentioned in A.4.3 had Y aperture dimensions ('transducer width') less than or equal to 1,0 cm, in which case $\frac{P}{X}$ and P_{1x1} yield the same numerical magnitude.~~

~~c) The derivation note presented in A.4.3.2, and in previous editions of this standard, for **non-scanning modes** states that, for both the below-surface and the at-surface case, when beam areas are < 1cm^2 the power controls the heating of tissue and for beam areas > 1cm^2, the spatial-average intensity controls the heating of tissue. This rationale is extended here to apply to scanning as well as non-scanning modes.~~

~~d) Many modern diagnostic ultrasound scanners and probes are capable of scanning in multiple scan planes (e.g. 3D / 4D scanning). The previously used $\frac{P}{X}$ parameter ('power per unit length in the scan direction') is ill-defined and/or inadequate for these cases.~~

In this document, the at-surface *TIS*-equations for all modes (**scanning** and **non-scanning**) use P_{1x1} and the at-surface *TIS* is calculated for all aperture sizes. See A.4.1.4 for the rationale for using the **attenuated bounded-square output power** in the numerator of the thermal index equations.

There is an expectation that **scanning mode** and **non-scanning mode** *TI* values should converge smoothly as the number of scan lines narrows to 1 (non-scanned), and as the depth of interest moves from below the surface ($z > 0$) to the surface ($z = 0$).

For the at-surface *TIS* equation, $P_{1x1,\alpha}(z)$ is the **bounded-square output power** P_{1x1} and equation A results (see Table A.2).

The *TIB* (bone below-surface) and *TIC* (bone at surface) equations are fundamentally the same. For *TIC*, the non-attenuated power is used, since it is an at-surface estimate. These approximations are discussed in A.4.3 (see Table A.2).

If the dimensions of the active aperture are larger than 1 cm × 1 cm, then the thermal perfusion length of one centimetre (1 cm) is assumed to be exceeded. In this case the **bounded-square output power** is measured by a radiation force balance using an intermediate absorbing mask with a one-square centimetre window (the mask is 1 cm × 1cm square), or by other masking means (e.g., electronic), or the **bounded-square output power** may be measured via hydrophone planar scanning.

~~For the at-surface *TIS* equation, $P_{1x1,\alpha}(z)$ is the **bounded-square output power**, P_{1x1}, and equation A results. (See Table A.2)~~

~~The *TIB* (bone below-surface) and *TIC* (bone at surface) equations are fundamentally the same. For *TIC* the non-attenuated power is used, since it is an at-surface estimate. These approximations are discussed in A.4.1.4. (See Table A.2)~~

NOTE Temperature rise in tissue due to transducer surface self-heating has not been taken into account in the determination of the **thermal index** [10]. (See Annex C.)

A.4.1.6 Rationale for below surface *TI* in non-scanning mode

In applying the basic *TIS* equation to the below-surface case, the parameter $P_{1x1,\alpha}(z)$ is approximated by using $\min\left(I_{spta,\alpha}(z) \text{ x } 1\text{cm}^2, P_{\alpha}(z)\right)$ as described in A.4.3.2, leading to equation B.1 in Table A.2.

For the bone-at-focus model, a different formulation is required for the power (P_{deg}) necessary to raise the bone temperature 1°C at an axial distance of $z_{b,ns}$. This different formulation is due to the observation that bone absorbs and dissipates acoustic power differently than soft tissue. The theory of this P_{deg}-formulation has been extensively developed in numerous published documents [1,12,14, 23]. The discussion in A.4.3.4 refers to key conclusions from these reports.

A.4.1.7 Rationale for below surface *TI* in scanning mode

Edition 1 of this standard, and [22], did not specify equations for below- surface *TIS* or *TIB* for **scanning modes**. This omission was intentional.

In IEC 62359 Edition 1, and in [22], the claim is made that for most **scanning mode** cases the below surface temperature in soft tissue and in bone is less than the at-surface temperature in soft tissue. Specifically (from [22]): '*the* (at-surface, scanning) *soft tissue model is used because the temperature increase at the surface is usually greater than or about the same as with the bone at the focus.*

This assumption may be true in most cases.

- The paper [25] is referenced as proof for the soft tissue below-surface case.
- Nothing is offered as proof for the bone below-surface case.

However, if there are **non-scanning mode** cases where the below-surface heating is greater than at-surface soft tissue heating, then it seems reasonable that there are a significant number of **scanning mode** operating conditions where the below-surface heating is larger than at-surface soft tissue heating.

- This seems particularly reasonable for the bone below-surface case.
- An ultrasound system operating condition with a narrow scan width should have heating characteristics approaching the non-scanned case. See [26].

Note that whether or not for **scanning modes** the at-surface soft tissue temperature rise exceeds the temperature rise in soft tissue or bone below-surface; in calculating the *TI* for **combined modes**, the below-surface contribution from **scanning modes** should not be neglected, and the below-surface sum (see Table 1) may be higher than the at-surface sum. So in Edition 2 equations for below-surface *TIB* and *TIS* for **scanning modes** are provided and are to be included in the below-surface sums.

An equation for the below surface *TIS* for **scanning modes** could be arrived at using the same principles applied in Edition 1 and [22] for deriving the below-surface *TIS* for **non-scanning modes** and the at-surface *TIS* for **scanning modes**. However, this Edition (Ed. 2) of the standard is not following that approach. Similarly, an equation for the below surface *TIB* for **scanning modes** could be arrived at using the same principals applied in Edition 1 and [22] for deriving the below-surface *TIB* for **non-scanning modes** and the at-surface *TIB*. However, again, Edition 2 is not following that approach.

There is considerably increased complexity and time associated with the measurement and estimation of $P_{1x1,\alpha}(z)$ and $d_{eq}(z)$ in **scanning modes**, and this is even more difficult in 3D and 4D **scanning modes**. It is preferable to choose formulas which give both reasonable results and which can be reasonably implemented in industrial measurement labs, where the constraints on measurement time and complexity must be considered. For the below-surface **non-scanning mode** case, suitable approximations for $P_{1x1,\alpha}(z)$ and $d_{eq}(z)$ were made in Edition 1 and [22]. But for scanning modes the complexity of approximations for $P_{1x1,\alpha}(z)$ and $d_{eq}(z)$ is significantly increased or their suitability are not well understood.

Therefore, use is made in Edition 2 of the claim in 62359 Edition 1 and in [22] that for most **scanning mode** cases the below surface temperature in soft tissue and in bone is less than the at-surface temperature in soft tissue. Though limited support for the claim is given in Edition 1 and in[22] particularly for the bone below-surface case, and though it seems reasonable that the claim is not true for some number of **scanning mode** operating conditions, this claim remains in Edition 2 and is made use of by setting the $TIS_{bs,sc}$ and the $TIB_{bs,sc}$ equal to the $TIS_{as,sc}$.

This compromise solution generally meets the requirement of satisfying the boundary conditions:

a) smooth convergence to the value of the TIB (or TIS) for **non-scanning modes** as the number of **ultrasonic scan lines** goes to one,

b) convergence to the at-surface TIB (or TIS) value as the region of interest moves from below-surface to the surface (z = 0).

NOTE Convergence does not happen, strictly speaking, when different approximations are used below-surface and at-surface. For instance, for non-scanning mode TIB, TIB_{ns}, D_{eq} (at-surface) and d_{eq} (below-surface) are approximated using different formulas. For non-scanning mode TIS, TIS_{ns}, P_{1x1} is estimated differently at-surface and below-surface. In the case of scanning modes, the below-surface TIB won't converge with the at-surface TIB (TIC), due to setting $TIB_{bs,sc}$ equal to $TIS_{as,sc}$

Table A.1 – Thermal index categories and models

Thermal Index category	Thermal Index models	
	Non-scanning mode	**Scanning mode**
TIS (soft tissue)	A) Soft tissue at-surface: non-scanning and scanning. B.1) Soft tissue below-surface: non-scanning	A) Soft tissue at-surface: non-scanning and scanning. B.2) Soft tissue below-surface: scanning. (= Equation A)
TIC=TIB_{as} (bone at-surface)	C) Bone at-surface: non-scanning and scanning	C) Bone at-surface: non-scanning and scanning
TIB_{bs} (bone below-surface)	A) Soft tissue at-surface: non-scanning and scanning. D.1) Bone below-surface: non-scanning	A) Soft tissue at-surface: non-scanning and scanning. D.2) Bone below-surface: -scanning. (=Equation A)

A.4.2 Derivation notes - General

A.4.2.1 Derivation of break-point depth

The expression for **break-point depth** in this edition is

$$z_{bp} = 1{,}5 \times D_{eq} \qquad \text{(A.2)}$$

D_{eq} is defined as the 'circular-equivalent' geometric mean diameter (the **equivalent aperture diameter**) of the transmit aperture for a single pulse of the **transmit pattern** being measured.

$$D_{eq} = \sqrt{\frac{4}{\pi} A_{ob}} = 1{,}13\sqrt{A_{ob}} \quad \text{(A.3)}$$

where A_{ob} is the **output beam area**.

NOTE 1 Equation (A.3) is a re-statement of Equation (8) (from 3.28), with a single pulse corresponding to a **non-scanning mode**.

Thus, for **scanning modes** or **non-scanning modes**, the same value of z_{bp} will be obtained if the **ultrasonic scan lines** (or at least the 'central scan line' of the lines making up the scan) use the same aperture and nominal focal point.

Figure A.1 shows a typical case. Here the focal point of the transducer and the position of maximum **attenuated spatial-peak temporal-average intensity** are shown to occur deeper than 1,5 × D_{eq}.

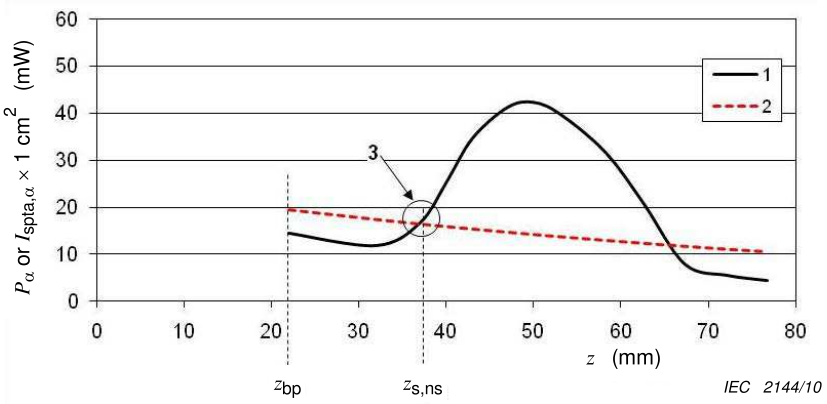

Key

1: graph of $I_{spta,\alpha}$ × 1 cm^2,

2: graph of P_α,

3: point where $P_p = P_\alpha(z_{s,ns}) = I_{spta,\alpha}$ × 1 cm^2

Figure A.1 – Focusing transducer with a f-number of about 7

For low **f-number** transmit conditions the 'legitimate' depth of maximum *pii* (including the focal point) might validly be shallower than 1,5 × D_{eq}. As pressure levels may be high in this region the definition of z_{bp} in this standard is only used for the determination of *TI*. Figure A.2 gives an example of such a situation.

NOTE The **f-number** denotes the ratio of the **geometric focal length** to the **transducer aperture width** in a specified longitudinal plane as defined in IEC 61828.

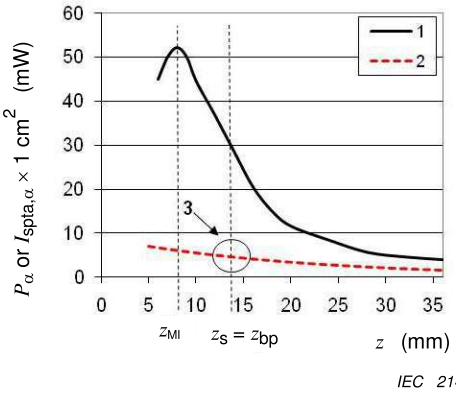

Key

1: graph of $I_{spta\cdot\alpha} \times 1$ cm^2,

2: graph of P_α,

3: point where $P_p = P_\alpha(z_{s,ns})$

z_{MI} is closer to the transducer surface than $1{,}5 \times D_{eq}$

Figure A.2 – Strongly focusing transducer with a low f-number of about 1

Close to the transducer acoustic field undulations and side lobe levels can vary from transducer to transducer of the same model type as sensitive functions of production tolerances. In most cases, adherence to the z_{bp} definition should serve to keep hydrophones not too close to the transducer, helping to obtain consistent intra-model measurement results and 'tighter' statistics. However, as shown in Figure A.3, if the undulations are extensive the determined value of z_{bp} may be close to the transducer.

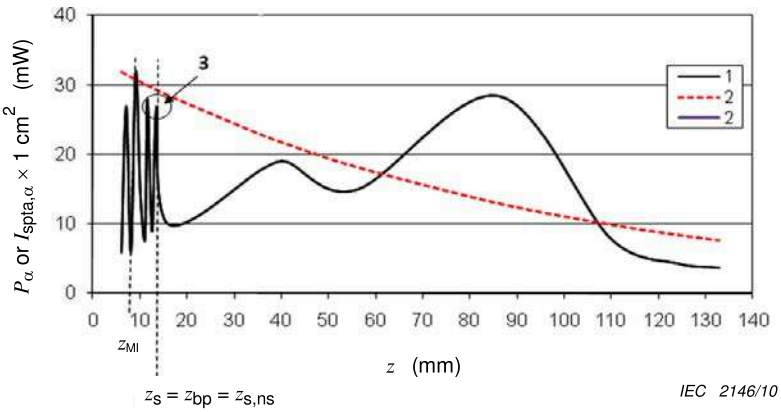

Key

1: graph of $I_{spta\cdot\alpha} \times 1$ cm^2,

2: graph of P_α,

3: point where $P_p = I_{spta\cdot\alpha} \times 1$ cm^2

Figure A.3 – Focusing transducer (f-number ≈ 10) with severe undulations close to the transducer

Another effect of employing the **break-point-depth** is that some separation between the at-surface and below-surface thermal indices positions is created. Thus, instead of finding the TI as the maximum value over all z values, including $z = 0$, (as discussed in A.4), we have two regions, $z = 0$ and $z \geq z_{bp}$, for TI.

Of course, one of the negative consequences of employing the **break-point-depth**, is the creation of a non-interrogated region which may contain the location of maximum TI.

To prevent collisions of expensive hydrophones into transducers being tested, care must be exercised when performing scans closer to the transducer than the **break-point depth** as required, if necessary, to find the **depth for mechanical index** (z_{MI}). This would happen with greater frequency if searching the beam axis all the way to the transducer surface were required. This could happen for probes with shallow focusing and/or high amplitude undulations close to the transducer.

Another effect of using z_{bp}, though not its intended purpose, is to obscure the fact that the below-surface TI values do not converge continuously to the at-surface TI values as z approaches 0. This is because different approximations for P_{1x1} and d_{eq} (D_{eq}) are used at-surface and below-surface. See A.4.1 and A.4.1.5 Note a.

A.4.2.2 Thermal index

In this annex the **thermal index**, TI, is defined by the relationship

$$TI = \frac{P_p}{P_{deg}} \tag{A.4}$$

where

P_p is the **power parameter** as defined in this annex, and

P_{deg} is the estimated power necessary to raise the target tissue 1 °C, based on the thermal models discussed in this annex.

The derivation of the temperature rise estimation models requires the understanding of four key concepts/parameters.

A.4.2.3 Attenuated output power and attenuated intensity

The **attenuated output power** and **attenuated intensity** are functions of the non-attenuated values, depth and the **acoustic attenuation coefficient**. **Attenuated output power** and **attenuated intensity** are denoted by the subscript α. Parameters without the subscript refer to non-attenuated values measured in water. Thus the **attenuated output power** P_α at a distance z is defined as

$$P_\alpha(z) = P\,10^{(-\alpha z\, f_{awf}/10\text{dB})} \tag{A.5}$$

where

P is the **output power**,
α is the **acoustic attenuation coefficient**,
f_{awf} is the **acoustic working frequency**, and
z is the distance from the **external transducer aperture** to the point of interest

The **attenuated spatial-peak temporal-average intensity** is denoted:

$$I_{spta,\alpha}(z) = I_{spta}(z)\,10^{(-\alpha z\, f_{awf}/10\text{dB})} \tag{A.6}$$

where

$I_{spta}(z)$ is the **spatial-peak temporal-average intensity** at distance z,

α is the **acoustic attenuation coefficient**,

f_{awf} is the **acoustic-working frequency**, and

z is the distance from the **external transducer aperture** to the point of interest.

A.4.2.4 Derivation of the equivalent beam area

The **equivalent beam area**, A_{eq}, is defined as

$$A_{eq}(z) = \frac{P_\alpha(z)}{I_{spta,\alpha}(z)} = \frac{P}{I_{spta}(z)} \quad \text{(A.7)}$$

where

$P_\alpha(z)$ is the **attenuated output power** at distance z,

$I_{spta,\alpha}(z)$ is the **attenuated spatial-peak temporal-average intensity** at distance z,

P is the **output power**,

$I_{spta}(z)$ is the **spatial-peak temporal-average intensity** at distance z, and

z is the distance from the **external transducer aperture** to the specified point.

A.4.2.5 Derivation of the equivalent beam diameter

The **equivalent beam diameter**, d_{eq}, is defined as

$$d_{eq}(z) = \sqrt{\frac{4}{\pi} A_{eq}(z)} \quad = \quad 2\sqrt{\frac{P_\alpha(z)}{\pi I_{spta,\alpha}(z)}} \quad \text{(A.8)}$$

where

$A_{eq}(z)$ is the **equivalent beam area** at distance z,

$P_\alpha(z)$ is the **attenuated output power** at distance z, and

$I_{spta,\alpha}(z)$ is the **attenuated spatial-peak temporal-average intensity** at distance z.

A minimum **beamwidth** of one millimetre (0,1 cm) is assumed because of the practical difficulty of holding a small beam steady on one target location. Therefore, for these derivations

$$d_{eq}(z) = \max\left(\sqrt{\frac{4}{\pi} A_{eq}(z)}, 0{,}1\,\text{cm}\right) = \max\left(2\sqrt{\frac{P_\alpha(z)}{\pi I_{spta,\alpha}(z)}}, 0{,}1\,\text{cm}\right) \quad \text{(A.9)}$$

This minimum **beamwidth** assumption is referred to in context in later sections of this annex.

A.4.3 Derivation notes for the thermal models used

As discussed in A.4.1 and in Table A.1, three **thermal indices** are defined, the *TIS*, the *TIB* and the *TIC*. Four temperature-rise estimation equations are used in calculating the *TI's*, as defined in Clause 5 of this standard. For the purposes of discussion and derivation, these four models are identified in Table A.2.

The soft tissue equations (A and B of Table A.2) are based on one model, derived primarily from a theoretical and experimental analysis [25,27]. According to [25], the mediating factor for temperature rise at the surface is the absorbed power per unit scan length, $\mu_o f\,[P/X]$, that normalizes the effect of frequency on the temperature rise (where μ_0 is the **acoustic absorption coefficient** in Np cm^{-1} MHz^{-1}). A series of calculations on 70 transducers of the absorbed power per unit scan length that caused a 1 °C rise at the skin surface produced results centred about:

$$\mu_0 f_{awf}[P_{deg}/X] = 21\,\text{Np mW/cm}^2 \quad \text{(A.10)}$$

This is a key concept in the development of the *TIS* models. A careful study of [25] is strongly recommended to ensure a thorough understanding of this important concept.

NOTE In [25] a study of typical linear array transducers available in 1991 is presented. Validation of the concept for more sophisticated modern transducers (e.g. 1,5 and 2D arrays) and 3D scanning formats has not yet been published.

For this study, the **acoustic absorption coefficient** intensity was selected as μ_o = 0,1 Np cm^{-1} MHz^{-1}, a value typical of soft tissue. The average perfusion rate for soft tissue has been estimated as the cardiac output divided by the body mass, resulting in a corresponding typical perfusion length of 1,0 cm. Selecting the unit scan length, X, as the perfusion length and combining these experimental approximations with equation A.10 results in the power required to cause a 1 °C temperature rise at the surface as

$$P_{\text{deg}} = \frac{(21\ \text{Np}\cdot\text{mW}\cdot\text{cm}^{-2})\,(1{,}0\ \text{cm})}{(0{,}1\ \text{Np}\cdot\text{cm}^{-1}\cdot\text{MHz}^{-1})\,(f_{\text{awf}})} \triangleq \frac{210\ \text{mW MHz}}{f_{\text{awf}}} \qquad \text{(A.11)}$$

This P_{deg} formula is shared by both the at-surface soft tissue equation (Equation A of Table A.2) and the below-surface soft tissue equation (eq. B.2 of Table A.2). In this standard, the value of 210 mW MHz is incorporated in constants $C_{TIS,1}$ and $C_{TIS,2}$.

Table A.2 – Consolidated thermal index formulae

Name	Formula
A Soft tissue at-surface non-scanning and scanning (see 5.4.1.1 and 5.5.1.1)	$TIS_{as} = \frac{P_{1x1}\, f_{awf}}{C_{TIS,1}}$
B.1 Soft tissue below-surface non-scanning (see 5.4.1.2)	$TIS_{bs,ns} = \min\left[\frac{P_{\alpha}(z_{s,ns}) f_{awf}}{C_{TIS,1}}, \frac{I_{spta,\alpha}(z_{s,ns}) f_{awf}}{C_{TIS,2}}\right]$ NOTE 1 $z_{s,ns} \geq z_{bp}$ NOTE 2 Where $\min\left[P_{\alpha}(z), I_{spta,\alpha}(z)\right]$ is an approximation of $P_{1x1,\alpha}(z)$ NOTE 3 $I_{spta,\alpha}(z)$ may be approximated by taking the $I_{ta,\alpha}(z)$ value on the beam axis.
B.2 Soft tissue below-surface scanning (see 5.4.1.2 and 5.5.1.2)	$TIS_{bs,sc} = TIS_{as,sc} = \frac{P_{1x1}\, f_{awf}}{C_{TIS,1}}$
C Bone at surface non-scanning and scanning (see 5.4.2.1 and 5.5.2.1)	~~$TIC = TIB_{as} = \frac{P / D_{eq}}{C_{TIC}}$~~ $TIC = \frac{P / D_{eq}}{C_{TIC}}$
D.1 Bone below-surface non-scanning (see 5.4.2.2)	$TIB_{bs,ns} = \min\left[\frac{\sqrt{P_{\alpha}(z_{b,ns}) I_{spta,\alpha}(z_{b,ns})}}{C_{TIB,1}}, \frac{P_{\alpha}(z_{b,ns})}{C_{TIB,2}}\right]$ NOTE 1 $z_{b,ns} \geq z_{bp}$ NOTE 2 $I_{spta,\alpha}(z)$ may be approximated by taking the $I_{ta,\alpha}(z)$ value on the beam axis.
D.2 Bone below-surface scanning (see 5.5.2.2)	$TIB_{bs,sc} = TIS_{as,sc} = \frac{P_{1x1}\, f_{awf}}{C_{TIS,1}}$

A.4.3.1 Derivation notes for soft tissue thermal index at-surface for non-scanning and scanning modes ($TIS_{\mathbf{as,ns}}$, $TIS_{\mathbf{as,sc}}$)

As noted in A.4.1.4, temperature increase in soft tissue is determined by the **bounded-square output power**.

Power from the one square-centimetre of the radiating- or active-aperture emitting the maximum value of the time average acoustic output power is measured (see Figure B.3). For active apertures having a scan dimension less than one centimetre in each dimension, no mask is necessary. The result of these power measurements, the **bounded-square output power**, P_{1x1}, is the **power parameter** used in the *TI*-formula for soft tissue at-surface.

Combining the **bounded-square output power** with the power required to cause a 1 °C temperature rise, P_{deg}, (equation A.11) into the general *TI*-formula (equation A.4) yields the soft tissue at-surface model for **scanning modes** and **non-scanning modes.**

$$TIS_{as} = \frac{P_{1x1}\, f_{awf}}{C_{TIS,1}} \tag{A.12}$$

where

$C_{TIS,1}$ = 210 mW MHz

A.4.3.2 Derivation notes for soft tissue thermal index below-surface for non-scanning mode ($TIS_{\mathbf{bs,ns}}$)

As discussed in A.4.2 and A.4.3 the perfusion assumption (1 cm thermal perfusion length) is critical to determining the location of the maximum temperature increase. Theory derived for a heated cylinder suggests that if the **beam area** is less than 1 cm^2, the power in the beam controls the temperature rise [14]. If the **beam area** is greater than 1 cm^2, intensity controls the temperature rise. Therefore, the **power parameter** P_p used in the numerator of the general formula (equation A.4) for narrow beams [**beam area** ≤ 1 cm^2] is the **attenuated output power**, $P_\alpha(z)$ and for broad beams [**beam area** > 1 cm^2] the **power parameter** is the **attenuated spatial-average temporal-average intensity**, $I_{sata,\alpha}(z)$, multiplied by an area of 1 cm^2 ($I_{sata,\alpha} \times 1$ cm^2), where the spatial averaging is carried out over a 1 cm^2 area.

Attenuated bounded-square output power', $P_{1x1,\alpha}(z)$ is defined as $P_\alpha,(z)$ when the **beam area** is < 1 cm^2 and $I_{sata,\alpha} \times 1$ cm^2 when the **beam area** is > 1 cm^2, where $I_{sata,\alpha}$ is the spatial average over the 1 cm x 1 cm area yielding the highest value.

Thus, for any location z on the beam axis, the local **power parameter** is $P_{1x1,\alpha}(z)$ and **the power parameter** P_p used in the numerator of the general formula (equation A.4) is then:

$$P_p = \max_{z>z_{bp}} \left[P_{1x1,\alpha}(z) \right] \tag{A.13}$$

Approximation Used:

Considering the measurement complexity and time associated with precise measurement of $P_{1x1,\alpha}(z)$, Edition 2 of the standard chooses an approximation of the local power parameter, using the **equivalent beam area** and using the **attenuated spatial-peak temporal-average intensity**, assumed to occur on the beam axis, rather than the spatial-average intensity.

Thus when the **equivalent beam area**, ($A_{\mathrm{eq}}(z) = \dfrac{P_\alpha(z)}{I_{\mathrm{spta},\alpha}(z)}$) is ≤ 1 cm^2 the attenuated output power, $P_\alpha(z)$, is the local **power parameter** and when $A_{\mathrm{eq}}(z)$ is > 1 cm^2, $I_{\mathrm{spta},\alpha}(z) \times 1$ cm^2 is the local **power parameter.**

That is, the local **power parameter** at a particular depth z is min($P_\alpha(z)$, $I_{\mathrm{spta},\alpha}(z) \times 1$ cm^2) and:

$$P_{\mathrm{p}} = \max_{z>z_{bp}} \left[\min\left(P_\alpha(z), I_{\mathrm{spta},\alpha}(z) \mathrm{x} 1 \mathrm{cm}^2 \right) \right] \tag{A.14}$$

This is a conservative approximation. The conservative nature of the approximation is further described in the following three notes:

NOTE 1 Equations such as A.17, A.18 and A.19 indicate that it is the -6 dB area which should be compared against the 1 cm^2 threshold, and equation A.29 shows that the -6 dB area is larger than A_{eq}.

NOTE 2 Because $I_{\mathrm{spta},\alpha}(z)$ is > $I_{\mathrm{sata},\alpha}(z)$ (averaged over 1×1 cm^2 and multiplied by 1 cm^2, = $P_{1\mathrm{x}1,\alpha}(z)$), then when $A_{\mathrm{eq}}(z) = \dfrac{P_\alpha(z)}{I_{\mathrm{spta},\alpha}(z)}$ = 1 cm^2 the actual -6dB beam area, per equation A.29, is larger than 1 cm^2, and therefore the power in the numerator can be larger than the power in a 1 cm^2 beam area (larger than $P_{1\mathrm{x}1,\alpha}(z)$). So for $A_{\mathrm{eq}}(z) \leq$ 1 cm^2, $P_{1\mathrm{x}1,\alpha}(z) \leq P_\alpha(z) < I_{\mathrm{spta},\alpha}(z)$, and for $A_{\mathrm{eq}}(z) >$ 1 cm^2, $P_{1\mathrm{x}1,\alpha}(z) < I_{\mathrm{spta},\alpha}(z) < P_\alpha(z)$.

NOTE 3 Because A_{eq} is smaller than the -6 dB area (A_6), then it is obviously < 1 cm^2 when A_6 is < 1 cm^2, and acoustic power is the 'power parameter' (controls heating), in this case.
For the region 1,0 cm^2 < A_6 < 1,28 cm^2, A_{eq} remains ≤ 1,0, and the **attenuated output power**, P_α, is used instead of $I_{\mathrm{spta},\alpha} \times 1$ cm^2 as the 'power parameter'. This is conservative (an over-estimate) for this region, because obviously the power passing through a 1,28 cm^2 area is > than the power through a 1 cm^2 area ($P_{1\mathrm{x}1,\alpha}$), and both are smaller than $I_{\mathrm{spta},\alpha} \times 1$ cm^2. So $P_{1\mathrm{x}1} < P \leq I_{\mathrm{spta},\alpha} \times 1$ cm^2.

Lastly, for $A_6 \geq$ 1,28 cm^2 the intensity (× 1 cm^2) is being used as the power parameter as it should be, $I_{\mathrm{spta},\alpha} \times$ 1 cm^2 is being used, which is always > $I_{\mathrm{sata},\alpha} \times 1$ cm^2 ($P_{1\mathrm{x}1,\alpha}$ when the spatial average is over 1 cm^2); so this is conservative ($I_{\mathrm{spta},\alpha} \times 1$ cm^2 > $P_{1\mathrm{x}1,\alpha}$).

Combining the **power parameter** expressed in equation A.14 with the power required to cause a 1 °C temperature rise, P_{deg}, (Equation A.11) into the general *TI*-formula (equation A.4) yields the soft tissue thermal index below-surface for non-scanning modes

$$TIS_{\mathrm{bs,ns}} = \max_{z>z_{\mathrm{bp}}} \left[\min\left(\frac{P_\alpha(z_{\mathrm{s,ns}}) f_{\mathrm{awf}}}{C_{TIS,1}}, \frac{I_{\mathrm{spta},\alpha}(z_{\mathrm{s,ns}}) f_{\mathrm{awf}}}{C_{TIS,2}} \right) \right] \tag{A.15}$$

where

$C_{TIS,1}$ = 210 mW MHz;

$C_{TIS,2}$ = 210 mW cm^{-2} MHz.

Figures A.4, A.5, A.6, and A.7 illustrate examples of possible locations and values of the **power parameter** (Equation A.14). These figures demonstrate examples of possible relationships between the intensity ($I_{\mathrm{spta},\alpha}(z) \times 1$ cm^2) and power ($P_\alpha(z)$) curves. Values within the region less than the **break-point depth** ($z < z_{\mathrm{bp}}$) are not considered.

It is helpful to consider what these curves indicate about beam focusing. Because the **equivalent beam area**, A_{eq}, is the ratio of $P_\alpha(z)$ to $I_{\mathrm{spta},\alpha}(z)$, in regions where the intensity curve is below (less than) the power curve, the **equivalent beam area** is greater than 1 cm^2. Similarly, where the intensity curve is above (greater than) the power curve, the **equivalent beam area** is less than 1 cm^2. The **equivalent beam area** is 1 cm^2 where the curves intersect.

Figure A.4 shows a focused beam for which the **equivalent beam area** first decreases to 1 cm^2, that is, the curves intersect at a depth greater than the **break-point depth**. The maximum value of the local **power parameter** is found at this intersection, and the location is denoted $z_{\mathrm{s,ns}}$.

Figure A.5 might represent a focused transducer with somewhat smaller aperture. At the **break-point depth**, the **equivalent beam area** is already less than 1 cm^2. The maximum value of the local **power parameter,** $P_\alpha(z)$, is the **attenuated output power** at the **break-point depth**, and $z_{s,ns}$ is at the **break-point depth**.

Figure A.6 might represent a focusing transducer with a relatively weak focus just beyond the **break-point depth**. This local intensity maximum may result from the elevation focus of a rectangular aperture transducer or, perhaps, a close to the transducer effect beyond the **break-point depth**. In this example, the location, $z_{s,ns}$, of the local **power parameter** maximum is at the weak focus. The value of the **power parameter** is $I_{spta,\alpha}(z) \times 1$ cm^2.

Figure A.7 represents a weakly focused transducer. The **equivalent beam diameter** always exceeds 1 cm^2. While such an example is unlikely in diagnostic ultrasound applications, the example is provided for the sake of a complete understanding of the model. The distribution of the local **power parameter** with depth is the intensity curve. The **power parameter** is the maximum value of the $I_{spta,\alpha}(z) \times 1$ cm^2. $z_{s,ns}$ is at the location on the beam axis of this maximum.

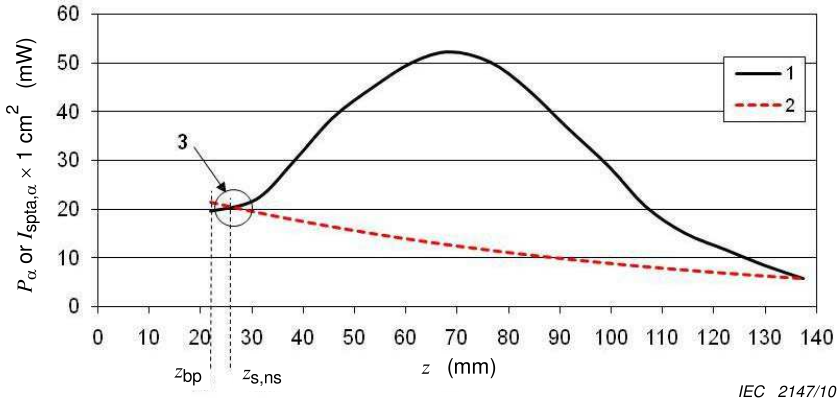

Key

1: graph of $I_{spta,\alpha} \times 1$ cm^2,

2: graph of P_α,

3: point where $P_p = P_\alpha(z_{s,ns}) = I_{spta,\alpha} \times 1$ cm^2

Figure A.4 – Focusing transducer

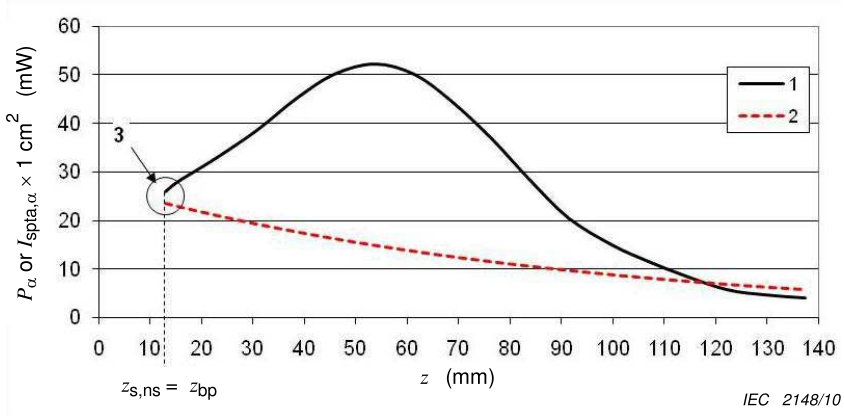

Key

1: graph of $I_{spta,\alpha} \times 1$ cm^2,

2: graph of P_α,

3: point where $P_p = P_\alpha(z_{s,ns})$

Figure A.5 – Focusing transducer with smaller aperture than that of Figure A.4

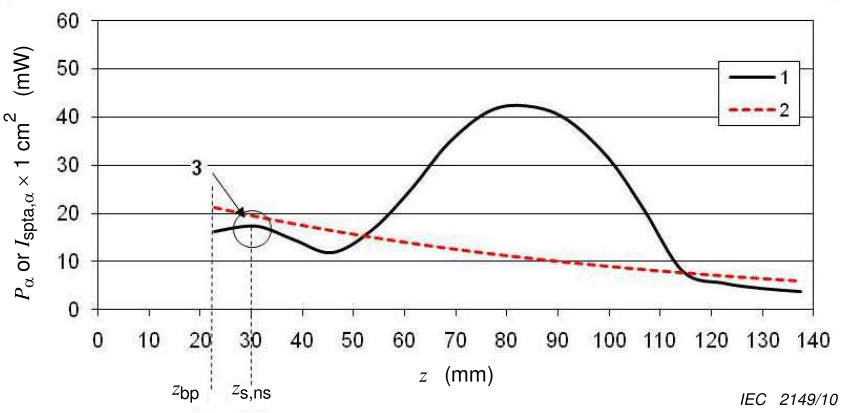

Key

1: graph of $I_{spta,\alpha} \times 1\ cm^2$,

2: graph of P_α,

3: point where $P_p = I_{spta,\alpha} \times 1\ cm^2$

Figure A.6 – Focusing transducer with a weak focus near z_{bp}

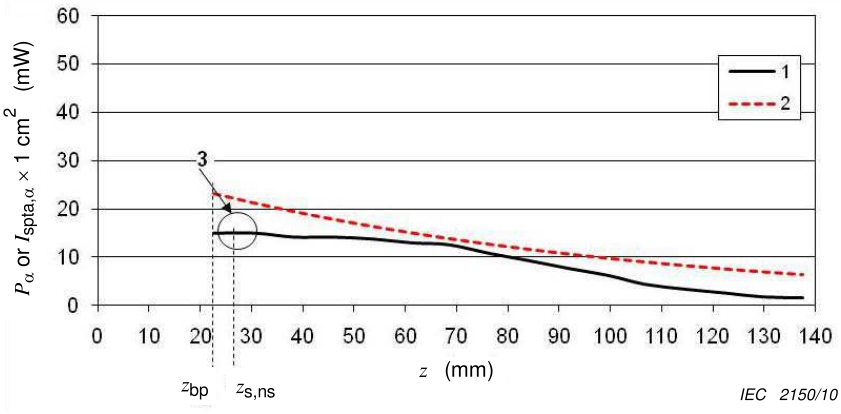

Key

1: graph of $I_{spta,\alpha} \times 1\ cm^2$,

2: graph of P_α,

3: point where $P_p = I_{spta,\alpha} \times 1\ cm^2$

Figure A.7 – Weakly focusing transducer

A.4.3.3 Derivation notes for soft tissue thermal index below-surface for scanning modes, ($TIS_{bs,sc}$)

An equation for the below surface TIS for **scanning modes** could be arrived at using the same principals applied in Edition 1 and [22] for deriving the below-surface TIS for **non-scanning modes** and the at-surface TIS for **scanning modes**. However, this Edition (Ed. 2) of the standard is not following that approach.

There is considerably increased complexity and time associated with the measurement and estimation of $P_{1x1,\alpha}(z)$ in **scanning modes**, and this is even more difficult in 3D and 4D **scanning modes**. It is preferable to choose formulas which give both reasonable results and which can be reasonably implemented in industrial measurement labs, where the constraints

on measurement time and complexity must be considered. For the below-surface **non-scanning mode** case, suitable approximations for $P_{1x1,\alpha}(z)$ were made in Edition 1 and [22]. But for scanning modes the complexity of approximations for $P_{1x1,\alpha}(z)$ is significantly increased or their suitability are not well understood.

Therefore, use is made in Edition 2 of the claim In IEC 62359 Edition 1 and in [22] that for most **scanning mode** cases the below surface temperature in soft tissue is less than the at-surface temperature in soft tissue. Though limited support for the claim is given in Edition 1 and in [22], this claim remains in Edition 2 and made use of by setting the $TIS_{bs,sc}$ equal to the $TIS_{as,sc}$.

So:

$$TIS_{bs,sc} = TIS_{as,sc} = \frac{P_{1x1}\, f_{awf}}{C_{TIS,1}} \qquad \text{(A.16)}$$

where

$C_{TIS,1}$ = 210 mW MHz

Justification for this simplification can be found in [25] and [26] which show calculations of at-surface soft tissue temperature rise for scanned modes to be higher than below-surface soft tissue temperature rise in a large majority of cases.

A.4.3.4 Derivation notes for bone at-focus for non-scanning modes ($TIB_{bs,ns}$)

For the bone-at-focus model for **non-scanning modes**, the location of the maximum temperature increase is at the proximal surface of the bone, located at the **depth for *TIB*** where the **depth for *TIB*** is the depth at which the *TIB*-expression is a maximum. The **power parameter** for the beam is the **attenuated output power**, P_α at $z_{b,ns}$.

NOTE The conservative assumption here is that the bone resides at the location where the *TIB* expression is a maximum.

The following derivation refers to key conclusions from the literature [1,12,14,23].

To determine the estimated power necessary to raise bone 1°C at an axial distance, $z_{b,ns}$, we begin with the point-source solution to the steady-state bio-heat equation [12,14], which gives the temperature rise on axis of a totally absorbing, very thin disc surrounded by a material of thermal conductivity, K,

$$\Delta T = \frac{I_{sata,\alpha}\, d_6}{4K} \qquad \text{(A.17)}$$

where

~~I_{sata} is spatial-average **temporal-average intensity**~~

$I_{sata,\alpha}$ is the **attenuated spatial-average temporal-average intensity**

d_6 is the –6 dB beam diameter and

K is the thermal conductivity of the surrounding medium

Since **attenuated output power** can be approximated as,

$$P_\alpha = \frac{\pi d_6^2}{4} I_{sata,\alpha} \qquad \text{(A.18)}$$

temperature rise can be expressed by combining A.17 and A.18:

$$\Delta T = \frac{P_\alpha}{\pi K d_6} \quad \text{(A.19)}$$

Using data adapted from [28] and selecting water at 37 °C as the surrounding medium gives a thermal conductivity, K, of 6,3 mW cm^{-1} °C^{-1}. Substituting this value for K into equation A.19 yields a temperature rise of approximately:

$$\Delta T \approx \frac{P_\alpha}{C_K d_6} \quad \text{(A.20)}$$

where

C_K= 20 mW cm^{-1} °C^{-1}.

While difficulties are obviously encountered in making accurate predictions of temperature rise that occur when bone is exposed to ultrasound *in vivo*, reasonable estimates can be made of upper limits to the temperature rise. Equation A.19, for a disc-like intensity distribution, yields a simple expression of temperature rise, ΔT, when the beam diameter is in the order of one-quarter of the perfusion length, a reasonable assumption for this model. Similar derivations are found for Gaussian or Bessinc beams and rectangular beams (within 10 % for Gaussian & Bessinc and within 30 % for rectangular).

Experimental data [29] suggest that a correction factor is required to formula A.17 (and results in changes to formulas A.19 and A.20). This correction factor is explained as being due, in part, to the effects of perfusion in relatively small volumes. The data available indicate that a factor of approximately 0,5 in temperature rise is needed to obtain correspondence between *in vivo* measurements and theory. Applying this correction factor yields

$$\Delta T = (0{,}5)\, P_\alpha / C_K d_6 = P_\alpha / 2C_K d_6 \quad \text{(A.21)}$$

Therefore, the power required to cause a 1 °C temperature rise, P_{deg}, becomes:

$$P_{\text{deg}} = 2C_K\, d_6 \,\text{x}\, 1^{\text{o}}\text{C} \quad \text{(A.22)}$$

The minimum **beamwidth** assumption noted in clause A.4.2.5 is made here insofar as the smallest beam diameter that can be maintained in a clinical exam is 0,1 cm, due to both operator- and patient-motion; then P_{deg} = 4 mW. This value yields the power required to cause a 1 °C temperature rise, P_{deg} in terms of d_6

$$P_{\text{deg}} = \max(2\text{C}_K\, d_6 \,\text{x}\, 1^{\text{o}}\text{C}, 4\,\text{mW}) \quad \text{(A.23)}$$

It is now necessary to express the beam diameter for typical beams, such as Gaussian or Bessinc, in terms of the **equivalent beam diameter**, d_{eq}. The equations for a uniform “disk” beam (A.18) and the **equivalent beam diameter** (A.8) are similar and result in

$$d_6 \approx d_{\text{eq}} = 2\sqrt{\frac{P}{\pi I_{\text{spta}}}} \quad \text{(A.24)}$$

For a Gaussian beam, see [1],

$$P_\alpha \approx \frac{\pi I_{\text{spta},\alpha} (d_6)^2}{5{,}5} \quad \text{(A.25)}$$

yielding a beam diameter of

$$d_6 = 2{,}34\sqrt{\frac{P_\alpha}{\pi I_{\text{spta},\alpha}}} = 1{,}17\, d_{\text{eq}} \tag{A.26}$$

where d_6 is the -6 dB beam diameter as discussed above. Similarly, for a Bessinc beam, see [1],

$$P_\alpha \approx \frac{\pi I_{\text{spta},\alpha}(d_6)^2}{4{,}8} \tag{A.27}$$

yielding a beam diameter of

$$d_6 = 2{,}19\sqrt{\frac{P_\alpha}{\pi I_{\text{spta},\alpha}}} = 1{,}10\, d_{\text{eq}} \tag{A.28}$$

Upon dividing equations A.26 and A.28 by A.24 and geometrically averaging the respective coefficients, the following correction is selected:

$$d_6 = 1{,}13\, d_{\text{eq}} \tag{A.29}$$

This expression is substituted for d_6 into Equation A.23, yielding the power required to cause a 1 °C temperature rise, P_{deg}

$$P_{\text{deg}} = \max\left(2{,}26\, C_K\, d_{\text{eq}} \times 1^{\text{o}}\text{C}\,,\, 4{,}52\,\text{mW}\right) \tag{A.30}$$

Expressing d_{eq} in terms of P_α and $I_{\text{spta},\alpha}$ and using equations A.7, A.8 and A.9 yields

$$P_{\text{deg}} = \max\left[2{,}26\, C_K\left(2\sqrt{\frac{P_\alpha}{\pi I_{\text{spta},\alpha}}}\right) \times 1^{\text{o}}\text{C}\,,\, 4{,}52\,\text{mW}\right] \tag{A.31}$$

which yields the approximation

$$P_{\text{deg}} = \max\left[2{,}55\, C_K\, \sqrt{\frac{P_\alpha}{I_{\text{spta},\alpha}}} \times 1^{\text{o}}\text{C}\,,\, 4{,}52\,\text{mW}\right] \tag{A.32}$$

NOTE 2 The actual computed values of 2,26 C_K and 4,52 in Equation A.31 (shown rounded in equation A.32) can be rounded further to 2,5C_K and 4,4, respectively, for compatibility with earlier editions of this standard.

Combining the **attenuated output power**, P_α, with the power required to cause a 1°C temperature rise, P_{deg}, (Equation A.32) into the general *TI*-formula A.4 yields the result for the bone-at-focus model for **non-scanning modes:**

$$TIB_{\text{bs,ns}} = \min\left[\frac{\sqrt{P_\alpha(z_{\text{b,ns}})\, I_{\text{spta},\alpha}(z_{\text{b,ns}})}}{C_{TIB,1}}, \frac{P_\alpha(z_{\text{b,ns}})}{C_{TIB,2}}\right] \tag{A.33}$$

where

$C_{TIB,1}$ = 50 mW cm^{-1}

$C_{TIB,2}$ = 4,4 mW

As described in section 5.4.2.2 and A.4.2.1, in Equation A.33 the depth at which the $TIB_{\text{bs,ns}}$ is calculated, $z_{\text{b,ns}}$, is the depth, for $z > z_{\text{bp}}$ where the product of the **attenuated spatial-peak temporal-average intensity** and the **attenuated output power** maximizes.

$$z_{\mathrm{b,ns}} = \text{depth of } \max\left(P_{\alpha}(z) \text{ x } I_{\mathrm{spta},\alpha}(z)\right) \quad \text{(A.34)}$$

A.4.3.5 Derivation notes for bone at focus for scanning modes ($TIB_{\mathrm{bs,sc}}$)

An equation for the below-surface TIB for **scanning modes** could be arrived at using the same principals applied in Edition 1 and [22] for deriving the below-surface TIB for **non-scanning modes** and the at-surface TIB. However, again, Edition 2 is not following that approach.

There is considerably increased complexity and time associated with the measurement and estimation of $d_{\mathrm{eq}}(z)$ in **scanning modes**, and this is even more difficult in 3D and 4D **scanning modes**. It is preferable to choose formulas which give both reasonable results and which can be reasonably implemented in industrial measurement labs, where the constraints on measurement time and complexity must be considered. For the below-surface **non-scanning mode** case, suitable approximations for $d_{\mathrm{eq}}(z)$ were made in Edition 1 and [22]. But for scanning modes the complexity of approximations for $d_{\mathrm{eq}}(z)$ is significantly increased or their suitability are not well understood.

Therefore, use is made in Edition 2 of the claim in 62359 Edition 1 and in [22] that for most **scanning mode** cases the below surface temperature in bone is less than the at-surface temperature in soft tissue. Though limited support for the claim is given in Edition 1 and in [22] and though it seems reasonable that the claim is not true for some number of **scanning mode** operating conditions, some support is offered [25,26] that it may be true in many cases. This claim remains in Edition 2 and made use of by setting the $TIB_{\mathrm{bs,sc}}$ equal to the $TIS_{\mathrm{as,sc}}$.

$$TIB_{\mathrm{bs,sc}} = TIS_{\mathrm{as,sc}} = \frac{P_{1\mathrm{x}1}\, f_{\mathrm{awf}}}{C_{TIS,1}} \quad \text{(A.35)}$$

where

$C_{TIS,1}$ = 210 mW MHz

A.4.3.6 Derivation notes for bone at-surface [TIC] for non-scanning modes (~~$TIB_{\mathrm{as,ns}}$~~ TIC_{ns}) and for scanning modes (~~$TIB_{\mathrm{as,sc}}$~~ TIC_{sc})

Like the bone-at-focus model (clauses A.4.3.4 and A.4.3.5), the location of the maximum temperature increase for the bone-at-surface (cranial) case is at the proximal surface of the bone. Since the bone is located at the surface, or beam entrance, there is no attenuation and there is no compensation for **scanning modes** vs., **non-scanning modes**. The power parameter is **output power**, P.

The thermal model for bone-at-surface for **non-scanning modes** and **scanning modes** is conceptually the same as for the bone-at-focus models, with the **equivalent aperture diameter** at the surface, D_{eq}, replacing the **equivalent beam diameter**, d_{eq}. Therefore, the power required to cause a 1 °C temperature rise, P_{deg}, is

$$P_{\mathrm{deg}} = C_{\mathrm{sb}}\, D_{\mathrm{eq}} \times 1\ ^{\circ}\mathrm{C} \quad \text{(A. 36)}$$

where

C_{sb} = 40 mW cm^{-1} °C^{-1}

NOTE 1 There is no beam correction factor applied to D_{eq} as it is a fixed aperture dimension.

NOTE 2 ~~D_{eq} is calculated as described in 3.28 and A.4.2.1 for non-scanning modes.~~ For **non-scanning modes** D_{eq} is calculated as described in A.4.2.1 and in 3.28 using the **output beam area** A_{ob}, and for **scanning modes** D_{eq} is calculated as described in 3.28 using the **scanned aperture area** A_{sa}.

Combining the **output power**, P, with the power required to cause a 1 °C temperature rise, P_{deg}, (equation A.36) into the general TI-formula (equation A.4) yields the bone-at-surface expression for **non-scanning modes** and **scanning modes:**

$$TIC_{ns}, TIC_{sc} = \frac{P / D_{eq}}{C_{TIC}} \quad \text{(A. 37)}$$

where

C_{TIC} = 40 mW cm^{-1}

Annex B
(informative)

Guidance notes for measurement of output power in combined modes, scanning modes and in 1 cm × 1 cm windows

B.1 General

This standard requires, for **non-scanning modes** and **scanning modes** the measurement of the **output power** transmitted from the 1 cm × 1 cm area of the active array which transmits the most power. This is termed the **bounded-square output power**. This standard also requires, for **non-scanning modes** and **scanning modes,** the determination of the total (non-bounded) **output power**.

This annex deals primarily with the exceptions that must be made from the standard acoustic **output power** measurement procedures and requirements set out in IEC 62127 and IEC 61161. The following clauses provide guidance and describe techniques for the measurement of **output power** in scanning modes, describe windowing techniques using a 1 cm × 1 cm absorbing mask, a 1 cm × 1 cm radiation-force-balance target or electronic masking techniques.

Acoustic **output power** is often measured using a radiation force balance with an absorbing target large enough to intercept all of the propagating energy. Hydrophone raster scan measurement methods may also be used, if accurate enough (see note 2).

It is important to always distinguish between **output power** and radiation force. Ultrasonic **output power** is a scalar and does not depend on the local angle of incidence. Radiation force is a vector that depends on the local angle of incidence (with respect to the direction of the force-measuring device). For a plane-progressive wave the relation is simply $P = cF$ (Equation (B.1) in IEC 61161). In real fields deviations from this relation occur, mainly due to (a) diffraction, (b) focussing and (c) scanning (steering of **ultrasonic scan lines**, variable and non-parallel angles of incidence relative to the force measurement equipment detection axis). Deviations from Equation (B.1) due to diffraction are dealt with in B.4.2 in IEC 61161, those due to focussing are dealt with in B.5 of IEC 61161 and those due to scanning are dealt with here. ~~Focused beams and/or~~ Steered beams are dealt with in the same way.

If the summation of deviations is low enough when compared to the uncertainties desired, then the above effects may not need to be taken into account.

Output power and bounded-square output power measurements should have an uncertainty of ~~20~~ 30 % or less (95 % confidence level).

NOTE 1 Reflecting targets are not recommended for the radiation force measurements discussed here, particularly for **scanning modes**.

NOTE 2 IEC 62127-1 recommends that usually it is more accurate to measure total **output power** by means of the radiation force method, and refers to IEC 61161 ~~Edition 2~~.

B.2 Measurements for combined operating modes

In a **combined-operating mode** with more than one type of **transmit pattern** employed during the scan period, the **output power** may be considered separately for different **transmit patterns**. Such separation is allowed when necessary to permit accurate measurement of **output power** and determination of the **thermal index** by combining values appropriately as shown in Table 1. Such an approach may, for example, enable the appropriate **acoustic working frequency** to be used for each calculation. Caution is needed to ensure that each

selected single **transmit pattern** is identical to those used during (by) the **combined-operating mode**.

B.3 Measurement of output power, P, in scanning modes

B.3.1 Measurement when scanning beam is arrested

The beam scan is arrested in the forward direction normal to the absorbing target and the radiation force F_1 is measured and converted into the **output power** P_1 taking into account the effects of diffraction and focusing (per IEC 61161) in so far as these effects cannot be ignored when compared to the uncertainties to be desired .

When performing measurements with the beam scan arrested, the measured **output power** should be corrected to compensate for any beam-former related output variability, dependent on beam scan angle and/or linear position, and should be corrected to the scanning mode **pulse repetition rate**. When the beam and pulse characteristics of each **ultrasonic scan line** are equal (e.g. aperture size, pulse amplitude, centre frequency**,** pulse shape, **pulse duration, beamwidth**, focus angle, and so on) then it is appropriate to measure one ultrasonic scan line (the one most parallel with the radiation force detection axis), adjust for **pulse repetition rate** and assume that P_2 (scanning mode **output power**) = P_1. If the characteristics of each **ultrasonic scan line** are not the same, adequate correction or weighting should be applied.

NOTE 1 Examples of non-constant beam or pulse characteristics:

a) In phased array sector scanning, **output power** is sometimes increased for non-normal scan angles because of decreased element (reception) sensitivity off axis.

b) Different aperture sizes may be used for different **ultrasonic scan lines**.

Hydrophone measurements of **output power** may also be performed with the beam scan arrested, and should also include appropriate compensations for beam-former related variations between **ultrasonic scan lines**, as described above.

B.3.2 Measurements with beams scanning

Hydrophone measurements of **output power** with the beams scanning may be made by making use of a synchronizing system to synchronize the transmitted acoustic signal with the measurement system, such that one ultrasonic scan line at a time is measured via raster scan. Hydrophone element directional response corrections, taking into account the angle between (the **beam axis** of) each **ultrasonic scan line** and the hydrophone active element should be considered and applied as necessary. An alternative hydrophone method, such as described in IEC 62127, which employs hydrophones and RF power meters, may allow measurement without synchronizing on individual **ultrasonic scan lines**; however angular corrections or scan-line-specific compensations may be more difficult.

When performing these measurements in **scanning mode** with radiation-force-balances, the (absorbing) target and **external transducer aperture** should be such that the effective **beam area** is intercepted by the target over the entire extent of the beam.

The radiation force F_2 in a **scanning mode** is measured, taking into account the effect of diffraction and focusing (per IEC 61161 and [30]), and a correction based on the cosine formula is applied in so far as these effects cannot be ignored when compared to the uncertainties to be desired.

Ideally, the alignment of the (**beam axis** of each) **ultrasonic scan lines** and the direction of sensing of the radiation-force balance should be co-linear to within ±10°. As this is often not possible in sector scan modes (with non-parallel ultrasonic scan lines and therefore larger scanning angles), then compensation should be applied to the measured values.

If the pulse repetition rate and the beam and pulse characteristics of each **ultrasonic scan line** are equal (e.g. aperture size, pulse amplitude, center frequency**,** pulse shape, **pulse duration, beamwidth**, focus angle, and so on) then it is appropriate to assume that the measured (and adjusted for focusing and diffraction) **output power** F_2c multiplied by a correction factor (such as given in B.3.3 below, see also [31]) represents the output power in the scanning mode P_2. If the characteristics of the **ultrasonic scan lines** are not the same, adequate correction or weighting should be applied (for instance using a summation instead of Equation B.1 below and weighting each **ultrasonic scan line** appropriately).

The associated error in measurement will depend upon the specific geometry of the transducer and radiation-force-balance target. A simple example for a correction is given in B.3.3.

B.3.3 Example of a radiation-force to acoustic output power correction based on cosine formula

When using an absorbing target, any deviation of any portion of the field from the forward propagation direction (i.e. from the direction parallel to the detection direction of the force-measuring device) leads to a reduction of the radiation force as approximately cos(θ). In this example θ is considered the angle between the propagation direction (or **ultrasonic scan line beam axis)** and the sense direction of the radiation force detector.

Considering here a curved linear array (CLA) with total scanning angle Θ. It is possible to make corrections for the beam that is at a representative angle of θ. It is assumed that the power is distributed equally over the transducer in the scan direction.

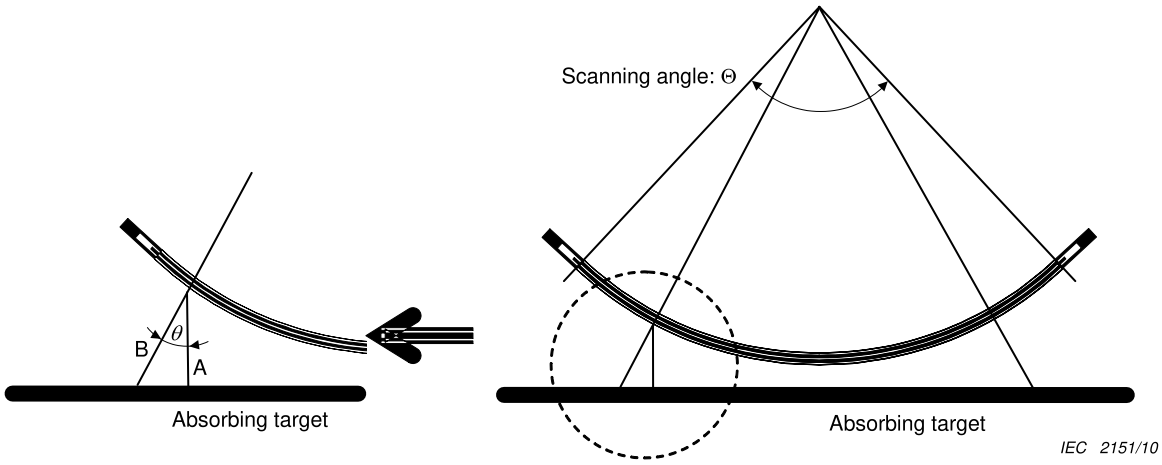

Figure B.1 – Example of curved linear array in scanning mode

Now assume that each **ultrasonic scan line** from –Θ/2 to Θ/2 is equal in average **output power** (although not in force directed parallel to the radiation-force detector sense direction). The force on the absorbing target that is actually measured is expressed as a vector A in Figure B.1, while vector B expresses what it should be. The radiation force measured by a large enough absorbing target for each scan line is expressed as $(P/c)\cos\theta$. The total measured radiation force F_2 can be obtained by integrating each force from –Θ/2 to Θ/2. F_2 can be calculated using the following equation:

$$F_2 = \frac{\frac{1}{c}\int_{-\Theta/2}^{\Theta/2} P\cos\theta d\theta}{\int_{-\Theta/2}^{\Theta/2} d\theta} = \frac{P_2}{c}\cdot\frac{2\sin\left(\frac{\Theta}{2}\right)}{\Theta} \qquad \text{(B.1)}$$

where

F_2 is the total radiation force from all scanning beams acting on the absorbing target;
P_2 is the true **scanning mode output power**;
c is the speed of sound in water;
θ is the angle between the propagation direction of incident beam and the direction of the force measuring device; and
Θ is the angle between the most widely separated **ultrasonic scanlines** of the active **scan plane,** in radians.

Therefore F_2 is converted to P_2 by multiplying F_2 by the reciprocal factor of above equation.

$$P_2 = \frac{\Theta}{2\sin\left(\frac{\Theta}{2}\right)}\cdot cF_2 \qquad \text{(B.2)}$$

If the total scanning angle is 60°, Θ = π/3 radian, the correction factor is calculated as 1,047 using equation B.2. If it is 90°, Θ = π/2, the correction factor would be 1,11.

NOTE 1 It has to be noted that to obtain the final power value, if not already taken care of in the determination of F_2, it may be needed to correct P_2 for diffraction and focusing.

B.4 Creating a 1 cm × 1 cm window using a mask of absorbing material or a 1 cm × 1 cm radiation force balance target

B.4.1 General

When a radiation force balance target is used to limit the aperture, its geometry and composition should be such as to detect all forward emissions from a 1 cm × 1 cm square area immediately in front of the **ultrasonic transducer** and not to detect emissions from outside that area.

The two techniques of defining the apertures in Clause B.4 have somewhat different sources of error. Agreement of the ~~two methods of defining the apertures~~ compared results from these methods, or compared to results from the method of Clause B.5, should give reasonable confidence that the aperture is defined accurately. Use of ~~an~~ these methods, absorbing mask (B.4.2) or ~~limited area radiation force balance absorber~~ absorbing target (B.4.3), to limit detection to a 1 cm × 1 cm area at the front surface of the active scan aperture is recommended ~~for mechanical sector probes, or third-party testing of all ultrasonic transducers~~ when the method of Clause B.5 is not feasible (e.g. for testing mechanically scanned sector probes, or third-party testing of all ultrasonic transducers).

B.4.2 1 cm × 1 cm aperture in a mask

When a mask is used, its geometry and composition should be such as to eliminate **output power** except that emitted by the designated 1 cm × 1 cm area of the active area of the transducer, to allow passage of all forward emissions from the unmasked area and to agree with the accuracy and other requirements of this standard.

The front surface of the **ultrasonic transducer** should be coplanar with the mask surfaces as illustrated in Figure B.3. This recommendation maintains consistency with B.3.2. The ultrasonic attenuation of the mask should be at least 30 dB and its window's inside walls should be lined with a reflective material to minimize loss in the walls.

Bounded-square output power measurements demonstrating that the mask meets the attenuation criteria should be made; otherwise **bounded-square output power** measurements should be made with two mask thicknesses, thereby demonstrating no (or marginal) influence of the mask thickness. Figure B.2 presents a sketch of a suggested geometry. A material with a maximum attenuation coefficient and minimum impedance mismatch with water is recommended. Materials are available commercially that are well matched to water (reflection coefficient: –30 dB) and have a loss in the range of 45 dB/cm at 3,5 MHz. Additional attenuation can be provided by sandwiching a stainless-steel, closed-pore foam or other high- or low-impedance reflector between two layers of the ultrasonic attenuating material.

For measurement of the **bounded-square output power**, the mask x- and y-dimensions should be aligned with respect to the transducer assembly under test and its x and y axis, as illustrated in Figure B.3. For instance, for 2D-**scanning modes** with simple 1D-transducer assemblies, the imaging plane axis can be set equal to x and the elevation dimension can be set equal to y. Lateral positioning is critical, **ultrasonic transducer** probe holders and jigs will be helpful in this regard. It is anticipated that an alignment of the beam alignment axis within ±5° of the normal to the mask plane and target plane and the x- and y-axes of the **transducer assembly** under test alignment within ±5° of the x- and y-axes of the mask are sufficient for the purposes of this test (see Figure B.3).

NOTE For a number of beams the mask requirements can be relaxed:

- For contact transducers, if an **output beam dimension** (X_{ob} or Y_{ob}) is less than 1 cm in any direction, then the mask's aperture may be greater than 1 cm wide in that direction.
- For transducers used with a standoff path, the mask's aperture may be larger than 1 cm in any direction in which hydrophone scanning has demonstrated that the –20 dB **beam- width** at the entrance plane is less than 1 cm.

B.4.3 1 cm × 1 cm area radiation-force-balance target

As an alternative to the use of an aperture-limiting mask, the measurement of the **bounded-square output power** may be made using a 1 cm × 1 cm area - radiation-force target. When the 1 cm × 1 cm area radiation-force-balance (RFB) target is used, it should be placed immediately in front of the **ultrasonic transducer** and its geometry and composition should be such that it detects all of, and only, the acoustic emissions from a 1 cm × 1 cm area of the **ultrasonic transducer**.

The accuracy and linearity of the measurement of **bounded-square output power** should conform to IEC 61161.

To minimize measurement errors due to reverberations, caution should be used to ensure that reflected acoustic energy does not reflect back onto the target. Further, the orientation of the target's x- and y-axes should remain co-linear with the chosen x- and y- axes of the **transducer assembly** under test, as illustrated in Figure B.4.

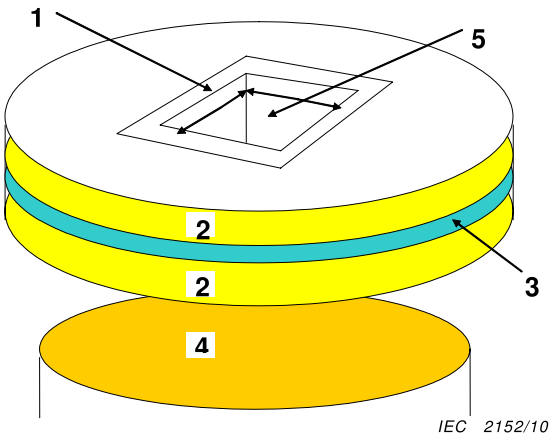

Key

1: Lining
2: Absorber
3: Sandwich layer
4: Ultrasonic transducer
5: 1 cm × 1 cm window

Figure B.2 – Suggested 1 cm × 1 cm square-aperture mask

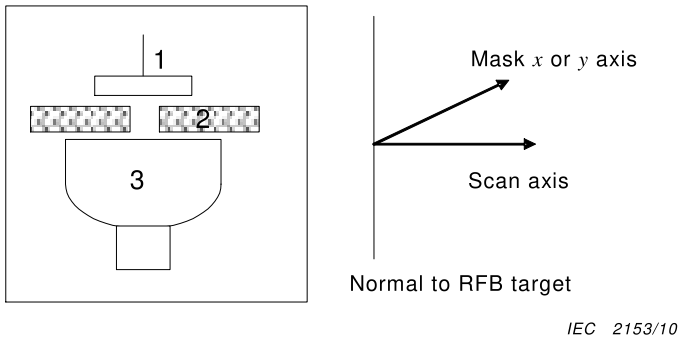

Key

1: RFB Target

2: Mask

3: Ultrasonic transducer

Figure B.3 – Suggested orientation of transducer, mask aperture and RFB target

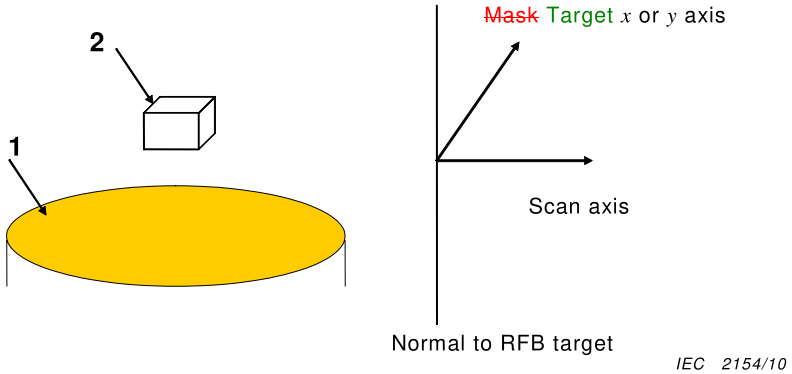

Key

1: Ultrasonic transducer

2: 1 cm-square RFB target

Figure B.4 – Suggested orientation of transducer and 1 cm-square RFB target

B.5 Creating a 1 cm × 1 cm window using electronic control or using calculations

Where the **equipment** control scheme and transducer geometry allow, masking a 1 cm × 1 cm square-area aperture may be accomplished electronically by de-energizing the aperture outside this area, provided that the **output power** emitted within the 1 cm × 1 cm square area aperture is not affected by the electronic masking.

Electronic means for masking the active aperture for a 1 cm × 1 cm square-area aperture are recommended where feasible with electronically controllable arrays (sequenced, phased, or combination).

In cases where arrays are electronically controllable in one dimension (e.g. scan-dimension, x) but not the other (e.g. transducer element lengths, $y > 1$ cm), the measurement of **bounded-square output power** can be achieved by electronically masking the elements outside 1 cm in the x dimension, making the power measurement and then mathematically adjusting the power value to a y-dimension of 1 cm.

Where transducer geometry and ultrasound radiation allows, mathematical~~ly~~ windowing, or a combination of acoustic windowing and mathematical~~ly~~ windowing, is allowed. ~~For example, in a case of linear scanning the ratio of scan width to 1 cm could be used in the calculation, although in a number of cases it is not simply the ratio of the two.~~

B.6 Measurement of bounded-square output power

While using the methods of B.4.2 or B.4.3 or Clause B.5 to ~~mask~~ eliminate all the **output power** except that originating through a 1 cm × 1 cm square window within the **output beam area** in **scanning mode**, the remaining **bounded-square output power** should be measured according to the procedures in IEC 61161.

In locating the mask used in either B.4.2 or Clause B.5, or the target used in B.4.3, the 1 cm × 1 cm square aperture emitting the largest bounded **output power**, should be exposed.

The uncertainty of the measurement of bounded-square power should be 20% or less.

Annex C
(informative)

The contribution of transducer self-heating to the temperature rise occurring during ultrasound exposure

The issue of temperature increase occurring during clinical exposure to diagnostic ultrasound is relevant to several current and future national and international standards. The present standard is particularly important in this regard as it specifies formulae for calculating a number of thermal indices (*TI*) which are used to provide safety-related real-time feedback to clinical users. The majority of manufacturers of ultrasound imaging equipment now comply with the IEC 60601-2-37 standard which refers to the present standard for the method of determining *TI* values to fulfil international regulations. Consequently, most modern scanners calculate and display *TI* values which are used by clinicians and sonographers in making their clinical risk assessments.

TI values are calculated from measurements of acoustic quantities made with hydrophones and radiation force balances. Essentially, the formulae used are a simplified method of estimating the temperature rise produced by the absorption of ultrasound. However, there is a second major cause of tissue heating which is ignored by the present standard and that is self-heating of the ultrasound transducer. This self-heating is caused by electrical inefficiency of the transducer; efficiencies are typically around 30% meaning that more than twice as much energy is liberated as heat in the transducer than is absorbed and converted to heat in the exposed tissue. For most transducers, most of the heat produced by the transducer is generated in the thin piezoelectric layer adjacent to the contact surface with the tissue.

Studies [32,33,34,35,36] with Thermal Test Objects (TTO) and a range of clinical pulsed Doppler transducers have shown that over three minutes exposure, self-heating accounts for approximately half of the temperature rise in the TTO at a distance of 7 mm from the transducer. At smaller distances or for longer exposure times, self-heating will be an even larger contribution. It is clear, therefore, that any proper evaluation of the thermal hazard must include transducer self-heating. One approach would be to model the transducer itself mathematically by consideration of the electrical and thermal properties of the piezoelectric element and the transducer case. This would certainly be feasible as an academic study (see Saunders [37]). However, in general, the properties and construction of the transducer will not be known (except, possibly, by the transducer manufacturer) so a simpler, more practicable method which could be implemented in future national and international standards should be proposed.

Studies are on-going which suggest that, subject to certain simplifying assumptions, the temperature profile (due to self-heating) as a function of distance from the transducer can be approximated from a single measurement of the temperature at or close to the transducer/tissue interface. The total temperature can then be given by the summation of the self-heating contribution and the contribution due to local ultrasound absorption within the medium. The need to take this approach in the present standard could not reach consensus and introduction of such methods is postponed to a third edition of this standard.

Annex D
(informative)

Guidance on the interpretation of *TI* and *MI*

D.1 General

It is beyond the scope of this standard to go into detail on the relation of the **thermal index** (*TI*) and **mechanical index** (*MI*) to safety. In addition to the short notice below, interested users are invited to consult the references in the Bibliography [5,7,8,11].

The relationship of various acoustic **output parameters** (for example, **acoustic intensity**, **acoustic pressure**, **output power**, etc...) to biological effects is not presently fully understood. Evidence to date has identified two fundamental mechanisms, thermal and mechanical, by which ultrasound may induce bioeffects [12,13,14,21,38,39], and in certain cases alteration or damage to tissue. The thermal mechanism is temperature rise due to energy absorption and the mechanical bioeffects may be caused by various kinds of cavitation, due to reduced instantaneous pressure.

The temperature rise and the possibility of cavitation seem to depend on such factors as the total energy output, the mode, the shape of the ultrasound beam, the position of the focus, the centre frequency, the shape of the waveform, the frame rate, and the duty factor. The *MI* and *TI* are designed to take the most important of these factors into account and give the user information in real time about the potential for thermal or mechanical bioeffects. Because the *MI* and *TI* reflect instantaneous output conditions, they do not take into account the cumulative effects of the total examination time, especially with regard to heating. It is relevant to emphasize that shortening insonation times can give a large safety margin under some conditions (wide, scanning beams in soft tissue) but no significant margin under other conditions (narrow , non-scanning beams on bone) [26]. It is the responsibility of the **operator** to understand the risk of the output of the equipment, and to act appropriately in order to obtain the needed diagnostic information with the minimum risk to the patient. To be able to do so, the manufacturer of the device will provide information to the user on how to interpret the displayed ultrasonic exposure parameters, **thermal index** and **mechanical index** (see IEC 60601-2-37). Further guidance on of the rationale and derivation of *MI* and *TI* are given in [27,40].

D.2 Limitations of the indices

- Although Table 1 gives a method to add the contributions of different discrete modes the method has some disadvantages. For example, the below-surface *TI*-formulation would ideally be a maximum of the summation, at each depth z, of the scanning and non-scanning—contributions. However, Table 1 specifies a summation of the individual maximum, and assumes (as per A.5.3.3 and A.5.3.5) that the maximum below surface *TI* value in scanned modes is less than or equal to the at-surface, soft tissue *TI* ($TIS_{\mathrm{as,sc}}$).
- Originally the formulations for *TI* were not intended for use in ophthalmic applications. Recently *TI* has been used for ophthalmic applications [41], However special caution is advised. This issue is further addressed in the following.
- Finite amplitude effects are known to alter intensities and pressures measured in water in a non-linear way. As the models used in this standard are linear, the *in situ* exposures may be 1,5 or 2,0 times the values indicated by *TI* or *MI* [42]. If a correction method for this effect has not been applied, this should be made known to the **operator**.
- The *TI value*s predict heating in tissue next to the transducer surface due only to the energy absorbed from the beam. No correction is made for the heating of superficial tissues by the transducer itself, which may be significant (see Annex C).

- As noted in Annex A, imposition of the **break-point depth** (z_{bp}) requirement, while useful for separating 'at-surface' and 'below-surface' *TI value*s, and for preventing hydrophone-to-transducer contact, creates an unexamined region which, particularly for **f-numbers** below 1,5, may contain the highest below-surface temperature.
- The *TI* represents average values calculated according to a model and should NOT be interpreted as the numerical value of the actual temperature rise in °C in the insonated tissues. Nevertheless, relationships between these quantities have been studied and resulting cautions are given in this annex. As has been explained, there are limitations on the models underlying both the *MI* and *TI*. These models contain practical simplifications to complex and incompletely understood bio-effects interactions. Because of this fact, their use is to be limited to relative indication of bio-effect risk. The operator should be aware that, in a limited number of cases, the actual worst-case temperature rise may be up to three times higher than the displayed *TI* value, if it were interpreted in °C [29]. The *TIS value*s are based on a model of linear array scanners, focussing energy on a line. For circular transducers with a point-focus, a theoretical calculation [11] for ratios between numerical value of temperature rise and the *TIS* value for the **non-scanning** mode yielded results that ranged from 0,24 to 109. The ratio 109 was calculated for a hypothetical 4-cm diameter transducer, f-number 0,7 at 12 MHz [11]. This is an (extreme) atypical case of medical diagnostic ultrasound and it should be noted the calculated temperature rise was less than 0,01°C, while the *TIS* value was less than 0,0001. As mentioned earlier and as indicated in [11], the ratio of 109 results primarily from limiting the axial search for the *TIS* to depths ≥ the **break-point depth**, 6 cm in this case, while the nominal focus of the transducer, and the position of maximum calculated temperature rise, is at 2,8 cm.
- The model for calculating *TI* assumes some cooling by blood perfusion. For applications where poorly perfused tissues are insonated, the *TI* may underestimate the numerical value of the worst-case temperature rise, and the *TI* displayed during such a clinical exam should accordingly be maintained at a lower value than is usually employed. Conversely, when scanning well-perfused organs, such as hepatic, cardiac or vascular structures, the value of *TI* displayed may overestimate the numerical value of the actual temperature rise.
- The models use a fixed attenuation coefficient and as such do not take long, low-attenuation fluid paths into account. In such cases, the ultrasound energy will not be absorbed as much as the model assumes with the result that the tissue distal to the fluid path may be exposed to higher energy levels than the models predict. For example, scanning through a full bladder or amniotic fluid may result in displayed *TI value*s that underestimate numerical value of the actual temperature rises. On the other hand, the fixed attenuation coefficient used (0,3 dB $cm^{-1}MHz^{-1}$) is considerably smaller than average values for human tissue. Therefore, in many cases, tissues may be exposed to lower levels of energy than the models predict.
- The meaning of "reasonable worst case" is taken as that given by the World Federation for Ultrasound in Medicine and Biology [43], namely "that set of tissue properties and dimensions such that less than 2,5% of patients have a higher calculated temperature increase or other thermal endpoint if their actual tissue properties or thicknesses differ from those employed in the calculations".

Annex E
(informative)

Differences from IEC 62359 Edition 1

E.1 General

The methods of determination set out in Edition 1 of this standard are based on those contained in the standard for Real–Time Display of Thermal and Mechanical Acoustic Output Indices on Diagnostic Ultrasound Equipment [22] and were intended to yield identical results.

The models on which these determinations are based and the measurement and calculation rationale are contained in [22] and in its secondary references. Edition 1 of this standard has followed [22]. While Edition 2 also follows [22] in principal and uses the same basic formulae and assumptions (see Annex A), it contains a few significant modifications which deviate from [22].

One of the primary issues dealt with in preparing the Edition 2 of this standard is 'missing' TI equations. In Edition 1 there were not enough equations to make complete 'at-surface' and 'below-surface' summations for TIS and TIB in combined-operating modes.

Annex F was added to Edition 2 of this standard to support the definition and determination of maximum positions and values of I_{spta}, $I_{\text{spta},\alpha}$, I_{sppa} and $I_{\text{sppa},\alpha}$ specified by IEC 60601-2-37.

NOTE Similar to the below-surface TI values, these are also specified to be found on the **beam axis** beyond the **break-point depth** z_{bp}.

E.2 Differences from IEC 62359 Edition 1

While there have been numerous editorial changes and clarifications, the technical changes and major editorial clarifications in Edition 2 come down to a relative few.

Some of the major changes from Edition 1 are related to the introduction of new calculations of thermal indices to take into account both "at-surface" and "below-surface" thermal effects:

TI in single modes of operation

TIS_{as}

- The substitution of $P_{1\text{x}1}$ for P_1 in $TIS_{\text{as,sc}}$.
  (See Annex A.4.1.4 and A.4.1.5)
- The calculation of $TIS_{\text{as,ns}}$ for all aperture sizes.
- Using the same TIS_{as} equation for both **non-scanning modes** and **scanning modes**.

TIS_{bs}

- For **non-scanning modes** the $TIS_{\text{bs,ns}}$ equation now applies (is calculated) for all aperture sizes.
- For **scanning modes** a $TIS_{\text{bs,sc}}$ equation has been added.

TIB_{bs}

- For **scanning modes** a $TIB_{\text{bs,sc}}$ equation has been added.

TI in combined modes of operation

- The TI is simply the maximum of the 'At-Surface Summation' or the 'Below-Surface Summation'. New in Edition 2 of the standard, there is an at-surface term (as) and a below-surface term (bs) for each active **Transmit Pattern** regardless of whether scanning or non-scanning or of aperture size. These at-surface and below-surface terms are calculated at all times.

- From Table 1 of section 5.6:

$$TIS = \mathrm{Max}\left[\sum_{\substack{Discrete\\Modes}} TIS_{\mathrm{as}}, \sum_{\substack{Discrete\\Modes}} TIS_{\mathrm{bs}}\right] \qquad TIB = \mathrm{Max}\left[\sum_{\substack{Discrete\\Modes}} TIS_{\mathrm{as}}, \sum_{\substack{Discrete\\Modes}} TIB_{\mathrm{bs}}\right]$$

z_{bp}

- Edition 2 makes clearer that z_{bp} is to be applied to $TIS_{\mathrm{bs,ns}}$, $TIB_{\mathrm{bs,ns}}$ and not to MI.
- In Edition 2 a **depth for** MI (z_{MI}) is specifically defined.

P_{sc}

- Explanation and equations have been added to Annex B describing the additional complexity and sources of error in the determination of acoustic output power in scanning modes (Psc). Recommended corrections are described for non-normal incidence (i.e. if measuring in **scanning modes** without arresting the beam scanning).

Beam-axis

- Edition 2 makes clearer that measurements are to be made on the **beam-axis**.

NOTE Transverse scans which, at depths of interest, re-affirm that the **beam-axis** remains found are recommended.

Table E.1 summarizes some of the major changes.

NOTE The $I_{\mathrm{spta},\alpha}(z_{\mathrm{b,ns}})$ and $I_{\mathrm{spta},\alpha}(z_{\mathrm{s,ns}})$ values shown in Table E.1 are not the "maximum" **attenuated spatial-peak temporal-average intensity** values described in Annex F, because they are at the **depth for** TIB and the **depth for** TIS, respectively.

Table E.1 – Summary of differences

Parameter	Edition 1	Edition 2
z_{bp}	$z_{bp} = 1{,}5 \times D_{eq}$	• No change to formula z_{bp} is only used in determining below-surface TI for non-scanned modes. z_{bp} is also applied to I_{spta}, $I_{spta,\alpha}$, I_{sppa} and $I_{sppa,\alpha}$ determination described in Annex F.
MI	$MI = \frac{p_{r,\alpha}(z_{MI}) \cdot f_{awf}^{-1/2}}{C_{MI}}$	• No change to formula • Measure at $z = z_{MI}$ is now stated.
$TIS_{as,ns}$	• TIS_{ns} is calculated at-surface only when **output beam area** (A_{ob}) is ≤ 1 cm^2 $TIS_{ns} = \frac{P f_{awf}}{C_{TIS,1}}$	• Calculate for all A_{ob} sizes. $TIS_{as,ns} = \frac{P_{1x1} f_{awf}}{C_{TIS,1}}$
$TIS_{as,sc}$	$TIS_{as,sc} = \frac{P_1 f_{awf}}{C_{TIS,1}}$	$TIS_{as,sc} = \frac{P_{1x1} f_{awf}}{C_{TIS,1}}$
$TIS_{bs,ns}$	• TIS_{ns} is calculated only when **output beam area** (A_{ob}) is > 1cm^2 $TIS_{ns} = \max_{z \geq z_{bp}} \left[\min \left[\frac{P_\alpha(z_{s,ns}) f_{awf}}{C_{TIS,1}}, \frac{I_{spta,\alpha}(z_{s,ns}) f_{awf}}{C_{TIS,2}} \right] \right]$	• Calculate for all A_{ob} sizes • No change to formula
$TIS_{bs,sc}$	• No formula specified.	• Same formula as $TIS_{as,sc}$ $TIB_{bs,sc} = TIS_{as,sc} = \frac{P_{1x1} f_{awf}}{C_{TIS,1}}$
$TIB_{bs,ns}$	$TIB_{bs,ns} = \min \left[\frac{\sqrt{P_\alpha(z_{b,ns}) I_{spta,\alpha}(z_{b,ns})}}{C_{TIB,1}}, \frac{P_\alpha(z_{b,ns})}{C_{TIB,2}} \right]$	• No change to formula • Measure at $z \geq z_{bp}$ is now stated.
$TIB_{bs,sc}$	• No formula specified.	• Same formula as $TIS_{as,sc}$ $TIB_{bs,sc} = TIS_{as,sc} = \frac{P_{1x1} f_{awf}}{C_{TIS,1}}$
$TIC_{as,ns}$ $TIC_{as,sc}$	$TIC = \frac{P / D_{eq}}{C_{TIC}}$	• No change to formula

Annex F
(informative)

Rationale and determination of maximum non-attenuated and attenuated spatial-peak temporal-average intensity and spatial-peak pulse-average intensity values

F.1 Rationale

This standard establishes parameters and methods related to thermal and non-thermal exposure aspects of diagnostic ultrasonic fields sufficient to calculate **mechanical index** (MI) and **thermal index** (TI) for display as specified in IEC 60601-2-37.

In the process of describing the determination of the **thermal index** and the **mechanical index**, this standard defines and describes the key components for deriving maximum non-attenuated and attenuated spatial-peak temporal-average and spatial-peak pulse-average intensities at any depth z in the acoustic field. Meanwhile, the acoustic output reporting tables specified in IEC 60601-2-37 require the provision of the spatial maximum values of these parameters in the acoustic field at specific depths z; including providing spatial maximum values over all depths z on the **beam axis** beyond the **break-point depth**, and "local" spatial maximum values at other depths on the **beam axis**.

NOTE 1 Other interested parties also require provision of these parameters at 'global' spatial maximum positions, and in some cases have established regulatory limits on their values.

NOTE 2 Recall from the definitions in Clause 3 that "spatial peak" in the terms "**attenuated spatial-peak temporal-average intensity**" and "**attenuated spatial-peak pulse-average intensity"** is the peak value at a given depth, z (i.e. not the peak value over all depths, z).

NOTE 3 The depths at which the MI and below-surface TIS and below-surface TIB are determined will not generally be the same depths at which the maximum values of I_{spta}, $I_{spta,\alpha}$, I_{sppa} or $I_{sppa,\alpha}$ occur.

This standard refers to IEC 62127-1, IEC 62127-2 and IEC 62127-3 for definitions, specifications of properties and calibration of measurement equipment and for hydrophone-based measurement methods. IEC 62127-1 defines various acoustic parameters which can be used to specify and characterize ultrasonic fields propagating in water using hydrophones. IEC 61157 also defines various acoustic parameters which can be used to specify and characterize ultrasonic fields propagating in water.

While these standards provide valuable information on the measurement of ultrasound fields, they do not describe standardized determination of maximum non-attenuated or **attenuated spatial-peak temporal-average intensity**, I_{spta} and $I_{spta,\alpha}$ nor non-attenuated or **attenuated spatial-peak pulse-average intensity** I_{sppa} and $I_{sppa,\alpha}$. Therefore, standardized means and definitions for their determination are provided in Annex F.

In combination with IEC 62127 and IEC 61161, this standard describes a complete set of methods for determining all acoustic output parameters for **medical diagnostic ultrasonic equipment** used within the ultrasound community, including those parameters called for by IEC 60601-2-37.

F.2 Overview

The goal of this Annex F is to describe standardized methods for determination of maximum positions and values of non-attenuated and **attenuated spatial-peak temporal-average intensity** I_{spta} and $I_{spta,\alpha}$, and non-attenuated and **attenuated spatial-peak pulse-average intensity** I_{sppa} and $I_{sppa,\alpha}$, in the acoustic field of a medical diagnostic ultrasound device.

Other, non-IEC, measurement standards define the determination of $I_{\text{spta},\alpha}$ and $I_{\text{sppa},\alpha}$ for regulatory agency purposes. Reference [44] is used widely and is referenced in IEC 62127-1. The methods listed in this Annex F are intended to be consistent with [44].

The standard attenuation coefficient value chosen is 0,3 dB cm^{-1} MHz^{-1}; the same value is introduced and used by this standard in the derivation of the below-surface **thermal index** and the **mechanical index**.

Another key similarity to the below-surface **thermal index** and the **mechanical index** is to remain on the **beam axis** when finding the position of spatial maximum values.

Similarly, this standard defines the **break-point depth**, and applies it in the determination of the below-surface thermal indices TIS and TIB for **non-scanning modes**. This same **break-point depth** is used for maximum I_{spta}, I_{sppa}, $I_{\text{spta},\alpha}$ and $I_{\text{sppa},\alpha}$ and is applied for both **scanning modes** and **non-scanning modes**.

As shown, for **non-scanning modes** one depth $z_{pii,\alpha}$ is used for the **depth of maximum $I_{\text{spta},\alpha}$** and **depth of maximum $I_{\text{sppa},\alpha}$**, and one depth z_{pii} is used for the **depth of maximum I_{spta}** and **depth of maximum I_{sppa}**.

However, as shown, for **scanning modes** the depths of maximum $I_{\text{spta},\alpha}$ and $I_{\text{sppa},\alpha}$ (and I_{spta} and I_{sppa}) can be different, and the depths of maximum I_{spta} and $I_{\text{spta},\alpha}$ often are not at the same depth as they occur for **non-scanning** modes.

Describing the determination of the $I_{\text{spta},\alpha}$ and I_{spta} for **scanning modes** is the most complicated and large part of Annex F. F.3.3.2 and F.3.1.4.2 give the summarized expressions while Clause F.4 gives more detailed information.

F.3 Test methods

F.3.1 Common parameters

F.3.1.1 Attenuation coefficient and frequency

The **acoustic attenuation coefficient** value α used for the determination of maximum $I_{\text{spta},\alpha}$ and $I_{\text{sppa},\alpha}$ is 0,3 dB cm^{-1} MHz^{-1} with linear frequency dependence.

NOTE 1 This value is the same as is used in the determination of the MI and TI, and it matches the attenuation coefficient used in [41] and [44].

Repeating Equation (A.6) in A.4.2.3:

The **attenuated spatial-peak temporal-average intensity** is denoted:

$$I_{\text{spta},\alpha}(z) = I_{\text{spta}}(z)\,10^{(-\alpha z\, f_{\text{awf}}/10\text{dB})}$$

where

$I_{\text{spta}}(z)$ is the **spatial-peak temporal-average intensity** at distance z,

α is the **acoustic attenuation coefficient**,

f_{awf} is the **acoustic-working frequency**, and

z is the distance from the **external transducer aperture** to the point of interest.

NOTE 2 In accordance with 3.4, NOTE 2, and 3.24, the **acoustic-working frequency** is determined at the **depth for peak pulse-intensity integral** on the **beam axis**.

NOTE 3 See A.4.2.3, 5.1 and Clause D.2 for additional discussion.

F.3.1.2 Use of the beam axis

Measurements for I_{sppa}, $I_{sppa,\alpha}$, I_{spta} and $I_{spta,\alpha}$ in **non-scanning modes** should be made on the **beam axis**.

NOTE While there can be side-lobes with higher intensity and pressure values, the same methodology and justification as is employed for the below-surface **thermal index** and the **mechanical index** is used, for the sake of measurement repeatability and ease.

F.3.1.3 Determination and use of the break-point depth

Measurements for I_{sppa}, $I_{sppa,\alpha}$, I_{spta} and $I_{spta,\alpha}$ in **scanning modes** and **non-scanning modes** are made at or beyond (farther-than) the **break-point depth** z_{bp}.

Care is to be taken when determining the z_{bp} so that the **equivalent aperture diameter** is correctly determined using only the –12 dB **output beam area**.

For **scanning modes** where **ultrasonic scan lines** that comprise a frame do not have the same –12 dB aperture size, the aperture size corresponding to the central scan line of each $sppsi$ sum is to be used in the determination of **the break-point depth**.

For **combined-operating modes** where measurement of multiple modes and **transmit patterns** is being performed simultaneously, the smallest **break-point depth** of the active modes is to be used.

For **combined-operating modes** in which measurements of contributing modes and **transmit patterns** are being performed sequentially, the **break-point depth** of each separated mode is to be used.

F.3.1.4 Calculation of $ppsi_\alpha(z)$, $ppsi(z)$, $sppsi_\alpha(z)$ and $sppsi(z)$

F.3.1.4.1 $ppsi_\alpha(z)$

The calculation of $ppsi_\alpha(z)$ is accomplished by using Equation (27) (see 3.63).

NOTE 1 For measurement purposes of this standard, pii_α is equivalent to $1/(\rho c)$ times the **attenuated pulse-pressure-squared integral** at depth z, when z is beyond the **break-point depth,** with ρc denoting the characteristic acoustic impedance of pure water.

NOTE 2 3.43 gives the non-attenuated version of this quantity.

F.3.1.4.2 $s_\alpha ppsi(z)$ and $sppsi_\alpha(z)$ and $sppsi(z)$

The following discussion is for the **sum of attenuated pulse-pressure-squared integrals**. Application to non-attenuated sum is the same, but can be more simple because the **acoustic working frequency** does not need to be known or estimated for each scan line.

The determination of the **sum of attenuated pulse-pressure-squared integrals** and the **attenuated sum of pulse-pressure-squared integrals** for adjacent **ultrasonic scan lines** at any depth z may be accomplished using one of the following methods. Generally, these methods require knowledge, a priori or determined, of the number of **ultrasonic scan lines** per scan frame, the number of transmit pulses per scan line and the **acoustic working frequency** or a frame trigger that signals the start/stop of repeating frames.

NOTE 1 See F.4.2 for additional discussion of these methods.

NOTE 2 See IEC 62127-1:2007, Annex F, for additional discussion of these $sppsi(z)$ determination methods.

While either method a) or b) can be employed, it can be seen that as the pulse sequencing becomes increasingly complicated, increased knowledge of the pulses and the pulse sequencing is required.

a) Scanning **ultrasonic scan lines** past a stationary hydrophone

This may be accomplished by:

1) using a long record digitizer to sum the $ppsi$ values in one long record, or

2) via an electronic mask or electronic trigger which signals one **ultrasonic scan line** at a time so that the $ppsi(z)$ for each transmit pulse down that line, n, can be acquired and added to the $sppsi$ sum.

For either method 1) or 2) above, if all transmit pulses included in the sum are NOT identical, then the f_{awf} value of each pulse is to be obtained and the **attenuated pulse-pressure-squared integral** $ppsi_\alpha(z)$ calculated for each transmit pulse. The **sum of attenuated pulse-pressure-squared integrals** $sppsi_\alpha(z)$ is thus obtained.

If all transmit pulses included in the sum are identical, then the $sppsi(z)$ value may be determined separately and one attenuation factor applied to obtain the **attenuated sum of pulse-pressure-squared integrals** $s_\alpha ppsi(z)$ which in this case is equivalent to the $sppsi_\alpha(z)$.

b) Scanning a hydrophone past a single stationary **ultrasonic scan line**

This method can yield estimates of the **attenuated sum of pulse-pressure-squared integrals** $s_\alpha ppsi(z)$ and the **sum of attenuated pulse-pressure-squared integrals** $sppsi_\alpha(z)$ which are reasonably accurate when all **ultrasonic scan lines** use identical transmit pulses (f_{awf}, pulse length, pulse shape, pulse focusing and aperture, etc.).

This method consists of scanning a hydrophone past a single stationary **ultrasonic scan line**, collecting **pulse-pressure-squared integrals** at multiple lateral beam (profile) locations with sufficient spatial step size (sampling) such that the **pulse-pressure-squared integrals** corresponding to the equivalent locations of adjacent **ultrasonic scan lines** scanning past a stationary hydrophone are calculated.

This method requires knowledge of the spacing between successive **ultrasonic scan lines**.

NOTE 1 A method for experimentally determining the spacing between **ultrasound scan lines** is provided in IEC 62127-1:2007, 7.2.6.3.

NOTE 2 Another reference is IEC 62127-1:2013+IEC 62127-1:2013/AMD1:2013, 8.2.

If the transmit pulses for all **ultrasonic scan lines** (pulse shape, **beamwidth**, etc.) are not all identical, then choosing a worst case pulse and scan line may provide a reasonable over-estimate. The **ultrasonic scan line** and pulse yielding the largest $s_\alpha ppsi(z)$ value should be chosen. Choosing an **ultrasonic scan line** in the centre of the scan should be sufficient.

NOTE 3 Multiple $s_\alpha ppsi$ sums may be needed at each depth z in order to find the largest sum.

F.3.1.5 Measurement depth for maximum $I_{spta,\alpha}$, I_{spta}, $I_{sppa,\alpha}$ and I_{sppa}

For **non-scanning modes**, the **depth for maximum** $I_{spta,\alpha}$, $z_{spta,\alpha,max}$ is the depth on the **beam axis**, at or beyond the **break-point depth**, where the maximum **attenuated pulse-pressure-squared integral** $\max_{z \geq z_{bp}} [ppsi_\alpha(z)]$ occurs. This is the **depth for maximum** pii_α, $z_{pii,\alpha}$.

NOTE 1 The **depth for maximum** $I_{spta,\alpha}$, $z_{spta,\alpha,max}$, for **non-scanning modes** is equal to the **depth for maximum** $I_{sppa,\alpha}$, $z_{sppa,\alpha,max}$, both occurring at $z_{pii,\alpha}$.

For **non-scanning modes**, the **depth for maximum** I_{spta}, $z_{spta,max}$ is the depth on the **beam axis,** at or beyond the **break-point depth**, where the maximum **pulse-pressure-squared integral** $\max_{z \geq z_{bp}} [ppsi(z)]$ occurs. This is the **depth for maximum** pii, z_{pii}.

NOTE 2 The **depth for maximum** I_{spta} ($z_{spta,max}$) for **non-scanning modes** is equal to the **depth for maximum** I_{sppa}, $z_{sppa,max}$, both occurring at z_{pii}.

For **scanning modes**, the **depth for maximum** $I_{\mathbf{spta},\alpha}$, $z_{\text{spta},\alpha,\text{max}}$, is the depth, on the **beam axis**, at or beyond the **break-point depth**, where the maximum **sum of attenuated pulse-pressure-squared integrals** $\max_{z \geq z_{\text{bp}}} \left[sppsi_{\alpha}(z) \right]$ occurs. This is the **depth for maximum** sii_{α}, $z_{sii,\alpha}$.

For **scanning modes**, the **depth for maximum** $I_{\mathbf{spta}}$, $z_{\text{spta,max}}$, is the depth, on the **beam axis**, at or beyond the **break-point depth**, where the maximum **sum of pulse-pressure-squared integrals** $\max_{z \geq z_{\text{bp}}} \left[sppsi(z) \right]$ occurs. This is the **depth for maximum** sii, z_{sii}.

NOTE 3 See F.3.1.3 regarding the **break-point depth** to use when the **ultrasonic scan lines** do not have the same –12 dB aperture size.

For **non-scanning modes** and for **scanning modes**, the **depth for maximum** $I_{\mathbf{sppa},\alpha}$, $z_{\text{sppa},\alpha,\text{max}}$, is the depth on the **beam axis**, at or beyond the **break-point depth**, where the maximum attenuated pulse-pressure-squared integral $\max_{z \geq z_{\text{bp}}} \left[ppsi_{\alpha}(z) \right]$ occurs. This is the depth for maximum pii_{α}, $z_{pii,\alpha}$.

NOTE 4 This is the same depth as for maximum $I_{\text{spta},\alpha}$ for **non-scanning modes**.

For non-scanning modes and for scanning modes, the depth for maximum I_{sppa}, $z_{\text{sppa,max}}$, is the depth on the beam axis, at or beyond the break-point depth, where the maximum pulse-pressure-squared integral $\max_{z \geq z_{\text{bp}}} \left[ppsi(z) \right]$ occurs. This is the depth for **maximum** pii, z_{pii}.

NOTE 5 This is the same depth as for maximum I_{spta} for **non-scanning modes**.

F.3.2 Determination of maximum $I_{\mathbf{sppa}}$ and $I_{\mathbf{sppa},\alpha}$

F.3.2.1 Non-scanning and scanning modes

For **non-scanning modes** and **scanning modes**, the maximum **attenuated spatial-peak pulse-average intensity** should be calculated using

$$I_{\text{sppa},\alpha} = \frac{1}{t_{\text{d}}\left(z_{\text{sppa},\alpha,\text{max}}\right)\rho c} ppsi_{\alpha}\left(z_{\text{sppa},\alpha,\text{max}}\right) \tag{F.1}$$

and the maximum **spatial-peak pulse-average intensity** should be calculated using:

$$I_{\text{sppa}} = \frac{1}{t_{\text{d}}\left(z_{\text{sppa,max}}\right)\rho c} ppsi\left(z_{\text{sppa,max}}\right) \tag{F.2}$$

where

ρc is the characteristic acoustic impedance of pure water (= 1,48 × 10^6 kg m^{-2} s^{-1} at 20 °C);

$t_{\text{d}}(z_{\text{sppa},\alpha,\text{max}})$ is the **pulse duration** at the **depth for maximum** $I_{\mathbf{sppa},\alpha}$;

$t_{\text{d}}(z_{\text{sppa,max}})$ is the **pulse duration** at the **depth for maximum** $I_{\mathbf{sppa}}$;

$ppsi_{\alpha}(z_{\text{sppa},\alpha,\text{max}})$ is the **attenuated pulse-pressure-squared integral** at the **depth for maximum** $I_{\mathbf{sppa},\alpha}$;

$ppsi(z_{\text{sppa,max}})$ is the **pulse-pressure-squared integral** at the **depth for maximum** $I_{\mathbf{sppa}}$.

NOTE 1 In contrast to Equations (28) and (29), Equations (F.1) and (F.2) describe one depth each.

NOTE 2 As shown in Equations (F.1) and (F.2) and per definition 3.65 and 3.81, the pulse duration value, t_d, is determined at $z_{sppa,\alpha,max}$ and $z_{sppa,max}$, respectively.

F.3.2.2 Combined-operating modes

For **combined-operating modes**, the maximum **attenuated spatial-peak pulse-average intensity** $I_{sppa,\alpha}$ value should be the largest of the $I_{sppa,\alpha}$ values of the constituent **transmit patterns**

$$I_{sppa,\alpha}\left(z_{sppa,\alpha,max}\right) = \max_{\text{all transmit patterns}}\left[I_{sppa,\alpha}\left(\text{transmit pattern } k, z_{pii,\alpha,k}\right)\right] \tag{F.3}$$

and the maximum **spatial-peak pulse-average intensity** I_{sppa} value should be the largest of the I_{sppa} values of the constituent **transmit patterns**

$$I_{sppa}\left(z_{sppa,max}\right) = \max_{\text{all transmit patterns}}\left[I_{sppa}\left(\text{transmit pattern } k, z_{pii,k}\right)\right] \tag{F.4}$$

F.3.3 Determination of maximum $I_{spta,\alpha}$ and I_{spta}

F.3.3.1 Non-scanning modes

For **non-scanning modes**, the maximum **attenuated spatial-peak temporal-average intensity** should be calculated using:

$$I_{spta,\alpha} = \frac{prr}{\rho c}\left(\max_{z \geq z_{bp}}\left[ppsi_\alpha(z)\right]\right) = \frac{prr}{\rho c}\, ppsi_\alpha\left(z_{pii,\alpha}\right) \tag{F.5}$$

and the maximum **spatial-peak temporal-average intensity** should be calculated using:

$$I_{spta} = \frac{prr}{\rho c}\left(\max_{z \geq z_{bp}}\left[ppsi(z)\right]\right) = \frac{prr}{\rho c}\, ppsi\left(z_{pii}\right) \tag{F.6}$$

where

$ppsi_\alpha$ is the **attenuated pulse-pressure-squared integral**;

$ppsi$ is the **pulse-pressure-squared integral**;

z_{bp} is the **break-point depth**;

z_{pii} is the **depth for maximum *pii*** (= $z_{spta,\alpha,max}$) on the **beam axis**;

$z_{pii,\alpha}$ is the **depth for maximum *pii*$_\alpha$** (= $z_{spta,\alpha,max}$) on the **beam axis**;

ρc is the characteristic acoustic impedance of pure water (1,48 × 10^6 kg m^{-2} s^{-1} at 20 °C);

prr is the pulse **repetition rate** of the **non-scanning mode**.

NOTE 1 In contrast to Equation (5) in 3.10 and to the description in 3.54, Equations (F.5) and (F.6) describe one depth each.

NOTE 2 Equation (F.6) is modified from IEC 62127-1:2007, as the **break-point depth** is applied to it.

NOTE 3 For these calculations, an average **pulse repetition period** is used (see 3.3, 3.44 and 3.55).

F.3.3.2 Scanning modes

For **scanning modes**, the maximum **attenuated spatial-peak temporal-average intensity** should be calculated using:

$$I_{\text{spta},\alpha} = \frac{srr}{\rho c}\left(\max_{z \geq z_{\text{bp}}}\left[sppsi_{\alpha}(z)\right]\right) = \frac{srr}{\rho c}\, sppsi_{\alpha}\left(z_{sii,\alpha}\right) \tag{F.7}$$

and the maximum **spatial-peak temporal-average intensity** should be calculated using:

$$I_{\text{spta}} = \frac{srr}{\rho c}\left(\max_{z \geq z_{\text{bp}}}\left[sppsi(z)\right]\right) = \frac{srr}{\rho c}\, sppsi\left(z_{sii}\right) \tag{F.8}$$

where

$\max_{z \geq z_{\text{bp}}}\left[sppsi_{\alpha}(z)\right]$ is the maximum **sum of attenuated pulse-pressure-squared integrals** in one frame of **ultrasonic scan lines** at depth z;

$\max_{z \geq z_{\text{bp}}}\left[sppsi(z)\right]$ is the maximum **sum of pulse-pressure-squared integrals** in one frame of **ultrasonic scan lines** at depth z;

z_{bp} is the **break-point depth**;

$z_{sii,\alpha}$ is the **depth for maximum** sii_{α};

z_{sii} is the **depth for maximum** sii;

srr is the **scan repetition rate**;

ρc is the characteristic acoustic impedance of pure water ($1{,}48 \times 10^6$ kg m^{-2} s^{-1} at 20 °C).

NOTE For these calculations, an average **scan repetition period** is used (see 3.3, 3.44 and 3.55).

It is recommended to review the more detailed derivation notes in Clause F.4, as well as the guidance in IEC 62127-1:2007+IEC 62127-1:2007/AMD1:2013, 7.2, 8.2 and Annex F, as well as clause 5.5 of [44].

F.3.3.3 Combined-operating modes

For **combined-operating modes**, the maximum **attenuated spatial-peak**, **temporal-average intensity** $I_{\text{spta},\alpha}$ should be calculated using:

$$I_{\text{spta},\alpha} = \frac{1}{\rho c}\max_{z \geq z_{\text{bp\_min}}}\left[\left(\sum_{\substack{\text{scanning}\\ \text{mode}\_i}} sppsi_{\alpha}(i,z)\, srr(i)\right) + \left(\sum_{\substack{\text{non-scanning}\\ \text{mode}\_j}} ppsi_{\alpha}(j,z)\, prr(j)\right)\right] \tag{F.9}$$

and the maximum **spatial-peak, temporal-average intensity** I_{spta} should be calculated using:

$$I_{\text{spta}} = \frac{1}{\rho c}\max_{z \geq z_{\text{bp\_min}}}\left[\left(\sum_{\substack{\text{scanning}\\ \text{mode}\_i}} sppsi(i,z)\, srr(i)\right) + \left(\sum_{\substack{\text{non-scanning}\\ \text{mode}\_j}} ppsi(j,z)\, prr(j)\right)\right] \tag{F.10}$$

where

$z_{\text{bp\_min}}$ is the smallest **break-point depth** of the active component modes.

A reasonably conservative estimate of time-average quantities for **combined-operating modes** may be made by determining each mode separately and then combining the time-average estimates of the constituent active modes.

$$I_{\text{spta},\alpha} = \sum_{\substack{\text{discrete} \\ \text{mode\_}k}} I_{\text{spta},\alpha}\left(k, z_{\text{spta},\alpha,\max}(k)\right) \tag{F.11}$$

where each $I_{\text{spta},\,\alpha}\,(k,\, z_{\text{spta}\cdot\alpha\cdot\max}(k))$ is determined according to F.3.3.1 and F.3.3.2.

That is

$$I_{\text{spta},\alpha} = \frac{1}{\rho c}\left[\left(\sum_{\substack{\text{scanning} \\ \text{mode\_}i}} \max_{z \geq z_{\text{bp},i}} \left[sppsi_{\alpha}(i,z)\right] srr(i)\right) + \left(\sum_{\substack{\text{non-scanning} \\ \text{mode\_}j}} \max_{z \geq z_{\text{bp},j}} \left[ppsi_{\alpha}(j,z)\right] prr(j)\right)\right] \tag{F.12}$$

For (non-attenuated) **spatial-peak temporal-average intensity** I_{spta} the equations are:

$$I_{\text{spta}} = \sum_{\substack{\text{discrete} \\ \text{mode\_}k}} I_{\text{spta},}\left(k, z_{\text{spta,max}}(k)\right) \tag{F.13}$$

and

$$I_{\text{spta}} = \frac{1}{\rho c}\left[\left(\sum_{\substack{\text{scanning} \\ \text{mode\_}i}} \max_{z \geq z_{\text{bp},i}} \left[sppsi(i,z)\right] srr(i)\right) + \left(\sum_{\substack{\text{non-scanning} \\ \text{mode\_}j}} \max_{z \geq z_{\text{bp},j}} \left[ppsi(j,z)\right] prr(j)\right)\right] \tag{F.14}$$

NOTE The application of Equations (F.9) through (F.14) requires use of the appropriate **break-point depths** for each of the discrete modes.

F.4 Additional rationale and derivation notes

F.4.1 Summary steps for measuring each active mode

The following steps are provided as a summary guide for measuring each active mode, separately.

- Determine and remain on the **beam axis** (see F.3.1.2).
- Find the **depth for maximum *pii***, z_{pii}, beyond (or at) the **break-point depth** z_{bp} (see F.3.1.3).
- Determine the **acoustic working frequency** f_{awf} (see 3.4) at this depth z_{pii} and the **pulse duration** t_{d} (see 3.41).
- For **scanning modes** and **non-scanning modes**, use the $ppsi$ and the t_{d} at z_{pii} for calculation of maximum I_{sppa}.
- For **non-scanning modes**, use the value of $ppsi$ at z_{pii} for the calculation of the maximum I_{spta}.
- Use f_{awf} and the acoustic attenuation coefficient value, α, to locate the depth for maximum $pii_{\alpha}(z)$ beyond or at the break-point depth z_{bp}.
- Determine the **pulse duration** t_{d} (see 3.41) at this depth $z_{pii\cdot\alpha}$.
- For **non-scanning modes,** use the value of $ppsi_{\alpha}$ at $z_{pii\cdot\alpha}$ for the calculation of maximum $I_{\text{spta}\cdot\alpha}$.
- For **scanning modes** and **non-scanning modes**, use $ppsi_{\alpha}$ at $z_{pii\cdot\alpha}$ and t_{d} at $z_{pii\cdot\alpha}$ for calculation of maximum $I_{\text{sppa},\alpha}$.

- For **scanning modes,** adhering to the **break-point depth** z_{bp} and referring to F.3.3.2 and F.4.2 and F.4.3, find the:
  - **depth for maximum** ***sii***, z_{sii}, and the value there of maximum I_{spta};
  - **depth for maximum** ***sii***$_\alpha$, $z_{sii,\alpha}$, and the value there of maximum $I_{spta,\alpha}$.

F.4.2 Notes regarding determination of $s_\alpha ppsi(z)$ and $sppsi_\alpha(z)$

F.4.2 gives additional notes to accompany F.3.1.4.2.

The general principles for measuring temporal average acoustic output parameters for **scanning modes** can be summarized as follows.

Temporal average parameters are determined by the cumulative effects of the overlap of beams generated during the **scan repetition period**. **Temporal average intensity** for a **scanning mode**, when measured at a point, is determined by the sum of the energy fluencies at the point resulting from the various beams transmitted during each scan and the **scan repetition rate**.

The determination of the sum of pulse-pressure-squared integrals and the sum of attenuated pulse-pressure-squared integrals are the key to determination of the temporal-average intensity in scanning modes.

The general form of the **sum of attenuated pulse-pressure-squared integrals** $sppsi_\alpha(z)$ is expressed as follows:

$$\begin{aligned} sppsi_\alpha(z) = {} & \ldots \\ & + \ldots \\ & + ppsi_{\alpha,m-2,1}(z) + ppsi_{\alpha,m-2,2}(z) + \ldots + ppsi_{\alpha,m-2,n_{m-2}}(z) \\ & + ppsi_{\alpha,m-1,1}(z) + ppsi_{\alpha,m-1,2}(z) + \ldots + ppsi_{\alpha,m-1,n_{m-1}}(z) \\ & + ppsi_{\alpha,m,1}(z) + ppsi_{\alpha,m,2}(z) + \ldots + ppsi_{\alpha,m,n_m}(z) \\ & + ppsi_{\alpha,m+1,1}(z) + ppsi_{\alpha,m+1,2}(z) + \ldots + ppsi_{\alpha,m+1,n_{m+1}}(z) \\ & + ppsi_{\alpha,m+2,1}(z) + ppsi_{\alpha,m+2,2}(z) + \ldots + ppsi_{\alpha,m+2,n_{m+2}}(z) \\ & + \ldots \end{aligned} \tag{F.15}$$

where

m is the central **ultrasonic scan line** of the scan or series of scan lines in a frame. By convention, the central line m can be considered the median line, and for sector scan formats the line with **beam axis** most closely parallel to the z axis (depth axis) of the hydrophone scanning system;

$m + j$ (j = … -2, -1, 0, 1, 2, …) is the **ultrasonic scan lines** adjacent to the central **ultrasonic scan line**;

n_{m+j} is the number of pulses transmitted down line $m + j$;

$ppsi_{\alpha,m+j,n}(z)$ is the **attenuated pulse-pressure-squared integral** of pulse number n down line $m + j$, as measured/detected by a hydrophone at depth z aligned with line m.

NOTE 1 This is an important distinction: $ppsi_{\alpha,m+j,n}(z)$ does not represent the $ppsi_\alpha$ measured on the **beam axis** of line '$m+j$', it is the $ppsi_\alpha(z)$ of the nth pulse down line $m+j$ as measured on the **beam axis** of the central **ultrasonic scan line** m.

For the case where the pulses transmitted down a particular **ultrasonic scan line** are identical, Equation (F.15) may be simplified to:

$$sppsi_{\alpha}(z) = \ldots + n_{m-2}\,ppsi_{\alpha,m-2}(z) + n_{m-1}\,ppsi_{\alpha,m-1}(z) + n_{m}\,ppsi_{\alpha,m}(z) + n_{m+1}\,ppsi_{\alpha,m+1}(z) + n_{m+2}\,ppsi_{\alpha,m+2}(z) + \ldots \quad \text{(F.16)}$$

where

n_{m+j} is the number of pulses per scan line for **ultrasonic scan line** $m + j$ (j = … –2, –1, 0, 1, 2, …).

If the pulses down all **ultrasonic scan lines** included in the sum are identical, then, because they share the same **acoustic working frequency**, they will share the same estimated attenuation at depth z. In this case, Equation (F.16) is equivalent to:

$$\begin{aligned} sppsi_{\alpha}(z) &= s_{\alpha}\,ppsi(z) \\ &= 10^{-\alpha z f_{\text{awf}}/10\,\text{dB}}(\ldots + n_{m-2}\,ppsi_{m-2}(z) + n_{m-1}\,ppsi_{m-1}(z) + n_{m}\,ppsi_{m}(z) + n_{m+1}\,ppsi_{m+1}(z) + n_{m+2}\,ppsi_{m+2}(z) + \ldots) \end{aligned} \quad \text{(F.17)}$$

In addition, when the number of pulses down each line included in the sum is the same ($n_{m+j} = n$), then Equation (F.16) simplifies further:

$$sppsi_{\alpha}(z) = n \times (\ldots + ppsi_{\alpha,m-2}(z) + ppsi_{\alpha,m-1}(z) + ppsi_{\alpha,m}(z) + ppsi_{\alpha,m+1}(z) + ppsi_{\alpha,m+2}(z) + \ldots) \quad \text{(F.18)}$$

and (again) if all the pulses down all lines in the sum are identical:

$$\begin{aligned} sppsi_{\alpha}(z) &= s_{\alpha}\,ppsi(z) \\ &= n \times 10^{-\alpha z f_{\text{awf}}/10\,\text{dB}}(\ldots + ppsi_{m-2}(z) + ppsi_{m-1}(z) + ppsi_{m}(z) + ppsi_{m+1}(z) + ppsi_{m+2}(z) + \ldots) \end{aligned} \quad \text{(F.19)}$$

NOTE 2 As illustrated by comparing Equations (F.15) to (F.19), the **sum of attenuated pulse-pressure-squared integrals** will be equal to the **attenuated sum of pulse-pressure-squared integrals** at depth z if each **ultrasonic scan line** in the frame which is included in the sum has the same **acoustic working frequency.** Therefore, when it is possible to partition scanned modes into groups of **ultrasonic scan lines** with the same f_{awf} values, then approximating $sppsi_{\alpha}$ with $s_{\alpha}ppsi$ may be a convenient alternative.

NOTE 3 Definitions in IEC 61157:2007+IEC 61157:2007/AMD1:2013, and IEC 60601-2-37:2007+IEC 60601-2-37/AMD1:2015 for "number of pulses per ultrasonic scan line" contain additional discussion and examples.

F.4.3 Further information regarding scanning modes

The discussion given in IEC 62127-1:2007 associated with its Equations (17) and (18) in 7.2.6.3 describes adjacent scan lines in a single scan plane. However, the **ultrasonic scan lines** adjacent to the central **ultrasonic scan line** could lie in multiple planes, as may be the case for 3D **scanning modes**. The equations would still apply, as would the methods and equations in F.3.1.4.2, F.3.3.2 and F.4.2. Knowledge of the location of the **ultrasonic scan lines** is still needed if applying method b) in F.3.1.4.2. A search in the azimuth (x) or elevation (y) direction at depth z may be needed to find the maximum $sppsi_{\alpha}$ value on a plane at depth z.

In **scanning modes**, a series of interrogating beams may be steered through a succession of azimuthal (i.e. in-plane lateral) directions within a single or succession of (elevation direction) target planes.

In the simplest **scanning mode**, all transmitted beams may exhibit the same focal characteristics along their respective **beam axes**; the beams may differ only in the orientation of the **beam axes**. Thus, the temporal peak and pulse average parameters of all beams (considered separately), as well as the **scanning mode** itself, are identical. The temporal average parameters for the mode are determined by the **pulse-pressure-squared integrals** of an individual beam, the degree of spatial overlap of the beams in the formation of the overall scan, and the **scan repetition rate**.

For 2D **scanning modes**, there is only one elevation target plane, and the rate at which the azimuthal scanning pattern is repeated is the **scan repetition rate** (srr). Multiplying the $\max_{z \geq z_{bp}} [sppsi(z)]$ and $\max_{z \geq z_{bp}} [sppsi_{\alpha}(z)]$ by this rate yields the maximum non-attenuated and attenuated **temporal average intensity** values.

In some 3D and 4D modes, the plane of examination is automatically swept through the target space in the elevation direction. Thus, while the scanning pattern may appear to be repetitive in the range-azimuth plane, the scanning pattern is not repetitive at any point in the target volume due to motion of the scan plane. As considered in this standard, two approaches may be taken.

This elevation motion is disregarded, and the **sum of pulse-pressure-squared integrals** is determined over the period of repetition in the range-azimuth plane, and then the **scan repetition rate** is determined from this period. This leads to a conservative over-estimate of the **temporal average intensity**.

The elevation motion is not disregarded, the **sum of pulse-pressure-squared integrals** is determined over all **ultrasonic scan lines** making one volume, with the **scan repetition rate** being the volume repetition rate.

In more complex **scanning modes**, the transmitted beams may exhibit two or more sets of focal characteristics. In some systems, certain scanning modes may employ two or more distinct focal patterns, each focused at a different depth, to create a single, overall scan. In still other systems, such as phased array sector devices, beam focal characteristics may vary with steering angle as well. In these more complex modes, the temporal-peak and pulse-average parameters for a given mode are determined by the maximum values that occur for any beam within the scan. The temporal average parameters for the mode are determined by the **pulse-pressure-squared integrals** and the **sum of pulse-pressure-squared integrals** and the **sum of attenuated pulse-pressure-squared integrals** of the different beam types, the degree and pattern of spatial overlap of the different beam types in the formation of the overall scan, and the **scan repetition rate**.

Bibliography

[1] AIUM. *Bio-effects and safety of diagnostic ultrasound*. American Institute of Ultrasound in Medicine, AIUM, 1470 Sweitzer Lane, suite 100, Laurel MD 20707-5906, 1993.

[2] HERMAN, BA, HARRIS, GR. Models and regulatory considerations for transient temperature rise during diagnostic ultrasound pulses. *Ultrasound Med Biol*, 28, 2002, p. 1217-12.

[3] IEC/TR 60854:1986, *Methods of measuring the performance of ultrasonic pulse-echo diagnostic equipment*

[4] IEC 61689, *Ultrasonics – Physiotherapy systems – Field specifications and methods of measurement in the frequency range 0,5 MHz to 5 MHz*

[5] BARNETT S.B, (ed.). Update on thermal bioeffects issues. *Ultrasound Med Biol,* Vol. 24, Suppl.1, 1998, p. S1-S10.

[6] European Committee for Medical Ultrasound Safety (ECMUS), *EFSUMB Newsletter* Vol. 15/1, 2001, p. 9 and EFSUMB Newsletter Vol. 15/2, 2002, p. 12.

[7] BARNETT S.B., TER HAAR G.R., ZISKIN M.C., ROTT H-D, DUCK F.A, MAEDA, K. International recommendations and guidelines for the safe use of diagnostic ultrasound in medicine. *Ultrasound in Medicine and Biology* 26, No. 3, 2000

[8] AIUM *Medical Ultrasound Safety,* © AIUM, 14750 Sweitzer Lane, Suite 100, Laurel MD 20707-5906, USA, 2009.

[9] ISO/IEC Guide 98-3, *Uncertainty of measurement – Part 3: Guide to the expression of uncertainty in measurement* (GUM 1995)

[10] HEKKENBERG R.T, BEZEMER R.A. On the development of a method to measure the surface temperature of ultrasonic diagnostic transducers. *Journal of Physics Conference Series* 1 (2004) 84-89 (Institute of Physics Publishing), 2004.

[11] O'BRIEN W.D. and ELLIS D.S. *IEEE Trans Ultrasonics Freq Control* 46, no. 6, Nov. 1999, p. 1459-1476.

[12] AIUM. Bio-effects considerations for the safety of diagnostic ultrasound. *J Ultrasound Med* 7: supplement, 1988.

[13] WFUMB. Conclusions and Recommendations on Thermal and Non-thermal Mechanisms for Biological Effects of Ultrasound. Report of the 1996 WFUMB Symposium on Safety of Ultrasound in Medicine. BARNETT S.B. (ed). *Ultrasound Med Biol*, 24, suppl 1, 1998.

[14] NCRP. *Exposure criteria for medical diagnostic ultrasound: I. Criteria based on thermal mechanisms*. NCRP Report No. 113, National Council on Radiation Protection and Measurements, Bethesda MD, 1992.

[15] CARSTENSEN E.L., CHILD S.Z., CRANE C., PARKER K.J. Lysis of cells in Elodera leaves by pulsed and continuous wave ultrasound. *Ultrasound Med Biol* 16, 1990, p. 167-173.

[16] CHILD S.Z., HARTMAN C.L., MCHALE L.A., CARSTENSEN E.L. Lung damage from exposure to pulsed ultrasound. *Ultrasound Med Biol*, 16, 1990, p. 817-825.

[17] CHURCH CC, O'BRIEN WD. Evaluation of the Threshold for Lung Hemorrhage by Diagnostic Ultrasound and a Proposed New Safety Index. *Ultrasound Med Biol*, 33, No.5, 2007, p. 810-818.

[18] CHURCH C.C. Spontaneous, homogeneous nucleation, inertial cavitation and the safety of diagnostic ultrasound. *Ultrasound Med Biol* 28, 2002, p. 1349-1364.

[19] HOLLAND C.K., APFEL R.E. Thresholds for transient cavitation produced by pulsed ultrasound in a controlled nuclei environment. *J Acoust Soc Am*, 88, 1989, p. 2059-2069.

[20] HERBERTZ J. Spontane Kavitation in keimfreien Flüssigkeiten (English translation: Spontaneous cavitation in liquids free of nuclei). In *Fortschritte der Akustik*, DAGA 88, DPG-GmbH Bad Honnef, 1988, p. 439-442.

[21] APFEL R.E., and HOLLAND C.K. Gauging the likelihood of cavitation from short-pulse low-duty cycle diagnostic ultrasound. *Ultrasound Med Biol*, 17, 1991, p. 179-185.

[22] AIUM / NEMA, *Standard for Real–Time Display of Thermal and Mechanical Acoustic Output Indices on Diagnostic Ultrasound Equipment*. AIUM, 1470 Sweitzer Lane, suite 100, Laurel MD 20707-5906, 2004.

[23] WFUMB, Second World Federation of Ultrasound in Medicine and Biology symposium on safety and standardization in medical ultrasound. *Ultrasound Med Biol.,* 15: supplement, 1989.

[24] NCRP, *Exposure criteria for medical diagnostic ultrasound: II. Criteria based on all known mechanisms.* NCRP Report No. 140, National Council on Radiation Protection and Measurements, Bethesda MD, 2002.

[25] CURLEY M.G., Soft tissue temperature rise caused by scanned, diagnostic ultrasound. *IEEE Trans Ultrasonics, Ferroelectrics and Frequency Control,* 49, 1993, p. 59-66.

[26] LUBBERS J., HEKKENBERG R.T., BEZEMER R.A. Time to Threshold (TT), a safety parameter for heating by diagnostic ultrasound. *Ultrasound in Med. & Biol.*, May 2003, Vol. 29, 5, p. 755-764.

[27] ABBOTT J.G. Rational and Derivation of MI and TI – a Review. *Ultrasound Med Biol.*, 25, No. 3, 1999, p. 431-441.

[28] SEKINS K.M., EMERY A.F. Thermal science for physical medicine. Chapter 3, p.70-132, in *Therapeutic Heat and Cold*. LEHMANN J.F. editor, Williams & Wilkins, Baltimore MD, 1982.

[29] CARSTENSEN E.L., CHILD S.Z., NORTON S., NYBORG W.L. Ultrasonic heating of the skull. *J Acoust Soc*. Am., 87, 1990, p. 1310-1317.

[30] BEISSNER K., Radiation force calculations for ultrasonic fields from rectangular weakly focusing transducers, *J. Acoust. Soc. Am*. 124, 1941 – 1949 (2008).

[31] BEISSNER K., Radiation force calculations for oblique ultrasonic beams, *J. Acoust. Soc. Am. 125,* 2827 – 2829 (2009).

[32] SHAW A., PAY NM. and PRESTON R.C. *Assessment of the likely thermal index values for pulsed Doppler ultrasonic equipment – Stages II and III: experimental assessment of*

scanner/transducer combinations. NPL Report cmAM 12, available from The National Physical Laboratory, Teddington, Middlesex TW11 OLW, UK, 1998.

[33] SHAW A, PAY N.M., PRESTON R.C., BOND A.D., Proposed Standard Thermal test object for medical ultrasound. *UMB*, Vol 25, No. 1, p. 121-132, 1999.

[34] HEKKENBERG R.T., BEZEMER R.A., *Aspects concerning the measurement of surface temperature of ultrasonic diagnostic transducers*. PG/TG/01.246r, ISBN 90-5412-078-9, March 2002.

[35] HEKKENBERG R.T., BEZEMER R.A., *Aspects concerning the measurement of surface temperature of ultrasonic diagnostic transducers, Part 2: On a human and artificial tissue*. PG/TG/2003.134, ISBN 90-5412-085-1, May 2003.

[36] HEKKENBERG R.T., BEZEMER R.A., On the development of a method to measure the surface temperature of ultrasonic diagnostic transducers. *Journal of Physics*: Conference Series 1 (2004) 84-89 (Institute of Physics Publishing), 2004.

[37] SAUNDERS O, CLIFT S AND DUCK F, Ultrasound transducer self heating: development of 3-D finite-element models. *Journal of Physics*: Conference Series 1 (2004) p. 72-77.

[38] AIUM, Mechanical Bioeffects from Diagnostic Ultrasound: AIUM Consensus Statements, *J Ultrasound Med*. 19, No. 2 or 3, 2000.

[39] SALVESEN K.A. Epidemiological studies of diagnostic ultrasound. Chapter 9, in: The safe use of ultrasound in medical diagnosis, British Medical Ultrasound Society/British Institute of Radiology. Editors TER HAAR G.R. and DUCK F.A., 2000, p. 86-93.

[40] DUCK F.A. The meaning of Thermal Index (TI) and Mechanical Index (MI) values. *BMUS Bulletin*, Nov. 1997, p. 36-40.

[41] FDA-CDRH, Guidance for Industry and FDA Staff, Information for Manufacturers Seeking Marketing Clearance of Diagnostic Ultrasound Systems and Transducers, September 9, 2008.

[42] CHRISTOPHER T., CARSTENSEN E.L. Finite amplitude distortion and its relationship to linear derating formulae for diagnostic ultrasound systems. *Ultrasound Med. Biol.,* 22, 1996, p. 1103-1116.

[43] World Federation for Ultrasound in Medicine and Biology. *(*WFUMB) Symposium on Safety and Standardisation in Medical Ultrasound, Synopsis. *Ultrasound Med Biol*, 18, 1992, p. 733-737.

[44] AIUM/NEMA, Acoustic output measurement standard for diagnostic ultrasound equipment, NEMA Standards Publication UD 2-2004, Revision 3

_____

IEC 62359

Edition 2.1 2017-09

FINAL VERSION

colour inside

Ultrasonics – Field characterization – Test methods for the determination of thermal and mechanical indices related to medical diagnostic ultrasonic fields

IEC 62359:2010-10+AMD1:2017-09 CSV(en)

CONTENTS

INTERNATIONAL ELECTROTECHNICAL COMMISSION

ULTRASONICS – FIELD CHARACTERIZATION – TEST METHODS FOR THE DETERMINATION OF THERMAL AND MECHANICAL INDICES RELATED TO MEDICAL DIAGNOSTIC ULTRASONIC FIELDS

FOREWORD

1) The International Electrotechnical Commission (IEC) is a worldwide organization for standardization comprising all national electrotechnical committees (IEC National Committees). The object of IEC is to promote international co-operation on all questions concerning standardization in the electrical and electronic fields. To this end and in addition to other activities, IEC publishes International Standards, Technical Specifications, Technical Reports, Publicly Available Specifications (PAS) and Guides (hereafter referred to as "IEC Publication(s)"). Their preparation is entrusted to technical committees; any IEC National Committee interested in the subject dealt with may participate in this preparatory work. International, governmental and non-governmental organizations liaising with the IEC also participate in this preparation. IEC collaborates closely with the International Organization for Standardization (ISO) in accordance with conditions determined by agreement between the two organizations.
2) The formal decisions or agreements of IEC on technical matters express, as nearly as possible, an international consensus of opinion on the relevant subjects since each technical committee has representation from all interested IEC National Committees.
3) IEC Publications have the form of recommendations for international use and are accepted by IEC National Committees in that sense. While all reasonable efforts are made to ensure that the technical content of IEC Publications is accurate, IEC cannot be held responsible for the way in which they are used or for any misinterpretation by any end user.
4) In order to promote international uniformity, IEC National Committees undertake to apply IEC Publications transparently to the maximum extent possible in their national and regional publications. Any divergence between any IEC Publication and the corresponding national or regional publication shall be clearly indicated in the latter.
5) IEC itself does not provide any attestation of conformity. Independent certification bodies provide conformity assessment services and, in some areas, access to IEC marks of conformity. IEC is not responsible for any services carried out by independent certification bodies.
6) All users should ensure that they have the latest edition of this publication.
7) No liability shall attach to IEC or its directors, employees, servants or agents including individual experts and members of its technical committees and IEC National Committees for any personal injury, property damage or other damage of any nature whatsoever, whether direct or indirect, or for costs (including legal fees) and expenses arising out of the publication, use of, or reliance upon, this IEC Publication or any other IEC Publications.
8) Attention is drawn to the Normative references cited in this publication. Use of the referenced publications is indispensable for the correct application of this publication.
9) Attention is drawn to the possibility that some of the elements of this IEC Publication may be the subject of patent rights. IEC shall not be held responsible for identifying any or all such patent rights.

This Consolidated version of IEC 62359 bears the edition number 2.1. It consists of the second edition (2010-10) [documents 87/445/FDIS and 87/453/RVD] and its corrigendum 1 (2011-03), and its amendment 1 (2017-09) [documents 87/661/FDIS and 87/665/RVD]. The technical content is identical to the base edition and its amendment.

This Final version does not show where the technical content is modified by amendment 1. A separate Redline version with all changes highlighted is available in this publication.

International standard IEC 62359 has been prepared by IEC technical committee 87: Ultrasonics.

This second edition It constitutes a technical revision.

Major changes with respect to the previous edition include the following:

- The methods of determination set out in the first edition of this standard were based on those contained in the American standard for Real–Time Display of Thermal and Mechanical Acoustic Output Indices on Diagnostic Ultrasound Equipment (ODS) and were intended to yield identical results. While this second edition also follows the ODS in principal and uses the same basic formulae and assumptions (see Annex A), it contains a few significant modifications which deviate from the ODS.

- One of the primary issues dealt with in preparing this second edition of IEC 62359 was “missing” TI equations. In Edition 1 there were not enough equations to make complete “at-surface” and “below-surface” summations for TIS and TIB in combined-operating modes. Thus major changes with respect to the previous edition are related to the introduction of new calculations of thermal indices to take into account both "at-surface" and "below-surface" thermal effects.

For the specific technical changes involved please see Annex E.

This publication has been drafted in accordance with the ISO/IEC Directives, Part 2.

This standard may be used to support the requirements of IEC 60601-2-37.

In this particular standard, the following print types are used:

– requirements, compliance with which can be tested, and definitions: in roman type
– notes, explanations, advice, introductions, general statements, exceptions, and references: in smaller type
– *test specifications: in italic type*
– words in **bold** are defined terms in Clause 3

The committee has decided that the contents of the base publication and its amendment will remain unchanged until the stability date indicated on the IEC web site under "http://webstore.iec.ch" in the data related to the specific publication. At this date, the publication will be

- reconfirmed,
- withdrawn,
- replaced by a revised edition, or
- amended.

A bilingual version of this publication may be issued at a later date.

IMPORTANT – The 'colour inside' logo on the cover page of this publication indicates that it contains colours which are considered to be useful for the correct understanding of its contents. Users should therefore print this document using a colour printer.

INTRODUCTION

Medical diagnostic ultrasonic equipment is widely used in clinical practice for imaging and monitoring purposes. Equipment normally operates at frequencies in the low megahertz frequency range and comprises an ultrasonic transducer acoustically coupled to the patient and associated electronics. There is an extremely wide range of different types of systems in current clinical practice.

The ultrasound entering the patient interacts with the patient's tissue, and this interaction can be considered in terms of both thermal and non-thermal effects. The purpose of this International standard is to specify methods of determining thermal and non-thermal exposure indices that can be used to help in assessing the hazard caused by exposure to a particular ultrasonic field used for medical diagnosis or monitoring. It is recognised that these indices have limitations, and knowledge of the indices at the time of an examination is not sufficient in itself to make an informed clinical risk assessment. It is intended that these limitations will be addressed in future revisions of this standard and as scientific understanding increases. While such increases remain pending, several organizations have published **prudent-use statements.**

Under certain conditions specified in IEC 60601-2-37, these indices are displayed on medical ultrasonic equipment intended for these purposes.

INTRODUCTION to Amendment

The second edition of IEC 62359 was published in 2010. Since then, IEC 60601-2-37:2007/AMD1:2015 has been published and calls for provision of **attenuated spatial peak temporal average intensity**, $I_{\mathrm{spta},\alpha}$, and **attenuated spatial peak pulse average intensity**, $I_{\mathrm{sppa},\alpha}$, at specific spatial maximum points in the ultrasonic field on the **beam axis**. No IEC standard describes the determination of these quantities at these specific positions. IEC 62359 for determining the thermal indices currently uses similar values at other positions, therefore, the determination of **attenuated spatial peak temporal average intensity**, $I_{\mathrm{spta},\alpha}$, and **attenuated spatial peak pulse average intensity**, $I_{\mathrm{sppa},\alpha}$, has been added as an annex in this amendment.

Additionally, references to newly published collateral standards have been updated.

ULTRASONICS – FIELD CHARACTERIZATION – TEST METHODS FOR THE DETERMINATION OF THERMAL AND MECHANICAL INDICES RELATED TO MEDICAL DIAGNOSTIC ULTRASONIC FIELDS

1 Scope

This International standard is applicable to medical diagnostic ultrasound fields.

This standard establishes

– parameters related to thermal and non-thermal exposure aspects of diagnostic ultrasonic fields;
– methods for the determination of an exposure parameter relating to temperature rise in theoretical tissue-equivalent models, resulting from absorption of ultrasound;
– methods for the determination of an exposure parameter appropriate to certain non-thermal effects.

NOTE 1 In Clause 3 of this standard, SI units are used (per ISO/IEC Directives, Part 2, ed. 5, Annex I b) in the Notes below definitions of certain parameters, such as beam areas and intensities; it may be convenient to use decimal multiples or submultiples in practice. Users must take care of decimal prefixes used in combination with the units when using and calculating numerical data. For example, beam area may be specified in cm^2 and intensities in W/cm^2 or mW/cm^2.

NOTE 2 Underlying calculations have been done from 0,25 MHz to 15 MHz for MI and 0,5 MHz to 15 MHz for *TI*.

NOTE 3 The thermal indices are steady state estimates based on the acoustic **output power** required to produce a 1°C temperature rise in tissue conforming to the "homogeneous tissue 0,3 $dBcm^{-1}MHz^{-1}$ attenuation model" [1] [1)] and may not be appropriate for radiation force imaging, or similar techniques that employ pulses or pulse bursts of sufficient duration to create a significant transient temperature rise. [2]

2 Normative references

The following referenced documents are indispensable for the application of this document. For dated references, only the edition cited applies. For undated references, the latest edition of the referenced document (including any amendments) applies.

IEC 60601-2-37:2007, *Medical electrical equipment – Part 2-37: Particular requirements for the basic safety and essential performance of ultrasonic medical diagnostic and monitoring equipment*
IEC 60601-2-37:2007/AMD1:2015

IEC 61157:2007, *Standard means for the reporting of the acoustic output of medical diagnostic ultrasonic equipment*
IEC 61157:2007/AMD1:2013

IEC 61161:2013, *Ultrasonics – Power measurement – Radiation force balances and performance requirements*

IEC 61828:2001, *Ultrasonics – Focusing transducers – Definitions and measurement methods for the transmitted fields*

---

1) Figures in square brackets refer to Bibliography.

IEC 62127-1:2007, *Ultrasonics – Hydrophones – Part 1: Measurement and characterization of medical ultrasonic fields up to 40 MHz*
IEC 62127-1:2007/AMD1:2013

IEC 62127-2:2007, *Ultrasonics – Hydrophones – Part 2: Calibration for ultrasonic fields up to 40 MHz*

IEC 62127-3:2007, *Ultrasonics – Hydrophones – Part 3: Properties of hydrophones for ultrasonic fields up to 40 MHz*

3 Terms and definitions

For the purposes of this document, the terms and definitions given in IEC 60601-2-37, IEC 62127-1, IEC 62127-2, IEC 62127-3, IEC 61157 and IEC 61161 apply. Several of these are repeated below for convenience and others are listed because they have been modified for application to this standard.

NOTE Units below definitions are given is SI units as per ISO/IEC Directives, Part 2, ed. 5, Annex I b). Users must be alert to possible need to convert units when using this standard in situations where data are received in units that are different from those used in the SI system.

3.1
acoustic attenuation coefficient
α
coefficient intended to account for ultrasonic attenuation of tissue between the **external transducer aperture** and a specified point

NOTE 1 A linear dependence on frequency is assumed.

NOTE 2 **Acoustic attenuation coefficient** is expressed in decibels per metre per hertz (dB m^{-1} Hz^{-1}).

3.2
acoustic absorption coefficient
μ_0
coefficient intended to account for ultrasonic absorption of tissue in the region of interest

NOTE 1 A linear dependence on frequency is assumed.

NOTE 2 **Acoustic absorption coefficient** is expressed in neper per metre per hertz (Np m^{-1} Hz^{-1}).

3.3
acoustic repetition period
arp
time interval between corresponding points of consecutive cycles, pulses or scans, depending on the current operating mode

NOTE 1 The **acoustic repetition period** is equal to the **pulse repetition period** for non-automatic scanning systems and to the **scan repetition period** for automatic scanning systems**.**

NOTE 2 For continuous wave modes, the **acoustic repetition period** is the time interval between corresponding points of consecutive cycles

NOTE 3 For **combined operating modes** where transmit pulsing of the constituent modes may be interrupted, the ***arp*** determination should take into account non-pulsing time to calculate an average period.

NOTE 4 The **acoustic repetition period** is expressed in seconds (s).

[IEC 62127-1:2007, definition 3.2, modified]

3.4
acoustic working frequency
frequency of an acoustic signal based on the observation of the output of a **hydrophone** placed in an acoustic field on the **beam axis**, beyond the **break-point depth**, corresponding to **depth of maximum pulse-intensity integral** z_{pii}.

NOTE 1 The signal is analysed using either the **zero-crossing acoustic-working frequency** technique or a spectrum analysis method. Specific acoustic-working frequencies are defined in 3.4.1 and 3.4.2.

NOTE 2 For pulsed waveforms the **acoustic-working frequency** shall be measured at the **depth for peak pulse-intensity integral**.

NOTE 3 **Acoustic frequency** is expressed in hertz (Hz).

[IEC 62127-1:2007, definition 3.3, modified]

3.4.1
zero-crossing acoustic-working frequency
$f_{\mathbf{awf}}$
number of consecutive half-cycles (irrespective of polarity) divided by twice the time between the commencement of the first half-cycle and the end of the n-th half-cycle

NOTE 1 Any half-cycle in which the waveform shows evidence of phase change shall not be counted.

NOTE 2 The measurement should be performed at terminals in the receiver, that are as close as possible to the receiving transducer (hydrophone) and, in all cases, before rectification.

NOTE 3 This frequency is determined according to the procedure specified in IEC/TR 60854 [3].

NOTE 4 This frequency is intended for continuous-wave systems only.

3.4.2
arithmetic-mean acoustic-working frequency
$f_{\mathbf{awf}}$
arithmetic mean of the most widely separated frequencies f_1 and f_2, within the range of three times f_1, at which the magnitude of the acoustic pressure spectrum is 3 dB below the peak magnitude

NOTE 1 This frequency is intended for pulse-wave systems only.

NOTE 2 It is assumed that $f_1 < f_2$.

NOTE 3 If f_2 is not found within the range < 3 f_1, f_2 is to be understood as the lowest frequency above this range at which the spectrum magnitude is -3 dB from the peak magnitude.

3.5
attenuated bounded-square output power
$P_{\mathbf{1x1},\alpha}(z)$
The maximum value of the **attenuated output power** passing through any one square centimeter of the plane perpendicular to the **beam axis** at depth z

NOTE 1 At z = 0 (the transducer surface) $P_{1x1,\alpha}(z)$ becomes the **bounded-square output power**, that is, at z = 0, $P_{1x1,\alpha} = P_{1x1}$.

NOTE 2 **Attenuated bounded-square output power** is expressed in watts (W).

3.6
attenuated output power
$P_{\alpha}(z)$
value of the acoustic **output power** after attenuation, at a specified distance from the **external transducer aperture**, and given by

$$P_{\alpha}(z) = P\,10^{(-\alpha z\, f_{\mathrm{awf}}/10\mathrm{dB})} \qquad (1)$$

where

α is the **acoustic attenuation coefficient**;

z is the distance from the **external transducer aperture** to the point of interest;

f_{awf} is the **acoustic working frequency**;

P is the **output power** measured in water.

NOTE 1 **Attenuated output power** is expressed in watts (W).

NOTE 2 In the case of stand-offs the P should represent the **output power** emanating from the stand-off.

3.7
attenuated peak-rarefactional acoustic pressure
$p_{\mathrm{r},\alpha}(z)$
value of the **peak-rarefactional acoustic pressure** after attenuation, on a plane perpendicular to the **beam axis** at a specified distance z from the **external transducer aperture**, and given by

$$p_{\mathrm{r},\alpha}(z) = p_{\mathrm{r}}(z) 10^{(-\alpha z\, f_{\mathrm{awf}}/20\mathrm{dB})} \tag{2}$$

where

α is the **acoustic attenuation coefficient**;

z is the distance from the **external transducer aperture** along the **beam axis** to the plane containing the point of interest;

f_{awf} is the **acoustic working frequency**;

$p_{\mathrm{r}}(z)$ is the **peak-rarefactional acoustic pressure** measured in water.

NOTE Attenuated peak-rarefactional acoustic pressure is expressed in pascals (Pa).

3.8
attenuated pulse-intensity integral
$pii_{\alpha}(z)$
value of the **pulse-intensity integral** after attenuation, on a plane perpendicular to the **beam axis** at a specified distance z from the **external transducer aperture**, and given by

$$pii_{\alpha}(z) = pii\, 10^{(-\alpha z\, f_{\mathrm{awf}}/10\mathrm{dB})} \tag{3}$$

where

α is the **acoustic attenuation coefficient**;

z is the distance from the **external transducer aperture** along the **beam axis** to the plane containing the point of interest;

f_{awf} is the **acoustic working frequency**;

pii is the **pulse-intensity integral** measured in water.

NOTE 1 **Attenuated pulse-intensity integral** is expressed in joules per metre squared, (J m^{-2}).

NOTE 2 For measurement purposes of this standard, pii_{α} is equivalent to $1/(\rho c)$ times the **attenuated pulse-pressure-squared integral** at depth z, with ρc denoting the characteristic acoustic impedance of pure water.

3.9
attenuated spatial-average temporal-average intensity
$I_{\mathrm{sata},\alpha}(z)$
value of the **spatial-average temporal-average intensity** after attenuation, on a plane perpendicular to the **beam axis** at a specified distance z from the **external transducer aperture**, and given by

$$I_{\mathrm{sata},\alpha}(z) = I_{\mathrm{sata}}\, 10^{(-\alpha z\, f_{\mathrm{awf}}/10\mathrm{dB})} \tag{4}$$

where

α is the **acoustic attenuation coefficient**;

z is the distance from the **external transducer aperture** along the **beam axis** to the plane containing the point of interest;

f_{awf} is the **acoustic working frequency**;

I_{sata} is the **spatial-average temporal-average intensity**, at a specified distance z measured in water.

NOTE **Attenuated spatial-average temporal-average intensity** is expressed in watts per metre squared, (W m^{-2}).

3.10
attenuated spatial-peak temporal-average intensity
$I_{spta,\alpha}(z)$
value of the **spatial-peak temporal-average intensity** after attenuation, on a plane perpendicular to the **beam axis** at a specified distance z from the **external transducer aperture**, and given by

$$I_{spta,\alpha}(z) = I_{spta}\, 10^{(-\alpha z\, f_{awf}/10dB)} \quad (5)$$

where

α is the **acoustic attenuation coefficient**;

z is the distance from the **external transducer aperture** along the **beam axis** to the plane containing the point of interest;

f_{awf} is the **acoustic working frequency**;

I_{spta} is the **spatial-peak temporal-average intensity**, at a specified distance z measured in water.

NOTE **Attenuated spatial-peak temporal-average intensity** is expressed in watts per metre squared, (W m^{-2}).

3.11
attenuated temporal-average intensity
$I_{ta,\alpha}(z)$
value of the **temporal-average intensity** after attenuation, on a plane perpendicular to the **beam axis** at a specified distance z from the **external transducer aperture**, and given by

$$I_{ta,\alpha}(z) = I_{ta}(z)\, 10^{(-\alpha z\, f_{awf}/10dB)} \quad (6)$$

where

α is the **acoustic attenuation coefficient**;

z is the distance from the **external transducer aperture** along the **beam axis** to the plane containing the point of interest;

f_{awf} is the **acoustic working frequency**;

$I_{ta}(z)$ is the **temporal-average intensity** measured in water.

NOTE **Attenuated temporal-average intensity** is expressed in watts per metre squared, (W m^{-2}).

3.12
beam area
$A_b(z)$
area in a specified plane perpendicular to the **beam axis** consisting of all points at which the **pulse-pressure-squared integral** is greater than a specified fraction of the maximum value of the **pulse-pressure-squared integral** in that plane

NOTE 1 If the position of the plane is not specified, it is the plane passing through the point corresponding to the **spatial-peak temporal-peak acoustic pressure** in the whole acoustic field.

NOTE 2 In a number of cases, the term **pulse-pressure-squared integral** is replaced everywhere in the above definition by any linearly related quantity, e.g.:

a) in the case of a continuous wave signal the term **pulse-pressure-squared integral** is replaced by mean square acoustic pressure as defined in IEC 61689 [4];

b) in cases where signal synchronisation with the scanframe is not available, the term **pulse-pressure-squared integral** may be replaced by **temporal average intensity.**

NOTE 3 Some specified levels are 0,25 and 0,01 for the -6 dB and -20 dB beam areas, respectively.

NOTE 4 Beam area is expressed in metres squared (m^2).

[IEC 62127-1:2007, definition 3.7, modified]

3.13
beam axis

straight line that passes through the beam centrepoints of two planes perpendicular to the line which connects the point of maximal pulse-pressure-squared integral with the centre of the external transducer aperture

NOTE 1 See Figure 1.

NOTE 2 The location of the first plane is the location of the plane containing the maximum **pulse-pressure-squared integral** or, alternatively, is one containing a single main lobe which is in the focal Fraunhofer zone. The location of the second plane is as far as is practicable from the first plane and parallel to the first with the same two orthogonal scan lines (*x* and *y* axes) used for the first plane.

NOTE 3 In a number of cases, the term **pulse-pressure-squared integral** is replaced in the above definition by any linearly related quantity, e.g.:

a) in the case of a continuous wave signal the term **pulse-pressure-squared integral** is replaced by mean square acoustic pressure as defined in IEC 61689,

b) in cases where signal synchronisation with the scan frame is not available the term **pulse-pressure-squared integral** may be replaced by **temporal average intensity**.

[IEC 62127-1:2007, definition 3.8]

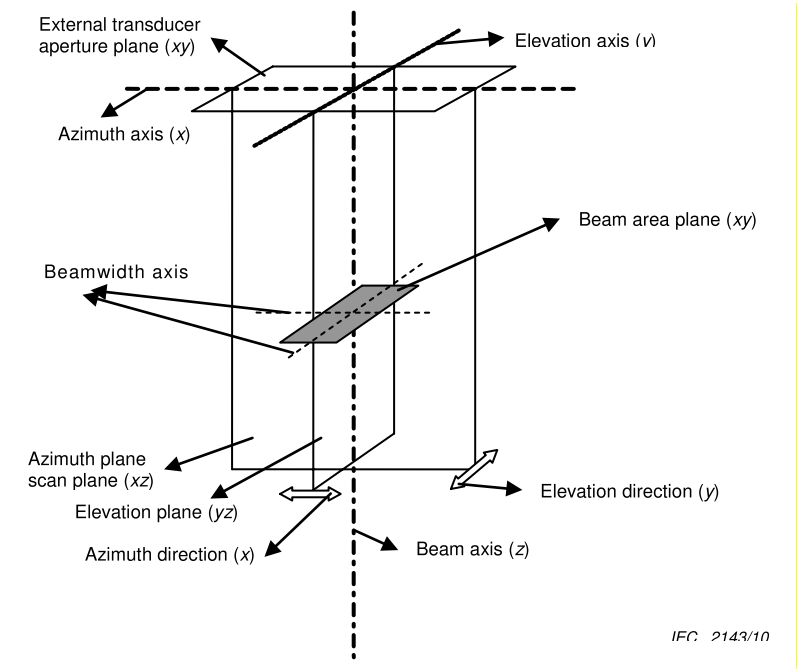

Figure 1 – Schematic diagram of the different planes and lines in an ultrasonic field
(modified from IEC 61828 and IEC 62127-1)

3.14
beam centrepoint

position determined by the 2D centroid of a set of **pulse-pressure-squared integrals** measured over the -6dB beam-area in a specified plane

NOTE Methods for determining 2D centroids are described in Annex B and C of IEC 61828.

3.15
beamwidth midpoint
linear average of the coordinates of the locations midway between each pair of points determining a **beamwidth** in a specified plane

NOTE The average is taken over as many **beamwidth** levels given in B.2 of IEC 61828 as signal level permits.

[IEC 62127-1:2007, definition 3.10, modified]

3.16
beamwidth
w_6, w_{12}, w_{20}
greatest distance between two points on a specified axis perpendicular to the **beam axis** where the **pulse-pressure-squared integral** falls below its maximum on the specified axis by a specified amount

NOTE 1 In a number of cases, the term **pulse-pressure-squared integral** is replaced in the above definition by any linearly related quantity, e.g.:

a) in the case of a continuous wave signal the term **pulse-pressure-squared integral** is replaced by mean square acoustic pressure as defined in IEC 61689 [4],

b) in cases where signal synchronisation with the scan frame is not available the term **pulse-pressure-squared integral** may be replaced by **temporal average intensity**.

NOTE 2 Commonly used **beamwidth**s are specified at –6 dB, –12 dB and –20 dB levels below the maximum. The decibel calculation implies taking 10 times the logarithm to the base of 10 of the ratios of the integrals.

NOTE 3 **Beamwidth** is expressed in metres (m).

[IEC 62127-1:2007, definition 3.11]

3.17
bone thermal index
TIB
thermal index for applications, such as foetal (second and third trimester), in which the ultrasound beam passes through soft tissue and a focal region is in the immediate vicinity of bone

NOTE 1 See 5.4.2 and 5.5.2 for methods of determining the bone thermal index.

NOTE 2 See Annex A for rationale and derivation notes.

3.18
bounded-square output power
P_{1x1}
maximum value of the time average **acoustic output power** emitted from any one-centimetre square region of the active area of the transducer, the one-centimetre square region having 1 cm dimensions in the x- and y-directions

NOTE 1 The side of the 1 cm × 1 cm square should be aligned with the azimuth axis in accordance with Figure 1. See A.4.1.4 and Annex B for more detail.

NOTE 2 **Bounded-square output power** is expressed in watts (W).

3.19
break-point depth
z_{bp}
closest distance, to the solid surface of the transducer or the enclosure of any stand-off path, used during a search to determine below-surface *TIS* and *TIB* **acoustic working frequency** and intensity parameters (such as **attenuated spatial-peak temporal-average intensity**)

$$z_{bp} = 1{,}5 \text{ x } D_{eq} \quad (7)$$

where D_{eq} is the **equivalent aperture diameter** for **non-scanning modes**.

NOTE 1 Specifically, for the **mechanical index**: the search should continue till the depth z_{MI}. Reasonable care should be taken not to go so close to the transducer face as to risk the integrity of the hydrophone or the validity of the measurement.

NOTE 2 For **scanning modes,** use the **non-scanning mode** D_{eq} value calculation [Equation (8)]. Do this using the **output beam area** of one **ultrasonic scan line**; the central scan line, corresponding to the **beam axis** (i.e. the line where pii, *MI, and* f_{awf} are measured).

NOTE 3 See Annex A for rationale and derivation notes.

NOTE 4 **Breakpoint depth** is expressed in metres (m).

3.20
combined-operating mode
mode of operation of an **equipment** that combines more than one **discrete-operating mode**

[IEC 61157:2007, definition 3.17.1]

3.21
cranial-bone thermal index
TIC
thermal index for applications in which the ultrasound beam passes through bone near the beam entrance into the body, such as paediatric and adult cranial or neonatal cephalic applications

NOTE 1 See 5.4.2.1 and 5.5.2.1 for methods of determining the **cranial bone thermal index**.

NOTE 2 See Annex A for rationale and derivation notes.

3.22
default setting
specific state of control that the **medical diagnostic ultrasonic equipment** will enter upon power-up, new **patient** selection or change from non-foetal to foetal applications

3.23
depth for mechanical index
z_{MI}
depth on the **beam axis** from the **external transducer aperture** to the plane of maximum **attenuated pulse-pressure-squared-integral** ($ppsi_{\alpha}$)

NOTE 1 Because z_{MI} may occur closer to the transducer than the **break-point depth** z_{bp}, use of $ppsi_{\alpha}$ rather than pii_{α} is technically more appropriate. If $z_{ppsi,\alpha}$ is larger than z_{bp}, then $z_{ppsi,\alpha}$ and $z_{pii,\alpha}$ are equal.

NOTE 2 **Depth for mechanical index** is expressed in metres (m).

3.24
depth for maximum pulse intensity integral
depth z on the **beam axis** and beyond the **break-point depth** z_{bp} from the **external transduscer aperture** to the plane of maximum **pulse-intensity integral** (pii) as approximated by the **pulse-pressure-squared integral** ($ppsi$)

NOTE 1 **Depth for maximum *pii*** is expressed in metres (m).

NOTE 2 **Depth for maximum** pii is termed "depth for peak pulse-intensity integral" in IEC 60601-2-37:2007/AMD1:2015.

NOTE 3 At this depth the **acoustic working frequency** is determined.

3.25
depth for TIB
$z_{b,ns}$ for **non-scanning modes**
for **non-scanning modes**, the distance along the **beam axis** from the **external transducer aperture** to the plane where the product of **attenuated output power** and **attenuated spatial-peak temporal-average intensity** is a maximum over the distance range equal to, or greater than, the **break-point depth**, z_{bp}

NOTE 1 **Depth for** TIB is expressed in metres (m).

NOTE 2 See Annex A for rationale and derivation notes.

3.26
depth for TIS
$z_{s,ns}$ for **non-scanning modes**
for **non-scanning modes**, the distance along the **beam axis** from the **external transducer aperture** to the plane at which the lower value of the **attenuated output power** and the product of the **attenuated spatial-peak temporal-average intensity** and 1 cm^2 is maximized over the distance range equal to, or greater than, the **break-point depth**, z_{bp}

NOTE 1 In this standard, the restricted definition of **spatial-peak temporal-average intensity** from IEC 62127-1, relating to a specified plane, is used where **spatial-peak temporal-average intensity** is replaced by **attenuated spatial-peak temporal-average intensity**.

NOTE 2 Depth for TIS is expressed in metres (m).

NOTE 3 See Annex A for rationale and derivation notes.

3.27
discrete-operating mode
mode of operation of **medical diagnostic ultrasonic equipment** in which the purpose of the excitation of the **ultrasonic transducer** or **ultrasonic transducer** element group is to utilize only one diagnostic methodology

[IEC 61157:2007, definition 3.17.2, modified]

3.28
equivalent aperture diameter
D_{eq}
diameter of a circle the area A of which is the –12 dB **output beam area** A_{ob} for **non-scanning modes** and the –12 dB **scanned aperture area** A_{sa} for **scanning modes**, given by

$$D_{eq} = \sqrt{\frac{4}{\pi} A} \tag{8}$$

where A_{ob} is the **output beam area**.

NOTE 1 Equation (8) is used in the calculation of the **cranial-bone thermal index**; for **non-scanning modes** with $A = A_{ob}$ and for **scanning modes** with $A = A_{sa}$.

NOTE 2 Equation (8) with $A = A_{ob}$ is also used in calculating the **break-point depth**.

NOTE 3 **Equivalent aperture diameter** is expressed in metres (m).

3.29
equivalent beam area
$A_{eq}(z)$
area of the acoustic beam at the distance z in terms of power and intensity and given by

$$A_{\mathrm{eq}}(z) = \frac{P_{\alpha}(z)}{I_{\mathrm{spta},\alpha}(z)} = \frac{P}{I_{\mathrm{spta}}} \tag{9}$$

where

$P_{\alpha}(z)$ is the **attenuated output power**, at the distance z;

$I_{\mathrm{spta},\alpha}(z)$ is the **attenuated spatial-peak temporal-average intensity**, at the distance z;

P is the **output power**;

I_{spta} is the **spatial-peak temporal-average intensity**, at the distance z; and

z is the distance from the **external transducer aperture** to the specified point.

NOTE **Equivalent beam area** is expressed in metres squared (m^2).

3.30
equivalent beam diameter
$d_{\mathrm{eq}}(z)$
diameter of the acoustic beam at the distance z in terms of the **equivalent beam area** and given by

$$d_{\mathrm{eq}}(z) = \sqrt{\frac{4}{\pi} A_{\mathrm{eq}}(z)} \tag{10}$$

where

$A_{\mathrm{eq}}(z)$ is the **equivalent beam area**;

z is the distance from the **external transducer aperture** to the specified point.

NOTE **Equivalent beam diameter** is expressed in metres (m).

3.31
external transducer aperture
part of the surface of the **ultrasonic transducer** or **ultrasonic transducer** element group assembly that emits ultrasonic radiation into the propagation medium

NOTE 1 This surface is assumed to be either directly in contact with the patient or in contact with a water or liquid path to the patient. See Figure 1.

NOTE 2 The **ultrasonic transducer** element group is usually offset from this surface by a lens, matching layers and possibly fluid.

[IEC 62127-1:2007, definition 3.27, modified]

3.32
mechanical index
MI
mechanical index is given by

$$MI = \frac{p_{\mathrm{r},\alpha}(z_{\mathrm{MI}})\, f_{\mathrm{awf}}^{-1/2}}{C_{MI}} \tag{11}$$

where

C_{MI} = 1 MPa·$MHz^{-1/2}$

$p_{\mathrm{r},\alpha}(z_{MI})$ is the **attenuated peak-rarefactional acoustic pressure** at the depth z_{MI}

f_{awf} *i*s the **acoustic-working frequency**.

NOTE 1 See Annex A for rationale and derivation notes.

3.33
medical diagnostic ultrasonic equipment (or **system)**
combination of the **ultrasound instrument console** and the **transducer assembly** making up a complete diagnostic system

[IEC 61157:2007, definition 3.15]

NOTE 1 For the purpose of this standard, **medical diagnostic ultrasonic equipment (or system)** means **electrical equipment** that is intended for *in vivo* ultrasonic examination and monitoring for obtaining a medical diagnosis.

NOTE 2 IEC 60601-2-37:2007 uses the term "ultrasonic diagnostic equipment" instead of **medical diagnostic ultrasonic equipment**.

3.34
non-scanning mode
mode of operation of **medical diagnostic ultrasonic equipment** that involves a sequence of ultrasonic pulses which give rise to **ultrasonic scan lines** that follow the same acoustic path

[IEC 62127-1:2007, definition 3.39.4, modified]

3.35
output beam area
A_{ob}
area of the ultrasonic beam derived from the -12 dB **beam area** at the **external transducer aperture**

NOTE 1 For reasons of measurement accuracy, the –12 dB **output beam area** may be derived from measurements at a distance chosen to be as close as possible to the face of the transducer, and, if possible, no more than 1 mm from the face.

NOTE 2 For contact transducers, this area can be taken as the geometrical area of the **ultrasonic transducer** or **ultrasonic transducer** element group.

NOTE 3 The **output beam area** is expressed in metres squared (m^2).

NOTE 4 Methodology for finding the beam area using the **pulse-pressure-squared integral** for focused fields is described in clauses 6.2 and 6.3 of IEC 61828.

[IEC 62127-1:2007, definition 3.40]

3.36
output beam dimensions
X_{ob} , Y_{ob}
dimensions of the ultrasonic beam (–12 dB **beamwidth**) in specified directions perpendicular to each other and in a direction normal to the **beam axis** and at the **external transducer aperture**

NOTE 1 For reasons of measurement accuracy, the –12 dB **output beam dimensions** may be derived from measurements at a distance chosen to be as close as possible to the face of the transducer and, if possible, no more than 1 mm from the face.

NOTE 2 For contact transducers, these dimensions can be taken as the geometrical dimensions of the **ultrasonic transducer** or **ultrasonic transducer** element group.

NOTE 3 **Output beam dimensions** are expressed in metres (m).

NOTE 4 Methodology for finding the beam area using the **pulse-pressure-squared integral** for focused fields is described in 6.2 and 6.3 of IEC 61828.

[IEC 62127-1:2007, definition 3.41, modified]

3.37
output power
P
time-average ultrasonic power emitted by an **ultrasonic transducer** into an approximately free field under specified conditions in a specified medium, preferably water

[IEC 61161:2013, definition 3.3]

NOTE 1 "time-average" means averaged over an integral multiple of the temporal periodicity.

NOTE 2 **Output power** is expressed in watts (W).

3.38
peak-rarefactional acoustic pressure
p_r
maximum of the modulus of the negative **instantaneous acoustic pressure** in an acoustic field or in a specified plane during an **acoustic repetition period**

NOTE 1 **Peak-rarefactional acoustic pressure** is expressed as a positive number.

NOTE 2 **Peak-rarefactional acoustic pressure** is expressed in pascals (Pa).

NOTE 3 The definition of **peak-rarefactional acoustic pressure** also applies to peak-negative acoustic pressure which is also in use in literature.

[IEC 62127-1:2007, definition 3.44]

3.39
power parameter
P_p
beam-related power quantity used in the numerator of the general **thermal index** relationship

NOTE 1 See Equation A.4

NOTE 2 The meaning of this quantity depends on the TI to be evaluated, see A.5.1 and A.5.2. In general terms, it will be the measured quantity responsible for the estimation of the specific temperature rise.

NOTE 3 **Power parameter** is expressed in watts (W).

3.40
prudent-use statements
affirmations of the principle that only necessary clinical information should be acquired and that high exposure levels and long exposure times should be avoided

NOTE See Bibliography [5,6,7,8].

3.41
pulse duration
t_d
1,25 times the interval between the time when the time integral of the square of the **instantaneous acoustic pressure** reaches 10 % and 90 % of its final value

NOTE 1 The final value of the time integral of the square of the **instantaneous acoustic pressure** is the **pulse-pressure-squared integral**.

NOTE 2 **Pulse duration** is expressed in seconds (s).

NOTE 3 See Figure 2 of IEC 62127-1.

[IEC 62127-1:2007, definition 3.48]

3.42
pulse-intensity integral
pii
time integral of the **instantaneous intensity** at a particular point in an acoustic field integrated over the **acoustic pulse waveform**

NOTE 1 For measurement purposes referred to in this International Standard, **pulse-intensity integral** is proportional to **pulse-pressure-squared integral**.

NOTE 2 The **pulse-intensity integral** is expressed in joules per metre squared (Jm^{-2}).

[IEC 62127-1:2007, definition 3.49]

3.43
pulse-pressure-squared integral
ppsi
time integral of the square of the **instantaneous acoustic pressure** at a particular point in an acoustic field integrated over the **acoustic pulse waveform**

NOTE The **pulse-pressure-squared integral** is expressed in pascal squared seconds (Pa^2s).

[IEC 62127-1:2007, definition 3.50]

3.44
pulse repetition period
prp
time interval between equivalent points on successive pulses or tone-bursts

NOTE 1 In general, for **non-scanning modes** the **pulse repetition period** needs to be adjusted to represent a 'per-second' average taking into account interruptions-in, or non-constant, pulsing; e.g. such as may occur in **combined operating modes**.

NOTE 2 The **pulse repetition period** is expressed in seconds (s).

[IEC 62127-1:2007, definition 3.51]

3.45
pulse repetition rate
prr
reciprocal of the **pulse repetition period**

NOTE The **pulse repetition rate** is expressed in hertz (Hz).

[IEC 62127-1:2007, definition 3.52]

3.46
scanned aperture area
A_{sa}
area at the **external transducer aperture** consisting of all points at which the **pulse-pressure-squared integral** is greater than -12 dB of the maximum value of the **pulse-pressure-squared integral** in that plane

NOTE 1 For reasons of measurement accuracy, the –12 dB **scanned aperture area** may be derived from measurements at a distance chosen to be as close as possible to the face of the transducer, and, if possible, no more than 1 mm from the face.

NOTE 2 For contact transducers, this area can be taken as the geometrical area of the active elements during one frame scan of the **ultrasonic transducer** or **ultrasonic transducer** element group.

NOTE 3 In a number of cases, the term **pulse-pressure-squared integral** is replaced everywhere in the above definition by any linearly related quantity, e.g.:

a) in the case of a continuous wave signal the term **pulse-pressure-squared integral** is replaced by mean square acoustic pressure as defined in IEC 61689,

b) in cases where signal synchronisation with the scanframe is not available the term **pulse-pressure-squared integral** may be replaced by **temporal average intensity**.

NOTE 4 **Scanned aperture area** is expressed in metres squared (m^2).

3.47
scan direction
for **systems** with scanning modes, the direction in the **scan plane** and perpendicular to a specified **ultrasonic scan line**

NOTE During one acquisition frame the scan direction may be azimuthal (x) and/or elevational (y) and may include combinations, e.g., polar.

[IEC 61157: 2007, definition 3.27]

3.48
scan plane
for automatic scanning systems, a plane containing all the **ultrasonic scan lines**

NOTE 1 See Figure 1.

NOTE 2 Some scanning systems have the ability to steer the ultrasound beam in two directions. In this case, there is no **scan plane** that meets this definition. However, it might be useful to consider a plane through the major-axis of symmetry of the **ultrasound transducer** and perpendicular to the transducer face (or another suitable plane) as being equivalent to the scan plane.

[IEC 62127-1:2007, definition 3.56]

3.49
scanning mode
mode of operation of **a medical diagnostic ultrasonic equipment** that involves a sequence of ultrasonic pulses which give rise to scan lines that do not follow the same acoustic path

[IEC 61157:2007, definition 3.17.5]

3.50
scan repetition period
srp
time interval between identical points on two successive frames, sectors or scans, applying to automatic scanning systems with a periodic scan sequence only

NOTE 1 In general, this International Standard assumes that an individual **ultrasonic scan line** repeats exactly after a number of acoustic pulses.

NOTE 2 The scan repetition period is expressed in seconds (s).

3.51
scanwidth
w_s
greatest distance between two points on the axis in the **scan plane** perpendicular to the central **ultrasonic scan line** where the **temporal average intensity** falls below its maximum in the **scan plane** by 12 dB at the distance of interest from the transducer surface

NOTE 1 This dimension may be determined by hydrophone measurements or by calculation using knowledge of the dimensions of the transducer aperture and scanning geometry.

NOTE 2 **Scanwidth** is expressed in metres (m).

3.52
soft tissue thermal index
TIS
thermal index related to soft tissues

NOTE 1 See 5.4.1 and the following sub-clauses and 5.5.1 for methods of determining the **soft tissue thermal index.**

NOTE 2 For the purposes of this document, soft tissue includes all body tissues and fluids except skeletal tissues.

NOTE 3 See Annex A for rationale and derivation notes.

3.53
spatial-average temporal-average intensity
I_{sata}
equal to the **temporal-average intensity** averaged over the **scan-area, beam area** or other defined area as appropriate

NOTE **Spatial-average temporal-average intensity** is expressed in watts per metre squared (Wm^{-2}).

[IEC 62127-1:2007, definition 3.59 slightly modified]

3.54
spatial-peak temporal-average intensity
I_{spta}
maximum value of the **temporal-average intensity** in an acoustic field or in a specified plane

NOTE 1 For systems in **combined-operating mode**, the averaging time period needs to be sufficient to include periods in which scanning or pulsing is interrupted.

NOTE 2 **Spatial-peak temporal-average intensity** is expressed in watts per metre squared (Wm^{-2}).

[IEC 62127-1:2007, definition 3.62]

3.55
temporal-average intensity
I_{ta}
time-average of the **instantaneous intensity** at a particular point in an acoustic field

NOTE 1 The time-average is taken normally over an integral number of **acoustic repetition periods**; if not, the period for averaging should be specified.

NOTE 2 **Temporal-average intensity** is expressed in watts per metre squared (Wm^{-2}).

[IEC 62127-1:2007, definition 3.65]

3.56
thermal index
TI
ratio of **attenuated output power** at a specified point to the **attenuated output power** required to raise the temperature at that point in a specific tissue model by 1 °C

NOTE See Annex A for rationale and derivation notes.

3.57
transducer assembly
those parts of **medical diagnostic ultrasonic equipment** comprising the **ultrasonic transducer** and/or **ultrasonic transducer** element group, together with any integral components, such as an acoustic lens or integral stand-off

NOTE The **transducer assembly** is usually separable from the ultrasound instrument console.

[IEC 62127-1:2007, definition 3.69]

3.58
transmit pattern
combination of a specific set of transducer beam-forming characteristics (determined by the transmit aperture size, apodization shape and relative timing/phase delay pattern across the aperture, resulting in a specific focal length and direction) and an electrical drive waveform of a specific fixed shape but variable amplitude

3.59
ultrasonic scan line
for scanning systems, the **beam axis** for a particular **ultrasonic transducer** element group, or for a particular excitation of an **ultrasonic transducer** or **ultrasonic transducer** element group

NOTE 1 Here an **ultrasonic scan line** refers to the path of acoustic pulses and not to a line on an image on the display screen of a system.

NOTE 2 The case where a single excitation produces ultrasonic beams propagating along more than one **beam axis** is not considered.

[IEC 62127-1:2007, definition 3.71, modified]

3.60
ultrasonic transducer
device capable of converting electrical energy to mechanical energy within the ultrasonic frequency range and/or reciprocally of converting mechanical energy to electrical energy

[IEC 62127-1:2007, definition 3.73]

3.61
instantaneous acoustic pressure
$p(t)$
pressure minus the ambient pressure at a particular instant in time and at a particular point in an acoustic field

NOTE **Instantaneous acoustic pressure** is expressed in pascals (Pa).

[SOURCE: IEC 62127-1:2007, 3.33, modified – The reference to IEV 801-01-19 has been removed in the definition]

3.62
attenuated instantaneous acoustic pressure
$p_\alpha(z,t)$
value of the **instantaneous acoustic pressure** at time t after attenuation on a plane perpendicular to the **beam axis** at a specified distance z from the source, and given by

$$p_\alpha(z,t) = p(z,t)10^{(-\alpha\, z\, f_{\text{awf}}/20\ \text{dB})} \tag{26}$$

where

α is the **acoustic attenuation coefficient**;

z is the distance from the source to the point (plane) of interest;

f_{awf} is the **acoustic working frequency**;

$p(z,t)$ is the **instantaneous acoustic pressure**

NOTE **Attenuated instantaneous acoustic pressure** is expressed in pascals (Pa).

3.63
attenuated pulse-pressure-squared integral
$ppsi_\alpha(z)$
time integral of the square of the **attenuated instantaneous acoustic pressure**, integrated over the acoustic pulse waveform, on a plane perpendicular to the **beam axis** at a specified distance z in an acoustic field

$$ppsi_\alpha(z) = \int p_\alpha{}^2(z,t)dt = \int \left[p(z,t)10^{(-\alpha\, z\, f_{\text{awf}}/20\ \text{dB})}\right]^2 dt = ppsi(z)\times 10^{(-\alpha\, z\, f_{\text{awf}}/10\ \text{dB})} \tag{27}$$

where

$p(z,t)$ is the **instantaneous acoustic pressure** at depth z.

α is the **acoustic attenuation coefficient**;

z is the distance from the source to the point (plane) of interest;

f_{awf} is the **acoustic working frequency**;

$ppsi$ is the **pulse-pressure-squared integral**

NOTE 1 **Attenuated pulse-pressure-squared integral** is expressed in pascal squared seconds (Pa^2s).

NOTE 2 See definition 3.43 for the non-attenuated version; with the addition here of the perpendicular plane at depth z.

3.64
attenuated scan intensity integral
$sii_\alpha(z)$
sum of the **attenuated pulse intensity integrals** in one scan (one frame of **ultrasonic scan lines**) at depth z

NOTE 1 **Attenuated scan intensity integral** is expressed in joules per square metre (Jm^{-2}).

NOTE 2 For measurement purposes of this standard, $sii_\alpha(z)$ is equivalent to $1/(\rho c)$ times the **sum of attenuated pulse-pressure-squared integrals** at depth z, for $z \geq z_{bp}$, with ρc denoting the characteristic acoustic impedance of pure water.

NOTE 3 See definition 3.79 for the non-attenuated version.

3.65
attenuated spatial-peak pulse-average intensity
$I_{sppa,\alpha}(z)$
maximum value of the **spatial-peak pulse-average intensity** after attenuation, on a plane perpendicular to the **beam axis** at a specified distance z from the source, and given by

$$I_{sppa,\alpha}(z) = \frac{1}{t_d(z)}\, pii_\alpha(z) \tag{28}$$

where

$t_d(z)$ is the **pulse duration** at the same depth z;

$pii_\alpha(z)$ is the **attenuated pulse-intensity integral** at depth z

NOTE 1 **Attenuated spatial-peak pulse-average intensity** is expressed in watts per square metre (Wm^{-2}).

NOTE 2 For measurement purposes of this standard, $pii_\alpha(z)$ is equivalent to $1/(\rho c)$ times the **attenuated pulse-pressure-squared integrals** at depth z, $ppsi_\alpha(z)$, for $z \geq z_{bp}$, with ρc denoting the characteristic acoustic impedance of pure water.

NOTE 3 See definition 3.81 for the non-attenuated version.

3.66
attenuated sum of pulse-pressure-squared integrals
$s_\alpha ppsi\ (z)$
attenuated value of the sum of **pulse-pressure-squared integrals** in one scan (one frame of **ultrasonic scan lines)** at depth z

NOTE 1 **Attenuated sum of pulse-pressure-squared integrals** is expressed in pascal squared seconds (Pa^2s).

NOTE 2 The **attenuated sum of pulse-pressure-squared integrals** at depth z will be equal to the **sum of attenuated pulse-pressure-squared integrals** if each **ultrasonic scan line** in the frame which is included in the sum has the same **acoustic working frequency**.

NOTE 3 See F.3.1.4.2 for additional explanation.

NOTE 4 See definition 3.83 for the non-attenuated version.

3.67
depth for maximum I_{sppa}
$z_{sppa,max}$
depth z on the **beam axis** and beyond the **break-point depth** z_{bp} of maximum **spatial-peak pulse-average intensity**

NOTE 1 **Depth for maximum I_{sppa}** is expressed in metres (m).

NOTE 2 This depth is equivalent to the **depth for maximum** pii.

3.68
depth for maximum $I_{sppa,\alpha}$
$z_{sppa,\alpha,max}$
depth z on the **beam axis** and beyond the **break-point depth** z_{bp} of maximum **attenuated spatial-peak pulse-average intensity**

NOTE 1 **Depth for maximum $I_{sppa,\alpha}$** is expressed in metres (m).

NOTE 2 This depth is equivalent to the **depth for maximum** pii_{α}.

3.69
depth for maximum I_{spta}
$z_{spta,max}$
depth z on the **beam axis** and beyond the **break-point depth** z_{bp} of maximum **spatial-peak temporal-average intensity**

NOTE 1 **Depth for maximum I_{spta}** is expressed in metres (m).

NOTE 2 For **non-scanning modes**, this depth is equivalent to the **depth for maximum** pii. For **scanning modes**, it is equivalent to the **depth for maximum** sii.

3.70
depth for maximum $I_{spta,\alpha}$
$z_{spta,\alpha,max}$
depth z on the **beam axis** and beyond the **break-point depth** z_{bp} of maximum **attenuated spatial-peak temporal-average intensity**

NOTE 1 **Depth for maximum $I_{spta,\alpha}$** is expressed in metres (m).

NOTE 2 For **non-scanning modes**, this depth is equivalent to the **depth for maximum** pii_{α}. For **scanning modes**, it is equivalent to the **depth for maximum** sii_{α}.

3.71
depth for maximum pii_{α}
$z_{pii,\alpha}$
depth z on the **beam axis** and beyond the **break-point depth** z_{bp} of maximum **attenuated pulse-intensity integral**

NOTE 1 **Depth for maximum pii_{α}** is expressed in metres (m).

NOTE 2 This depth is equivalent to the **depth for maximum** $ppsi_{\alpha}$, $z_{ppsi,\alpha}$, when $z_{ppsi,\alpha}$ occurs beyond the **break-point depth** (see 3.73).

NOTE 3 **Depth for maximum** pii_{α} is termed "depth for peak attenuated pulse-intensity integral" in IEC 60601-2-37:2007+IEC 60601-2-37:2007/AMD1:2015.

3.72
depth for maximum $ppsi$
z_{ppsi}
depth z on the **beam axis** of maximum **pulse-pressure-squared integral**

NOTE 1 **Depth for maximum** $ppsi$ is expressed in metres (m).

NOTE 2 When it occurs beyond the **break-point depth**, this depth is equivalent to the **depth for maximum** pii, z_{pii} (see 3.24).

3.73
depth for maximum $ppsi_\alpha$

$z_{ppsi,\alpha}$
depth z on the **beam axis** of maximum **attenuated pulse-pressure-squared integral**

NOTE 1 **Depth for maximum** $ppsi_\alpha$ is expressed in metres (m).

NOTE 2 When it occurs beyond the **break-point depth**, this depth is equivalent to the **depth for maximum** pii_α, $z_{pii,\alpha}$ (i.e. depth for maximum **attenuated pulse-intensity integral**).

NOTE 3 This depth is the **depth for mechanical index**, z_{MI} (see 3.23).

3.74
depth for maximum sii

z_{sii}
depth z on the **beam axis** and beyond the **break-point depth** z_{bp} of maximum **scan-intensity integral**

NOTE 1 **Depth for maximum** sii is expressed in metres (m).

NOTE 2 This depth is equivalent to the **depth for maximum** $sppsi$, z_{sppsi}, when z_{sppsi} occurs beyond the **break-point depth** (see 3.76).

NOTE 3 **Depth for maximum** sii is termed "depth for peak sum of pulse-intensity integrals" in IEC 60601-2-37:2007+IEC 60601-2-37:2007/AMD1:2015.

3.75
depth for maximum sii_α

$z_{sii,\alpha}$
depth z on the **beam axis** and beyond the **break-point depth** z_{bp} of maximum **attenuated scan-intensity integral**

NOTE 1 **Depth for maximum** sii_α is expressed in metres (m).

NOTE 2 This depth is equivalent to the **depth for maximum** $sppsi_\alpha$, $z_{sppsi,\alpha}$, when $z_{sppsi,\alpha}$ occurs beyond the **break-point depth** (see 3.77).

NOTE 3 **Depth for maximum** sii_α is termed "depth for peak sum of attenuated pulse-intensity integrals" in IEC 60601-2-37:2007+IEC 60601-2-37:2007/AMD1:2015.

3.76
depth for maximum $sppsi$

z_{sppsi}
depth z on the **beam axis** of maximum **sum of pulse-pressure-squared integrals**

NOTE 1 **Depth for maximum** $sppsi$ is expressed in metres (m).

NOTE 2 When it occurs beyond the **break-point depth**, this depth is equivalent to the **depth for maximum** sii, z_{sii} (see 3.74).

NOTE 3 **Depth for maximum** $sppsi$ is termed "depth for peak sum of pulse-intensity integrals" in IEC 60601-2-37:2007+IEC 60601-2-37:2007/AMD1:2015.

3.77
depth for maximum $sppsi_\alpha$

$z_{sppsi,\alpha}$
depth z on the **beam axis** of maximum **sum of attenuated pulse-pressure-squared integrals**

NOTE 1 **Depth for maximum** $sppsi_\alpha$ is expressed in metres (m).

NOTE 2 When it occurs beyond the **break-point depth**, this depth is equivalent to the **depth for maximum** sii_α, $z_{sii,\alpha}$ (see 3.75).

NOTE 3 **Depth for maximum** $sppsi_\alpha$ is termed "depth for peak sum of attenuated pulse-intensity integrals" in IEC 60601-2-37:2007+IEC 60601-2-37:2007/AMD1:2015.

3.78
pulse-average intensity
I_{pa}
quotient of the **pulse-intensity integral** to the **pulse duration** at a particular point in an acoustic field

NOTE 1 This definition applies to pulses and bursts.

NOTE 2 **Pulse-average intensity** is expressed in watts per square metre (Wm^{-2}).

[IEC 62127-1:2007+IEC 62127-1:2007/AMD1:2013, 3.47]

3.79
scan intensity integral
sii
sum of the **pulse intensity integrals** in one scan (one frame of **ultrasonic scan lines**) at depth z in the acoustic field

NOTE 1 **Scan intensity integral** is expressed in joules per square metre (Jm^{-2}).

NOTE 2 For measurement purposes of this standard, sii is equivalent to $1/(\rho c)$ times the **sum of pulse-pressure-squared integral** at depth z where ρc is the characteristic acoustic impedance of pure water.

3.80
scan repetition rate
srr
inverse of the **scan repetition period** (see 3.50)

NOTE **Scan repetition rate** is expressed in hertz (Hz).

3.81
spatial-peak pulse-average intensity
$I_{sppa}(z)$
maximum value of the **pulse-average intensity** on a plane perpendicular to the **beam axis** at a specified distance z from the source, and given by

$$I_{\text{sppa}}(z) = \frac{1}{t_{\text{d}}(z)}\, pii(z) \tag{29}$$

where

$t_{\text{d}}(z)$ is the **pulse duration** at the same depth z;

$pii(z)$ is the **pulse-intensity integral** at depth z

NOTE 1 **Spatial-peak pulse-average intensity** is expressed in watts per square metre (Wm^{-2}).

NOTE 2 For measurement purposes of this standard, $pii(z)$ is equivalent to $1/(\rho c)$ times the **pulse-pressure-squared integral** at depth z, $ppsi(z)$, for $z \geq z_{\text{bp}}$, with ρc denoting the characteristic acoustic impedance of pure water.

NOTE 3 See IEC 62127-1:2007, 3.60, which has been modified to specify the perpendicular plane at depth z. Equation (29) and Note 2 have been added, in accordance with IEC 62127-1:2007, Equation (15).

3.82
sum of attenuated pulse-pressure-squared integrals
$sppsi_\alpha(z)$
sum of the **attenuated pulse-pressure-squared integrals** in one scan (one frame of **ultrasonic scan lines**) at depth z

NOTE 1 **Sum of attenuated pulse-pressure-squared integrals** is expressed in pascal squared seconds (Pa^2s).

NOTE 2 Closely related to the **attenuated scan intensity integral**, see 3.64.

NOTE 3 The **sum of attenuated pulse-pressure-squared integrals** at depth z will be equal to the **attenuated sum of pulse-pressure-squared integrals** at depth z if each **ultrasonic scan line** in the frame which is included in the sum has the same **acoustic working frequency**.

3.83
sum of pulse-pressure-squared integrals
***sppsi*(*z*)**
sum of **pulse-pressure-squared integrals** in one scan (one frame of **ultrasonic scan lines**) at depth z

NOTE 1 **Sum of pulse-pressure-squared integrals** is expressed in pascal squared seconds (Pa^2s).

NOTE 2 The *sppsi* at depth z may also be referred to as the scan pulse pressure squared integral and is proportional to the **scan intensity integral** for $z \geq z_{bp}$.

4 List of symbols

α	**acoustic attenuation coefficient**
$A_b(z)$	**beam area**
$A_{eq}(z)$	**equivalent beam area**
A_{ob}	**output beam area**
A_{sa}	scanned aperture area
arp	**acoustic repetition period**
C_{MI}	normalizing coefficient
$C_{TIS,1}$	normalizing coefficient
$C_{TIS,2}$	normalizing coefficient
$C_{TIB,1}$	normalizing coefficient
$C_{TIB,2}$	normalizing coefficient
C_{TIC}	normalizing coefficient
C_K	normalizing coefficient
C_{sb}	normalizing coefficient
d_6	–6 dB beam diameter
D_{eq}	**equivalent aperture diameter**
$d_{eq}(z)$	**equivalent beam diameter**
f_{awf}	**acoustic working frequency**
I_{ta}	**temporal-average intensity**
$I_{ta,\alpha}(z)$	**attenuated temporal-average intensity**
I_{sata}	**spatial-average temporal-average intensity**
$I_{sata,\alpha}(z)$	attenuated spatial-average temporal-average intensity
I_{sppa}	**spatial-peak pulse-average intensity**
$I_{sppa,\alpha}$	**attenuated spatial-peak pulse-average intensity**
I_{spta}	**spatial-peak temporal-average intensity**
$I_{spta,\alpha}(z)$	**attenuated spatial-peak temporal-average intensity**
I_{ta}	**temporal-average intensity**
K	thermal conductivity
MI	**mechanical index**
μ_0	**acoustic absorption coefficient**

P	**output power**
$P_{\alpha(z)}$	**attenuated output power**
P_{1x1}	**bounded-square output power**
$P_{1x1,\alpha(z)}$	**attenuated bounded-square output power**
pii	**pulse-intensity integral**
$pii_{\alpha(z)}$	**attenuated pulse-intensity integral**
P_p	**power parameter**
$ppsi_\alpha$	**attenuated pulse-pressure-squared integral**
$ppsi(z)$	**pulse-pressure-squared integral**
p_r	**peak-rarefactional acoustic pressure**
$p_{r,\alpha(z)}$	**attenuated peak-rarefactional acoustic pressure**
prp	**pulse repetition period**
prr	**pulse repetition rate**
sii	**scan intensity integral**
sii_α	**attenuated scan intensity integral**
$sppsi$	**sum of pulse-pressure-squared integrals**
$s_\alpha ppsi$	**attenuated sum of pulse-pressure-squared integrals**
$sppsi_\alpha$	**sum of attenuated pulse-pressure-squared integrals**
srp	**scan repetition period**
srr	**scan repetition rate**
TI	**thermal index**
TIB	**bone thermal index**
TIC_{sc}	**bone thermal index** at-surface, scanning
TIC_{ns}	**bone thermal index** at surface, non-scanning
$TIB_{bs,sc}$	**bone thermal index** below surface, scanning
$TIB_{bs,ns}$	**bone thermal index** below surface, non-scanning
TIC	**cranial-bone thermal index**
TIS	**soft tissue thermal index**
$TIS_{as,sc}$	**soft tissue thermal index** at-surface, scanning
$TIS_{as,ns}$	**soft tissue thermal index** at surface, non-scanning
$TIS_{bs,sc}$	**soft tissue thermal index** below surface, scanning
$TIS_{bs,ns}$	**soft tissue thermal index** below surface, non-scanning
t_d	**pulse duration**
w_6, w_{12}, w_{20}	**beamwidth**
X_{ob} , Y_{ob}	**output beam dimensions**
z	distance from the **external transducer aperture** to a specified point
$z_{b,ns}$	**depth for *TIB*** below surface for non- scanned modes
z_{bp}	**break-point depth**
z_{pii}	**depth for maximum *pii***
$z_{pii,\alpha}$	**depth for maximum pii_α**
z_{ppsi}	**depth for maximum *ppsi***
$z_{ppsi,\alpha}$	**depth for maximum $ppsi_\alpha$**
z_{MI}	**depth for *MI***

z_{sii}	**depth for maximum** sii
$z_{sii,\alpha}$	**depth for maximum** sii_{α}
$z_{s,ns}$	**depth for** TIS below surface for non- scanned modes
$z_{sppa,max}$	**depth for maximum** I_{sppa}
$z_{sppa,\alpha,max}$	**depth for maximum** $I_{sppa,\alpha}$
$z_{spta,max}$	**depth for maximum** I_{spta}
$z_{spta,\alpha,max}$	**depth for maximum** $I_{spta,\alpha}$
z_{sppsi}	**depth for maximum** $sppsi$
$z_{sppsi,\alpha}$	**depth for maximum** $sppsi_{\alpha}$

5 Test methods for determining the mechanical index and the thermal index

5.1 General

This clause defines methods for determining an exposure parameter relating to temperature rise in theoretical tissue-equivalent models, and also an exposure parameter for non-thermal effects. These exposure parameters, referred to as indices, are related to the safe use of **medical diagnostic ultrasonic equipment**. The indices are intended to be used in IEC 60601-2-37.

These indices shall be determined in accordance with 5.2 to 5.5 for a particular ultrasonic field configuration generated by a **discrete-operating mode** of specific **medical diagnostic ultrasonic equipment**. For **combined-operating modes**, the procedures specified in 5.6 shall be used. Background material is given in Annex A. “Rationale and derivation”.

Acoustic output measurements shall be undertaken using test methods based on the use of hydrophones in accordance with IEC 62127-1 or the use of radiation force balances for power measurements in accordance with IEC 61161. All such measurements shall be made in water (see also Annex B). The measurement uncertainty is to be determined by following [9].

In all cases where **bounded-square output power** is determined, the location of the bounding mask or equivalent means (see Annex B) shall be such as to determine the largest value.

The value of the **acoustic attenuation coefficient** shall be 0,3 dB cm^{-1} MHz^{-1}. This value is selected as an appropriate attenuating coefficient for a homogeneous model intended to be equivalent to the attenuation in reasonable worst-case conditions of clinical use.

The **output beam area** may be determined by using a line scanning or a raster-scanning hydrophone. If the output beam area is expected to be circular it may be sufficient to measure the w_{20} **beamwidth** along the x and y axes. If the **beamwidth**s are equal within 5 %, then also measure the diagonal widths of the aperture at $\pm 45°$ to the x axis. If the diagonal widths are also within 5 %, then the symmetry is circular for present purposes. If the diagonal widths differ by more than 5 % compared to the x or y widths, the symmetry is not circular and measurements may be performed by raster scanning, but not line scanning. See IEC 61828 for more.

NOTE 1 Temperature rise in tissue due to transducer surface self-heating has not been taken into account in the determination of the **thermal index** [10]. See Annex C.

NOTE 2 The attenuation model used is not always applicable. Recent literature suggests that sometimes other models should be used [11]. See Annex D for more discussion.

NOTE 3 See Annex D for more discussion of ‘reasonable worst case’.

NOTE 4 Basic SI units have been specified in Clause 3. The expressions in the following clauses and annexes were formulated using, e.g. centimetres (cm), milliwatts (mW), and megahertz (MHz)

5.2 Determination of mechanical index

5.2.1 Determination of attenuated peak-rarefactional acoustic pressure

The calculation of **mechanical index** requires determination of the value of the **attenuated peak-rarefactional acoustic pressure** at the location of the maximum **attenuated pulse-intensity integral** ($z_{pii,\alpha}$). This location should be determined according to the procedures set out in IEC 62127-1 for the location of peak **pulse-pressure-squared integral**, with the addition that for all measurement locations an **acoustic attenuation coefficient** shall be applied to the **pulse-pressure-squared integral.**

5.2.2 Calculation of mechanical index

The **mechanical index** shall be calculated, at depth z_{MI}, from the expression as defined under 3.32:

$$MI = \frac{p_{\mathrm{r},\alpha} \cdot f_{\mathrm{awf}}^{-1/2}}{C_{MI}} \tag{11}$$

where

C_{MI} = 1 MPa MHz$^{-1/2}$

$p_{\mathrm{r},\alpha}(z_{MI})$ is the **attenuated peak-rarefactional acoustic pressure** at the depth z_{MI}

f_{awf} is the **acoustic-working frequency**.

5.3 Determination of thermal index – general

The method of determination of the **thermal index** depends on the tissue model being assumed (*TIS*, *TIB* or *TIC* tissue model) and, for the *TIS* and *TIB* models, it requires the calculation of ‘at surface’ and ‘below surface’ values and taking the larger. For **combined-operating modes**, ‘at surface’ and ‘below surface’ contributions from **scanning modes** and **non-scanning modes** are calculated and summed, the displayed *TI* being the larger sum.

The determination methods for these ‘at surface’, ‘below surface’, ‘scanning’ and ‘non-scanning’ components are described in the following sections.

NOTE 1 The thermal indices are steady state estimates based on the acoustic **output power** required to produce a 1 °C temperature rise in tissue conforming to the “homogeneous tissue 0,3 dBcm^{-1}MHz^{-1} attenuation model” [1] and may not be appropriate for radiation force imaging, or similar techniques that employ pulses or pulse bursts of sufficient duration to create a significant transient temperature rise. [2].

NOTE 2 At present the heat conduction from transducer surface is not evaluated nor included in the methods for determining the exposure parameters. See Annex C.

5.4 Determination of thermal index in non-scanning mode

5.4.1 Determination of soft tissue thermal index for non-scanning modes

5.4.1.1 Determination of soft tissue thermal index at-surface for non-scanning modes, $TIS_{\mathrm{as,ns}}$

For each **transmit pattern** in a **non-scanning mode** the **soft tissue thermal index** at-surface for a **non-scanning mode**, $TIS_{\mathrm{as,ns}}$, shall be calculated from:

$$TIS_{\mathrm{as,ns}} = \frac{P_{1x1} \, f_{\mathrm{awf}}}{C_{TIS,1}} \tag{12}$$

where

$C_{TIS,1}$ = 210 mW MHz;

P_{1x1} is the **bounded-square output power**;

f_{awf} is the **acoustic working frequency**.

5.4.1.2 Determination of soft tissue thermal index *TIS* below-surface for non-scanning modes, $TIS_{bs,ns}$

For each **transmit pattern** in a **non-scanning mode,** the **depth for** ***TIS***, $z_{s,ns}$, shall be determined by the range along the **beam axis** to the plane at which the lower value of the **attenuated output power** and the product of the **attenuated spatial-peak temporal-average intensity** multiplied by 1 cm^2 is maximized. The position of the maximum value of this parameter, for $z \geq z_{bp}$, shall be $z_{s,ns}$.

$$z_{s,ns} = \text{depth of max} \left[\min \left(I_{spta,\alpha}(z) \times 1\,\text{cm}^2, P_\alpha(z) \right) \right] \tag{13}$$

NOTE See Annex A for discussion of the $z_{s,ns} \geq z_{bp}$ convention.

For each **transmit pattern** in a **non-scanning mode** the **soft tissue thermal index** below surface for a **non-scanning mode**, $TIS_{bs,ns}$, shall be calculated from:

$$TIS_{bs,ns} = \frac{P_\alpha(z_{s,ns})\, f_{awf}}{C_{TIS,1}} \tag{14}$$

or

$$TIS_{bs,ns} = \frac{I_{spta,\alpha}(z_{s,ns})\, f_{awf}}{C_{TIS,2}} \tag{15}$$

whichever yields the smaller value,

where

$C_{TIS,1}$ = 210 mW MHz;

$C_{TIS,2}$ = 210 mW cm^{-2} MHz;

$P_\alpha(z_{s,ns})$ is the **attenuated output power** at $z_{s,ns}$, the **depth for** ***TIS***

f_{awf} is the **acoustic working frequency**;

$I_{spta,\alpha}(z_{s,ns})$ is the attenuated spatial-peak temporal-average intensity at $z_{s,ns}$, the **depth for** ***TIS.***

NOTE As $TIS_{bs,ns}$ is to be determined on the beam axis, $I_{spta}(z)$, may be approximated by taking the $I_{ta}(z)$ value on the beam axis.

Thus, $TIS_{bs,ns}$ is determined at depth $z_{s,ns}$ from:

$$TIS_{bs,ns} = \min\left[\frac{P_\alpha(z_{s,ns}) f_{awf}}{C_{TIS,1}}, \frac{I_{spta,\alpha}(z_{s,ns}) f_{awf}}{C_{TIS,2}} \right] \tag{16}$$

[see Table A.2 “B”]

5.4.2 Determination of bone thermal index, *TIB*, for non-scanning modes

5.4.2.1 Determination of bone thermal index at surface for non-scanning modes, TIC_{ns}

For each **transmit pattern** in a **non-scanning mode**, the (**cranial) bone thermal index** at-surface shall be calculated from:

$$TIC_{\mathrm{ns}} = \frac{P / D_{\mathrm{eq}}}{C_{TIC}} \qquad (17)$$

where

C_{TIC} = 40 mW cm^{-1};

P is the **output power**;

D_{eq} is the **equivalent aperture diameter**; calculation for **non-scanning modes** as described in 3.28 using the **output beam area** A_{ob}.

NOTE TIC_{ns} applies to the bone-at-surface case for **non-scanning modes**.

5.4.2.2 Determination of bone thermal index below-surface for non-scanning modes, $TIB_{\mathrm{bs,ns}}$

For each **transmit pattern** in a **non-scanning mode,** the **depth for *TIB*** shall be determined from the dependence, on distance, of the product of the **attenuated output power and** the **attenuated spatial-peak temporal-average intensity**, or equivalently the square root of this product. The position of the maximum value of this product, for depths >= z_{bp}, shall determine $z_{\mathrm{b,ns}}$.

$$z_{\mathrm{b,ns}} = \text{depth of max } \left(P_{\alpha}(z) \times I_{\mathrm{spta},\alpha}(z)\right) \qquad (18)$$

NOTE 1 See Annex A for discussion of the $z_{\mathrm{b,ns}} \geq z_{\mathrm{bp}}$ convention.

The **bone thermal index** below-surface for **non-scanning mode**, $TIB_{\mathrm{bs,ns}}$, shall be calculated from:

$$TIB_{\mathrm{bs,ns}} = \frac{\sqrt{P_{\alpha}(z_{\mathrm{b,ns}}) I_{\mathrm{spta},\alpha}(z_{\mathrm{b,ns}})}}{C_{TIB,1}} \qquad (19)$$

or

$$TIB_{\mathrm{bs,ns}} = \frac{P_{\alpha}(z_{\mathrm{b,ns}})}{C_{TIB,2}} \qquad (20)$$

whichever yields the smallest value;

where

$C_{TIB,1}$ = 50 mW cm^{-1};

$C_{TIB,2}$ = 4,4 mW;

$P_{\alpha}(z_{\mathrm{b,ns}})$ is the **attenuated output power** at the **depth for *TIB***;

$I_{\mathrm{spta},\alpha}(z_{\mathrm{b,ns}})$ is the **attenuated spatial-peak temporal-average intensity** at the **depth for *TIB***.

NOTE As $TIB_{\mathrm{bs,ns}}$ is to be determined on the beam axis, $I_{\mathrm{spta}}(z)$, may be approximated by taking the $I_{\mathrm{ta}}(z)$ value on the beam axis.

Thus, $TIB_{\mathrm{bs,ns}}$ is determined at depth $z_{\mathrm{b,ns}}$ from:

$$TIB_{\mathrm{bs,ns}} = \min\left[\frac{\sqrt{P_{\alpha}(z_{\mathrm{b,ns}}) I_{\mathrm{spta},\alpha}(z_{\mathrm{b,ns}})}}{C_{TIB,1}}, \frac{P_{\alpha}(z_{\mathrm{b,ns}})}{C_{TIB,2}}\right] \qquad (21)$$

[see Table A.2 “D1”]

5.5 Determination of thermal index in scanning modes

5.5.1 Determination of soft tissue thermal index for scanning modes

5.5.1.1 Determination of soft tissue thermal index at-surface for scanning modes, $TIS_{\mathbf{as,sc}}$

For each **transmit pattern** in a **scanning mode**, the **soft tissue thermal index** at-surface shall be calculated from:

$$TIS_{\mathrm{as,sc}} = \frac{P_{1\mathrm{x}1}\, f_{\mathrm{awf}}}{C_{TIS,1}} \tag{22}$$

where

$C_{TIS,1}$ = 210 mW MHz;

$P_{1\mathrm{x}1}$ is the **bounded-square-output-power** (z = 0);

f_{awf} is the **acoustic working frequency**.

5.5.1.2 Determination of soft tissue thermal index below-surface for scanning modes, $TIS_{\mathbf{bs,sc}}$

For each **transmit pattern** in a **scanning mode** the **soft tissue thermal index** below-surface for a **scanning mode**, $TIS_{\mathrm{bs,sc}}$, shall be calculated from:

$$TIS_{\mathrm{bs,sc}} = TIS_{\mathrm{as,sc}} = \frac{P_{1\mathrm{x}1}\, f_{\mathrm{awf}}}{C_{TIS,1}} \tag{23}$$

[see Table A.2 “B2”]

5.5.2 Determination of bone thermal index for scanning modes

5.5.2.1 Determination of bone thermal index at surface for scanning modes, $TIC_{\mathbf{sc}}$

The determination of the **bone thermal index** at-surface for **scanning modes** shall be identical to that for **bone thermal index** at-surface for **non-scanning modes**, as specified in 5.4.2.1, except that D_{eq} is calculated by using the **scanned aperture area** A_{sa} as described in 3.28.

$$TIC_{\mathrm{sc}} = \frac{P / D_{\mathrm{eq}}}{C_{TIC}} \tag{24}$$

where

C_{TIC} = 40 mW cm^{-1};

P is the **output power**;

D_{eq} is the **equivalent aperture diameter**; calculation for **scanning modes** as described in 3.28 using the **scanned aperture area** A_{sa}.

NOTE TIC_{sc} applies to the bone-at-surface case for **scanning modes.**

5.5.2.2 Determination of bone thermal index below-surface for scanning mode, $TIB_{\mathbf{bs,sc}}$

The **bone thermal index** below-surface, $TIB_{\mathrm{bs,sc}}$, shall be calculated from:

$$TIB_{\mathrm{bs,sc}} = TIS_{\mathrm{as,sc}} = \frac{P_{1\mathrm{x}1}\, f_{\mathrm{awf}}}{\mathrm{C}_{TIS1}} \qquad (25)$$

where

$C_{TIS,1}$ = 210 mW MHz;

$P_{1\mathrm{x}1}$ is the **bounded-square-output-power** (z = 0);

f_{awf} is the **acoustic working frequency**.

[see Table A.2 “D.2”]

5.6 Calculations for combined-operating mode

5.6.1 Acoustic working frequency

In a **combined-operating mode** with more than one type of **transmit pattern** employed during the scan period, the **acoustic working frequency** shall be considered separately for each different **transmit pattern** as appropriate in calculating the **thermal index** or the **mechanical index**.

5.6.2 Thermal index

For **combined-operating modes**, the at-surface and the below-surface **thermal index** contributions for each **discrete-operating mode** shall be calculated separately and the individual values summed appropriately, as shown in Table 1. For *TIC* the location of the maximum temperature increase is near the surface of the **transducer assembly**. For *TIB* the location of the maximum temperature increase depends on whether (as shown in Table 1) the at-surface *TIS*-summation or the below-surface *TIB*-summation is larger. In the latter case, choose z_{b} as the depth corresponding to the non-scanning mode, $TIB_{\mathrm{bs,ns}}$, since the scanning mode contribution to TIB_{bs} is estimated from the at-surface value. For *TIS* the location of the maximum temperature increase depends on the combination process. *TIS* shall be the summation of at-surface TIS_{as} contributions for all modes, or the summation of below-surface TIS_{bs} contributions for all modes, whichever is the larger. If the at-surface *TIS*-summation is larger, z_{s} is equal to 0. If the below-surface *TIS*-summation is larger choose z_{s} as the depth corresponding to the non-scanning mode, $TIS_{\mathrm{bs,ns}}$, since the scanning mode contribution to TIS_{bs} is estimated from the at-surface value. Table 1 summarizes the combination formulae for each of the **thermal index** categories.

Table 1 – Summary of combination formulae for each of the THERMAL INDEX categories

Thermal index categories	Combinations of discrete mode values of thermal index [equations for each discrete mode are shown in Tables A.2]
TIC	$\sum_{\substack{Discrete\\Modes}} TIC_{as} = \sum_{non-scanned\_TPs} TIC_{ns} + \sum_{scanned\_TPs} TIC_{sc}$
TIB	$\mathrm{Max}\left[\sum_{\substack{Discrete\\Modes}} TIS_{as}, \sum_{\substack{Discrete\\Modes}} TIB_{bs}\right]$ $= \sum_{scanned\_TPs} TIS_{as,sc} + \mathrm{Max}\left[\sum_{non-scanned\_TPs} TIS_{as,ns}, \sum_{non-scanned\_TPs} TIB_{bs,ns}\right]$
TIS	$\mathrm{Max}\left[\sum_{\substack{Discrete\\Modes}} TIS_{as}, \sum_{\substack{Discrete\\Modes}} TIS_{bs}\right]$ $= \sum_{scanned\_TPs} TIS_{as,sc} + \mathrm{Max}\left[\sum_{non-scanned\_TPs} TIS_{as,ns}, \sum_{non-scanned\_TPs} TIS_{bs,ns}\right]$ NOTE '*scanned_TPs'* means Scanned **Transmit Patterns** e.g. B mode, Color Mode *'non-scanned_TPs'* means Non-Scanned **Transmit Patterns** e.g. Pulsed Doppler, CW, M

5.6.3 Mechanical index

For **combined-operating modes**, the **mechanical index** shall be that for the **discrete-operating mode** with the largest **mechanical index**.

5.7 Summary of measured quantities for index determination

Table 2 gives a summary of the acoustic quantities required for the determination of each of the defined safety-related indices. Since attenuated quantities are derived by calculation from associated measured free-field quantities, both attenuated and free-field quantities are included.

Table 2 – Summary of the acoustic quantities required for the determination of the indices

Index	*MI*	TIS_{as} (at surface)	TIS_{bs} *(below surface)*		TIB_{bs} *(below surface)*		*TIC* *(at surface)*
Mode		**Scanning and non-scanning**	**Scanning** (=$TIS_{as,sc}$)	**non-scanning**	**Scanning** (= $TIS_{as,sc}$)	**non-scanning**	**Scanning and non-scanning**
f_{awf} at z_{pii}	x	x	x	x	x	x	
P							x
P_{1x1}		x	x		x		
P_{α}				x		x	
$I_{spta,\alpha}$				x		x	
pii	x			x		x	
pii_{α}	x			x		x	
$p_{r,\alpha}$	x						
d_{eq}						x	
D_{eq}							x
z_{bp}	x			x		x	
$z_{s,ns}$				x			
$z_{b,ns}$						x	
z_{MI}	x						
z_{pii}	x			x		x	

Annex A
(informative)

Rationale and derivation of index models

A.1 Overview

This annex provides in summary a rationale and derivation guidance for the formulas presented in the body of this standard for **mechanical index** and **thermal index**. Numerous references are made to the root publications from which the formulas were derived. As will be discussed in the derivation notes that follow, key parts of the MI and TI models rely on experimental data. This annex does not attempt to do more than describe relevant results of the experiments. A thorough reading of the referenced papers is strongly recommended in order to obtain a full understanding of the model derivation notes presented herein.

The relationship of various acoustic output parameters (for example, acoustic intensity, pressure, power, etc.) to biological endpoints is not well understood at the present time. Evidence to date has identified two fundamental mechanisms, thermal and mechanical, by which ultrasound may induce bio-effects [12,13]. This standard provides a uniform means for the calculation of acoustic output parameters relevant to these potential biological effects. The rationale behind these calculation methods is twofold:

a) that information be provided that is representative of what is occurring *in vivo* with regard to mechanical and thermal bio-effects. It is for this reason that indices were chosen as opposed to absolute quantities not shown to have a direct correlation to bio-effects;
b) that ultrasonically induced heating and acoustic pressure levels should be maintained at a level as low as practical while still providing acceptable diagnostic information (the "ALARA Principle").

A.2 General rationale

A.2.1 Rationale for attenuation coefficient of the tissue path used

The **absorption coefficient** of typical soft tissue is 0,87 dB cm^{-1} MHz^{-1}. Since the **attenuation coefficient** includes scattering and diffusion as well as absorption, the **attenuation coefficient** is always greater than the **absorption coefficient** for the same tissue and conditions. However, the **attenuation coefficient** of 0,3 dB cm^{-1} MHz^{-1} is frequently used to provide a conservative safety margin when modelling the attenuation of the sound path reaching a target tissue.

The choice of a homogeneous tissue path to the region of interest and an **acoustic attenuation coefficient** of 0,3 dB cm^{-1} MHz^{-1} is a compromise. Other attenuation models were evaluated and rejected, such as fixed distance models [14] and the use of a homogeneous tissue model with an attenuation coefficient of 0,5 dB cm^{-1} MHz^{-1}, a value more representative of many radiological and cardiac imaging applications. However, use of more than one attenuation model would entail an increase in **equipment** complexity and could create a further need for user input to select appropriate attenuation schemes. With the selected compromise in the attenuation model, the **mechanical index** and **thermal index** are simple to implement and use and, most importantly, are sufficient to allow users to minimize acoustic output and any corresponding potential mechanical or thermal bio-effects.

A.2.2 Thermal properties of tissue used in calculation of the thermal index

The rationale related to tissue properties used in the determination of the **thermal index** (TI) is given in [14,22,**Error! Bookmark not defined.**,26].

A.2.3 Mechanical properties of tissue used in calculation of the mechanical index

The rationale related to tissue properties used in the determination of the **mechanical index** (MI) is given in [21,22,24,26].

A.3 Mechanical index (MI)

A.3.1 Rationale

A **mechanical index** is selected as a value to be calculated as an indicator related to mechanical effects. The index is intended to estimate the potential for mechanical bio-effects. Examples of mechanical effects include motion (or streaming) around compressible gas bubbles as ultrasound pressure waves pass through tissues, and energy released in the inertial collapse, i.e., cavitation, of micrometer-sized gas bubbles.

While no adverse mechanical bio-effects in humans have been reported to date from exposure to ultrasound output levels typical of **medical diagnostic ultrasonic equipment**, several observations have contributed to the development of the **mechanical index**.

– In lithotripsy, mechanical bio-effects are induced by ultrasound with peak pressures in the same range as those that are sometimes used in diagnostic imaging, albeit at significantly lower frequencies.
– *In vitro* experiments and observations with lower organisms have demonstrated the possibility of cavitation at ultrasound peak pressures and frequencies in ranges utilized by some **medical diagnostic ultrasonic equipment** [15].
– Lung haemorrhage has been demonstrated in several laboratory animal models exposed to levels of pulsed ultrasound similar to those used in **medical diagnostic ultrasonic equipment.** Although this effect has been demonstrated in juvenile and adult animals, similar effects have not been found in foetuses [16,17].

A.3.2 Derivation notes

The conditions that affect the likelihood of mechanical effects are not yet well understood; however, it is generally agreed that the likelihood increases as **peak-rarefactional acoustic pressure** increases, and decreases as the ultrasound frequency increases. Further, it is generally believed to be a threshold effect, such that no effect occurs unless a certain output level is exceeded [18,19,20].

While the existing limited experimental data [21] suggest a linear frequency relationship, a more conservative root-frequency relationship was selected. The **mechanical index** is defined as in 3.32 as

$$MI = \frac{p_{\mathrm{r},\alpha}\left(z_{MI}\right) \times f_{\mathrm{awf}}{}^{-1/2}}{C_{MI}} \qquad \text{(A.1)}$$

where

C_{MI} = 1 MPa MHz$^{-1/2}$

$p_{\mathrm{r}\cdot\alpha}(z_{MI})$ is the **attenuated peak-rarefactional acoustic pressure** at the depth z_{MI}

z_{MI} is the **depth for** MI

f_{awf} is the **acoustic-working frequency**.

The convention adopted in [22] and continued here is to use the $p_{\mathrm{r}\cdot\alpha}$ value determined at the position on the beam axis of maximum **attenuated pulse-intensity integral**, z_{MI}. The intent is to reduce measurement burden, as the position and value of $p_{\mathrm{r}\cdot\alpha}(z_{MI})$ is assumed to be close to the position and value of the maximum $p_{\mathrm{r}\cdot\alpha}(z)$. This assumption is more accurate when pressure wave propagation is more nearly linear. While, the position and value of the maximum $p_{\mathrm{r},\alpha}(z)$ diverges (typically becoming shallower and larger) from that of $p_{\mathrm{r}\cdot\alpha}(z_{MI})$ as the effects of nonlinear propagation become more pronounced.

A.4 Thermal index (TI)

A.4.1 Rationales

A.4.1.1 General

The relationship between temperature rise and thermal bio-effects in tissues is well established (numerous studies,[1,5,7,8,14,23,24]). While present acoustic output measurement parameters, such as

P **output power**,

I_{ta} **temporal-average intensity**, and

I_{spta} **spatial-peak temporal-average intensity**

are not suitable individually as indicators or estimators of ultrasound-induced temperature rise, combinations of these parameters (together with specific geometric information) can be used to calculate indices that provide an estimate of risk of hazard from temperature rise in soft tissue or bone.

Because of the difficulties of anticipating and thermally modelling the many possible ultrasound scan planes of the human body, simplified models based on average conditions are used. Three user-selectable **thermal index** categories corresponding to different anatomical combinations of soft tissue and bone that are encountered in imaging applications are defined (see Table A.1). Each category uses one or more TI-models. Values for each model listed in Table A.1 are calculated and the larger or largest value is displayed.

A.4.1.2 Rationale for the location of the maximum temperature increase

The location of the maximum temperature increase depends on the ultrasound propagation conditions in the human body. The maximum temperature increase is assumed to be near the surface if the ultrasound beam passes through bone near the surface (TIC). For TIB, the assumption is that the maximum temperature rise is either below the surface at the tissue/bone interface, or at the soft tissue surface, thus the at-surface soft tissue equation (Equation A in Table A.2) and the below-surface bone equation (Equation D in Table A.2)) are both calculated and the maximum displayed. Likewise, for the homogeneous soft tissue model, the maximum temperature rise may be at the surface or below the surface, so TIS is the maximum value of the results of evaluating Equations A and B in Table A.2.

A.4.1.3 Rationale for choosing a break-point depth (z_{bp})

Searching the beam axis methodically up to but no closer than the **break-point depth**, z_{bp}, is imposed on the measurement of all below-surface TI parameters.

The intent of the z_{bp} as originally stated [22] was to prevent measurements from being made in the acoustic field too close to the transducer. One reason for this is to reduce violation of the assumption that acoustic particle velocity and pressure are in phase when estimating the **pulse-intensity integral**, (pii), from the **pulse-pressure-squared integral**, ($ppsi$).

NOTE 1 As discussed in section A.4.1.6 and A.4.1.7, below-surface **thermal index** values are basically functions of **acoustic output power**, and the **mechanical index** is a function of acoustic pressure. Therefore the phase between particle velocity and acoustic pressure may not seem so important. However due to the approximations and conventions used in this standard, the measurement of intensity, by way of the **pulse-pressure-squared integral** is required.

NOTE 2 In AIUM / NEMA measurement standards prior to UD-3 ([22] and all previous editions thereof), a break-point value of z_min = min(X_Dim, Y_Dim), i.e. the minimum dimension of the active transmit aperture, was used. This value proved to be inside the acoustic field close to the transducer of some transducer/system combinations.

A.4.1.4 Rationale for the bounded-square output power and attenuated bounded-square output power

As discussed in A.4.1.2, A.4.3.1 and A.4.3.2, for the soft tissue case, the interaction between acoustic beam dimensions and the cooling effect of perfusion determines the position of maximum temperature increase. A perfusion rate characterized by a perfusion length of 1 cm is assumed. This translates to a situation where, for **beam areas** less than 1 cm^2, **output power** is the relevant **power parameter,** and for **beam areas** greater than 1 cm^2, spatial average acoustic intensity multiplied by 1 cm^2 is the relevant **power parameter**. This leads to the concept of the **bounded-square output power,** P_{1x1}, as the **power parameter** "at-surface", and the **"attenuated bounded-square output power,** $P_{1x1,\alpha}(z)$, as the **power parameter** "below-surface".

Interpretation of [**Error! Bookmark not defined.**] and the information in [22] have led previously, in [22], to using $\frac{P}{X}$ = '**output power** per unit scan length' as the power parameter of interest for 'at-surface' *TIS* estimates for **scanning modes**. In Edition 1 of this standard $\frac{P}{X}$ was symbolized as P_1 and titled the 'bounded output power'. Edition 1 of this standard also used an approximation of the, presently used, **bounded-square output power**, P_{1x1}, for the at-surface *TIS* for **non-scanning modes**, calculated only when the output beam area, A_{ob}, is <= 1,0 cm^2, and an approximation of **attenuated bounded-square output power**, $P_{1x1,\alpha}(z)$, for below-surface **non-scanning modes**.

In the present 2nd edition of the IEC 62359 standard the at-surface *TIS*-equations for all modes (**scanning** and **non-scanning**) use P_{1x1}. And the at-surface *TIS* is calculated for all aperture sizes. This is rationalized as follows:

A) Clearly P_{1x1} should be used for **non-scanning modes** for the at-surface *TIS* and $P_{1x1,\alpha}(z)$ for the below surface *TIS*.

B) There is an expectation that **scanned mode** and **non-scanned mode** *TIS value*s should converge smoothly as the number of scan lines narrows to 1 (from the **scanned mode** case to the **non-scanned mode** case). This occurs when P_{1x1} is used for both cases.

C) A majority of the 70 probes/cases simulated in [**Error! Bookmark not defined.**] had Y aperture dimensions ('transducer width') ≤ 1,0 cm, in which case $\frac{P}{X}$(P_1) and P_{1x1} yield the same numerical magnitude.

D) Many modern diagnostic ultrasound scanners and probes are capable of scanning in multiple scan planes (e.g. 3D / 4D scanning). The previously used $\frac{P}{X}$(P_1) parameter ('power per unit length in the scan direction') is ill-defined and/or inadequate for these cases.

An approximation of the **attenuated bounded-square output power** is used in equation B in Table A.2, for the below-surface *TIS*.

A.4.1.5 Rationale for at surface *TI* in non-scanning mode and scanning mode

Implementation of the **soft tissue thermal index** (*TIS*) assumes a homogenous tissue-path model. One basic equation covers all cases for the at-surface case, **scanning modes** (such as colour-flow mapping and B-mode) and **non-scanning modes** (such as Doppler and M-mode).

In this document, the at-surface *TIS*-equations for all modes (**scanning** and **non-scanning**) use P_{1x1} and the at-surface *TIS* is calculated for all aperture sizes. See A.4.1.4 for the rationale for using the **attenuated bounded-square output power** in the numerator of the thermal index equations.

There is an expectation that **scanning mode** and **non-scanning mode** TI values should converge smoothly as the number of scan lines narrows to 1 (non-scanned), and as the depth of interest moves from below the surface ($z > 0$) to the surface ($z = 0$).

For the at-surface TIS equation, $P_{1x1,\alpha}(z)$ is the **bounded-square output power** P_{1x1} and equation A results (see Table A.2).

The TIB (bone below-surface) and TIC (bone at surface) equations are fundamentally the same. For TIC, the non-attenuated power is used, since it is an at-surface estimate. These approximations are discussed in A.4.3 (see Table A.2).

If the dimensions of the active aperture are larger than 1 cm × 1 cm, then the thermal perfusion length of one centimetre (1 cm) is assumed to be exceeded. In this case the **bounded-square output power** is measured by a radiation force balance using an intermediate absorbing mask with a one-square centimetre window (the mask is 1 cm × 1cm square), or by other masking means (e.g., electronic), or the **bounded-square output power** may be measured via hydrophone planar scanning.

NOTE Temperature rise in tissue due to transducer surface self-heating has not been taken into account in the determination of the **thermal index** [10]. (See Annex C.)

A.4.1.6 Rationale for below surface TI in non-scanning mode

In applying the basic TIS equation to the below-surface case, the parameter $P_{1x1,\alpha}(z)$ is approximated by using $\min\left(I_{spta,\alpha}(z) \text{ x } 1\text{cm}^2, P_\alpha(z)\right)$ as described in A.4.3.2, leading to equation B.1 in Table A.2.

For the bone-at-focus model, a different formulation is required for the power (P_{deg}) necessary to raise the bone temperature 1°C at an axial distance of $z_{b,ns}$. This different formulation is due to the observation that bone absorbs and dissipates acoustic power differently than soft tissue. The theory of this P_{deg}-formulation has been extensively developed in numerous published documents [1,12,14, 23]. The discussion in A.4.3.4 refers to key conclusions from these reports.

A.4.1.7 Rationale for below surface TI in scanning mode

Edition 1 of this standard, and [22], did not specify equations for below- surface TIS or TIB for **scanning modes**. This omission was intentional.

In IEC 62359 Edition 1, and in [22], the claim is made that for most **scanning mode** cases the below surface temperature in soft tissue and in bone is less than the at-surface temperature in soft tissue. Specifically (from [22]): '*the* (at-surface, scanning) *soft tissue model is used because the temperature increase at the surface is usually greater than or about the same as with the bone at the focus.*

This assumption may be true in most cases.

- The paper [**Error! Bookmark not defined.**] is referenced as proof for the soft tissue below-surface case.
- Nothing is offered as proof for the bone below-surface case.

However, if there are **non-scanning mode** cases where the below-surface heating is greater than at-surface soft tissue heating, then it seems reasonable that there are a significant number of **scanning mode** operating conditions where the below-surface heating is larger than at-surface soft tissue heating.

- This seems particularly reasonable for the bone below-surface case.

- An ultrasound system operating condition with a narrow scan width should have heating characteristics approaching the non-scanned case. See [25].

Note that whether or not for **scanning modes** the at-surface soft tissue temperature rise exceeds the temperature rise in soft tissue or bone below-surface; in calculating the *TI* for **combined modes**, the below-surface contribution from **scanning modes** should not be neglected, and the below-surface sum (see Table 1) may be higher than the at-surface sum. So in Edition 2 equations for below-surface *TIB* and *TIS* for **scanning modes** are provided and are to be included in the below-surface sums.

An equation for the below surface *TIS* for **scanning modes** could be arrived at using the same principles applied in Edition 1 and [22] for deriving the below-surface *TIS* for **non-scanning modes** and the at-surface *TIS* for **scanning modes**. However, this Edition (Ed. 2) of the standard is not following that approach. Similarly, an equation for the below surface *TIB* for **scanning modes** could be arrived at using the same principals applied in Edition 1 and [22] for deriving the below-surface *TIB* for **non-scanning modes** and the at-surface *TIB*. However, again, Edition 2 is not following that approach.

There is considerably increased complexity and time associated with the measurement and estimation of $P_{1x1,\alpha}(z)$ and $d_{eq}(z)$ in **scanning modes**, and this is even more difficult in 3D and 4D **scanning modes**. It is preferable to choose formulas which give both reasonable results and which can be reasonably implemented in industrial measurement labs, where the constraints on measurement time and complexity must be considered. For the below-surface **non-scanning mode** case, suitable approximations for $P_{1x1,\alpha}(z)$ and $d_{eq}(z)$ were made in Edition 1 and [22]. But for scanning modes the complexity of approximations for $P_{1x1,\alpha}(z)$ and $d_{eq}(z)$ is significantly increased or their suitability are not well understood.

Therefore, use is made in Edition 2 of the claim in 62359 Edition 1 and in [22] that for most **scanning mode** cases the below surface temperature in soft tissue and in bone is less than the at-surface temperature in soft tissue. Though limited support for the claim is given in Edition 1 and in[22] particularly for the bone below-surface case, and though it seems reasonable that the claim is not true for some number of **scanning mode** operating conditions, this claim remains in Edition 2 and is made use of by setting the $TIS_{bs,sc}$ and the $TIB_{bs,sc}$ equal to the $TIS_{as,sc}$.

This compromise solution generally meets the requirement of satisfying the boundary conditions:

a) smooth convergence to the value of the *TIB* (or *TIS*) for **non-scanning modes** as the number of **ultrasonic scan lines** goes to one,

b) convergence to the at-surface *TIB* (or *TIS*) value as the region of interest moves from below-surface to the surface ($z = 0$).

NOTE Convergence does not happen, strictly speaking, when different approximations are used below-surface and at-surface. For instance, for non-scanning mode *TIB*, TIB_{ns}, D_{eq} (at-surface) and d_{eq} (below-surface) are approximated using different formulas. For non-scanning mode *TIS*, TIS_{ns}, P_{1x1} is estimated differently at-surface and below-surface. In the case of scanning modes, the below-surface *TIB* won't converge with the at-surface *TIB* (*TIC*), due to setting $TIB_{bs,sc}$ equal to $TIS_{as,sc}$

Table A.1 – Thermal index categories and models

Thermal Index category	Thermal Index models	
	Non-scanning mode	Scanning mode
TIS (soft tissue)	A) Soft tissue at-surface: non-scanning and scanning. B.1) Soft tissue below-surface: non-scanning	A) Soft tissue at-surface: non-scanning and scanning. B.2) Soft tissue below-surface: scanning. (= Equation A)

TIC=TIB_{as} (bone at-surface)	C) Bone at-surface: non-scanning and scanning	C) Bone at-surface: non-scanning and scanning
TIB_{bs} (bone below-surface)	A) Soft tissue at-surface: non-scanning and scanning. D.1) Bone below-surface: non-scanning	A) Soft tissue at-surface: non-scanning and scanning. D.2) Bone below-surface: -scanning. (=Equation A)

A.4.2 Derivation notes - General

A.4.2.1 Derivation of break-point depth

The expression for **break-point depth** in this edition is

$$z_{bp} = 1{,}5 \times D_{eq} \quad \text{(A.2)}$$

D_{eq} is defined as the 'circular-equivalent' geometric mean diameter (the **equivalent aperture diameter**) of the transmit aperture for a single pulse of the **transmit pattern** being measured.

$$D_{eq} = \sqrt{\frac{4}{\pi} A_{ob}} = 1{,}13\sqrt{A_{ob}} \quad \text{(A.3)}$$

where A_{ob} is the **output beam area**.

NOTE 1 Equation (A.3) is a re-statement of Equation (8) (from 3.28), with a single pulse corresponding to a **non-scanning mode**.

Thus, for **scanning modes** or **non-scanning modes**, the same value of z_{bp} will be obtained if the **ultrasonic scan lines** (or at least the 'central scan line' of the lines making up the scan) use the same aperture and nominal focal point.

Figure A.1 shows a typical case. Here the focal point of the transducer and the position of maximum **attenuated spatial-peak temporal-average intensity** are shown to occur deeper than 1,5 × D_{eq}.

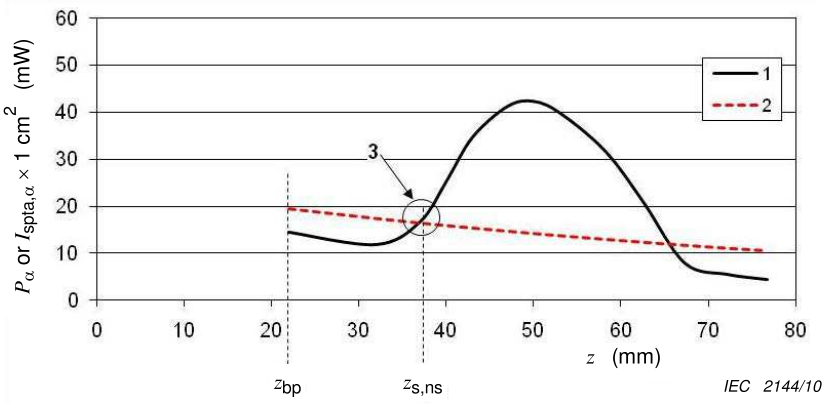

Key

1: graph of $I_{spta\cdot\alpha}$ × 1 cm^2,

2: graph of P_α,

3: point where P_p= $P_\alpha(z_{s,ns})$=$I_{spta\cdot\alpha}$ × 1 cm^2

Figure A.1 – Focusing transducer with a f-number of about 7

For low **f-number** transmit conditions the 'legitimate' depth of maximum *pii* (including the focal point) might validly be shallower than 1,5 × D_{eq}. As pressure levels may be high in this region the definition of z_{bp} in this standard is only used for the determination of *TI*. Figure A.2 gives an example of such a situation.

NOTE The **f-number** denotes the ratio of the **geometric focal length** to the **transducer aperture width** in a specified longitudinal plane as defined in IEC 61828.

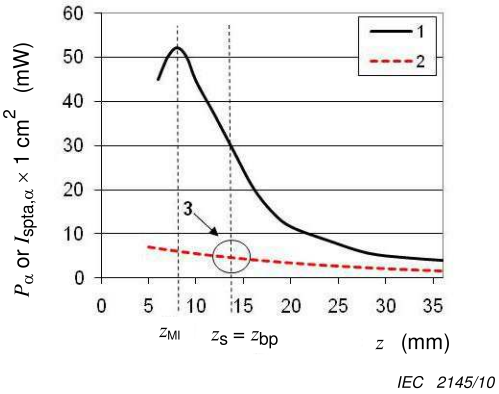

Key

1: graph of $I_{spta\cdot\alpha}$ × 1 cm^2,

2: graph of P_α,

3: point where $P_p = P_\alpha(z_{s,ns})$

z_{MI} is closer to the transducer surface than 1,5 × D_{eq}

Figure A.2 – Strongly focusing transducer with a low f-number of about 1

Close to the transducer acoustic field undulations and side lobe levels can vary from transducer to transducer of the same model type as sensitive functions of production tolerances. In most cases, adherence to the z_{bp} definition should serve to keep hydrophones not too close to the transducer, helping to obtain consistent intra-model measurement results and 'tighter' statistics. However, as shown in Figure A.3, if the undulations are extensive the determined value of z_{bp} may be close to the transducer.

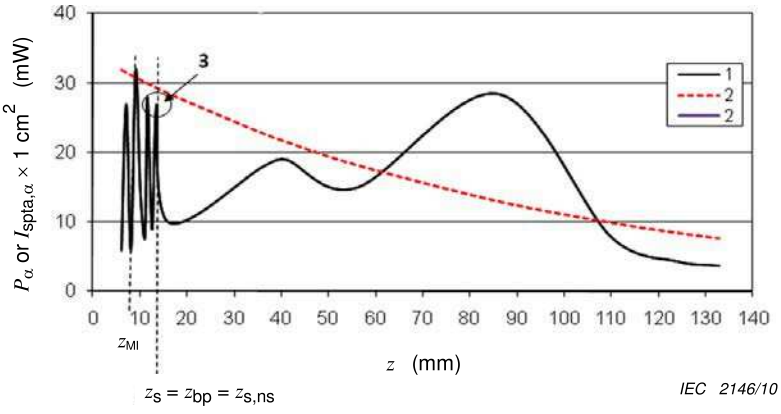

Key

1: graph of $I_{spta\cdot\alpha}$ × 1 cm^2,

2: graph of P_α,

3: point where $P_p = I_{spta\cdot\alpha}$ × 1 cm^2

Figure A.3 – Focusing transducer (f-number ≈ 10) with severe undulations close to the transducer

Another effect of employing the **break-point-depth** is that some separation between the at-surface and below-surface thermal indices positions is created. Thus, instead of finding the TI as the maximum value over all z values, including z = 0, (as discussed in A.4), we have two regions, z = 0 and $z \geq z_{bp}$, for TI.

Of course, one of the negative consequences of employing the **break-point-depth**, is the creation of a non-interrogated region which may contain the location of maximum TI.

To prevent collisions of expensive hydrophones into transducers being tested, care must be exercised when performing scans closer to the transducer than the **break-point depth** as required, if necessary, to find the **depth for mechanical index** (z_{MI}). This would happen with greater frequency if searching the beam axis all the way to the transducer surface were required. This could happen for probes with shallow focusing and/or high amplitude undulations close to the transducer.

Another effect of using z_{bp}, though not its intended purpose, is to obscure the fact that the below-surface TI values do not converge continuously to the at-surface TI values as z approaches 0. This is because different approximations for P_{1x1} and d_{eq} (D_{eq}) are used at-surface and below-surface. See A.4.1 and A.4.1.5 Note a.

A.4.2.2 Thermal index

In this annex the **thermal index**, TI, is defined by the relationship

$$TI = \frac{P_{p}}{P_{deg}} \tag{A.4}$$

where

P_{p} is the **power parameter** as defined in this annex, and

P_{deg} is the estimated power necessary to raise the target tissue 1 °C, based on the thermal models discussed in this annex.

The derivation of the temperature rise estimation models requires the understanding of four key concepts/parameters.

A.4.2.3 Attenuated output power and attenuated intensity

The **attenuated output power** and **attenuated intensity** are functions of the non-attenuated values, depth and the **acoustic attenuation coefficient**. **Attenuated output power** and **attenuated intensity** are denoted by the subscript α. Parameters without the subscript refer to non-attenuated values measured in water. Thus the **attenuated output power** P_{α} at a distance z is defined as

$$P_{\alpha}(z) = P\,10^{(-\alpha z\, f_{awf}/10\text{dB})} \tag{A.5}$$

where

P is the **output power**,
α is the **acoustic attenuation coefficient**,
f_{awf} is the **acoustic working frequency**, and
z is the distance from the **external transducer aperture** to the point of interest

The **attenuated spatial-peak temporal-average intensity** is denoted:

$$I_{spta,\alpha}(z) = I_{spta}(z)10^{(-\alpha z\, f_{awf}/10\text{dB})} \tag{A.6}$$

where

$I_{spta}(z)$ is the **spatial-peak temporal-average intensity** at distance z,

α is the **acoustic attenuation coefficient**,

f_{awf} is the **acoustic-working frequency**, and

z is the distance from the **external transducer aperture** to the point of interest.

A.4.2.4 Derivation of the equivalent beam area

The **equivalent beam area**, A_{eq}, is defined as

$$A_{eq}(z) = \frac{P_\alpha(z)}{I_{spta,\alpha}(z)} = \frac{P}{I_{spta}(z)} \quad \text{(A.7)}$$

where

$P_\alpha(z)$ is the **attenuated output power** at distance z,

$I_{spta,\alpha}(z)$ is the **attenuated spatial-peak temporal-average intensity** at distance z,

P is the **output power**,

$I_{spta}(z)$ is the **spatial-peak temporal-average intensity** at distance z, and

z is the distance from the **external transducer aperture** to the specified point.

A.4.2.5 Derivation of the equivalent beam diameter

The **equivalent beam diameter**, d_{eq}, is defined as

$$d_{eq}(z) = \sqrt{\frac{4}{\pi} A_{eq}(z)} \quad = \quad 2\sqrt{\frac{P_\alpha(z)}{\pi I_{spta,\alpha}(z)}} \quad \text{(A.8)}$$

where

$A_{eq}(z)$ is the **equivalent beam area** at distance z,

$P_\alpha(z)$ is the **attenuated output power** at distance z, and

$I_{spta,\alpha}(z)$ is the **attenuated spatial-peak temporal-average intensity** at distance z.

A minimum **beamwidth** of one millimetre (0,1 cm) is assumed because of the practical difficulty of holding a small beam steady on one target location. Therefore, for these derivations

$$d_{eq}(z) = \max\left(\sqrt{\frac{4}{\pi} A_{eq}(z)}, 0{,}1\,\text{cm}\right) = \max\left(2\sqrt{\frac{P_\alpha(z)}{\pi I_{spta,\alpha}(z)}}, 0{,}1\,\text{cm}\right) \quad \text{(A.9)}$$

This minimum **beamwidth** assumption is referred to in context in later sections of this annex.

A.4.3 Derivation notes for the thermal models used

As discussed in A.4.1 and in Table A.1, three **thermal indices** are defined, the *TIS*, the *TIB* and the *TIC*. Four temperature-rise estimation equations are used in calculating the *TI's*, as defined in Clause 5 of this standard. For the purposes of discussion and derivation, these four models are identified in Table A.2.

The soft tissue equations (A and B of Table A.2) are based on one model, derived primarily from a theoretical and experimental analysis [**Error! Bookmark not defined.**,26]. According to [**Error! Bookmark not defined.**], the mediating factor for temperature rise at the surface is the absorbed power per unit scan length, $\mu_o f\,[P/X]$, that normalizes the effect of frequency on the temperature rise (where μ_0 is the **acoustic absorption coefficient** in Np cm^{-1} MHz^{-1}). A

series of calculations on 70 transducers of the absorbed power per unit scan length that caused a 1 °C rise at the skin surface produced results centred about:

$$\mu_0 f_{\text{awf}}[P_{\text{deg}} / X] = 21\,\text{Np mW/cm}^2 \qquad \text{(A.10)}$$

This is a key concept in the development of the *TIS* models. A careful study of [**Error! Bookmark not defined.**] is strongly recommended to ensure a thorough understanding of this important concept.

NOTE In [**Error! Bookmark not defined.**] a study of typical linear array transducers available in 1991 is presented. Validation of the concept for more sophisticated modern transducers (e.g. 1,5 and 2D arrays) and 3D scanning formats has not yet been published.

For this study, the **acoustic absorption coefficient** intensity was selected as μ_o = 0,1 Np cm^{-1} MHz^{-1}, a value typical of soft tissue. The average perfusion rate for soft tissue has been estimated as the cardiac output divided by the body mass, resulting in a corresponding typical perfusion length of 1,0 cm. Selecting the unit scan length, X, as the perfusion length and combining these experimental approximations with equation A.10 results in the power required to cause a 1 °C temperature rise at the surface as

$$P_{\text{deg}} = \frac{(21\ \text{Np}\cdot\text{mW}\cdot\text{cm}^{-2})\,(1{,}0\ \text{cm})}{(0{,}1\ \text{Np}\cdot\text{cm}^{-1}\cdot\text{MHz}^{-1})\,(f_{\text{awf}})} \triangleq \frac{210\ \text{mW MHz}}{f_{\text{awf}}} \qquad \text{(A.11)}$$

This P_{deg} formula is shared by both the at-surface soft tissue equation (Equation A of Table A.2) and the below-surface soft tissue equation (eq. B.2 of Table A.2). In this standard, the value of 210 mW MHz is incorporated in constants $C_{TIS,1}$ and $C_{TIS,2}$.

Table A.2 – Consolidated thermal index formulae

Name	Formula
A Soft tissue at-surface non-scanning and scanning (see 5.4.1.1 and 5.5.1.1)	$$TIS_{\text{as}} = \frac{P_{1\text{x}1}\, f_{\text{awf}}}{C_{TIS,1}}$$
B.1 Soft tissue below-surface non-scanning (see 5.4.1.2)	$$TIS_{\text{bs,ns}} = \min\left[\frac{P_{\alpha}\left(z_{\text{s,ns}}\right) f_{\text{awf}}}{C_{TIS,1}}, \frac{I_{\text{spta},\alpha}\left(z_{\text{s,ns}}\right) f_{\text{awf}}}{C_{TIS,2}}\right]$$ NOTE 1 $z_{\text{s,ns}} \geq z_{\text{bp}}$ NOTE 2 Where $\min\left[P_{\alpha}(z), I_{\text{spta},\alpha}(z)\right]$ is an approximation of $P_{1x1,\alpha}(z)$ NOTE 3 $I_{\text{spta},\alpha}(z)$ may be approximated by taking the $I_{\text{ta},\alpha}(z)$ value on the beam axis.
B.2 Soft tissue below-surface scanning (see 5.4.1.2 and 5.5.1.2)	$$TIS_{\text{bs,sc}} = TIS_{\text{as,sc}} = \frac{P_{1\text{x}1}\, f_{\text{awf}}}{C_{TIS,1}}$$
C Bone at surface non-scanning and scanning (see 5.4.2.1 and 5.5.2.1)	$$TIC = \frac{P / D_{\text{eq}}}{C_{TIC}}$$
D.1 Bone below-surface non-scanning (see 5.4.2.2)	$$TIB_{\text{bs,ns}} = \min\left[\frac{\sqrt{P_{\alpha}\left(z_{\text{b,ns}}\right) I_{\text{spta},\alpha}\left(z_{\text{b,ns}}\right)}}{C_{TIB,1}}, \frac{P_{\alpha}\left(z_{\text{b,ns}}\right)}{C_{TIB,2}}\right]$$ NOTE 1 $z_{\text{b,ns}} \geq z_{\text{bp}}$ NOTE 2 $I_{\text{spta},\alpha}(z)$ may be approximated by taking the $I_{\text{ta},\alpha}(z)$ value on the beam axis.
D.2 Bone below-surface scanning (see 5.5.2.2)	$$TIB_{\text{bs,sc}} = TIS_{\text{as,sc}} = \frac{P_{1\text{x}1}\, f_{\text{awf}}}{C_{TIS,1}}$$

A.4.3.1 Derivation notes for soft tissue thermal index at-surface for non-scanning and scanning modes ($TIS_{\mathbf{as,ns}}$, $TIS_{\mathbf{as,sc}}$)

As noted in A.4.1.4, temperature increase in soft tissue is determined by the **bounded-square output power**.

Power from the one square-centimetre of the radiating- or active-aperture emitting the maximum value of the time average acoustic output power is measured (see Figure B.3). For active apertures having a scan dimension less than one centimetre in each dimension, no mask is necessary. The result of these power measurements, the **bounded-square output power**, P_{1x1}, is the **power parameter** used in the TI-formula for soft tissue at-surface.

Combining the **bounded-square output power** with the power required to cause a 1 °C temperature rise, P_{deg}, (equation A.11) into the general TI-formula (equation A.4) yields the soft tissue at-surface model for **scanning modes** and **non-scanning modes.**

$$TIS_{as} = \frac{P_{1x1}\, f_{awf}}{C_{TIS,1}} \tag{A.12}$$

where

$C_{TIS,1}$ = 210 mW MHz

A.4.3.2 Derivation notes for soft tissue thermal index below-surface for non-scanning mode ($TIS_{\mathbf{bs,ns}}$)

As discussed in A.4.2 and A.4.3 the perfusion assumption (1 cm thermal perfusion length) is critical to determining the location of the maximum temperature increase. Theory derived for a heated cylinder suggests that if the **beam area** is less than 1 cm^2, the power in the beam controls the temperature rise [14]. If the **beam area** is greater than 1 cm^2, intensity controls the temperature rise. Therefore, the **power parameter** P_p used in the numerator of the general formula (equation A.4) for narrow beams [**beam area** ≤ 1 cm^2] is the **attenuated output power**, $P_\alpha(z)$ and for broad beams [**beam area** > 1 cm^2] the **power parameter** is the **attenuated spatial-average temporal-average intensity**, $I_{sata,\alpha}(z)$, multiplied by an area of 1 cm^2 ($I_{sata,\alpha} \times 1$ cm^2), where the spatial averaging is carried out over a 1 cm^2 area.

Attenuated bounded-square output power', $P_{1x1,\alpha}(z)$ is defined as $P_\alpha,(z)$ when the **beam area** is < 1 cm^2 and $I_{sata,\alpha} \times 1$ cm^2 when the **beam area** is > 1 cm^2, where $I_{sata,\alpha}$ is the spatial average over the 1 cm x 1 cm area yielding the highest value.

Thus, for any location z on the beam axis, the local **power parameter** is $P_{1x1,\alpha}(z)$ and **the power parameter** P_p used in the numerator of the general formula (equation A.4) is then:

$$P_p = \max_{z>z_{bp}} \left[P_{1x1,\alpha}(z) \right] \tag{A.13}$$

Approximation Used:

Considering the measurement complexity and time associated with precise measurement of $P_{1x1,\alpha}(z)$, Edition 2 of the standard chooses an approximation of the local power parameter, using the **equivalent beam area** and using the **attenuated spatial-peak temporal-average intensity**, assumed to occur on the beam axis, rather than the spatial-average intensity.

Thus when the **equivalent beam area**, ($A_{eq}(z) = \frac{P_\alpha(z)}{I_{spta,\alpha}(z)}$) is ≤ 1 cm^2 the attenuated output power, $P_\alpha(z)$, is the local **power parameter** and when $A_{eq}(z)$ is > 1 cm^2, $I_{spta,\alpha}(z) \times 1$ cm^2 is the local **power parameter.**

That is, the local **power parameter** at a particular depth z is min($P_\alpha(z)$, $I_{spta,\alpha}(z) \times 1$ cm^2) and:

$$P_p = \max_{z>z_{bp}} \left[\min\left(P_\alpha(z), I_{spta,\alpha}(z) \text{x} 1\text{cm}^2 \right) \right] \quad \text{(A.14)}$$

This is a conservative approximation. The conservative nature of the approximation is further described in the following three notes:

NOTE 1 Equations such as A.17, A.18 and A.19 indicate that it is the -6 dB area which should be compared against the 1 cm^2 threshold, and equation A.29 shows that the -6 dB area is larger than A_{eq}.

NOTE 2 Because $I_{spta,\alpha}(z)$ is > $I_{sata,\alpha}(z)$ (averaged over 1×1 cm^2 and multiplied by 1 cm^2, = $P_{1x1,\alpha}(z)$), then when $A_{eq}(z) = \frac{P_\alpha(z)}{I_{spta,\alpha}(z)}$ = 1 cm^2 the actual -6dB beam area, per equation A.29, is larger than 1 cm^2, and therefore the power in the numerator can be larger than the power in a 1 cm^2 beam area (larger than $P_{1x1,\alpha}(z)$). So for $A_{eq}(z) \leq$ 1 cm^2, $P_{1x1,\alpha}(z) \leq P_\alpha(z) < I_{spta,\alpha}(z)$, and for $A_{eq}(z) >$ 1 cm^2 , $P_{1x1,\alpha}(z) < I_{spta,\alpha}(z) < P_\alpha(z)$.

NOTE 3 Because A_{eq} is smaller than the -6 dB area (A_6), then it is obviously < 1 cm^2 when A_6 is < 1 cm^2, and acoustic power is the 'power parameter' (controls heating), in this case.
For the region 1,0 cm^2 < A_6 < 1,28 cm^2, A_{eq} remains ≤ 1,0, and the **attenuated output power**, P_α, is used instead of $I_{spta,\alpha} \times 1$ cm^2 as the 'power parameter'. This is conservative (an over-estimate) for this region, because obviously the power passing through a 1,28 cm^2 area is > than the power through a 1 cm^2 area ($P_{1x1,\alpha}$), and both are smaller than $I_{spta,\alpha} \times 1$ cm^2. So $P_{1x1} < P \leq I_{spta,\alpha} \times 1$ cm^2.

Lastly, for $A_6 \geq$ 1,28 cm^2 the intensity (× 1 cm^2) is being used as the power parameter as it should be, $I_{spta,\alpha} \times$ 1 cm^2 is being used, which is always > $I_{sata,\alpha} \times 1$ cm^2 ($P_{1x1,\alpha}$ when the spatial average is over 1 cm^2); so this is conservative ($I_{spta,\alpha} \times 1$ cm^2 > $P_{1x1,\alpha}$).

Combining the **power parameter** expressed in equation A.14 with the power required to cause a 1 °C temperature rise, P_{deg}, (Equation A.11) into the general *TI*-formula (equation A.4) yields the soft tissue thermal index below-surface for non-scanning modes

$$TIS_{bs,ns} = \max_{z>z_{bp}} \left[\min\left(\frac{P_\alpha(z_{s,ns}) f_{awf}}{C_{TIS,1}}, \frac{I_{spta,\alpha}(z_{s,ns}) f_{awf}}{C_{TIS,2}} \right) \right] \quad \text{(A.15)}$$

where

$C_{TIS,1}$ = 210 mW MHz;

$C_{TIS,2}$ = 210 mW cm^{-2} MHz.

Figures A.4, A.5, A.6, and A.7 illustrate examples of possible locations and values of the **power parameter** (Equation A.14). These figures demonstrate examples of possible relationships between the intensity ($I_{spta,\alpha}(z) \times 1$ cm^2) and power ($P_\alpha(z)$) curves. Values within the region less than the **break-point depth** ($z < z_{bp}$) are not considered.

It is helpful to consider what these curves indicate about beam focusing. Because the **equivalent beam area**, A_{eq}, is the ratio of $P_\alpha(z)$ to $I_{spta,\alpha}(z)$, in regions where the intensity curve is below (less than) the power curve, the **equivalent beam area** is greater than 1 cm^2. Similarly, where the intensity curve is above (greater than) the power curve, the **equivalent beam area** is less than 1 cm^2. The **equivalent beam area** is 1 cm^2 where the curves intersect.

Figure A.4 shows a focused beam for which the **equivalent beam area** first decreases to 1 cm^2, that is, the curves intersect at a depth greater than the **break-point depth**. The maximum value of the local **power parameter** is found at this intersection, and the location is denoted $z_{s,ns}$.

Figure A.5 might represent a focused transducer with somewhat smaller aperture. At the **break-point depth**, the **equivalent beam area** is already less than 1 cm^2. The maximum value of the local **power parameter,** $P_\alpha(z)$, is the **attenuated output power** at the **break-point depth**, and $z_{s,ns}$ is at the **break-point depth**.

Figure A.6 might represent a focusing transducer with a relatively weak focus just beyond the **break-point depth**. This local intensity maximum may result from the elevation focus of a rectangular aperture transducer or, perhaps, a close to the transducer effect beyond the **break-point depth**. In this example, the location, $z_{s,ns}$, of the local **power parameter** maximum is at the weak focus. The value of the **power parameter** is $I_{spta,\alpha}(z) \times 1$ cm^2.

Figure A.7 represents a weakly focused transducer. The **equivalent beam diameter** always exceeds 1 cm^2. While such an example is unlikely in diagnostic ultrasound applications, the example is provided for the sake of a complete understanding of the model. The distribution of the local **power parameter** with depth is the intensity curve. The **power parameter** is the maximum value of the $I_{spta,\alpha}(z) \times 1$ cm^2. $z_{s,ns}$ is at the location on the beam axis of this maximum.

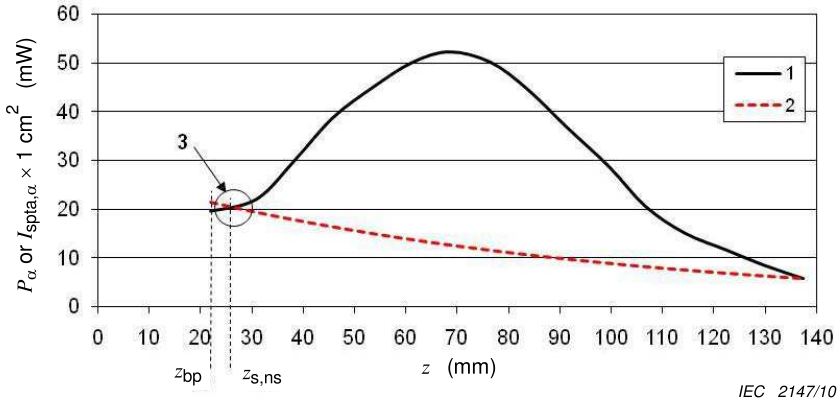

Key

1: graph of $I_{spta,\alpha} \times 1$ cm^2,

2: graph of P_α,

3: point where $P_p = P_\alpha(z_{s,ns}) = I_{spta,\alpha} \times 1$ cm^2

Figure A.4 – Focusing transducer

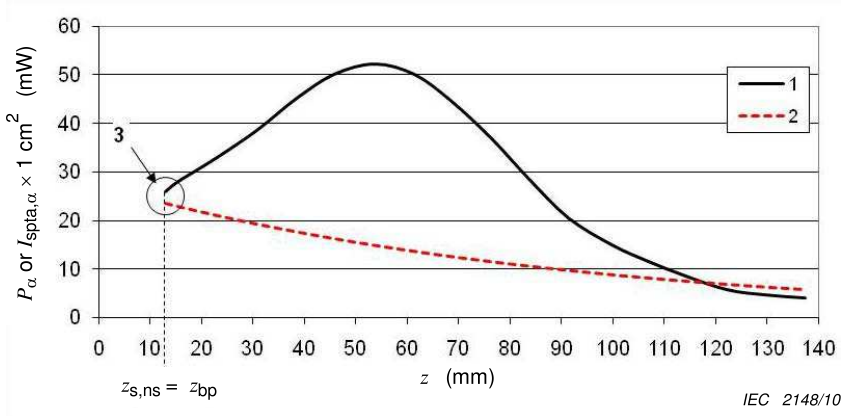

Key

1: graph of $I_{spta,\alpha} \times 1$ cm^2,

2: graph of P_α,

3: point where $P_p = P_\alpha(z_{s,ns})$

Figure A.5 – Focusing transducer with smaller aperture than that of Figure A.4

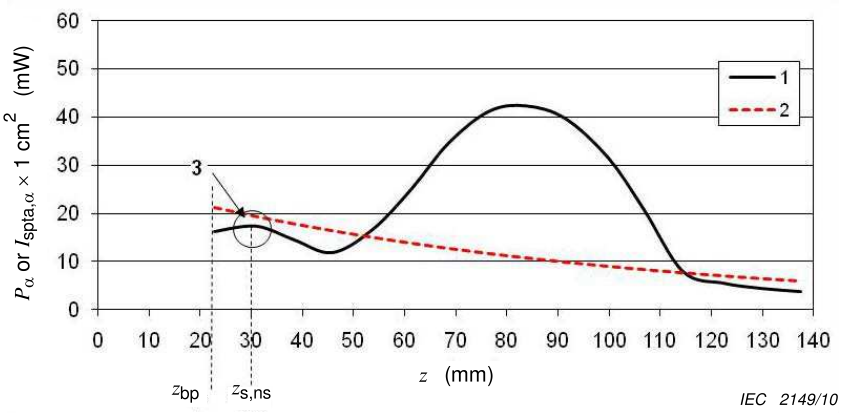

Key

1: graph of $I_{spta,\alpha} \times 1\ cm^2$,

2: graph of P_α,

3: point where $P_p = I_{spta,\alpha} \times 1\ cm^2$

Figure A.6 – Focusing transducer with a weak focus near z_{bp}

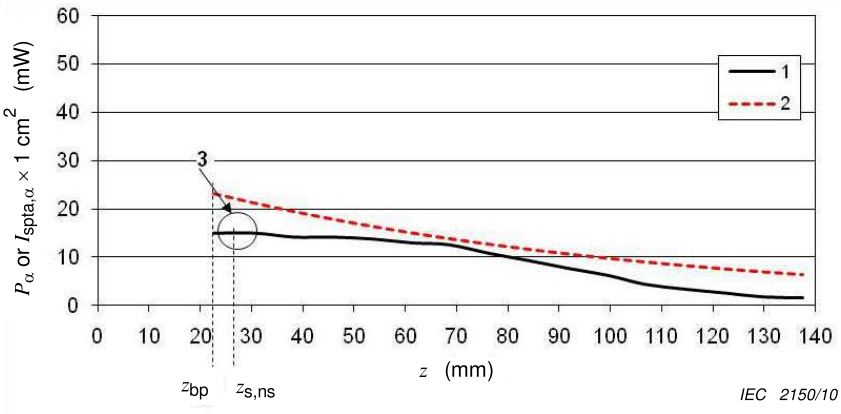

Key

1: graph of $I_{spta,\alpha} \times 1\ cm^2$,

2: graph of P_α,

3: point where $P_p = I_{spta,\alpha} \times 1\ cm^2$

Figure A.7 – Weakly focusing transducer

A.4.3.3 Derivation notes for soft tissue thermal index below-surface for scanning modes, ($TIS_{bs,sc}$)

An equation for the below surface TIS for **scanning modes** could be arrived at using the same principals applied in Edition 1 and [22] for deriving the below-surface TIS for **non-scanning modes** and the at-surface TIS for **scanning modes**. However, this Edition (Ed. 2) of the standard is not following that approach.

There is considerably increased complexity and time associated with the measurement and estimation of $P_{1x1,\alpha}(z)$ in **scanning modes**, and this is even more difficult in 3D and 4D **scanning modes**. It is preferable to choose formulas which give both reasonable results and which can be reasonably implemented in industrial measurement labs, where the constraints

on measurement time and complexity must be considered. For the below-surface **non-scanning mode** case, suitable approximations for $P_{1x1,\alpha}(z)$ were made in Edition 1 and [22]. But for scanning modes the complexity of approximations for $P_{1x1,\alpha}(z)$ is significantly increased or their suitability are not well understood.

Therefore, use is made in Edition 2 of the claim In IEC 62359 Edition 1 and in [22] that for most **scanning mode** cases the below surface temperature in soft tissue is less than the at-surface temperature in soft tissue. Though limited support for the claim is given in Edition 1 and in [22], this claim remains in Edition 2 and made use of by setting the $TIS_{\mathrm{bs,sc}}$ equal to the $TIS_{\mathrm{as,sc}}$.

So:

$$TIS_{\mathrm{bs,sc}} = TIS_{\mathrm{as,sc}} = \frac{P_{1x1}\, f_{\mathrm{awf}}}{C_{TIS,1}} \qquad \text{(A.16)}$$

where

$C_{TIS,1}$ = 210 mW MHz

Justification for this simplification can be found in [**Error! Bookmark not defined.**] and [25] which show calculations of at-surface soft tissue temperature rise for scanned modes to be higher than below-surface soft tissue temperature rise in a large majority of cases.

A.4.3.4 Derivation notes for bone at-focus for non-scanning modes ($TIB_{\mathrm{bs,ns}}$)

For the bone-at-focus model for **non-scanning modes**, the location of the maximum temperature increase is at the proximal surface of the bone, located at the **depth for *TIB*** where the **depth for *TIB*** is the depth at which the *TIB*-expression is a maximum. The **power parameter** for the beam is the **attenuated output power**, P_α at $z_{\mathrm{b,ns}}$.

NOTE The conservative assumption here is that the bone resides at the location where the *TIB* expression is a maximum.

The following derivation refers to key conclusions from the literature [1,12,14,23].

To determine the estimated power necessary to raise bone 1°C at an axial distance, $z_{\mathrm{b,ns}}$, we begin with the point-source solution to the steady-state bio-heat equation [12,14], which gives the temperature rise on axis of a totally absorbing, very thin disc surrounded by a material of thermal conductivity, K,

$$\Delta T = \frac{I_{\mathrm{sata},\alpha}\, d_6}{4K} \qquad \text{(A.17)}$$

where

$I_{\mathrm{sata},\alpha}$ is the **attenuated spatial-average temporal-average intensity**

d_6 is the –6 dB beam diameter and

K is the thermal conductivity of the surrounding medium

Since **attenuated output power** can be approximated as,

$$P_\alpha = \frac{\pi d_6^2}{4} I_{\mathrm{sata},\alpha} \qquad \text{(A.18)}$$

temperature rise can be expressed by combining A.17 and A.18:

$$\Delta T = \frac{P_\alpha}{\pi K d_6} \quad \text{(A.19)}$$

Using data adapted from [27] and selecting water at 37 °C as the surrounding medium gives a thermal conductivity, K, of 6,3 mW cm^{-1} °C^{-1}. Substituting this value for K into equation A.19 yields a temperature rise of approximately:

$$\Delta T \approx \frac{P_\alpha}{C_K d_6} \quad \text{(A.20)}$$

where

C_K= 20 mW cm^{-1} °C^{-1}.

While difficulties are obviously encountered in making accurate predictions of temperature rise that occur when bone is exposed to ultrasound *in vivo*, reasonable estimates can be made of upper limits to the temperature rise. Equation A.19, for a disc-like intensity distribution, yields a simple expression of temperature rise, ΔT, when the beam diameter is in the order of one-quarter of the perfusion length, a reasonable assumption for this model. Similar derivations are found for Gaussian or Bessinc beams and rectangular beams (within 10 % for Gaussian & Bessinc and within 30 % for rectangular).

Experimental data [28] suggest that a correction factor is required to formula A.17 (and results in changes to formulas A.19 and A.20). This correction factor is explained as being due, in part, to the effects of perfusion in relatively small volumes. The data available indicate that a factor of approximately 0,5 in temperature rise is needed to obtain correspondence between *in vivo* measurements and theory. Applying this correction factor yields

$$\Delta T = (0{,}5)\, P_\alpha / C_K d_6 = P_\alpha / 2C_K d_6 \quad \text{(A.21)}$$

Therefore, the power required to cause a 1 °C temperature rise, P_{deg}, becomes:

$$P_{\text{deg}} = 2C_K\, d_6 \,\text{x}\, 1^{\text{o}}\text{C} \quad \text{(A.22)}$$

The minimum **beamwidth** assumption noted in clause A.4.2.5 is made here insofar as the smallest beam diameter that can be maintained in a clinical exam is 0,1 cm, due to both operator- and patient-motion; then P_{deg} = 4 mW. This value yields the power required to cause a 1 °C temperature rise, P_{deg} in terms of d_6

$$P_{\text{deg}} = \max(2\text{C}_K\, d_6 \,\text{x}\, 1^{\text{o}}\text{C}, 4\,\text{mW}) \quad \text{(A.23)}$$

It is now necessary to express the beam diameter for typical beams, such as Gaussian or Bessinc, in terms of the **equivalent beam diameter**, d_{eq}. The equations for a uniform “disk” beam (A.18) and the **equivalent beam diameter** (A.8) are similar and result in

$$d_6 \approx d_{\text{eq}} = 2\sqrt{\frac{P}{\pi I_{\text{spta}}}} \quad \text{(A.24)}$$

For a Gaussian beam, see [1],

$$P_\alpha \approx \frac{\pi I_{\text{spta},\alpha} (d_6)^2}{5{,}5} \quad \text{(A.25)}$$

yielding a beam diameter of

$$d_6 = 2{,}34\sqrt{\frac{P_\alpha}{\pi I_{\text{spta},\alpha}}} = 1{,}17\, d_{\text{eq}} \tag{A.26}$$

where d_6 is the -6 dB beam diameter as discussed above. Similarly, for a Bessinc beam, see [1],

$$P_\alpha \approx \frac{\pi I_{\text{spta},\alpha}(d_6)^2}{4{,}8} \tag{A.27}$$

yielding a beam diameter of

$$d_6 = 2{,}19\sqrt{\frac{P_\alpha}{\pi I_{\text{spta},\alpha}}} = 1{,}10\, d_{\text{eq}} \tag{A.28}$$

Upon dividing equations A.26 and A.28 by A.24 and geometrically averaging the respective coefficients, the following correction is selected:

$$d_6 = 1{,}13\, d_{\text{eq}} \tag{A.29}$$

This expression is substituted for d_6 into Equation A.23, yielding the power required to cause a 1 °C temperature rise, P_{deg}

$$P_{\text{deg}} = \max(2{,}26\, C_K\, d_{\text{eq}} \times 1^{\text{o}}\text{C}\,,\, 4{,}52\,\text{mW}) \tag{A.30}$$

Expressing d_{eq} in terms of P_α and $I_{\text{spta},\alpha}$ and using equations A.7, A.8 and A.9 yields

$$P_{\text{deg}} = \max\left[2{,}26\, C_K \left(2\sqrt{\frac{P_\alpha}{\pi I_{\text{spta},\alpha}}}\right) \times 1^{\text{o}}\text{C}\,,\, 4{,}52\,\text{mW}\right] \tag{A.31}$$

which yields the approximation

$$P_{\text{deg}} = \max\left[2{,}55\, C_K \sqrt{\frac{P_\alpha}{I_{\text{spta},\alpha}}} \times 1^{\text{o}}\text{C}\,,\, 4{,}52\,\text{mW}\right] \tag{A.32}$$

NOTE 2 The actual computed values of 2,26 C_K and 4,52 in Equation A.31 (shown rounded in equation A.32) can be rounded further to 2,5C_K and 4,4, respectively, for compatibility with earlier editions of this standard.

Combining the **attenuated output power**, P_α, with the power required to cause a 1°C temperature rise, P_{deg}, (Equation A.32) into the general *TI*-formula A.4 yields the result for the bone-at-focus model for **non-scanning modes:**

$$TIB_{\text{bs,ns}} = \min\left[\frac{\sqrt{P_\alpha(z_{\text{b,ns}})\, I_{\text{spta},\alpha}(z_{\text{b,ns}})}}{C_{TIB,1}}, \frac{P_\alpha(z_{\text{b,ns}})}{C_{TIB,2}}\right] \tag{A.33}$$

where

$C_{TIB,1}$ = 50 mW cm^{-1}

$C_{TIB,2}$ = 4,4 mW

As described in section 5.4.2.2 and A.4.2.1, in Equation A.33 the depth at which the $TIB_{\text{bs,ns}}$ is calculated, $z_{\text{b,ns}}$, is the depth, for $z > z_{\text{bp}}$ where the product of the **attenuated spatial-peak temporal-average intensity** and the **attenuated output power** maximizes.

$$z_{\mathrm{b,ns}} = \text{depth of } \max\left(P_{\alpha}(z) \text{ x } I_{\mathrm{spta},\alpha}(z)\right) \quad \text{(A.34)}$$

A.4.3.5 Derivation notes for bone at focus for scanning modes ($TIB_{\mathrm{bs,sc}}$)

An equation for the below-surface TIB for **scanning modes** could be arrived at using the same principals applied in Edition 1 and [22] for deriving the below-surface TIB for **non-scanning modes** and the at-surface TIB. However, again, Edition 2 is not following that approach.

There is considerably increased complexity and time associated with the measurement and estimation of $d_{\mathrm{eq}}(z)$ in **scanning modes**, and this is even more difficult in 3D and 4D **scanning modes**. It is preferable to choose formulas which give both reasonable results and which can be reasonably implemented in industrial measurement labs, where the constraints on measurement time and complexity must be considered. For the below-surface **non-scanning mode** case, suitable approximations for $d_{\mathrm{eq}}(z)$ were made in Edition 1 and [22]. But for scanning modes the complexity of approximations for $d_{\mathrm{eq}}(z)$ is significantly increased or their suitability are not well understood.

Therefore, use is made in Edition 2 of the claim in 62359 Edition 1 and in [22] that for most **scanning mode** cases the below surface temperature in bone is less than the at-surface temperature in soft tissue. Though limited support for the claim is given in Edition 1 and in [22] and though it seems reasonable that the claim is not true for some number of **scanning mode** operating conditions, some support is offered [**Error! Bookmark not defined.**,25] that it may be true in many cases. This claim remains in Edition 2 and made use of by setting the $TIB_{\mathrm{bs,sc}}$ equal to the $TIS_{\mathrm{as,sc}}$.

$$TIB_{\mathrm{bs,sc}} = TIS_{\mathrm{as,sc}} = \frac{P_{1\mathrm{x}1}\, f_{\mathrm{awf}}}{C_{TIS,1}} \quad \text{(A.35)}$$

where

$C_{TIS,1}$ = 210 mW MHz

A.4.3.6 Derivation notes for bone at-surface [TIC] for non-scanning modes (TIC_{ns}) and for scanning modes (TIC_{sc})

Like the bone-at-focus model (clauses A.4.3.4 and A.4.3.5), the location of the maximum temperature increase for the bone-at-surface (cranial) case is at the proximal surface of the bone. Since the bone is located at the surface, or beam entrance, there is no attenuation and there is no compensation for **scanning modes** vs., **non-scanning modes**. The power parameter is **output power**, P.

The thermal model for bone-at-surface for **non-scanning modes** and **scanning modes** is conceptually the same as for the bone-at-focus models, with the **equivalent aperture diameter** at the surface, D_{eq}, replacing the **equivalent beam diameter**, d_{eq}. Therefore, the power required to cause a 1 °C temperature rise, P_{deg}, is

$$P_{\mathrm{deg}} = C_{\mathrm{sb}}\, D_{\mathrm{eq}} \times 1\ ^{\circ}\mathrm{C} \quad \text{(A. 36)}$$

where

C_{sb} = 40 mW cm^{-1} °C^{-1}

NOTE 1 There is no beam correction factor applied to D_{eq} as it is a fixed aperture dimension.

NOTE 2 For **non-scanning modes** D_{eq} is calculated as described in A.4.2.1 and in 3.28 using the **output beam area** A_{ob}, and for **scanning modes** D_{eq} is calculated as described in 3.28 using the **scanned aperture area** A_{sa}.

Combining the **output power**, P, with the power required to cause a 1 °C temperature rise, P_{deg}, (equation A.36) into the general TI-formula (equation A.4) yields the bone-at-surface expression for **non-scanning modes** and **scanning modes:**

$$TIC_{ns}, TIC_{sc} = \frac{P / D_{eq}}{C_{TIC}} \quad \text{(A. 37)}$$

where

C_{TIC} = 40 mW cm^{-1}

Annex B
(informative)

Guidance notes for measurement of output power in combined modes, scanning modes and in 1 cm × 1 cm windows

B.1 General

This standard requires, for **non-scanning modes** and **scanning modes** the measurement of the **output power** transmitted from the 1 cm × 1 cm area of the active array which transmits the most power. This is termed the **bounded-square output power**. This standard also requires, for **non-scanning modes** and **scanning modes,** the determination of the total (non-bounded) **output power**.

This annex deals primarily with the exceptions that must be made from the standard acoustic **output power** measurement procedures and requirements set out in IEC 62127 and IEC 61161. The following clauses provide guidance and describe techniques for the measurement of **output power** in scanning modes, describe windowing techniques using a 1 cm × 1 cm absorbing mask, a 1 cm × 1 cm radiation-force-balance target or electronic masking techniques.

Acoustic **output power** is often measured using a radiation force balance with an absorbing target large enough to intercept all of the propagating energy. Hydrophone raster scan measurement methods may also be used, if accurate enough (see note 2).

It is important to always distinguish between **output power** and radiation force. Ultrasonic **output power** is a scalar and does not depend on the local angle of incidence. Radiation force is a vector that depends on the local angle of incidence (with respect to the direction of the force-measuring device). For a plane-progressive wave the relation is simply $P = cF$ (Equation (B.1) in IEC 61161). In real fields deviations from this relation occur, mainly due to (a) diffraction, (b) focussing and (c) scanning (steering of **ultrasonic scan lines**, variable and non-parallel angles of incidence relative to the force measurement equipment detection axis). Deviations from Equation (B.1) due to diffraction are dealt with in B.4.2 in IEC 61161, those due to focussing are dealt with in B.5 of IEC 61161 and those due to scanning are dealt with here. Steered beams are dealt with in the same way.

If the summation of deviations is low enough when compared to the uncertainties desired, then the above effects may not need to be taken into account.

Output power and bounded-square output power measurements should have an uncertainty of 30 % or less (95 % confidence level).

NOTE 1 Reflecting targets are not recommended for the radiation force measurements discussed here, particularly for **scanning modes**.

NOTE 2 IEC 62127-1 recommends that usually it is more accurate to measure total **output power** by means of the radiation force method, and refers to IEC 61161.

B.2 Measurements for combined operating modes

In a **combined-operating mode** with more than one type of **transmit pattern** employed during the scan period, the **output power** may be considered separately for different **transmit patterns**. Such separation is allowed when necessary to permit accurate measurement of **output power** and determination of the **thermal index** by combining values appropriately as shown in Table 1. Such an approach may, for example, enable the appropriate **acoustic working frequency** to be used for each calculation. Caution is needed to ensure that each

selected single **transmit pattern** is identical to those used during (by) the **combined-operating mode**.

B.3 Measurement of output power, P, in scanning modes

B.3.1 Measurement when scanning beam is arrested

The beam scan is arrested in the forward direction normal to the absorbing target and the radiation force F_1 is measured and converted into the **output power** P_1 taking into account the effects of diffraction and focusing (per IEC 61161) in so far as these effects cannot be ignored when compared to the uncertainties to be desired .

When performing measurements with the beam scan arrested, the measured **output power** should be corrected to compensate for any beam-former related output variability, dependent on beam scan angle and/or linear position, and should be corrected to the scanning mode **pulse repetition rate**. When the beam and pulse characteristics of each **ultrasonic scan line** are equal (e.g. aperture size, pulse amplitude, centre frequency**,** pulse shape, **pulse duration, beamwidth**, focus angle, and so on) then it is appropriate to measure one ultrasonic scan line (the one most parallel with the radiation force detection axis), adjust for **pulse repetition rate** and assume that P_2 (scanning mode **output power**) = P_1. If the characteristics of each **ultrasonic scan line** are not the same, adequate correction or weighting should be applied.

NOTE 1 Examples of non-constant beam or pulse characteristics:

a) In phased array sector scanning, **output power** is sometimes increased for non-normal scan angles because of decreased element (reception) sensitivity off axis.

b) Different aperture sizes may be used for different **ultrasonic scan lines**.

Hydrophone measurements of **output power** may also be performed with the beam scan arrested, and should also include appropriate compensations for beam-former related variations between **ultrasonic scan lines**, as described above.

B.3.2 Measurements with beams scanning

Hydrophone measurements of **output power** with the beams scanning may be made by making use of a synchronizing system to synchronize the transmitted acoustic signal with the measurement system, such that one ultrasonic scan line at a time is measured via raster scan. Hydrophone element directional response corrections, taking into account the angle between (the **beam axis** of) each **ultrasonic scan line** and the hydrophone active element should be considered and applied as necessary. An alternative hydrophone method, such as described in IEC 62127, which employs hydrophones and RF power meters, may allow measurement without synchronizing on individual **ultrasonic scan lines**; however angular corrections or scan-line-specific compensations may be more difficult.

When performing these measurements in **scanning mode** with radiation-force-balances, the (absorbing) target and **external transducer aperture** should be such that the effective **beam area** is intercepted by the target over the entire extent of the beam.

The radiation force F_2 in a **scanning mode** is measured, taking into account the effect of diffraction and focusing (per IEC 61161 and [29]), and a correction based on the cosine formula is applied in so far as these effects cannot be ignored when compared to the uncertainties to be desired.

Ideally, the alignment of the (**beam axis** of each) **ultrasonic scan lines** and the direction of sensing of the radiation-force balance should be co-linear to within ±10°. As this is often not possible in sector scan modes (with non-parallel ultrasonic scan lines and therefore larger scanning angles), then compensation should be applied to the measured values.

If the pulse repetition rate and the beam and pulse characteristics of each **ultrasonic scan line** are equal (e.g. aperture size, pulse amplitude, center frequency**,** pulse shape, **pulse duration, beamwidth**, focus angle, and so on) then it is appropriate to assume that the measured (and adjusted for focusing and diffraction) **output power** F_2c multiplied by a correction factor (such as given in B.3.3 below, see also [31]) represents the output power in the scanning mode P_2. If the characteristics of the **ultrasonic scan lines** are not the same, adequate correction or weighting should be applied (for instance using a summation instead of Equation B.1 below and weighting each **ultrasonic scan line** appropriately).

The associated error in measurement will depend upon the specific geometry of the transducer and radiation-force-balance target. A simple example for a correction is given in B.3.3.

B.3.3 Example of a radiation-force to acoustic output power correction based on cosine formula

When using an absorbing target, any deviation of any portion of the field from the forward propagation direction (i.e. from the direction parallel to the detection direction of the force-measuring device) leads to a reduction of the radiation force as approximately cos(θ). In this example θ is considered the angle between the propagation direction (or **ultrasonic scan line beam axis)** and the sense direction of the radiation force detector.

Considering here a curved linear array (CLA) with total scanning angle Θ. It is possible to make corrections for the beam that is at a representative angle of θ. It is assumed that the power is distributed equally over the transducer in the scan direction.

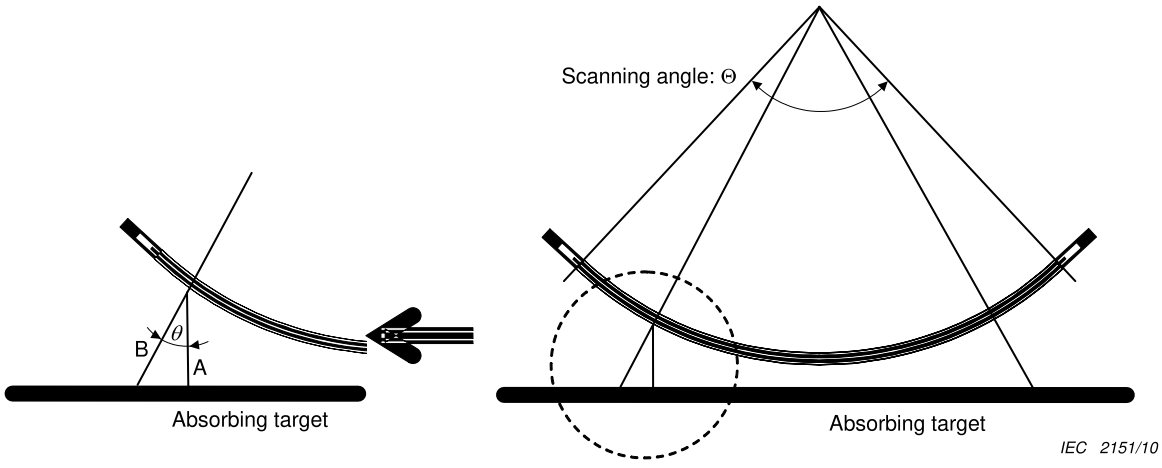

Figure B.1 – Example of curved linear array in scanning mode

Now assume that each **ultrasonic scan line** from –Θ/2 to Θ/2 is equal in average **output power** (although not in force directed parallel to the radiation-force detector sense direction). The force on the absorbing target that is actually measured is expressed as a vector A in Figure B.1, while vector B expresses what it should be. The radiation force measured by a large enough absorbing target for each scan line is expressed as $(P/c)\cos\theta$. The total measured radiation force F_2 can be obtained by integrating each force from –Θ/2 to Θ/2. F_2 can be calculated using the following equation:

$$F_2 = \frac{\frac{1}{c}\int_{-\Theta/2}^{\Theta/2} P\cos\theta d\theta}{\int_{-\Theta/2}^{\Theta/2} d\theta} = \frac{P_2}{c}\cdot\frac{2\sin\left(\frac{\Theta}{2}\right)}{\Theta} \tag{B.1}$$

where

F_2 is the total radiation force from all scanning beams acting on the absorbing target;
P_2 is the true **scanning mode output power**;
c is the speed of sound in water;
θ is the angle between the propagation direction of incident beam and the direction of the force measuring device; and
Θ is the angle between the most widely separated **ultrasonic scanlines** of the active **scan plane,** in radians.

Therefore F_2 is converted to P_2 by multiplying F_2 by the reciprocal factor of above equation.

$$P_2 = \frac{\Theta}{2\sin\left(\frac{\Theta}{2}\right)}\cdot cF_2 \tag{B.2}$$

If the total scanning angle is 60°, Θ = π/3 radian, the correction factor is calculated as 1,047 using equation B.2. If it is 90°, Θ = π/2, the correction factor would be 1,11.

NOTE 1 It has to be noted that to obtain the final power value, if not already taken care of in the determination of F_2, it may be needed to correct P_2 for diffraction and focusing.

B.4 Creating a 1 cm × 1 cm window using a mask of absorbing material or a 1 cm × 1 cm radiation force balance target

B.4.1 General

When a radiation force balance target is used to limit the aperture, its geometry and composition should be such as to detect all forward emissions from a 1 cm × 1 cm square area immediately in front of the **ultrasonic transducer** and not to detect emissions from outside that area.

The two techniques of defining the apertures in Clause B.4 have somewhat different sources of error. Agreement of the compared results from these methods, or compared to results from the method of Clause B.5, should give reasonable confidence that the aperture is defined accurately. Use of these methods, absorbing mask (B.4.2) or absorbing target (B.4.3), to limit detection to a 1 cm × 1 cm area at the front surface of the active scan aperture is recommended when the method of Clause B.5 is not feasible (e.g. for testing mechanically scanned sector probes, or third-party testing of all ultrasonic transducers).

B.4.2 1 cm × 1 cm aperture in a mask

When a mask is used, its geometry and composition should be such as to eliminate **output power** except that emitted by the designated 1 cm × 1 cm area of the active area of the transducer, to allow passage of all forward emissions from the unmasked area and to agree with the accuracy and other requirements of this standard.

The front surface of the **ultrasonic transducer** should be coplanar with the mask surfaces as illustrated in Figure B.3. This recommendation maintains consistency with B.3.2. The ultrasonic attenuation of the mask should be at least 30 dB and its window's inside walls should be lined with a reflective material to minimize loss in the walls.

Bounded-square output power measurements demonstrating that the mask meets the attenuation criteria should be made; otherwise **bounded-square output power** measurements should be made with two mask thicknesses, thereby demonstrating no (or marginal) influence of the mask thickness. Figure B.2 presents a sketch of a suggested geometry. A material with a maximum attenuation coefficient and minimum impedance mismatch with water is recommended. Materials are available commercially that are well matched to water (reflection coefficient: –30 dB) and have a loss in the range of 45 dB/cm at 3,5 MHz. Additional attenuation can be provided by sandwiching a stainless-steel, closed-pore foam or other high- or low-impedance reflector between two layers of the ultrasonic attenuating material.

For measurement of the **bounded-square output power**, the mask x- and y-dimensions should be aligned with respect to the transducer assembly under test and its x and y axis, as illustrated in Figure B.3. For instance, for 2D-**scanning modes** with simple 1D-transducer assemblies, the imaging plane axis can be set equal to x and the elevation dimension can be set equal to y. Lateral positioning is critical, **ultrasonic transducer** probe holders and jigs will be helpful in this regard. It is anticipated that an alignment of the beam alignment axis within ±5° of the normal to the mask plane and target plane and the x- and y-axes of the **transducer assembly** under test alignment within ±5° of the x- and y-axes of the mask are sufficient for the purposes of this test (see Figure B.3).

NOTE For a number of beams the mask requirements can be relaxed:

- For contact transducers, if an **output beam dimension** (X_{ob} or Y_{ob}) is less than 1 cm in any direction, then the mask's aperture may be greater than 1 cm wide in that direction.
- For transducers used with a standoff path, the mask's aperture may be larger than 1 cm in any direction in which hydrophone scanning has demonstrated that the –20 dB **beam width** at the entrance plane is less than 1 cm.

B.4.3 1 cm × 1 cm area radiation-force-balance target

As an alternative to the use of an aperture-limiting mask, the measurement of the **bounded-square output power** may be made using a 1 cm × 1 cm area - radiation-force target. When the 1 cm × 1 cm area radiation-force-balance (RFB) target is used, it should be placed immediately in front of the **ultrasonic transducer** and its geometry and composition should be such that it detects all of, and only, the acoustic emissions from a 1 cm × 1 cm area of the **ultrasonic transducer**.

The accuracy and linearity of the measurement of **bounded-square output power** should conform to IEC 61161.

To minimize measurement errors due to reverberations, caution should be used to ensure that reflected acoustic energy does not reflect back onto the target. Further, the orientation of the target's x- and y-axes should remain co-linear with the chosen x- and y- axes of the **transducer assembly** under test, as illustrated in Figure B.4.

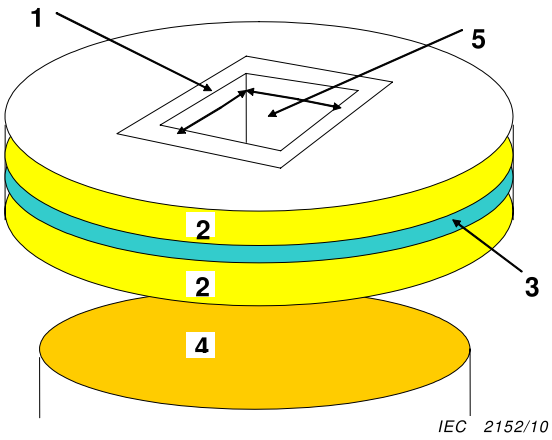

Key

1: Lining
2: Absorber
3: Sandwich layer
4: Ultrasonic transducer
5: 1 cm × 1 cm window

Figure B.2 – Suggested 1 cm × 1 cm square-aperture mask

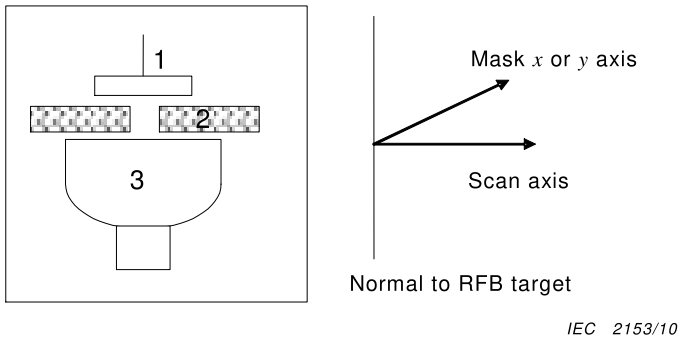

Key

1: RFB Target

2: Mask

3: Ultrasonic transducer

Figure B.3 – Suggested orientation of transducer, mask aperture and RFB target

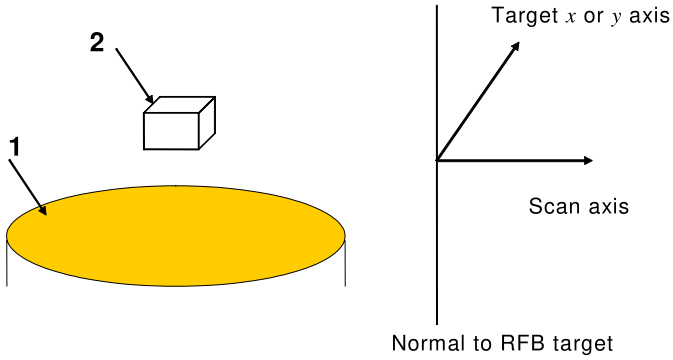

Key

1: Ultrasonic transducer

2: 1 cm-square RFB target

Figure B.4 – Suggested orientation of transducer and 1 cm-square RFB target

B.5 Creating a 1 cm × 1 cm window using electronic control or using calculations

Where the **equipment** control scheme and transducer geometry allow, masking a 1 cm × 1 cm square-area aperture may be accomplished electronically by de-energizing the aperture outside this area, provided that the **output power** emitted within the 1 cm × 1 cm square area aperture is not affected by the electronic masking.

Electronic means for masking the active aperture for a 1 cm × 1 cm square-area aperture are recommended where feasible with electronically controllable arrays (sequenced, phased, or combination).

In cases where arrays are electronically controllable in one dimension (e.g. scan-dimension, x) but not the other (e.g. transducer element lengths, $y > 1$ cm), the measurement of **bounded-square output power** can be achieved by electronically masking the elements outside 1 cm in the x dimension, making the power measurement and then mathematically adjusting the power value to a y-dimension of 1 cm.

Where transducer geometry and ultrasound radiation allows, mathematical windowing, or a combination of acoustic windowing and mathematical windowing, is allowed.

B.6 Measurement of bounded-square output power

While using the methods of B.4.2 or B.4.3 or Clause B.5 to eliminate all the **output power** except that originating through a 1 cm × 1 cm square window within the **output beam area** in **scanning mode**, the remaining **bounded-square output power** should be measured according to the procedures in IEC 61161.

In locating the mask used in either B.4.2 or Clause B.5, or the target used in B.4.3, the 1 cm × 1 cm square aperture emitting the largest bounded **output power**, should be exposed.

The uncertainty of the measurement of bounded-square power should be 20% or less.

Annex C
(informative)

The contribution of transducer self-heating to the temperature rise occurring during ultrasound exposure

The issue of temperature increase occurring during clinical exposure to diagnostic ultrasound is relevant to several current and future national and international standards. The present standard is particularly important in this regard as it specifies formulae for calculating a number of thermal indices (*TI*) which are used to provide safety-related real-time feedback to clinical users. The majority of manufacturers of ultrasound imaging equipment now comply with the IEC 60601-2-37 standard which refers to the present standard for the method of determining *TI* values to fulfil international regulations. Consequently, most modern scanners calculate and display *TI* values which are used by clinicians and sonographers in making their clinical risk assessments.

TI values are calculated from measurements of acoustic quantities made with hydrophones and radiation force balances. Essentially, the formulae used are a simplified method of estimating the temperature rise produced by the absorption of ultrasound. However, there is a second major cause of tissue heating which is ignored by the present standard and that is self-heating of the ultrasound transducer. This self-heating is caused by electrical inefficiency of the transducer; efficiencies are typically around 30% meaning that more than twice as much energy is liberated as heat in the transducer than is absorbed and converted to heat in the exposed tissue. For most transducers, most of the heat produced by the transducer is generated in the thin piezoelectric layer adjacent to the contact surface with the tissue.

Studies [32,33,34,35,36] with Thermal Test Objects (TTO) and a range of clinical pulsed Doppler transducers have shown that over three minutes exposure, self-heating accounts for approximately half of the temperature rise in the TTO at a distance of 7 mm from the transducer. At smaller distances or for longer exposure times, self-heating will be an even larger contribution. It is clear, therefore, that any proper evaluation of the thermal hazard must include transducer self-heating. One approach would be to model the transducer itself mathematically by consideration of the electrical and thermal properties of the piezoelectric element and the transducer case. This would certainly be feasible as an academic study (see Saunders [37]). However, in general, the properties and construction of the transducer will not be known (except, possibly, by the transducer manufacturer) so a simpler, more practicable method which could be implemented in future national and international standards should be proposed.

Studies are on-going which suggest that, subject to certain simplifying assumptions, the temperature profile (due to self-heating) as a function of distance from the transducer can be approximated from a single measurement of the temperature at or close to the transducer/tissue interface. The total temperature can then be given by the summation of the self-heating contribution and the contribution due to local ultrasound absorption within the medium. The need to take this approach in the present standard could not reach consensus and introduction of such methods is postponed to a third edition of this standard.

Annex D
(informative)

Guidance on the interpretation of *TI* and *MI*

D.1 General

It is beyond the scope of this standard to go into detail on the relation of the **thermal index** (*TI*) and **mechanical index** (*MI*) to safety. In addition to the short notice below, interested users are invited to consult the references in the Bibliography [5,7,8,11].

The relationship of various acoustic **output parameters** (for example, **acoustic intensity**, **acoustic pressure**, **output power**, etc...) to biological effects is not presently fully understood. Evidence to date has identified two fundamental mechanisms, thermal and mechanical, by which ultrasound may induce bioeffects [12,13,14,21,38,39], and in certain cases alteration or damage to tissue. The thermal mechanism is temperature rise due to energy absorption and the mechanical bioeffects may be caused by various kinds of cavitation, due to reduced instantaneous pressure.

The temperature rise and the possibility of cavitation seem to depend on such factors as the total energy output, the mode, the shape of the ultrasound beam, the position of the focus, the centre frequency, the shape of the waveform, the frame rate, and the duty factor. The *MI* and *TI* are designed to take the most important of these factors into account and give the user information in real time about the potential for thermal or mechanical bioeffects. Because the *MI* and *TI* reflect instantaneous output conditions, they do not take into account the cumulative effects of the total examination time, especially with regard to heating. It is relevant to emphasize that shortening insonation times can give a large safety margin under some conditions (wide, scanning beams in soft tissue) but no significant margin under other conditions (narrow , non-scanning beams on bone) [25]. It is the responsibility of the **operator** to understand the risk of the output of the equipment, and to act appropriately in order to obtain the needed diagnostic information with the minimum risk to the patient. To be able to do so, the manufacturer of the device will provide information to the user on how to interpret the displayed ultrasonic exposure parameters, **thermal index** and **mechanical index** (see IEC 60601-2-37). Further guidance on of the rationale and derivation of *MI* and *TI* are given in [26,40].

D.2 Limitations of the indices

- Although Table 1 gives a method to add the contributions of different discrete modes the method has some disadvantages. For example, the below-surface *TI*-formulation would ideally be a maximum of the summation, at each depth z, of the scanning and non-scanning—contributions. However, Table 1 specifies a summation of the individual maximum, and assumes (as per A.5.3.3 and A.5.3.5) that the maximum below surface *TI* value in scanned modes is less than or equal to the at-surface, soft tissue *TI* ($TIS_{\mathrm{as,sc}}$).
- Originally the formulations for *TI* were not intended for use in ophthalmic applications. Recently *TI* has been used for ophthalmic applications [41], However special caution is advised. This issue is further addressed in the following.
- Finite amplitude effects are known to alter intensities and pressures measured in water in a non-linear way. As the models used in this standard are linear, the *in situ* exposures may be 1,5 or 2,0 times the values indicated by *TI* or *MI* [42]. If a correction method for this effect has not been applied, this should be made known to the **operator**.
- The *TI value*s predict heating in tissue next to the transducer surface due only to the energy absorbed from the beam. No correction is made for the heating of superficial tissues by the transducer itself, which may be significant (see Annex C).

- As noted in Annex A, imposition of the **break-point depth** (z_{bp}) requirement, while useful for separating 'at-surface' and 'below-surface' *TI value*s, and for preventing hydrophone-to-transducer contact, creates an unexamined region which, particularly for **f-numbers** below 1,5, may contain the highest below-surface temperature.
- The *TI* represents average values calculated according to a model and should NOT be interpreted as the numerical value of the actual temperature rise in °C in the insonated tissues. Nevertheless, relationships between these quantities have been studied and resulting cautions are given in this annex. As has been explained, there are limitations on the models underlying both the *MI* and *TI*. These models contain practical simplifications to complex and incompletely understood bio-effects interactions. Because of this fact, their use is to be limited to relative indication of bio-effect risk. The operator should be aware that, in a limited number of cases, the actual worst-case temperature rise may be up to three times higher than the displayed *TI* value, if it were interpreted in °C [28]. The *TIS value*s are based on a model of linear array scanners, focussing energy on a line. For circular transducers with a point-focus, a theoretical calculation [11] for ratios between numerical value of temperature rise and the *TIS* value for the **non-scanning** mode yielded results that ranged from 0,24 to 109. The ratio 109 was calculated for a hypothetical 4-cm diameter transducer, f-number 0,7 at 12 MHz [11]. This is an (extreme) atypical case of medical diagnostic ultrasound and it should be noted the calculated temperature rise was less than 0,01°C, while the *TIS* value was less than 0,0001. As mentioned earlier and as indicated in [11], the ratio of 109 results primarily from limiting the axial search for the *TIS* to depths ≥ the **break-point depth**, 6 cm in this case, while the nominal focus of the transducer, and the position of maximum calculated temperature rise, is at 2,8 cm.
- The model for calculating *TI* assumes some cooling by blood perfusion. For applications where poorly perfused tissues are insonated, the *TI* may underestimate the numerical value of the worst-case temperature rise, and the *TI* displayed during such a clinical exam should accordingly be maintained at a lower value than is usually employed. Conversely, when scanning well-perfused organs, such as hepatic, cardiac or vascular structures, the value of *TI* displayed may overestimate the numerical value of the actual temperature rise.
- The models use a fixed attenuation coefficient and as such do not take long, low-attenuation fluid paths into account. In such cases, the ultrasound energy will not be absorbed as much as the model assumes with the result that the tissue distal to the fluid path may be exposed to higher energy levels than the models predict. For example, scanning through a full bladder or amniotic fluid may result in displayed *TI value*s that underestimate numerical value of the actual temperature rises. On the other hand, the fixed attenuation coefficient used (0,3 dB $cm^{-1}MHz^{-1}$) is considerably smaller than average values for human tissue. Therefore, in many cases, tissues may be exposed to lower levels of energy than the models predict.
- The meaning of "reasonable worst case" is taken as that given by the World Federation for Ultrasound in Medicine and Biology [43], namely "that set of tissue properties and dimensions such that less than 2,5% of patients have a higher calculated temperature increase or other thermal endpoint if their actual tissue properties or thicknesses differ from those employed in the calculations".

Annex E
(informative)

Differences from IEC 62359 Edition 1

E.1 General

The methods of determination set out in Edition 1 of this standard are based on those contained in the standard for Real–Time Display of Thermal and Mechanical Acoustic Output Indices on Diagnostic Ultrasound Equipment [22] and were intended to yield identical results.

The models on which these determinations are based and the measurement and calculation rationale are contained in [22] and in its secondary references. Edition 1 of this standard has followed [22]. While Edition 2 also follows [22] in principal and uses the same basic formulae and assumptions (see Annex A), it contains a few significant modifications which deviate from [22].

One of the primary issues dealt with in preparing the Edition 2 of this standard is 'missing' TI equations. In Edition 1 there were not enough equations to make complete 'at-surface' and 'below-surface' summations for TIS and TIB in combined-operating modes.

Annex F was added to Edition 2 of this standard to support the definition and determination of maximum positions and values of I_{spta}, $I_{\text{spta},\alpha}$, I_{sppa} and $I_{\text{sppa},\alpha}$ specified by IEC 60601-2-37.

NOTE Similar to the below-surface TI values, these are also specified to be found on the **beam axis** beyond the **break-point depth** z_{bp}.

E.2 Differences from IEC 62359 Edition 1

While there have been numerous editorial changes and clarifications, the technical changes and major editorial clarifications in Edition 2 come down to a relative few.

Some of the major changes from Edition 1 are related to the introduction of new calculations of thermal indices to take into account both "at-surface" and "below-surface" thermal effects:

TI in single modes of operation

TIS_{as}

- The substitution of $P_{1\text{x}1}$ for P_1 in $TIS_{\text{as,sc}}$.
  (See Annex A.4.1.4 and A.4.1.5)
- The calculation of $TIS_{\text{as,ns}}$ for all aperture sizes.
- Using the same TIS_{as} equation for both **non-scanning modes** and **scanning modes**.

TIS_{bs}

- For **non-scanning modes** the $TIS_{\text{bs,ns}}$ equation now applies (is calculated) for all aperture sizes.
- For **scanning modes** a $TIS_{\text{bs,sc}}$ equation has been added.

TIB_{bs}

- For **scanning modes** a $TIB_{\text{bs,sc}}$ equation has been added.

TI in combined modes of operation

- The TI is simply the maximum of the 'At-Surface Summation' or the 'Below-Surface Summation'. New in Edition 2 of the standard, there is an at-surface term (as) and a below-surface term (bs) for each active **Transmit Pattern** regardless of whether scanning or non-scanning or of aperture size. These at-surface and below-surface terms are calculated at all times.

- From Table 1 of section 5.6:

$$TIS = \mathrm{Max}\left[\sum_{\substack{Discrete\\Modes}} TIS_{\mathrm{as}}, \sum_{\substack{Discrete\\Modes}} TIS_{\mathrm{bs}}\right] \qquad TIB = \mathrm{Max}\left[\sum_{\substack{Discrete\\Modes}} TIS_{\mathrm{as}}, \sum_{\substack{Discrete\\Modes}} TIB_{\mathrm{bs}}\right]$$

z_{bp}

- Edition 2 makes clearer that z_{bp} is to be applied to $TIS_{\mathrm{bs,ns}}$, $TIB_{\mathrm{bs,ns}}$ and not to MI.
- In Edition 2 a **depth for** MI (z_{MI}) is specifically defined.

P_{sc}

- Explanation and equations have been added to Annex B describing the additional complexity and sources of error in the determination of acoustic output power in scanning modes (Psc). Recommended corrections are described for non-normal incidence (i.e. if measuring in **scanning modes** without arresting the beam scanning).

Beam-axis

- Edition 2 makes clearer that measurements are to be made on the **beam-axis**.

NOTE Transverse scans which, at depths of interest, re-affirm that the **beam-axis** remains found are recommended.

Table E.1 summarizes some of the major changes.

NOTE The $I_{\mathrm{spta},\alpha}(z_{\mathrm{b,ns}})$ and $I_{\mathrm{spta},\alpha}(z_{\mathrm{s,ns}})$ values shown in Table E.1 are not the "maximum" **attenuated spatial-peak temporal-average intensity** values described in Annex F, because they are at the **depth for** TIB and the **depth for** TIS, respectively.

Table E.1 – Summary of differences

Parameter	Edition 1	Edition 2
z_{bp}	$z_{bp} = 1{,}5 \times D_{eq}$	• No change to formula z_{bp} is only used in determining below-surface TI for non-scanned modes. z_{bp} is also applied to I_{spta}, $I_{spta,\alpha}$, I_{sppa} and $I_{sppa,\alpha}$ determination described in Annex F.
MI	$MI = \frac{p_{r,\alpha}(z_{MI}) \cdot f_{awf}^{-1/2}}{C_{MI}}$	• No change to formula • Measure at $z = z_{MI}$ is now stated.
$TIS_{as,ns}$	• TIS_{ns} is calculated at-surface only when **output beam area** (A_{ob}) is ≤ 1 cm^2 $TIS_{ns} = \frac{P f_{awf}}{C_{TIS,1}}$	• Calculate for all A_{ob} sizes. $TIS_{as,ns} = \frac{P_{1x1} f_{awf}}{C_{TIS,1}}$
$TIS_{as,sc}$	$TIS_{as,sc} = \frac{P_1 f_{awf}}{C_{TIS,1}}$	$TIS_{as,sc} = \frac{P_{1x1} f_{awf}}{C_{TIS,1}}$
$TIS_{bs,ns}$	• TIS_{ns} is calculated only when **output beam area** (A_{ob}) is > 1cm^2 $TIS_{ns} = \max_{z \geq z_{bp}} \left[\min \left[\frac{P_\alpha(z_{s,ns}) f_{awf}}{C_{TIS,1}}, \frac{I_{spta,\alpha}(z_{s,ns}) f_{awf}}{C_{TIS,2}} \right] \right]$	• Calculate for all A_{ob} sizes • No change to formula
$TIS_{bs,sc}$	• No formula specified.	• Same formula as $TIS_{as,sc}$ $TIB_{bs,sc} = TIS_{as,sc} = \frac{P_{1x1} f_{awf}}{C_{TIS,1}}$
$TIB_{bs,ns}$	$TIB_{bs,ns} = \min \left[\frac{\sqrt{P_\alpha(z_{b,ns}) I_{spta,\alpha}(z_{b,ns})}}{C_{TIB,1}}, \frac{P_\alpha(z_{b,ns})}{C_{TIB,2}} \right]$	• No change to formula • Measure at $z \geq z_{bp}$ is now stated.
$TIB_{bs,sc}$	• No formula specified.	• Same formula as $TIS_{as,sc}$ $TIB_{bs,sc} = TIS_{as,sc} = \frac{P_{1x1} f_{awf}}{C_{TIS,1}}$
$TIC_{as,ns}$ $TIC_{as,sc}$	$TIC = \frac{P / D_{eq}}{C_{TIC}}$	• No change to formula

Annex F
(informative)

Rationale and determination of maximum non-attenuated and attenuated spatial-peak temporal-average intensity and spatial-peak pulse-average intensity values

F.1 Rationale

This standard establishes parameters and methods related to thermal and non-thermal exposure aspects of diagnostic ultrasonic fields sufficient to calculate **mechanical index** (MI) and **thermal index** (TI) for display as specified in IEC 60601-2-37.

In the process of describing the determination of the **thermal index** and the **mechanical index**, this standard defines and describes the key components for deriving maximum non-attenuated and attenuated spatial-peak temporal-average and spatial-peak pulse-average intensities at any depth z in the acoustic field. Meanwhile, the acoustic output reporting tables specified in IEC 60601-2-37 require the provision of the spatial maximum values of these parameters in the acoustic field at specific depths z; including providing spatial maximum values over all depths z on the **beam axis** beyond the **break-point depth**, and "local" spatial maximum values at other depths on the **beam axis**.

NOTE 1 Other interested parties also require provision of these parameters at 'global' spatial maximum positions, and in some cases have established regulatory limits on their values.

NOTE 2 Recall from the definitions in Clause 3 that "spatial peak" in the terms "**attenuated spatial-peak temporal-average intensity**" and "**attenuated spatial-peak pulse-average intensity"** is the peak value at a given depth, z (i.e. not the peak value over all depths, z).

NOTE 3 The depths at which the MI and below-surface TIS and below-surface TIB are determined will not generally be the same depths at which the maximum values of I_{spta}, $I_{\text{spta},\alpha}$, I_{sppa} or $I_{\text{sppa},\alpha}$ occur.

This standard refers to IEC 62127-1, IEC 62127-2 and IEC 62127-3 for definitions, specifications of properties and calibration of measurement equipment and for hydrophone-based measurement methods. IEC 62127-1 defines various acoustic parameters which can be used to specify and characterize ultrasonic fields propagating in water using hydrophones. IEC 61157 also defines various acoustic parameters which can be used to specify and characterize ultrasonic fields propagating in water.

While these standards provide valuable information on the measurement of ultrasound fields, they do not describe standardized determination of maximum non-attenuated or **attenuated spatial-peak temporal-average intensity**, I_{spta} and $I_{\text{spta},\alpha}$ nor non-attenuated or **attenuated spatial-peak pulse-average intensity** I_{sppa} and $I_{\text{sppa},\alpha}$. Therefore, standardized means and definitions for their determination are provided in Annex F.

In combination with IEC 62127 and IEC 61161, this standard describes a complete set of methods for determining all acoustic output parameters for **medical diagnostic ultrasonic equipment** used within the ultrasound community, including those parameters called for by IEC 60601-2-37.

F.2 Overview

The goal of this Annex F is to describe standardized methods for determination of maximum positions and values of non-attenuated and **attenuated spatial-peak temporal-average intensity** I_{spta} and $I_{\text{spta},\alpha}$, and non-attenuated and **attenuated spatial-peak pulse-average intensity** I_{sppa} and $I_{\text{sppa},\alpha}$, in the acoustic field of a medical diagnostic ultrasound device.

Other, non-IEC, measurement standards define the determination of $I_{spta,\alpha}$ and $I_{sppa,\alpha}$ for regulatory agency purposes. Reference [44] is used widely and is referenced in IEC 62127-1. The methods listed in this Annex F are intended to be consistent with [44].

The standard attenuation coefficient value chosen is 0,3 dB cm^{-1} MHz^{-1}; the same value is introduced and used by this standard in the derivation of the below-surface **thermal index** and the **mechanical index**.

Another key similarity to the below-surface **thermal index** and the **mechanical index** is to remain on the **beam axis** when finding the position of spatial maximum values.

Similarly, this standard defines the **break-point depth**, and applies it in the determination of the below-surface thermal indices TIS and TIB for **non-scanning modes**. This same **break-point depth** is used for maximum I_{spta}, I_{sppa}, $I_{spta,\alpha}$ and $I_{sppa,\alpha}$ and is applied for both **scanning modes** and **non-scanning modes**.

As shown, for **non-scanning modes** one depth $z_{pii,\alpha}$ is used for the **depth of maximum $I_{spta,\alpha}$** and **depth of maximum $I_{sppa,\alpha}$**, and one depth z_{pii} is used for the **depth of maximum I_{spta}** and **depth of maximum I_{sppa}**.

However, as shown, for **scanning modes** the depths of maximum $I_{spta,\alpha}$ and $I_{sppa,\alpha}$ (and I_{spta} and I_{sppa}) can be different, and the depths of maximum I_{spta} and $I_{spta,\alpha}$ often are not at the same depth as they occur for **non-scanning** modes.

Describing the determination of the $I_{spta,\alpha}$ and I_{spta} for **scanning modes** is the most complicated and large part of Annex F. F.3.3.2 and F.3.1.4.2 give the summarized expressions while Clause F.4 gives more detailed information.

F.3 Test methods

F.3.1 Common parameters

F.3.1.1 Attenuation coefficient and frequency

The **acoustic attenuation coefficient** value α used for the determination of maximum $I_{spta,\alpha}$ and $I_{sppa,\alpha}$ is 0,3 dB cm^{-1} MHz^{-1} with linear frequency dependence.

NOTE 1 This value is the same as is used in the determination of the MI and TI, and it matches the attenuation coefficient used in [41] and [44].

Repeating Equation (A.6) in A.4.2.3:

The **attenuated spatial-peak temporal-average intensity** is denoted:

$$I_{spta,\alpha}(z) = I_{spta}(z)\,10^{(-\alpha z\, f_{awf}/10\,dB)}$$

where

$I_{spta}(z)$ is the **spatial-peak temporal-average intensity** at distance z,

α is the **acoustic attenuation coefficient**,

f_{awf} is the **acoustic-working frequency**, and

z is the distance from the **external transducer aperture** to the point of interest.

NOTE 2 In accordance with 3.4, NOTE 2, and 3.24, the **acoustic-working frequency** is determined at the **depth for peak pulse-intensity integral** on the **beam axis**.

NOTE 3 See A.4.2.3, 5.1 and Clause D.2 for additional discussion.

F.3.1.2 Use of the beam axis

Measurements for I_{sppa}, $I_{sppa,\alpha}$, I_{spta} and $I_{spta,\alpha}$ in **non-scanning modes** should be made on the **beam axis**.

NOTE While there can be side-lobes with higher intensity and pressure values, the same methodology and justification as is employed for the below-surface **thermal index** and the **mechanical index** is used, for the sake of measurement repeatability and ease.

F.3.1.3 Determination and use of the break-point depth

Measurements for I_{sppa}, $I_{sppa,\alpha}$, I_{spta} and $I_{spta,\alpha}$ in **scanning modes** and **non-scanning modes** are made at or beyond (farther-than) the **break-point depth** z_{bp}.

Care is to be taken when determining the z_{bp} so that the **equivalent aperture diameter** is correctly determined using only the –12 dB **output beam area**.

For **scanning modes** where **ultrasonic scan lines** that comprise a frame do not have the same –12 dB aperture size, the aperture size corresponding to the central scan line of each *sppsi* sum is to be used in the determination of **the break-point depth**.

For **combined-operating modes** where measurement of multiple modes and **transmit patterns** is being performed simultaneously, the smallest **break-point depth** of the active modes is to be used.

For **combined-operating modes** in which measurements of contributing modes and **transmit patterns** are being performed sequentially, the **break-point depth** of each separated mode is to be used.

F.3.1.4 Calculation of $ppsi_\alpha(z)$, $ppsi(z)$, $sppsi_\alpha(z)$ and $sppsi(z)$

F.3.1.4.1 $ppsi_\alpha(z)$

The calculation of $ppsi_\alpha(z)$ is accomplished by using Equation (27) (see 3.63).

NOTE 1 For measurement purposes of this standard, pii_α is equivalent to $1/(\rho c)$ times the **attenuated pulse-pressure-squared integral** at depth z, when z is beyond the **break-point depth,** with ρc denoting the characteristic acoustic impedance of pure water.

NOTE 2 3.43 gives the non-attenuated version of this quantity.

F.3.1.4.2 $s_\alpha ppsi(z)$ and $sppsi_\alpha(z)$ and $sppsi(z)$

The following discussion is for the **sum of attenuated pulse-pressure-squared integrals**. Application to non-attenuated sum is the same, but can be more simple because the **acoustic working frequency** does not need to be known or estimated for each scan line.

The determination of the **sum of attenuated pulse-pressure-squared integrals** and the **attenuated sum of pulse-pressure-squared integrals** for adjacent **ultrasonic scan lines** at any depth z may be accomplished using one of the following methods. Generally, these methods require knowledge, a priori or determined, of the number of **ultrasonic scan lines** per scan frame, the number of transmit pulses per scan line and the **acoustic working frequency** or a frame trigger that signals the start/stop of repeating frames.

NOTE 1 See F.4.2 for additional discussion of these methods.

NOTE 2 See IEC 62127-1:2007, Annex F, for additional discussion of these $sppsi(z)$ determination methods.

While either method a) or b) can be employed, it can be seen that as the pulse sequencing becomes increasingly complicated, increased knowledge of the pulses and the pulse sequencing is required.

a) Scanning **ultrasonic scan lines** past a stationary hydrophone

This may be accomplished by:

1) using a long record digitizer to sum the $ppsi$ values in one long record, or

2) via an electronic mask or electronic trigger which signals one **ultrasonic scan line** at a time so that the $ppsi(z)$ for each transmit pulse down that line, n, can be acquired and added to the $sppsi$ sum.

For either method 1) or 2) above, if all transmit pulses included in the sum are NOT identical, then the f_{awf} value of each pulse is to be obtained and the **attenuated pulse-pressure-squared integral** $ppsi_\alpha(z)$ calculated for each transmit pulse. The **sum of attenuated pulse-pressure-squared integrals** $sppsi_\alpha(z)$ is thus obtained.

If all transmit pulses included in the sum are identical, then the $sppsi(z)$ value may be determined separately and one attenuation factor applied to obtain the **attenuated sum of pulse-pressure-squared integrals** $s_\alpha ppsi(z)$ which in this case is equivalent to the $sppsi_\alpha(z)$.

b) Scanning a hydrophone past a single stationary **ultrasonic scan line**

This method can yield estimates of the **attenuated sum of pulse-pressure-squared integrals** $s_\alpha ppsi(z)$ and the **sum of attenuated pulse-pressure-squared integrals** $sppsi_\alpha(z)$ which are reasonably accurate when all **ultrasonic scan lines** use identical transmit pulses (f_{awf}, pulse length, pulse shape, pulse focusing and aperture, etc.).

This method consists of scanning a hydrophone past a single stationary **ultrasonic scan line**, collecting **pulse-pressure-squared integrals** at multiple lateral beam (profile) locations with sufficient spatial step size (sampling) such that the **pulse-pressure-squared integrals** corresponding to the equivalent locations of adjacent **ultrasonic scan lines** scanning past a stationary hydrophone are calculated.

This method requires knowledge of the spacing between successive **ultrasonic scan lines**.

NOTE 1 A method for experimentally determining the spacing between **ultrasound scan lines** is provided in IEC 62127-1:2007, 7.2.6.3.

NOTE 2 Another reference is IEC 62127-1:2013+IEC 62127-1:2013/AMD1:2013, 8.2.

If the transmit pulses for all **ultrasonic scan lines** (pulse shape, **beamwidth**, etc.) are not all identical, then choosing a worst case pulse and scan line may provide a reasonable over-estimate. The **ultrasonic scan line** and pulse yielding the largest $s_\alpha ppsi(z)$ value should be chosen. Choosing an **ultrasonic scan line** in the centre of the scan should be sufficient.

NOTE 3 Multiple $s_\alpha ppsi$ sums may be needed at each depth z in order to find the largest sum.

F.3.1.5 Measurement depth for maximum $I_{\mathbf{spta},\alpha}$, $I_{\mathbf{spta}}$, $I_{\mathbf{sppa},\alpha}$ and $I_{\mathbf{sppa}}$

For **non-scanning modes**, the **depth for maximum** $I_{\mathbf{spta},\alpha}$, $z_{\mathrm{spta},\alpha,\mathrm{max}}$ is the depth on the **beam axis**, at or beyond the **break-point depth**, where the maximum **attenuated pulse-pressure-squared integral** $\max_{z \geq z_{\mathrm{bp}}} [ppsi_\alpha(z)]$ occurs. This is the **depth for maximum** $\boldsymbol{pii}_\alpha$, $z_{pii,\alpha}$.

NOTE 1 The **depth for maximum** $I_{\mathbf{spta},\alpha}$, $z_{\mathrm{spta},\alpha,\mathrm{max}}$, for **non-scanning modes** is equal to the **depth for maximum** $I_{\mathbf{sppa},\alpha}$, $z_{\mathrm{sppa},\alpha,\mathrm{max}}$, both occurring at $z_{pii,\alpha}$.

For **non-scanning modes**, the **depth for maximum** $I_{\mathbf{spta}}$, $z_{\mathrm{spta,max}}$ is the depth on the **beam axis,** at or beyond the **break-point depth**, where the maximum **pulse-pressure-squared integral** $\max_{z \geq z_{\mathrm{bp}}} [ppsi(z)]$ occurs. This is the **depth for maximum** $\boldsymbol{pii}$, z_{pii}.

NOTE 2 The **depth for maximum** $I_{\mathbf{spta}}$ ($z_{\mathrm{spta,max}}$) for **non-scanning modes** is equal to the **depth for maximum** $I_{\mathbf{sppa}}$, $z_{\mathrm{sppa,max}}$, both occurring at z_{pii}.

For **scanning modes**, the **depth for maximum** $I_{\mathbf{spta},\alpha}$, $z_{\text{spta},\alpha,\text{max}}$, is the depth, on the **beam axis**, at or beyond the **break-point depth**, where the maximum **sum of attenuated pulse-pressure-squared integrals** $\max_{z \geq z_{\text{bp}}} \left[sppsi_{\alpha}(z) \right]$ occurs. This is the **depth for maximum** sii_{α}, $z_{sii,\alpha}$.

For **scanning modes**, the **depth for maximum** $I_{\mathbf{spta}}$, $z_{\text{spta,max}}$, is the depth, on the **beam axis**, at or beyond the **break-point depth**, where the maximum **sum of pulse-pressure-squared integrals** $\max_{z \geq z_{\text{bp}}} \left[sppsi(z) \right]$ occurs. This is the **depth for maximum** sii, z_{sii}.

NOTE 3 See F.3.1.3 regarding the **break-point depth** to use when the **ultrasonic scan lines** do not have the same –12 dB aperture size.

For **non-scanning modes** and for **scanning modes**, the **depth for maximum** $I_{\mathbf{sppa},\alpha}$, $z_{\text{sppa},\alpha,\text{max}}$, is the depth on the **beam axis**, at or beyond the **break-point depth**, where the maximum attenuated pulse-pressure-squared integral $\max_{z \geq z_{\text{bp}}} \left[ppsi_{\alpha}(z) \right]$ occurs. This is the depth for maximum pii_{α}, $z_{pii,\alpha}$.

NOTE 4 This is the same depth as for maximum $I_{\text{spta},\alpha}$ for **non-scanning modes**.

For non-scanning modes and for scanning modes, the depth for maximum I_{sppa}, $z_{\text{sppa,max}}$, is the depth on the beam axis, at or beyond the break-point depth, where the maximum pulse-pressure-squared integral $\max_{z \geq z_{\text{bp}}} \left[ppsi(z) \right]$ occurs. This is the depth for **maximum** pii, z_{pii}.

NOTE 5 This is the same depth as for maximum I_{spta} for **non-scanning modes**.

F.3.2 Determination of maximum $I_{\mathbf{sppa}}$ and $I_{\mathbf{sppa},\alpha}$

F.3.2.1 Non-scanning and scanning modes

For **non-scanning modes** and **scanning modes**, the maximum **attenuated spatial-peak pulse-average intensity** should be calculated using

$$I_{\text{sppa},\alpha} = \frac{1}{t_{\text{d}}\left(z_{\text{sppa},\alpha,\text{max}}\right)\rho c} ppsi_{\alpha}\left(z_{\text{sppa},\alpha,\text{max}}\right) \tag{F.1}$$

and the maximum **spatial-peak pulse-average intensity** should be calculated using:

$$I_{\text{sppa}} = \frac{1}{t_{\text{d}}\left(z_{\text{sppa,max}}\right)\rho c} ppsi\left(z_{\text{sppa,max}}\right) \tag{F.2}$$

where

ρc is the characteristic acoustic impedance of pure water (= 1,48 × 10^6 kg m^{-2} s^{-1} at 20 °C);

$t_{\text{d}}(z_{\text{sppa},\alpha,\text{max}})$ is the **pulse duration** at the **depth for maximum** $I_{\mathbf{sppa},\alpha}$;

$t_{\text{d}}(z_{\text{sppa,max}})$ is the **pulse duration** at the **depth for maximum** $I_{\mathbf{sppa}}$;

$ppsi_{\alpha}(z_{\text{sppa},\alpha,\text{max}})$ is the **attenuated pulse-pressure-squared integral** at the **depth for maximum** $I_{\mathbf{sppa},\alpha}$;

$ppsi(z_{\text{sppa,max}})$ is the **pulse-pressure-squared integral** at the **depth for maximum** $I_{\mathbf{sppa}}$.

NOTE 1 In contrast to Equations (28) and (29), Equations (F.1) and (F.2) describe one depth each.

NOTE 2 As shown in Equations (F.1) and (F.2) and per definition 3.65 and 3.81, the pulse duration value, t_d, is determined at $z_{sppa,\alpha,max}$ and $z_{sppa,max}$, respectively.

F.3.2.2 Combined-operating modes

For **combined-operating modes**, the maximum **attenuated spatial-peak pulse-average intensity** $I_{sppa,\alpha}$ value should be the largest of the $I_{sppa,\alpha}$ values of the constituent **transmit patterns**

$$I_{sppa,\alpha}\left(z_{sppa,\alpha,max}\right) = \max_{\text{all transmit patterns}}\left[I_{sppa,\alpha}\left(\text{transmit pattern } k, z_{pii,\alpha,k}\right)\right] \tag{F.3}$$

and the maximum **spatial-peak pulse-average intensity** I_{sppa} value should be the largest of the I_{sppa} values of the constituent **transmit patterns**

$$I_{sppa}\left(z_{sppa,max}\right) = \max_{\text{all transmit patterns}}\left[I_{sppa}\left(\text{transmit pattern } k, z_{pii,k}\right)\right] \tag{F.4}$$

F.3.3 Determination of maximum $I_{spta,\alpha}$ and I_{spta}

F.3.3.1 Non-scanning modes

For **non-scanning modes**, the maximum **attenuated spatial-peak temporal-average intensity** should be calculated using:

$$I_{spta,\alpha} = \frac{prr}{\rho c}\left(\max_{z \geq z_{bp}}\left[ppsi_{\alpha}(z)\right]\right) = \frac{prr}{\rho c}\, ppsi_{\alpha}\left(z_{pii,\alpha}\right) \tag{F.5}$$

and the maximum **spatial-peak temporal-average intensity** should be calculated using:

$$I_{spta} = \frac{prr}{\rho c}\left(\max_{z \geq z_{bp}}\left[ppsi(z)\right]\right) = \frac{prr}{\rho c}\, ppsi\left(z_{pii}\right) \tag{F.6}$$

where

$ppsi_{\alpha}$ is the **attenuated pulse-pressure-squared integral**;

$ppsi$ is the **pulse-pressure-squared integral**;

z_{bp} is the **break-point depth**;

z_{pii} is the **depth for maximum *pii*** (= $z_{spta,\alpha,max}$) on the **beam axis**;

$z_{pii,\alpha}$ is the **depth for maximum *pii*$_{\alpha}$** (= $z_{spta,\alpha,max}$) on the **beam axis**;

ρc is the characteristic acoustic impedance of pure water (1,48 × 10^6 kg m^{-2} s^{-1} at 20 °C);

prr is the pulse **repetition rate** of the **non-scanning mode**.

NOTE 1 In contrast to Equation (5) in 3.10 and to the description in 3.54, Equations (F.5) and (F.6) describe one depth each.

NOTE 2 Equation (F.6) is modified from IEC 62127-1:2007, as the **break-point depth** is applied to it.

NOTE 3 For these calculations, an average **pulse repetition period** is used (see 3.3, 3.44 and 3.55).

F.3.3.2 Scanning modes

For **scanning modes**, the maximum **attenuated spatial-peak temporal-average intensity** should be calculated using:

$$I_{\text{spta},\alpha} = \frac{srr}{\rho c}\left(\max_{z \geq z_{\text{bp}}}\left[sppsi_{\alpha}(z)\right]\right) = \frac{srr}{\rho c} sppsi_{\alpha}\left(z_{sii,\alpha}\right) \quad \text{(F.7)}$$

and the maximum **spatial-peak temporal-average intensity** should be calculated using:

$$I_{\text{spta}} = \frac{srr}{\rho c}\left(\max_{z \geq z_{\text{bp}}}\left[sppsi(z)\right]\right) = \frac{srr}{\rho c} sppsi\left(z_{sii}\right) \quad \text{(F.8)}$$

where

$\max_{z \geq z_{\text{bp}}}\left[sppsi_{\alpha}(z)\right]$ is the maximum **sum of attenuated pulse-pressure-squared integrals** in one frame of **ultrasonic scan lines** at depth z;

$\max_{z \geq z_{\text{bp}}}\left[sppsi(z)\right]$ is the maximum **sum of pulse-pressure-squared integrals** in one frame of **ultrasonic scan lines** at depth z;

z_{bp} is the **break-point depth**;

$z_{sii,\alpha}$ is the **depth for maximum** sii_{α};

z_{sii} is the **depth for maximum** sii;

srr is the **scan repetition rate**;

ρc is the characteristic acoustic impedance of pure water ($1{,}48 \times 10^6$ kg m^{-2} s^{-1} at 20 °C).

NOTE For these calculations, an average **scan repetition period** is used (see 3.3, 3.44 and 3.55).

It is recommended to review the more detailed derivation notes in Clause F.4, as well as the guidance in IEC 62127-1:2007+IEC 62127-1:2007/AMD1:2013, 7.2, 8.2 and Annex F, as well as clause 5.5 of [44].

F.3.3.3 Combined-operating modes

For **combined-operating modes**, the maximum **attenuated spatial-peak**, **temporal-average intensity** $I_{\text{spta},\alpha}$ should be calculated using:

$$I_{\text{spta},\alpha} = \frac{1}{\rho c} \max_{z \geq z_{\text{bp\_min}}}\left[\left(\sum_{\substack{\text{scanning}\\ \text{mode}\_i}} sppsi_{\alpha}(i,z)srr(i)\right) + \left(\sum_{\substack{\text{non-scanning}\\ \text{mode}\_j}} ppsi_{\alpha}(j,z)prr(j)\right)\right] \quad \text{(F.9)}$$

and the maximum **spatial-peak, temporal-average intensity** I_{spta} should be calculated using:

$$I_{\text{spta}} = \frac{1}{\rho c} \max_{z \geq z_{\text{bp\_min}}}\left[\left(\sum_{\substack{\text{scanning}\\ \text{mode}\_i}} sppsi(i,z)srr(i)\right) + \left(\sum_{\substack{\text{non-scanning}\\ \text{mode}\_j}} ppsi(j,z)prr(j)\right)\right] \quad \text{(F.10)}$$

where

$z_{\text{bp\_min}}$ is the smallest **break-point depth** of the active component modes.

A reasonably conservative estimate of time-average quantities for **combined-operating modes** may be made by determining each mode separately and then combining the time-average estimates of the constituent active modes.

$$I_{\text{spta},\alpha} = \sum_{\substack{\text{discrete} \\ \text{mode\_}k}} I_{\text{spta},\alpha}\left(k, z_{\text{spta},\alpha,\max}(k)\right) \tag{F.11}$$

where each $I_{\text{spta},\,\alpha}\,(k,\, z_{\text{spta},\alpha,\max}(k))$ is determined according to F.3.3.1 and F.3.3.2.

That is

$$I_{\text{spta},\alpha} = \frac{1}{\rho c}\left[\left(\sum_{\substack{\text{scanning} \\ \text{mode\_}i}} \max_{z \geq z_{\text{bp},i}} \left[sppsi_{\alpha}(i,z)\right] srr(i)\right) + \left(\sum_{\substack{\text{non-scanning} \\ \text{mode\_}j}} \max_{z \geq z_{\text{bp},j}} \left[ppsi_{\alpha}(j,z)\right] prr(j)\right)\right] \tag{F.12}$$

For (non-attenuated) **spatial-peak temporal-average intensity** I_{spta} the equations are:

$$I_{\text{spta}} = \sum_{\substack{\text{discrete} \\ \text{mode\_}k}} I_{\text{spta},}\left(k, z_{\text{spta,max}}(k)\right) \tag{F.13}$$

and

$$I_{\text{spta}} = \frac{1}{\rho c}\left[\left(\sum_{\substack{\text{scanning} \\ \text{mode\_}i}} \max_{z \geq z_{\text{bp},i}} \left[sppsi(i,z)\right] srr(i)\right) + \left(\sum_{\substack{\text{non-scanning} \\ \text{mode\_}j}} \max_{z \geq z_{\text{bp},j}} \left[ppsi(j,z)\right] prr(j)\right)\right] \tag{F.14}$$

NOTE The application of Equations (F.9) through (F.14) requires use of the appropriate **break-point depths** for each of the discrete modes.

F.4 Additional rationale and derivation notes

F.4.1 Summary steps for measuring each active mode

The following steps are provided as a summary guide for measuring each active mode, separately.

- Determine and remain on the **beam axis** (see F.3.1.2).
- Find the **depth for maximum *pii***, z_{pii}, beyond (or at) the **break-point depth** z_{bp} (see F.3.1.3).
- Determine the **acoustic working frequency** f_{awf} (see 3.4) at this depth z_{pii} and the **pulse duration** t_{d} (see 3.41).
- For **scanning modes** and **non-scanning modes**, use the $ppsi$ and the t_{d} at z_{pii} for calculation of maximum I_{sppa}.
- For **non-scanning modes**, use the value of $ppsi$ at z_{pii} for the calculation of the maximum I_{spta}.
- Use f_{awf} and the acoustic attenuation coefficient value, α, to locate the depth for maximum $pii_{\alpha}(z)$ beyond or at the break-point depth z_{bp}.
- Determine the **pulse duration** t_{d} (see 3.41) at this depth $z_{pii,\alpha}$.
- For **non-scanning modes,** use the value of $ppsi_{\alpha}$ at $z_{pii,\alpha}$ for the calculation of maximum $I_{\text{spta},\alpha}$.
- For **scanning modes** and **non-scanning modes**, use $ppsi_{\alpha}$ at $z_{pii,\alpha}$ and t_{d} at $z_{pii,\alpha}$ for calculation of maximum $I_{\text{sppa},\alpha}$.

- For **scanning modes,** adhering to the **break-point depth** z_{bp} and referring to F.3.3.2 and F.4.2 and F.4.3, find the:
  - **depth for maximum** ***sii***, z_{sii}, and the value there of maximum I_{spta};
  - **depth for maximum** ***sii***$_\alpha$, $z_{sii,\alpha}$, and the value there of maximum $I_{spta,\alpha}$.

F.4.2 Notes regarding determination of $s_\alpha ppsi(z)$ and $sppsi_\alpha(z)$

F.4.2 gives additional notes to accompany F.3.1.4.2.

The general principles for measuring temporal average acoustic output parameters for **scanning modes** can be summarized as follows.

Temporal average parameters are determined by the cumulative effects of the overlap of beams generated during the **scan repetition period**. **Temporal average intensity** for a **scanning mode**, when measured at a point, is determined by the sum of the energy fluencies at the point resulting from the various beams transmitted during each scan and the **scan repetition rate**.

The determination of the sum of pulse-pressure-squared integrals and the sum of attenuated pulse-pressure-squared integrals are the key to determination of the temporal-average intensity in scanning modes.

The general form of the **sum of attenuated pulse-pressure-squared integrals** $sppsi_\alpha(z)$ is expressed as follows:

$$\begin{aligned} sppsi_\alpha(z) = & \ldots \\ & + \ldots \\ & + ppsi_{\alpha,m-2,1}(z) + ppsi_{\alpha,m-2,2}(z) + \ldots + ppsi_{\alpha,m-2,n_{m-2}}(z) \\ & + ppsi_{\alpha,m-1,1}(z) + ppsi_{\alpha,m-1,2}(z) + \ldots + ppsi_{\alpha,m-1,n_{m-1}}(z) \\ & + ppsi_{\alpha,m,1}(z) + ppsi_{\alpha,m,2}(z) + \ldots + ppsi_{\alpha,m,n_m}(z) \\ & + ppsi_{\alpha,m+1,1}(z) + ppsi_{\alpha,m+1,2}(z) + \ldots + ppsi_{\alpha,m+1,n_{m+1}}(z) \\ & + ppsi_{\alpha,m+2,1}(z) + ppsi_{\alpha,m+2,2}(z) + \ldots + ppsi_{\alpha,m+2,n_{m+2}}(z) \\ & + \ldots \end{aligned} \tag{F.15}$$

where

m	is the central **ultrasonic scan line** of the scan or series of scan lines in a frame. By convention, the central line m can be considered the median line, and for sector scan formats the line with **beam axis** most closely parallel to the z axis (depth axis) of the hydrophone scanning system;
$m + j$ (j = … -2, -1, 0, 1, 2, …)	is the **ultrasonic scan lines** adjacent to the central **ultrasonic scan line**;
n_{m+j}	is the number of pulses transmitted down line $m + j$;
$ppsi_{\alpha,m+j,n}(z)$	is the **attenuated pulse-pressure-squared integral** of pulse number n down line $m + j$, as measured/detected by a hydrophone at depth z aligned with line m.

NOTE 1 This is an important distinction: $ppsi_{\alpha,m+j,n}(z)$ does not represent the $ppsi_\alpha$ measured on the **beam axis** of line '$m+j$', it is the $ppsi_\alpha(z)$ of the nth pulse down line $m+j$ as measured on the **beam axis** of the central **ultrasonic scan line** m.

For the case where the pulses transmitted down a particular **ultrasonic scan line** are identical, Equation (F.15) may be simplified to:

$$sppsi_{\alpha}(z) = \ldots + n_{m-2}\,ppsi_{\alpha,m-2}(z) + n_{m-1}\,ppsi_{\alpha,m-1}(z) + n_{m}\,ppsi_{\alpha,m}(z) + n_{m+1}\,ppsi_{\alpha,m+1}(z) + n_{m+2}\,ppsi_{\alpha,m+2}(z) + \ldots \quad \text{(F.16)}$$

where

n_{m+j} is the number of pulses per scan line for **ultrasonic scan line** $m + j$ (j = … –2, –1, 0, 1, 2, …).

If the pulses down all **ultrasonic scan lines** included in the sum are identical, then, because they share the same **acoustic working frequency**, they will share the same estimated attenuation at depth z. In this case, Equation (F.16) is equivalent to:

$$\begin{aligned} sppsi_{\alpha}(z) &= s_{\alpha}\,ppsi(z) \\ &= 10^{-\alpha z f_{\text{awf}}/10\,\text{dB}}(\ldots + n_{m-2}\,ppsi_{m-2}(z) + n_{m-1}\,ppsi_{m-1}(z) + n_{m}\,ppsi_{m}(z) + n_{m+1}\,ppsi_{m+1}(z) + n_{m+2}\,ppsi_{m+2}(z) + \ldots) \end{aligned} \quad \text{(F.17)}$$

In addition, when the number of pulses down each line included in the sum is the same ($n_{m+j} = n$), then Equation (F.16) simplifies further:

$$sppsi_{\alpha}(z) = n \times (\ldots + ppsi_{\alpha,m-2}(z) + ppsi_{\alpha,m-1}(z) + ppsi_{\alpha,m}(z) + ppsi_{\alpha,m+1}(z) + ppsi_{\alpha,m+2}(z) + \ldots) \quad \text{(F.18)}$$

and (again) if all the pulses down all lines in the sum are identical:

$$\begin{aligned} sppsi_{\alpha}(z) &= s_{\alpha}\,ppsi(z) \\ &= n \times 10^{-\alpha z f_{\text{awf}}/10\,\text{dB}}(\ldots + ppsi_{m-2}(z) + ppsi_{m-1}(z) + ppsi_{m}(z) + ppsi_{m+1}(z) + ppsi_{m+2}(z) + \ldots) \end{aligned} \quad \text{(F.19)}$$

NOTE 2 As illustrated by comparing Equations (F.15) to (F.19), the **sum of attenuated pulse-pressure-squared integrals** will be equal to the **attenuated sum of pulse-pressure-squared integrals** at depth z if each **ultrasonic scan line** in the frame which is included in the sum has the same **acoustic working frequency.** Therefore, when it is possible to partition scanned modes into groups of **ultrasonic scan lines** with the same f_{awf} values, then approximating $sppsi_{\alpha}$ with $s_{\alpha}ppsi$ may be a convenient alternative.

NOTE 3 Definitions in IEC 61157:2007+IEC 61157:2007/AMD1:2013, and IEC 60601-2-37:2007+IEC 60601-2-37/AMD1:2015 for "number of pulses per ultrasonic scan line" contain additional discussion and examples.

F.4.3 Further information regarding scanning modes

The discussion given in IEC 62127-1:2007 associated with its Equations (17) and (18) in 7.2.6.3 describes adjacent scan lines in a single scan plane. However, the **ultrasonic scan lines** adjacent to the central **ultrasonic scan line** could lie in multiple planes, as may be the case for 3D **scanning modes**. The equations would still apply, as would the methods and equations in F.3.1.4.2, F.3.3.2 and F.4.2. Knowledge of the location of the **ultrasonic scan lines** is still needed if applying method b) in F.3.1.4.2. A search in the azimuth (x) or elevation (y) direction at depth z may be needed to find the maximum $sppsi_{\alpha}$ value on a plane at depth z.

In **scanning modes**, a series of interrogating beams may be steered through a succession of azimuthal (i.e. in-plane lateral) directions within a single or succession of (elevation direction) target planes.

In the simplest **scanning mode**, all transmitted beams may exhibit the same focal characteristics along their respective **beam axes**; the beams may differ only in the orientation of the **beam axes**. Thus, the temporal peak and pulse average parameters of all beams (considered separately), as well as the **scanning mode** itself, are identical. The temporal average parameters for the mode are determined by the **pulse-pressure-squared integrals** of an individual beam, the degree of spatial overlap of the beams in the formation of the overall scan, and the **scan repetition rate**.

For 2D **scanning modes**, there is only one elevation target plane, and the rate at which the azimuthal scanning pattern is repeated is the **scan repetition rate** (srr). Multiplying the $\max_{z \geq z_{bp}} [sppsi(z)]$ and $\max_{z \geq z_{bp}} [sppsi_{\alpha}(z)]$ by this rate yields the maximum non-attenuated and attenuated **temporal average intensity** values.

In some 3D and 4D modes, the plane of examination is automatically swept through the target space in the elevation direction. Thus, while the scanning pattern may appear to be repetitive in the range-azimuth plane, the scanning pattern is not repetitive at any point in the target volume due to motion of the scan plane. As considered in this standard, two approaches may be taken.

This elevation motion is disregarded, and the **sum of pulse-pressure-squared integrals** is determined over the period of repetition in the range-azimuth plane, and then the **scan repetition rate** is determined from this period. This leads to a conservative over-estimate of the **temporal average intensity**.

The elevation motion is not disregarded, the **sum of pulse-pressure-squared integrals** is determined over all **ultrasonic scan lines** making one volume, with the **scan repetition rate** being the volume repetition rate.

In more complex **scanning modes**, the transmitted beams may exhibit two or more sets of focal characteristics. In some systems, certain scanning modes may employ two or more distinct focal patterns, each focused at a different depth, to create a single, overall scan. In still other systems, such as phased array sector devices, beam focal characteristics may vary with steering angle as well. In these more complex modes, the temporal-peak and pulse-average parameters for a given mode are determined by the maximum values that occur for any beam within the scan. The temporal average parameters for the mode are determined by the **pulse-pressure-squared integrals** and the **sum of pulse-pressure-squared integrals** and the **sum of attenuated pulse-pressure-squared integrals** of the different beam types, the degree and pattern of spatial overlap of the different beam types in the formation of the overall scan, and the **scan repetition rate**.

Bibliography

[1] AIUM. *Bio-effects and safety of diagnostic ultrasound*. American Institute of Ultrasound in Medicine, AIUM, 1470 Sweitzer Lane, suite 100, Laurel MD 20707-5906, 1993.

[2] HERMAN, BA, HARRIS, GR. Models and regulatory considerations for transient temperature rise during diagnostic ultrasound pulses. *Ultrasound Med Biol*, 28, 2002, p. 1217-12.

[3] IEC/TR 60854:1986, *Methods of measuring the performance of ultrasonic pulse-echo diagnostic equipment*

[4] IEC 61689, *Ultrasonics – Physiotherapy systems – Field specifications and methods of measurement in the frequency range 0,5 MHz to 5 MHz*

[5] BARNETT S.B, (ed.). Update on thermal bioeffects issues. *Ultrasound Med Biol,* Vol. 24, Suppl.1, 1998, p. S1-S10.

[6] European Committee for Medical Ultrasound Safety (ECMUS), *EFSUMB Newsletter* Vol. 15/1, 2001, p. 9 and EFSUMB Newsletter Vol. 15/2, 2002, p. 12.

[7] BARNETT S.B., TER HAAR G.R., ZISKIN M.C., ROTT H-D, DUCK F.A, MAEDA, K. International recommendations and guidelines for the safe use of diagnostic ultrasound in medicine. *Ultrasound in Medicine and Biology* 26, No. 3, 2000

[8] AIUM *Medical Ultrasound Safety,* © AIUM, 14750 Sweitzer Lane, Suite 100, Laurel MD 20707-5906, USA, 2009.

[9] ISO/IEC Guide 98-3, *Uncertainty of measurement – Part 3: Guide to the expression of uncertainty in measurement* (GUM 1995)

[10] HEKKENBERG R.T, BEZEMER R.A. On the development of a method to measure the surface temperature of ultrasonic diagnostic transducers. *Journal of Physics Conference Series* 1 (2004) 84-89 (Institute of Physics Publishing), 2004.

[11] O'BRIEN W.D. and ELLIS D.S. *IEEE Trans Ultrasonics Freq Control* 46, no. 6, Nov. 1999, p. 1459-1476.

[12] AIUM. Bio-effects considerations for the safety of diagnostic ultrasound. *J Ultrasound Med* 7: supplement, 1988.

[13] WFUMB. Conclusions and Recommendations on Thermal and Non-thermal Mechanisms for Biological Effects of Ultrasound. Report of the 1996 WFUMB Symposium on Safety of Ultrasound in Medicine. BARNETT S.B. (ed). *Ultrasound Med Biol*, 24, suppl 1, 1998.

[14] NCRP. *Exposure criteria for medical diagnostic ultrasound: I. Criteria based on thermal mechanisms*. NCRP Report No. 113, National Council on Radiation Protection and Measurements, Bethesda MD, 1992.

[15] CARSTENSEN E.L., CHILD S.Z., CRANE C., PARKER K.J. Lysis of cells in Elodera leaves by pulsed and continuous wave ultrasound. *Ultrasound Med Biol* 16, 1990, p. 167-173.

[16] CHILD S.Z., HARTMAN C.L., MCHALE L.A., CARSTENSEN E.L. Lung damage from exposure to pulsed ultrasound. *Ultrasound Med Biol*, 16, 1990, p. 817-825.

[17] CHURCH CC, O'BRIEN WD. Evaluation of the Threshold for Lung Hemorrhage by Diagnostic Ultrasound and a Proposed New Safety Index. *Ultrasound Med Biol*, 33, No.5, 2007, p. 810-818.

[18] CHURCH C.C. Spontaneous, homogeneous nucleation, inertial cavitation and the safety of diagnostic ultrasound. *Ultrasound Med Biol* 28, 2002, p. 1349-1364.

[19] HOLLAND C.K., APFEL R.E. Thresholds for transient cavitation produced by pulsed ultrasound in a controlled nuclei environment. *J Acoust Soc Am*, 88, 1989, p. 2059-2069.

[20] HERBERTZ J. Spontane Kavitation in keimfreien Flüssigkeiten (English translation: Spontaneous cavitation in liquids free of nuclei). In *Fortschritte der Akustik*, DAGA 88, DPG-GmbH Bad Honnef, 1988, p. 439-442.

[21] APFEL R.E., and HOLLAND C.K. Gauging the likelihood of cavitation from short-pulse low-duty cycle diagnostic ultrasound. *Ultrasound Med Biol*, 17, 1991, p. 179-185.

[22] AIUM / NEMA, *Standard for Real–Time Display of Thermal and Mechanical Acoustic Output Indices on Diagnostic Ultrasound Equipment*. AIUM, 1470 Sweitzer Lane, suite 100, Laurel MD 20707-5906, 2004.

[23] WFUMB, Second World Federation of Ultrasound in Medicine and Biology symposium on safety and standardization in medical ultrasound. *Ultrasound Med Biol.,* 15: supplement, 1989.

[24] NCRP, *Exposure criteria for medical diagnostic ultrasound: II. Criteria based on all known mechanisms.* NCRP Report No. 140, National Council on Radiation Protection and Measurements, Bethesda MD, 2002.

[25] LUBBERS J., HEKKENBERG R.T., BEZEMER R.A. Time to Threshold (TT), a safety parameter for heating by diagnostic ultrasound. *Ultrasound in Med. & Biol.*, May 2003, Vol. 29, 5, p. 755-764.

[26] ABBOTT J.G. Rational and Derivation of MI and TI – a Review. *Ultrasound Med Biol.*, 25, No. 3, 1999, p. 431-441.

[27] SEKINS K.M., EMERY A.F. Thermal science for physical medicine. Chapter 3, p.70-132, in *Therapeutic Heat and Cold*. LEHMANN J.F. editor, Williams & Wilkins, Baltimore MD, 1982.

[28] CARSTENSEN E.L., CHILD S.Z., NORTON S., NYBORG W.L. Ultrasonic heating of the skull. *J Acoust Soc*. Am., 87, 1990, p. 1310-1317.

[29] BEISSNER K., Radiation force calculations for ultrasonic fields from rectangular weakly focusing transducers, *J. Acoust. Soc. Am*. 124, 1941 – 1949 (2008).

[31] BEISSNER K., Radiation force calculations for oblique ultrasonic beams, *J. Acoust. Soc. Am. 125,* 2827 – 2829 (2009).

[32] SHAW A., PAY NM. and PRESTON R.C. *Assessment of the likely thermal index values for pulsed Doppler ultrasonic equipment – Stages II and III: experimental assessment of scanner/transducer combinations*. NPL Report cmAM 12, available from The National Physical Laboratory, Teddington, Middlesex TW11 OLW, UK, 1998.

[33] SHAW A, PAY N.M., PRESTON R.C., BOND A.D., Proposed Standard Thermal test object for medical ultrasound. *UMB*, Vol 25, No. 1, p. 121-132, 1999.

[34] HEKKENBERG R.T., BEZEMER R.A., *Aspects concerning the measurement of surface temperature of ultrasonic diagnostic transducers*. PG/TG/01.246r, ISBN 90-5412-078-9, March 2002.

[35] HEKKENBERG R.T., BEZEMER R.A., *Aspects concerning the measurement of surface temperature of ultrasonic diagnostic transducers, Part 2: On a human and artificial tissue*. PG/TG/2003.134, ISBN 90-5412-085-1, May 2003.

[36] HEKKENBERG R.T., BEZEMER R.A., On the development of a method to measure the surface temperature of ultrasonic diagnostic transducers. *Journal of Physics*: Conference Series 1 (2004) 84-89 (Institute of Physics Publishing), 2004.

[37] SAUNDERS O, CLIFT S AND DUCK F, Ultrasound transducer self heating: development of 3-D finite-element models. *Journal of Physics*: Conference Series 1 (2004) p. 72-77.

[38] AIUM, Mechanical Bioeffects from Diagnostic Ultrasound: AIUM Consensus Statements, *J Ultrasound Med*. 19, No. 2 or 3, 2000.

[39] SALVESEN K.A. Epidemiological studies of diagnostic ultrasound. Chapter 9, in: The safe use of ultrasound in medical diagnosis, British Medical Ultrasound Society/British Institute of Radiology. Editors TER HAAR G.R. and DUCK F.A., 2000, p. 86-93.

[40] DUCK F.A. The meaning of Thermal Index (TI) and Mechanical Index (MI) values. *BMUS Bulletin*, Nov. 1997, p. 36-40.

[41] FDA-CDRH, Guidance for Industry and FDA Staff, Information for Manufacturers Seeking Marketing Clearance of Diagnostic Ultrasound Systems and Transducers, September 9, 2008.

[42] CHRISTOPHER T., CARSTENSEN E.L. Finite amplitude distortion and its relationship to linear derating formulae for diagnostic ultrasound systems. *Ultrasound Med. Biol.,* 22, 1996, p. 1103-1116.

[43] World Federation for Ultrasound in Medicine and Biology. *(*WFUMB) Symposium on Safety and Standardisation in Medical Ultrasound, Synopsis. *Ultrasound Med Biol*, 18, 1992, p. 733-737.

[44] AIUM/NEMA, Acoustic output measurement standard for diagnostic ultrasound equipment, NEMA Standards Publication UD 2-2004, Revision 3

_____

INTERNATIONAL
ELECTROTECHNICAL
COMMISSION

3, rue de Varembé
PO Box 131
CH-1211 Geneva 20
Switzerland

Tel: + 41 22 919 02 11
Fax: + 41 22 919 03 00
info@iec.ch
www.iec.ch